224.
4-29-82

CONTRACTOR REPORT ②

SAND81-7013
Unlimited Release
UC-63a

LR.463

I-2803

MASTER

Photovoltaic Subsystem Optimization and Design Tradeoff Study Final Report

SAND--81-7013

DE82 013393

W. J. Stolte, Project Manager
Bechtel Group Inc., San Francisco, CA

Printed March 1982

NOTICE
PORTIONS OF THIS REPORT ARE ILLEGIBLE.
It has been reproduced from the best
available copy to permit the broadest
possible availability.

DISCLAIMER

SAND81-7013
Unlimited Distribution
Printed March 1982

SAND--81-7013

DE82 013393

PHOTOVOLTAIC SUBSYSTEM OPTIMIZATION
AND DESIGN TRADEOFF STUDY: FINAL REPORT

W. J. Stolte, Project Manager
Bechtel Group, Inc.
Research and Engineering Operation
San Francisco, California

ABSTRACT

This work examines tradeoffs and subsystem choices
in photovoltaic array subfield design, power-
conditioning sizing and selection, roof- and
ground-mounted structure installation, energy
loss, operating voltage, power conditioning cost,
and subfield size. Line- and self-commutated
power conditioning options are analyzed to
determine the most cost-effective technology in
the megawatt power range. Methods for reducing
field installation of flat panels and roof
mounting of intermediate load centers are
discussed, including the cost of retrofit
installations.

ACKNOWLEDGMENTS

13908
T1002415

CONTENTS

ILLUSTRATIONS

xiv

Section 1

INTRODUCTION

Successful commercialization of large-scale terrestrial photovoltaic power systems will require identification of reliable, low cost, and efficient subsytem components and system configurations. This report documents an engineering study conducted to identify and evaluate engineering design tradeoffs for several key subsystems. The Research and Engineering Operation of Bechtel Group, Inc. performed the study, with United Technologies Corporation as a subcontractor, for Sandia National Laboratories under Contract Number 46-0042, as part of the U.S. Department of Energy's National Photovoltaic Program.

1.1 OBJECTIVES

The overall objectives were to identify and evaluate engineering design options with regard to:

- Array field layout and wiring
- Power conditioning
- Array support structure design and installation.

Specific objectives for these three areas of study were to:

- Provide parametric data and tradeoff analyses on array subfield layout and wiring, in a form that will facilitate future subsystem and system design optimizations

- Identify and evaluate techniques having the potential to reduce wiring subsystem installation costs

- Provide parametric data on power conditioner costs and operating characteristics, as well as tradeoff analyses in conjunction with field layout and wiring subsystems data

- Provide a comparative assessment of power conditioners, indicating which type(s) is best suited for photovoltaic applications and areas needing further development

- Provide characterizations and assessments of flat roof types and array structural requirements for roof-mounted nontracking arrays, and detailed analyses of promising concepts

- Identify and assess cost reduction techniques for the fabrication and installation of roof- and ground-mounted arrays.

1.2 REPORT FORMAT

This section presents a discussion of terminology, assumptions, costing methodologies, and other design bases used in the study. Study results are summarized in Section 2. Field layout and wiring considerations are presented in Section 3. Section 4 covers the power conditioning subsystem and Section 5 presents optimization and design tradeoff analyses combining the data contained in Sections 3 and 4. Requirements for array structures mounted on flat roofs, as well as installation cost reduction techniques for both roof- and ground-mounted arrays are presented in Section 6. Major conclusions are presented in Section 7, along with recommendations and identification of areas requiring additional study.

1.3 TERMINOLOGY

At present, several institutions are working to establish a consistent set of terms and a nomenclature hierarchy to describe the components and subsystems that comprise a photovoltaic (PV) power system. Attempts are

being made to make these terms as consistent as possible for both flat-plate and concentrator array designs. Figure 1-1 illustrates the hierarchy of system elements used in this study. The terminology presented in the figure is consistent with the Interim Performance Criteria for Photovoltaic Energy Systems draft document (Ref. 1-1). While this terminology may not be completely applicable for all PV applications, it provides a common basis for discussion of the analyses presented in this report.

The term "subsystem" is used to identify specific portions of photovoltaic power systems (e.g., dc power collection wiring subsystem) evaluated during this study. The subsystems are defined to include all elements (e.g., cable, terminations, etc. and installation for the dc power collection wiring subsystem) necessary to accomplish a specific function within the power system.

1.4   DESIGN AND COST BASES

To conduct this study, it was necessary to make certain initial assumptions and to establish study bases and guidelines for use during the design optimization and tradeoff analyses. This was necessitated by both the diverse nature of potential terrestrial photovoltaic applications and the relatively immature state of present technology development. Also, it was realized that the economic parameters (e.g., material costs, labor rates, and the value of energy used in the analyses) significantly affect the results and conclusions of a study of this type.

The reader is cautioned that, because the primary purpose of this study was to identify major cost drivers and to compare alternate design

MODULE – THE SMALLEST COMPLETE ENVIRONMENTALLY PROTECTED ASSEMBLY OF SOLAR CELLS/OPTICS AND OTHER COMPONENTS (EXCLUSIVE OF TRACKING), DESIGNED TO GENERATE DC POWER WHEN UNDER UNCONCENTRATED TERRESTRIAL SUNLIGHT

PANEL – A COLLECTION OF ONE OR MORE MODULES, OPTICS AND OTHER COMPONENTS FASTENED TOGETHER, FACTORY PREASSEMBLED AND WIRED, FORMING A FIELD INSTALLABLE UNIT.

ARRAY – A MECHANICALLY INTEGRATED ASSEMBLY OF PANELS TOGETHER WITH SUPPORT STRUCTURE (INCLUDING FOUNDATIONS) AND OTHER COMPONENTS, AS REQUIRED, TO FORM A FREE-STANDING FIELD INSTALLED UNIT THAT PRODUCES DC POWER

BRANCH CIRCUIT – A GROUP OF PANELS OR PARALLELED PANELS CONNECTED IN A SERIES TO PROVIDE DC POWER AT THE DC VOLTAGE LEVEL OF THE POWER CONDITIONING UNIT (PCU). A BRANCH CIRCUIT MAY INVOLVE THE INTERCONNECTION OF PANELS LOCATED IN SEVERAL ARRAYS.
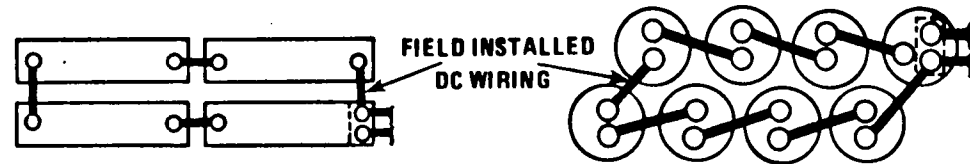
ARRAY SUBFIELD – A GROUP OF SOLAR PHOTOVOLTAIC ARRAYS ASSOCIATED BY THE COLLECTION OF BRANCH CIRCUITS THAT ACHIEVES THE RATED DC POWER LEVEL OF THE POWER CONDITIONING UNIT.
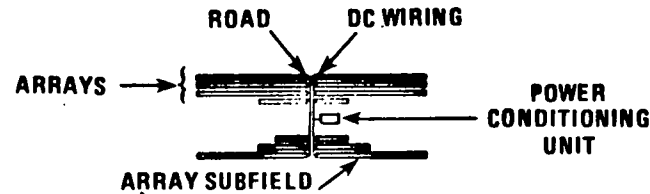
ARRAY FIELD – THE AGGREGATE OF ALL ARRAY SUBFIELDS THAT GENERATE POWER WITHIN THE PHOTOVOLTAIC POWER SYSTEM.

PHOTOVOLTAIC POWER SYSTEM –
THE ARRAY FIELD TOGETHER WITH AUXILIARY SYSTEMS (POWER CONDITIONING, WIRING, SWITCHYARD, PROTECTION, CONTROL) AND FACILITIES REQUIRED TO CONVERT TERRESTRIAL SUNLIGNT INTO AC ELECTRICAL ENERGY SUITABLE FOR DELIVERY TO THE LOAD.
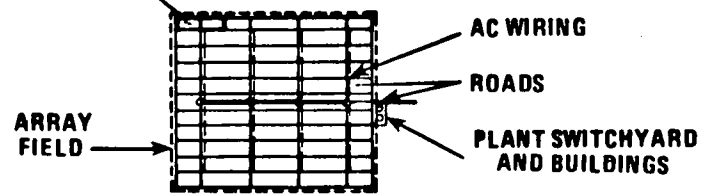
1-4

Figure 1-1 Photovoltaic Power System Terminology

configurations, several inaccuracies may be present. These include the use of engineering approximations and the unavailability of data on similar construction projects and their historical costs. Also, subsystems were generally evaluated individually, rather than as an integral part of a larger system; therefore the costs of the tradeoff analyses may not accurately reflect the true costs of the subsystems in an integrated plant design. For example, the estimated costs for underground field wiring subsystems include dedicated trenches. However, in an actual plant design it might be possible to install wiring in array foundation trenches, thereby reducing the combined cost of the integrated subsystems.

Therefore, although these inaccuracies do not significantly affect the design tradeoff analyses or identification of optimum subsystem configurations, they are inherent in much of the cost data presented in the following sections. Detailed system design and cost estimating studies are required to better define absolute values of installed costs for specific system configurations and site conditions.

Unless otherwise indicated, all costs are reported in terms of 1980 dollars. To the extent possible, costs are reported in appropriate units, such as $/Wp for power conditioning equipment or $/m^2$ for array support structures.

Costs reported in Section 3 (for wiring subsystems) and in Section 6 (for array support structures) were estimated by Bechtel using standard historical construction cost references (e.g., Refs. 1-2 and 1-3). Where necessary, these sources were supplemented using Bechtel's in-house construction cost data base.

Power conditioning equipment costs reported in Section 4 were generated by United Technologies Corporation (a subcontractor) using their existing in-house data base. The sources of these data are discussed in Section 4.

In many cases, the evaluation of design alternatives and identification of optimum configurations requires a tradeoff between equipment first costs (all costs for material and installation) and the value of energy losses resulting from equipment/subsystem inefficiencies. An example of this is the tradeoff between the size of electrical conductors installed (first cost) and the value of the resulting I^2R energy losses.

Such tradeoffs can be accomplished by using life cycle costs methods to calculate the present worth of all losses occurring during the plant lifetime. However, this approach requires that several key assumptions be made with regard to interest rates, capital recovery factors, the future value of energy, and other economic factors. These factors are subject to a degree of uncertainty regarding future economic conditions. In addition, these factors will also exhibit variations for different application categories and geographic locations.

A second method of analyzing the tradeoff between first costs and energy losses is to determine the equivalent cost of all PV plant equipment (essentially all of the area related costs) necessary to provide a yearly energy production equal to the yearly energy losses, as follows:

$$V = (\frac{100}{n} - 1) \times Ca$$

Where: V = equivalent value of energy losses
n = yearly energy efficiency (%)
Ca = area related costs ($/Wp)

For example, if it is desired to evaluate the equivalent value of the energy losses occurring in a dc power collection wiring subsystem that operates at a yearly energy efficiency of 98 percent, and is a part of a photovoltaic power system having an area related cost of $1.00/Wp, then:

$$V = (\frac{100}{98} - 1) \times \$1.00/Wp = \$0.02/Wp$$

The equivalent cost of $0.02/Wp can then be compared with the increased first costs incurred for decreasing the wiring system losses (by installing larger conductors). The optimum configuration is that which results in the lowest total of first cost and equivalent value of energy lost. This analysis does not result in a determination of life cycle energy costs, but it does identify subsystem and system configurations that result in the lowest system cost per unit of annual energy production.

Unless otherwise indicated, therefore, all tradeoffs between first costs and energy losses presented in this report are based on the equivalent value of the losses, as discussed above. The area-related costs were assumed to be $1.00/Wp (1980 dollars) in all cases. While this value is also subject to some uncertainty and variation between applications, it is generally in the range of expected costs based on the DOE price goals (Ref. 1-4). In most cases, first costs and energy losses (in percent) are presented parametrically for each analysis, to facilitate evaluation of optimum configurations using other economic assumptions and/or methodologies.

Section 2

SUMMARY

This report documents an engineering study conducted to identify and evaluate engineering design tradeoffs for several key subsystems for large (> 500 kW) photovoltaic power plants. The Research and Engineering Operation of Bechtel Group, Inc. performed the study, with United Technologies Corporation as a subcontractor, for Sandia National Laboratories under Contract Number 46-0042, as part of the U.S. Department of Energy's National Photovoltaic Program.

The study evaluated the effects of array characteristics, system power, and voltage levels, as well as other design and application specific factors, on first and operating (e.g., the value of energy losses) costs with regard to:

- Array field layout and wiring subsystems

- Power conditioning equipment

- Array field design optimization.

In addition, initial evaluation of the requirements for mounting fixed flat plate arrays on flat-roofed commercial and industrial buildings was conducted, along with an analysis of potential array support structure installation cost reduction techniques.

A hierarchy of terminology used to identify the photovoltaic power system elements was established, as described in Figure 1-1.

2.1 ARRAY FIELD LAYOUT AND WIRING SUBSYSTEMS

For most large photovoltaic power systems, it will be necessary to provide a field-installed dc wiring subsystem to collect the power outputs of the individual arrays for power conditioning and eventual delivery to the load. Other field-installed subsystems, such as ac power collection, grounding, lightning protection, instrumentation and control, and tracking power wiring may also be required.

Insofar as subfield layout and wiring subsystem design are concerned, a major distinction exists between arrays that rotate about a vertical axis (primarily two axis tracking concentrator designs) and horizontal axis systems such as flat-plate and line focus designs. This difference results from the fact that the vertical axis arrays are discrete physical structures having their electrical terminals at their centers. This generally requires a larger (and more costly) field-installed dc wiring subsystem than would be necessary for equivalently rated horizontal axis arrays.

For this study, vertical axis arrays having diameters of 10, 25, and 45m, and efficiencies of 10, 15, and 20% were evaluated. Horizontal axis arrays having slant heights of 1.2, 2.4, and 4.8m, and efficiencies of 10, 13, and 16% were also studied. These array parameters resulted in peak power densities in the ranges of 80 to 200 kW/acre for the vertical axis arrays and 120 and 385 kW/acre for the horizontal axis arrays (for 1 kW/m^2 insolation).

Several computer programs were developed to facilitate evaluation of dc wiring subsystem first costs and I^{2}R energy losses (for underground direct buried copper conductors) for dc voltages ranging from 500 to

5000 volts and subfield peak power ratings ranging from 500 to 25,000 kW.
In general, costs and losses tend to decrease with increasing dc voltage
level, although above about 2000 Vdc the decreases are less significant.
For example, first costs and energy losses for a 5000 kWp subfield consisting
of 25m diameter, 15% efficient vertical axis arrays operating at 500 Vdc
are 32 mills/ Wp and 5.8% (of yearly array output energy), respectively.
At 2000 Vdc the values are 13 mills/Wp and 1.9%, while at 5000 Vdc the
first costs are 11 mills/Wp and the energy losses are 1.1% of yearly
array energy output. For a given subfield dc voltage level, first costs
and energy losses tend to increase with increasing subfield power level.
Also, first costs and energy losses tend to decrease with increasing
array diameter and/or increasing array efficiency. Similar trends are
observed for horizontal axis arrays, although the values of first costs
and energy losses are generally lower than for equivalently rated vertical
axis array subfields. The cost impacts of using copper versus aluminum
conductors, as well as using oversized or undersized conductors were also
evaluated. Further details and results of these analyses are presented
in Section 3.2.

Large photovoltaic power systems may consist of several array subfields,
each with its own dc/ac power conditioner, operating in parallel (on the
ac side). An ac power collection wiring subsystem will therefore be required.
This study evaluated the first costs and energy losses for this subsystem
as functions of array field power density, array field peak power rating,
array subfield (i.e., power conditioner) power rating, and ac collection
voltage for both overhead and underground wiring systems. First costs
for overhead construction are generally slightly lower than for equivalent

underground installations. Also, costs tend to decrease for increasing array field power density, increasing ac voltage level, and/or increasing power conditioner power rating. However, ac power collection wiring first costs are relatively small (compared with total plant costs). For example, first costs for a 35 kV ac power collecting wiring subsystem for a 100 MWp array field, having a power density of 200 kWp/acre and consisting of 5 MWp array subfields, are 3 mills/Wp and 6.5 mills/Wp for overhead and underground installations, respectively. I^2R energy losses are relatively small ($< 0.5\%$ of yearly power conditioner energy output) and do not significantly affect the selection of optimum ac power collection wiring subsystem configurations. Further details and results of this analysis are presented in Section 3.3.

Most photovoltaic power systems will require a grounding subsystem both to ensure proper plant equipment operation and to maintain equipment and personnel safety during normal operating and upset conditions. Design requirements for grounding in large photovoltaic power systems are presently not well defined. This results from uncertainties with regard to both the required levels of protection and the nature of specific array configurations. In lieu of detailed design criteria, standard industry practice for the design of ac substation ground grids was used to evaluate the effects of array size, array efficiency, plant size and soil resistivity on grounding subsystem requirements and costs. Using existing design criteria, soil resistivity was found to be the most significant cost driver. For example, for vertical axis arrays and for 10 Ω-m soil resistivity, grounding subsystem costs are in the range of 10 mills/Wp. However, for 1000 Ω-m soil resistivity costs can increase by as much as one

or two orders of magnitude, depending on plant peak power rating. The results of this analysis are discussed further in Section 3.4.

In many applications it will be necessary (or economically attractive) to protect the arrays from transient voltage surges, either lightning induced or generated within the power system. As is the case for grounding, the design requirements for surge protection are uncertain at present. These requirements can be affected by site specific characteristics, such as soil resistivity and isokeraunic level, as well as by array and system design characteristics. To obtain order-of-magnitude cost estimates for surge protection and to assess the effects of array size, array efficiency, and dc voltage, the use of varistors was investigated. For example, for 10m diameter, 10% efficient arrays, the costs for locating two varistors at each branch circuit terminal box, plus one varistor at each array, were estimated to be about 10 mills/Wp. The results of this analysis are discussed further in Section 3.5.

The requirements for control, instrumentation, and auxiliary power wiring are extremely array- and application-specific, and were not addressed in detail in this study. These requirements are discussed briefly in Section 3.6.

Reductions in installed costs for the field-installed wiring subsystems can potentially be obtained by the use of innovative factory prefabrication and field installation methods. These are discussed in Section 3.7.

2.2 POWER CONDITIONING EQUIPMENT

Most PV systems require some type of interface between the array dc output

terminals and the load to provide voltage matching, dc/ac inversion, or other power conditioning functions. For this study, the power conditioning subsystem, sometimes referred to as the power conditioning unit (PCU), was defined to include all equipment necessary to receive the dc power outputs of all branch circuit feeders and deliver ac power of acceptable quality to the photovoltaic system load.

United Technologies Corporation, under subcontract to Bechtel, conducted a study to:

- Evaluate the effects of power level (1 to 25MWp) and dc voltage (600 to 5000V) on PCU first cost and operating efficiency

- Evaluate the effects of dc voltage window (i.e., operating voltage range) on PCU first costs and operating efficiency

- Evaluate the first cost and operating efficiency of in-field dc-to-dc up-converters

- Provide an overall assessment of self-commutated inverter (SCI) versus line-commutated inverter (LCI) technologies for use in large photovoltaic power systems.

The results of the study indicate that for equivalently rated systems (in terms of dc power and voltage, as well as ac power factor and harmonic injection) average selling prices for SCI systems are equal to or less than LCI selling prices. This is primarily due to the costs of power factor correction and harmonic filter equipment necessary with the LCI systems. For example, for 5000 kW, 2000 Vdc systems having a 1.5 voltage window, the

average selling prices are estimated to be $55/kW and $62/kW for SCI and LCI systems, respectively. In general, selling price ($/kW) for both converter types decreases with increasing power level. Also, selling prices for fixed power level converters are relatively insensitive to dc voltage level, especially for the higher power levels. The results of this analysis are presented in detail in Section 4.1.

For the designs evaluated in this study, the full- and part-load operating efficiencies of identically rated LCI and SCI systems are approximately equal. Efficiencies generally increase with increasing power level for both converter types. SCI efficiencies tend to decrease slightly with increasing dc voltage, especially at part-load. For the lower power level LCI systems, efficiency tends to decrease with increasing dc voltage, while for the higher power systems efficiency increases with increasing dc voltage. These results are also quantified and discussed in Section 4.1.

For voltage windows in the range of 1.5 to 1.1, selling prices of both LCI and SCI converters decrease for narrower voltage windows. For example, selling prices for 5000 kW, 2000 Vdc systems decrease by 15 and 24% for SCI and LCI systems, respectively, when going from a voltage window of 1.5 to 1.1. Narrower voltage windows also result in improved operating efficiencies. The effects of voltage window are discussed further in Section 4.2.

Also evaluated during this study were selling prices and operating efficiencies for two in-field dc up-converter schemes: (1) dc boost regulators and (2) inverter-transformer-rectifier, for use with large, centrally located inverters. These schemes generally result in higher selling

prices and lower operating efficiencies than would be incurred with the use of smaller, in-field dc to ac converters.

No clear-cut advantage for either the SCI or LCI converter technologies can be discerned from the data developed during this study. However, the SCI technology exhibits several attractive operating characteristics, especially with regard to power factor control and harmonic injection. Further evaluations, including identification of installation requirements, site-dependent design requirements, and refinement of full- and part-load efficiencies estimates are required to determine which type of converter is best suited for specific photovoltaic power system applications.

Subsequent to the completion of the initial work, a follow-on contract was awarded to further analyze LCI and SCI operational characteristics and estimate installation costs. These results are presented and summarized separately in the appendix.

2.3 ARRAY FIELD DESIGN OPTIMIZATION

The identification of optimum system design parameters requires consideration of the interactions between the various subsystems as well as the effects of application-specific factors. This study evaluated such trade-offs with regard to:

- Total equivalent PCU costs

- Total equivalent dc subsystem costs

- PCU voltage window

- Total equivalent dc up-converter costs

- Array spacing.

To compare the various PCU design alternatives, it is necessary to evaluate their yearly energy efficiencies so that the total equivalent PCU costs (first costs plus the value of the losses) can be identified. This was accomplished using the full- and part-load efficiency data supplied by United Technologies Corporation (as discussed in Section 4) and SOLMET TMY insolation data for Albuquerque, Boston, and Miami. The results of this analysis indicate that yearly PCU energy efficiency is affected by: inverter type (being slightly higher for LCI systems, especially at the lower power levels), array type (e.g., two axis tracking or fixed flat-plate), and location. In general, PCU yearly energy efficiencies were in the range of about 90 to 96% of yearly array output energy. The values of the energy losses (as described in Section 1.4) were then combined with PCU first costs to identify total equivalent PCU costs. Comparison of these costs indicates that, considering both first costs and operating efficiencies, LCI and SCI systems have comparable total equivalent costs. Costs for both systems tend to decrease with increasing power level, although the decreases become less significant above about 5MW. Equivalent costs for the LCI systems are essentially unaffected by dc voltage level. However, equivalent costs for the SCI systems generally increase with increasing dc voltage level, except at the higher power ratings. These results are further quantified and discussed in Section 5.1.1.

Selection of optimum (lowest cost) subfield voltage and power levels requires evaluation of the combined costs for dc wiring, power conditioning, and other related components. Evaluation of total costs for the dc wiring and PCU subsystems indicates that at the 1000 and 2000 Vdc levels, cost minima occur in the area of about 5MW peak subfield power.

At the higher voltage levels, costs generally continue to decrease, although at a slower rate (particularly for the LCI systems).

However, other considerations, including the need for branch circuit isolating and/or shorting switches, as well as the cost of electrically insulating the solar cell modules, may result in somewhat lower optimum voltage levels. This is discussed further in Section 5.1.2.

Evaluation of total equivalent PCU costs as a function of voltage window indicates that for 5000 kW, 2000 Vdc units, costs can be reduced by as much as 9 or 10% for both SCI and LCI systems, when the voltage window is decreased from 1.5 to 1.1. Additionally, analyses indicate that with proper selection of the dc center voltage, acceptable yearly array energy output can be obtained for voltage windows as narrow as 1.1 or 1.2. This is discussed further in Section 5.1.3.

For the in-field dc up-converter schemes analyzed in this study, their high first costs and/or low operating efficiencies cause them to be economically unattractive for use in large photovoltaic power systems. This is further illustrated in Section 5.1.4.

The spacing provided between adjacent array structures is a tradeoff between access requirements; shadowing losses; and the costs of land, wiring and other subsystems affected by the spacing. Analyses conducted during this study indicate that, depending on site latitude and land costs, spacings of up to 3 times the vertical array height may be economically attractive for fixed flat-plate arrays. This is discussed further in Section 5.2, along with the effects of vertical axis array spacing on dc wiring costs.

2.4 ARRAY SUPPORT STRUCTURES

Mounting photovoltaic arrays on building rooftops requires that consideration be given to the consequences of additional structural loadings imposed by the arrays, as well as to other factors such as the need to maintain the watertight integrity of the roof membrane.

A review of the various roof construction types used throughout the United States on flat-roofed commercial and industrial buildings reveals a wide range of characteristics. This makes generalization of array design requirements and optimum array configurations extremely difficult.

Also, no existing building codes could be found that specifically address the installation of photovoltaic arrays on building roofs. Therefore, identification of structural loadings and other design criteria must be based on engineering judgment and are subject to interpretation by individual building code officials. Of particular concern in the design of roof mounted photovoltaic arrays are the resulting additional wind and, in some areas, snow loadings. Additional study is required (and is in progress) to adequately define these loadings.

Roof-mounted arrays must be capable of transferring their loadings to the building structure in a manner that does not overstress the building's structural members. In general, two methods of accomplishing this can be identified: roof supports, the array support structures are located over and supported by structural components of the roof system (such as the membane, beams or joists), or wall supports, wherein the array support structures transfer their loads directly into vertical building members (such as walls or columns).

Structural evaluations conducted during this study indicate that many
existing roofs may have relatively small design margins, and that the
inclusion of photovoltaic arrays using the roof support method may result
in overstress conditions. This is, of course, dependent on design loadings
and design details for specific buildings, and underscores the need for
better definition of array loading conditions. Retrofit may not be practi-
cal for some existing buildings.

Installed cost estimates indicate that a torque-tube type of array support
structure has the potential for lower cost than the more conventional truss
structure presently used for solar thermal array installations. As with
ground mounted support structures, loading is a major cost driver. How-
ever, for roof mounted arrays the cost of roof penetrations is also a
significant cost factor, especially in retrofit applications. These pene-
trations must be capable of transferring the array loads to the building's
structural members, while maintaining the watertight integrity of the roof.
Identification of innovative, low cost roof penetrations having relatively
minor maintenance requirements is a key factor in attaining low cost
roof-mounted photovoltaic array support structures.

The mounting of photovoltaic arays on flat-roofed commercial and industrial
buildings is discussed in more detail in Section 6.1.

In the area of array support structure cost reduction, baseline construction
scenarios for three support structure designs (torque tube) were established
to identify major cost drivers. Labor costs ranged from about 12 to 21%
of the total installed costs. It is expected that the lowest total
installed costs will be obtained for designs that fully consider the

integration of panel and array structural members. Such studies are being conducted by Bechtel for Sandia for release in early 1982. Additional cost reductions can be obtained via design optimizations that utilize factory prefabrication techniques, as well as low cost structural materials and labor reducing in-field mechanical connections. Details are discussed in Section 6.2.

Highly speculative automated installation scenarios were postulated during this study to assess the installation cost reduction potential of such techniques. Based on these scenarios, it appears that potential cost benefits may be achieved through optimum blends of conventional and automated installation methods for specific array field designs. This will require further study to identify construction activities and procedures that are amenable to automation as well as to improve the cost tradeoff data. This is discussed in Section 6.2.

Section 3

ARRAY FIELD LAYOUT AND WIRING SUBSYSTEMS

The nature of solar radiation is such that a large array field area is required to generate significant amounts of power. As shown in Figure 1-1, the array field consists of photovoltaic panels mounted on support structures to form arrays. Each array is a mechanically integrated assembly of solar cell panels, support structure, foundations, and other components needed to form a free-standing dc power producing unit. Large photovoltaic power systems will consist of many arrays dispersed over relatively large land areas. Thus, it will be necessary to provide a field-installed dc wiring subsystem to collect the power outputs of the individual arrays for power conditioning and eventual delivery to the load. Other field-installed subsystems, such as ac power collection, grounding, lightning protection, instrumentation and control, and tracking power wiring may also be required.

The number of arrays required for a specific application is determined by load power (and energy) requirements; array type and efficiency; site location; and other application-specific factors. In addition, subsystem design requirements are likely to be somewhat determined by array characteristics. However, in most situations the system designer must select between a large number of design alternatives with regard to system configurations, voltage levels, non PV equipment ratings, and many other factors. A number of parameters that can influence array field layout and wiring subsystem designs are summarized in Table 3-1.

Table 3-1

ARRAY SUBFIELD DESIGN PARAMETERS

I   ARRAY CHARACTERISTICS

    1) Configuration
       a) Flat-plate or horizontal-axis tracking
       b) Vertical-axis tracking
    2) Design Characteristics
       a) Voltage level
       b) Current level
       c) Electrical insulation level
    3) Performance Characteristics
       a) Peak power per unit area (efficiency)
       b) Diurnal power output shape
       c) Ratio of peak power to yearly energy
    4) Other
       a) Tracking control and drive power wiring
       b) Instrumentation wiring

II SYSTEMS CHARACTERISTICS

    1) System Power Level
    2) DC System (Branch Circuit) Voltage
    3) Wiring Layout
       a) Individual feeders vs tapered bus
       b) DC ground (floating, center, or one-pole grounded)
       c) Disconnect switches, transient overcurrent, and reverse
          current protection
    4) Value of I^2R Energy Losses
    5) Grounding and Lightning Protection
    6) AC Power Collection Costs

III SITE CHARACTERISTICS

    1) Latitude
       a) Tilt angle (fixed array only)
       b) Interarray spacing
    2) Soil Conditions
       a) Ground resistance
       b) Installation requirements
    3) Weather
       a) Installation requirements
       b) Temperature
       c) Isokeraunic Level

IV OTHER CONSIDERATIONS

    1) Codes and Utility Practice
    2) Safety
    3) Equipment
       a) Suitability of standard designs
       b) Potential for cost reduction or need for custom designs
    4) Reliability

Identification of optimum (lowest cost per unit of annual energy production) system configurations requires identification and evaluation of these and other relevant parameters for the specific application under study. The evaluation should consider the first costs, the value of energy losses, and the costs of maintenance over the life of the system for the various design options.

This section discusses some of the various field wiring subsystems design options available to the system designer for the design of large (i.e., 0.5 to 1000 MWp) PV power systems. First costs, energy losses, and other significant characteristics are presented parametrically to facilitate identification of optimum configurations for specific applications and/or array characteristics. Methods of reducing installation costs for the field-installed wiring subsystems are also discussed.

3.1 DESIGN CONSIDERATIONS

Subsystem requirements and optimum subsystem design configurations are determined by both application specific characteristics and array design. For example, while all large PV systems will likely require dc power collection and equipment grounding subsystems, the need for control, auxiliary power, and other similar subsystems is determined by the requirements of specific array types.

Site-specific factors, such as soil characteristics and the degree of lightning activity, can also influence optimum design configurations. Local and/or national safety codes and standards may also impose additional requirements.

Therefore, subsystem requirements and appropriate design alternatives must be identified prior to the conduct of trade off analyses and design optimization. This is facilitated by consideration of:

- Array characteristics
- Field layout
- Site characteristics
- Code requirements.

3.1.1   Array Characteristics

A wide variety of array designs are presently in use, under development, or proposed for large photovoltaic power systems. The appropriate array for a specific application is influenced by array costs and application-specific factors such as potential uses for thermal energy rejected by actively cooled concentrators. The array selected for a particular application will influence wiring subsystem design requirements, optimum subsytem configurations and, therefore, subsystem costs.

Insofar as subfield layout and wiring subsystems design are concerned, a major distinction exists between arrays that rotate about a vertical axis (primarily two axis tracking concentrator designs) and horizontal axis systems such as flat-plate and line focus designs. This is primarily due to the location of the electrical terminals. Examples of the various array types are illustrated in Figure 3-1.

Vertical Axis Arrays. A number of array designs (Ref. 3-1) are configured so as to rotate about their vertical axes. The carousel and pedestal-mount designs, illustrated in Figures 3-1(a) and 3-1(b) respectively, are

VERTICAL AXIS
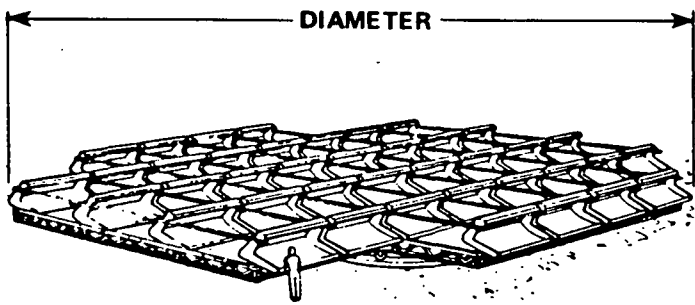
(a)
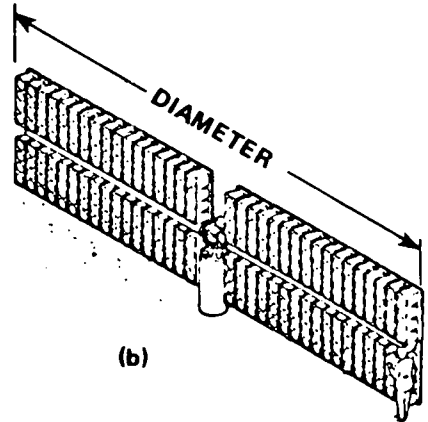
(b)

HORIZONTAL AXIS
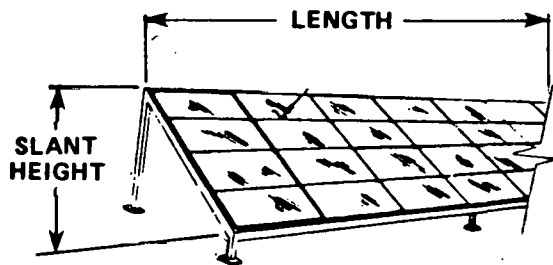
(c)
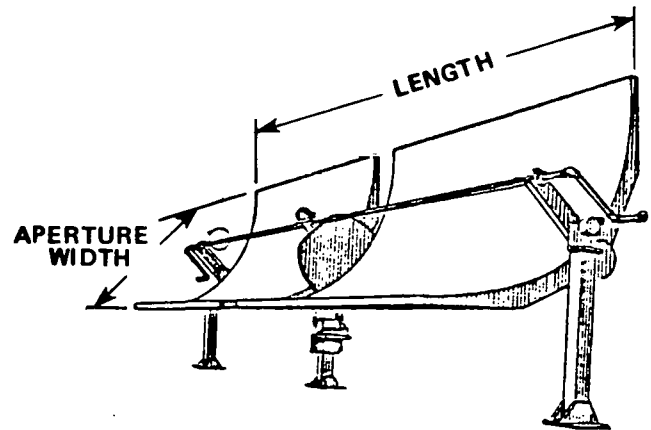
(d)

Figure 3-1 Generic Array Types

representative of this array type. The major distinguishing feature, in terms of field-installed wiring subsystems, is the location of the array electrical terminals at the center of the structure. This necessitates field installed dc wiring between each set of array terminals to provide the required series/parallel array connections. The quantity of array terminals requiring interconnection depends on the system power level as well as array size and array efficiency. For purposes of this study, a range of vertical axis array sizes (horizontal diameter) and efficiencies was assumed, as illustrated in Table 3-2.

The efficiencies listed in Table 3-2 are assumed to be at the Nominal Operating Cell Temperature (NOCT). Array peak power data are based on an insolation of 1 kW/m^2 and an aperture packing factor of 0.25. The aperture packing factor is defined as the ratio between active aperture area and the total ground area swept by the array. The effects of other aperture packing factors can be assessed by calculating the equivalent efficiency of an array having the new packing factor and then interpolating the data presented in this report. For example, a 10 m diameter array having an aperture packing factor of 0.2 and operating at 15% efficiency, would have a calculated peak power output of 2.36kW. This would be equivalent to a 12% efficient, 10 m diameter array having a 0.25 aperture packing factor. While these parameters may not represent a specific array design, they were selected to provide a reasonable range of characteristics for use during the parametric analyses.

Many vertical axis array designs will likely require an auxiliary ac power supply for tracking motors and, possibly, control circuits. Power

Table 3-2

VERTICAL AXIS ARRAY PARAMETERS

Array Diameter (m)	Array[1] Efficiency (%)	Array Peak [2] Power (kW)
10	10	1.96
10	15	2.95
10	20	3.93
25	10	12.27
25	15	18.41
25	20	24.54
45	10	39.76
45	15	59.64
45	20	79.52

1) Nominal array efficiency at NOCT

2) Assumes array aperture packing factor of 0.25 and 1 kW/m^2 insolation

requirements will vary depending on array size and other design characteristics. In general, array auxiliary power requirements will be relatively small, perhaps a few amperes per array at 110 volts single phase, or 120/208 volts (or 277/480 volts) three phase.

Requirements for control wiring will also be design specific, but might consist of a twisted pair or a coaxial cable routed to each array.

Horizontal Axis Arrays. A second category of array configurations is represented by the fixed flat-plate and single axis tracking designs as illustrated in Figures 3-1(c) and 3-1(d), respectively. Since these arrays are either totally fixed (nontracking) or constrained to rotate about a single axis, there is no inherent limit to the length of an individual array structure. Individual panels can be mounted adjacent to each other on the support structure and electrically interconnected using factory installed wiring devices, as described in Ref. 3-2. This situation is analogous to the interconnection of field-installed collector panels on a carousel type array structure.

In this case, however, the length of the array is limited by the maximum number of solar cells that can be connected in series before reaching the dc system voltage level.

For example, consider a flat-plate array consisting of solar cells having a center-to-center spacing of 8 cm and connected in series along the east-west (long) axis of the array. If each cell has an NOCT maximum power point voltage of 0.45 volts the array voltage at NOCT would be 5.63 volts per meter of array length. An array operating at 1000 volts would therefore be approximately 178 meters long. Obviously, physical breaks could be

inserted in the array at selected intervals to facilitate personnel movement and array access for normal maintenance or repair work. However, a horizontal axis configuration generally results in reduced field-installed wiring requirements, especially for the dc power collection wiring, as compared to vertical axis arrays with equivalent power ratings. This is illustrated in Section 3.2.

The output power of a horizontal axis array is a function of array length, aperture width, and array efficiency. Table 3-3 presents the range of parameters used in this study for horizontal axis arrays.

The efficiencies listed in Table 3-3 are assumed to be for array operation at NOCT. The array peak power data are based on an insolation of 1 kW/m^2 and are shown in terms of kW per meter of array length. The data presented in Table 3-3 are intended to span the range of likely horizontal axis array parameters.

Although not required for fixed flat-plate arrays, single axis tracking arrays may require auxiliary ac power and control wiring, depending on design-specific array characteristics.

3.1.2 Field Layout

As mentioned, individual array dc terminals are interconnected, via field-installed wiring, in an appropriate series/parallel configuration as required to meet the dc voltage and input power ratings of the power conditioning unit (PCU).

Table 3-3

HORIZONTAL AXIS ARRAY PARAMETERS

Array[1] Width (m)	Array[2] Efficiency (%)	Array Peak[3] Power (kW/m^2)
1.2	10	0.12
1.2	13	0.16
1.2	16	0.19
2.4	10	0.24
2.4	13	0.31
2.4	16	0.38
4.8	10	0.48
4.8	13	0.62
4.8	16	0.77

1) Collector aperture width (sometimes referred to as array slant height for flat-plate arrays)

2) Nominal array efficiency at NOCT

3) Peak power per meter of array length at 1 kW/m^2 insolation

Referring to Figure 1-1, a photovoltaic power system may be discussed in the following terms:

- Branch circuits
- Array subfields
- Array field.

Branch Circuits. In many large PV systems, practical array terminal voltages (especially for vertical axis arrays) will be lower than the most economic dc system voltage. Therefore, it will be necessary to connect several sets of array dc terminals in series. A group of panels (or arrays) connected in series and operating at the nominal system dc voltage level is referred to as a branch circuit. Generic branch circuit configurations are illustrated in Figures 3-2(a) and 3-2(b) for vertical and horizontal axis arrays, respectively.

The interconnection of vertical axis arrays to form a branch circuit is illustrated schematically in Figure 3-2(a). As shown, the arrays are physically arranged in a staggered or nested configuration. This is consistent with presently proposed system designs (Ref. 3-1) and results in the most efficient land use. Spacing between arrays is primarily determined by shadowing criteria and access requirements. For purposes of this study, a nominal spacing of one meter was assumed between arrays. Vehicle access to each array is accommodated by increasing the space between adjacent branch circuits. This is discussed further under Array Subfields. The effects of array spacing on wiring subsystems designs and system economics are illustrated in Section 5.
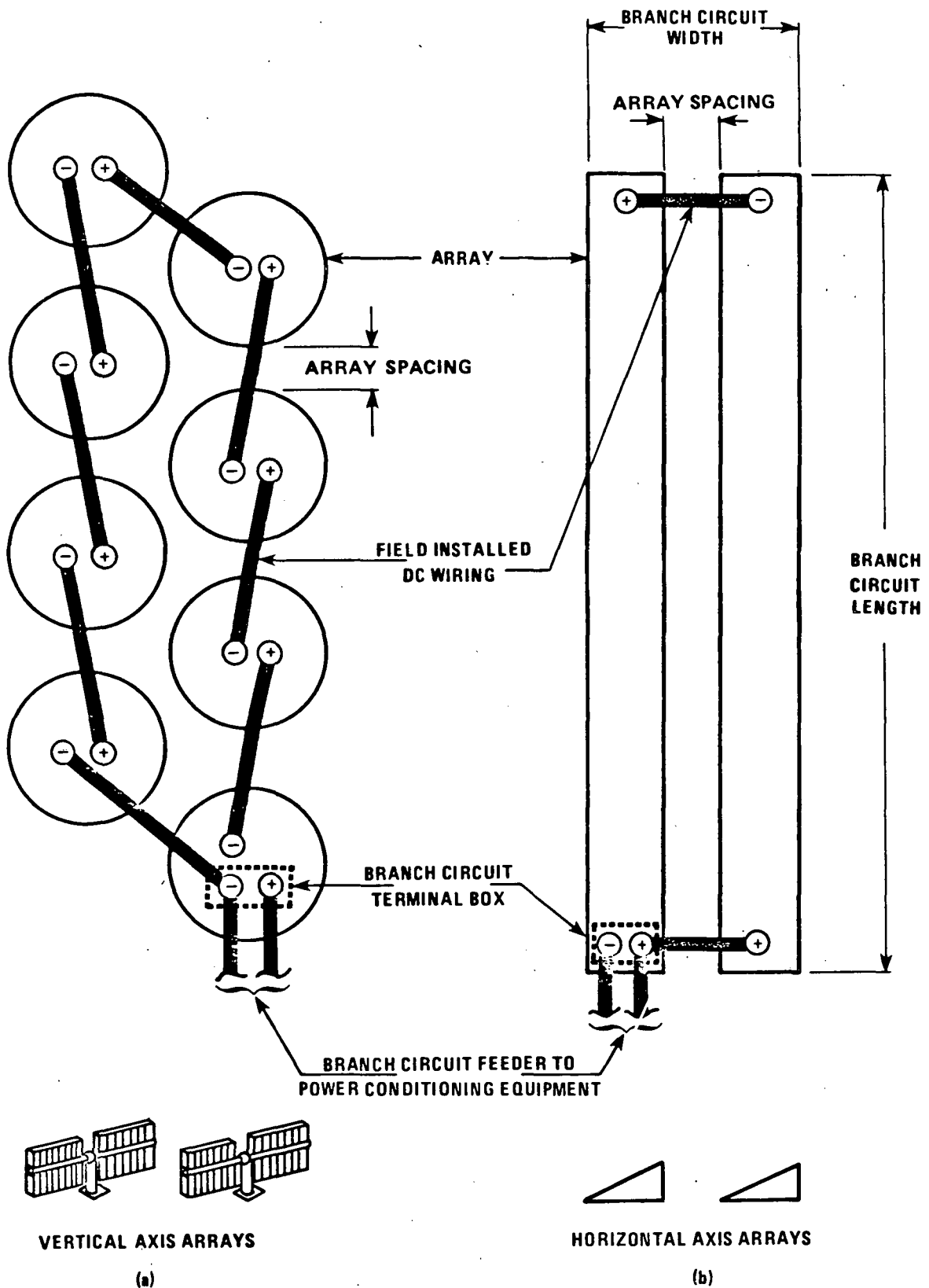
Figure 3-2 Generic Branch Circuit Configurations

The width of the branch circuit is determined by array width and array spacing, while branch circuit length is proportional to array diameter, array spacing, array voltage, and dc system voltage (i.e., the number of arrays connected in series per branch circuit).

Figure 3-2(a) also illustrates a branch circuit terminal box. This box contains the plus and minus branch circuit dc terminals as well as blocking diodes, transient surge suppressors, switches, fuses, and other equipment. This is discussed further in Section 3.2.

The horizontal axis array branch circuit configuration is illustrated in Figure 3-2(b). The solar cells are assumed to be connected in series along the long axis of the array, with one dc terminal located at each end of the array. The spacing between adjacent arrays is primarily determined by shadowing criteria. These criteria are in turn affected by site latitude, array size, and other considerations. For purposes of this study, the spacing was assumed to be 1.5 times the vertical array height, or 3 meters minimum. The effects of alternate spacings on wiring subsystems designs and system economics are discussed in Section 5. Vehicle access is again accommodated by increasing the space (if necessary) between adjacent branch circuits.

The width of a horizontal axis array branch circuit is determined by array size, tilt angle, and spacing, while the length is proportional to the dc system voltage level.

Array Subfields. The dc power outputs of individual branch circuits are collected by field-installed dc wiring (branch circuit feeders) and delivered to the power conditioning unit (PCU), as illustrated in

Figure 3-3. Branch circuits are grouped around the PCU to minimize the total lengths of the dc and other wiring subsystems. Vehicle access is accommodated by providing additional space between adjacent branch circuits (referred to in the figure as branch circuit roads), and by providing access space along the center line of the subfield (referred to in the figure as the subfield road). For this study, baseline road widths of 3 and 5 meters were assumed for the branch circuit and subfield roads, respectively.

The nominal subfield power densities obtainable for the range of array configurations and design parameters listed in Tables 3-1 and 3-2 are illustrated in Table 3-4.

Subfield peak power level is determined by the rating of the PCU. This is in turn determined by either: the system power level or, especially for the larger systems, by the effects of power level on dc power collection subystems costs. For this study, subfield peak dc power levels in the range of 0.5 to 25 MWp were evaluated.

In general, there will be a maximum practical subfield size, in terms of peak power rating. This is due to the economics of dc wiring and PCU subsystems, as well as upper limits on practical array operating dc voltage levels. The latter is a result of electrical isolation requirements placed on the solar cell encapsulation system (Ref. 3-3). This is discussed in more detail in Section 5.
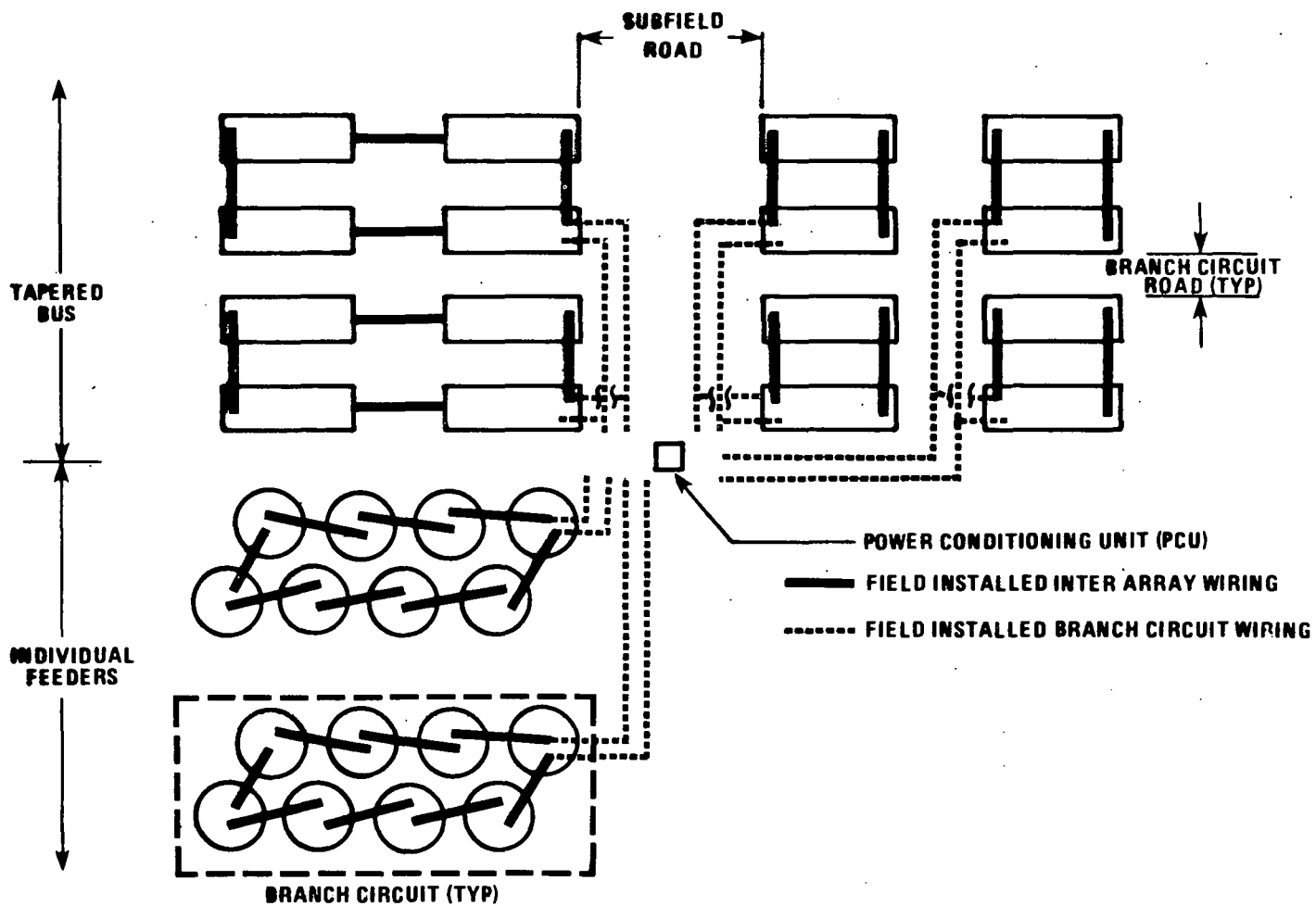
Figure 3-3 Generic Array Subfield Configurations

Table 3-4

NOMINAL SUBFIELD POWER DENSITIES

Array Type	Array[1] Size (m)	Array[2] Efficiency (%)	Subfield Power[3] Density (kWp/acre)
Vertical Axis	10	10	80
Vertical Axis	10	15	125
Vertical Axis	10	20	165
Vertical Axis	25	10	95
Vertical Axis	25	15	145
Vertical Axis	25	20	195
Vertical Axis	45	10	100
Vertical Axis	45	15	150
Vertical Axis	45	20	200
Horizontal Axis	1.2	10	120
Horizontal Axis	1.2	13	160
Horizontal Axis	1.2	16	195
Horizontal Axis	2.4	10	195
Horizontal Axis	2.4	13	255
Horizontal Axis	2.4	16	310
Horizontal Axis	4.8	10	240
Horizontal Axis	4.8	13	310
Horizontal Axis	4.8	16	385

1) Diameter for vertical axis arrays; aperture width for horizontal axis arrays

2) At NOCT

3) Based on array peak dc power output at NOCT and 1 kW/m^2 insolation

Array Field. Where PCU and PV system power ratings are equivalent, the array field and array subfield are essentially the same. If, however, the PV system power rating is higher than the practical PCU rating, the array field will consist of several array subfields. The ac power outputs of the individual PCUs are collected, via a field-installed ac power collection wiring subsytem, for delivery to the load.

The array field and any necessary control buildings, warehouses, and other support facilities comprise the photovoltaic power system.

3.1.3 Site Characteristics

Subsystem design requirements, optimum configurations, and installed costs can be affected by various site-specific conditions. These include soil and weather conditions and site latitude. For example, soil resistivity influences grounding grid design; soil density affects the cost of installation for underground wiring subsystems.

The impacts of specific site characteristics on subsystem designs and costs for each field-installed wiring subsystem is discussed in the remainder of this section where relevant.

3.1.4 Code Requirements

Various codes have been developed to ensure that electrical systems are designed and operated to provide adequate personnel and equipment safety. Although at present there are no electrical safety codes that specifically address photovoltaic power system design, it is reasonable to assume that specific PV power systems will be required to comply with the applicable provisions of locally enforced codes.

3-17

Two significant codes are discussed briefly:

- National Electric Code (NEC)
- National Electric Safety Code (NESC).

National Electric Code. The NEC (Ref. 3-4) is probably the most widely known and accepted electrical code. The code is sponsored by the National Fire Protection Association (NFPA) and is intended to be a source of advisory information for use by government and other agencies responsible for regulating the safety of electrical installations. The NEC is widely used by local inspectors and it is likely that the vast majority of commercial and industrial PV system applications will fall under its jurisdiction. Utility owned central station plants will generally not be included in this category and are discussed separately.

A comprehensive review of the NEC with regard to its impact on residential photovoltaic power systems is presented in Ref. 3-5. Based on this review, as well as in-house review of the NEC by Bechtel as a part of this and previous studies, there do not appear to be any significant restrictions or impediments with regard to the design and installation of PV power systems.

Certain specific design requirements will no doubt require further analysis and clarification. Examples of these include system grounding requirements and the use of modular, quick-disconnect type connectors for solar cell panel interconnection. These issues are beginning to receive attention by organizations such as the IEEE Standards and Coordinating Committee on Photovoltaics (Ref. 3-6). However, since they do not generally affect the design tradeoff and optimization analyses, they were not considered to be within the scope of this study.

Relevant sections of the NEC, such as maximum conductor ampacity ratings and underground conductor burial depths, were used as guidelines during the conduct of the study.

National Electric Safety Code. The NESC (Ref. 3-7) is similar to the NEC in that it provides guidelines for the practical safeguarding of equipment and personnel during the installation and operation of electrical systems. However, the NESC is principally concerned with electric supply systems used by railways, communications utilities, electric supply, and other similar utilities. Therefore, the requirements of the NESC may apply, even though central station PV power plants may not fall under the jurisdiction of the NEC.

Like the NEC, the NESC is not intended to be a system design manual, but rather to recommend minimum requirements necessary to ensure the safety of utility employees and the general public.

A brief review of the NESC did not reveal any significant impediments to the design and installation of central station PV power systems. However, this was not a comprehensive review and should not be considered conclusive.

Relevant sections of the NESC, such as high voltage overhead transmission line clearance requirements, were used as guidelines during the conduct of this study.

3.1.5   Parametric Analysis

As mentioned, identification of optimum subsystems designs requires consideration of a wide range of parameters and design alternatives.

These result from variations in array and site characteristics, as discussed in Section 3.1, as well as from the range of voltage levels, subsystem configurations, and other alternatives available to the system designer. Many of the design parameters interact strongly. For example, the optimum dc system voltage level, for a specific array configuration and subfield power level, can be determined by parametrically evaluating system design requirements for various voltage levels. One aspect of such an analysis is the determination of energy losses resulting from I^2R wiring losses at each voltage level. However, calculation of these losses involves a further tradeoff between wire size (installed cost) and the value of losses (operating cost) at each voltage level. Therefore, the selection of specific parameters for analysis, as well as the order in which the parametric analyses are performed, is critical to ensuring that the results of the study can be meaningfully applied.

The range of parameters selected for analysis in this study is presented in Figure 3-4. While this may appear to be an overwhelming effort, analyzing a range as broad as possible greatly enhances the usefulness of the results.

Several computer programs were developed to calculate field layouts, subsystem first costs, and energy (I^2R) losses. These programs are described in the following subsections, in conjunction with specific subsystems that were evaluated. Where appropriate, design alternatives, such as the use of copper versus aluminum conductors and overhead versus underground construction, were also evaluated.

SUBSYSTEM

VERTICAL AXIS		HORIZONTAL AXIS

ARRAY TYPE

10	25	45		1.2	2.4	4.8

ARRAY SIZE (M)

10	15	20		10	13	16

ARRAY EFF. (%)

DC POWER COLLECTION

50	100	250	500	750	1000		250	500	1000	2000	4000	5000

ARRAY Vmp (VOLTS)

250	500	1000	2000	3500	5000

SUBFIELD Vmp (VOLTS)

POWER CONDITIONING

500	1000	2500	5000	10000	25000

SUBFIELD Pmax (kW)

AC POWER COLLECTION

15	35	69

AC COLLECTION VOLTAGE (kv)

0.5 to 1000

FIELD POWER (MWp)

Figure 3-4 Field Layout and Wiring Subsystems Parameter Range

3.2 DC POWER COLLECTION WIRING

The dc power collection wiring subsystem provides interconnection of the field-installed solar cell panels into the desired series/parallel configuration, and delivers the PV-generated dc power to the PCU input bus. The subsystem also contains components and equipment needed to ensure equipment and personnel safety, as well as to provide the desired degree of operating and maintenance flexibility.

For many array types, it will be necessary to interconnect individual solar cell panels after installation on each array support structure. Panel interconnection methods and requirements have been investigated, primarily for flat-plate arrays, in several previous studies (e.g., Refs. 3-2 and 3-8). Results of these studies indicate that panel interconnection will likely be facilitated by the use of factory installed quick-disconnects, or other types of prefabricated terminations. These methods generally minimize the amount of additional material and labor used in the field to accomplish the panel interconnections. While these terminations are a potentially significant system cost contributor, the interconnection of panels within an individual array structure does not significantly affect the field layout and field-installed wiring subsystems tradeoff analyses. Therefore, primary emphasis was placed on the wiring and equipment necessary to connect each set of array dc power output terminals to the PCU dc power input bus.

3.2.1 Design Requirements

The primary requirement of the dc power collection subsystem is to connect the array terminals into appropriate series/parallel configurations and to collect the array dc power outputs in an efficient and cost effective

manner. The subsystem must also be designed to maintain adequate voltage isolation of all energized components, to ensure efficient operation, and to provide personnel protection.

In addition, the dc wiring subsystem is required to provide protection against transient overvoltages, overcurrents, and other potentially damaging conditions. Equipment to short circuit and/or isolate individual branch circuit terminals may also be required.

The dc wiring subsystem should also be designed to minimize interference with both normal system operation and maintenance activities (e.g., array shadowing caused by utility poles, or restricted vehicle access caused by energized overhead conductors).

To design a power wiring system, it is necessary to establish design point voltage and current levels. This enables specification of system components that will ensure both safe operation and compliance with applicable codes and standards. Identification of these parameters in most conventional applications is relatively straightforward, and is based on standardized voltage levels, load current calculations, and other criteria established by organizations such as the National Electric Code Committee. However, at the present time, the design of PV power systems is not specifically addressed by the National Electric Code or other standards. In general, no specific guidelines exist for the establishment of design voltage and current levels for PV dc wiring subsystems.

For purposes of this study, the following criteria were used to establish dc wiring subsystem design point operating parameters:

- Dc power ratings are based on array operation at NOCT and 1 kW/m^2 insolation.

- Dc voltage and current are based on array peak power point operation at NOCT and 1 kW/m^2 insolation.

As more experience is gained from the design and operation of PV power systems, it is likely that more definitive criteria will be developed.

3.2.2 Design Alternatives

Numerous alternatives can be considered with regard to dc wiring subsystem design. In addition to the selection of subfield dc voltage and power levels, design options also exist with regard to:

- Subsystem configuration

- Construction methods.

Subsystem Configuration. Several possible dc wiring subsystem configurations are illustrated in Figure 3-5. Of particular interest is the location (or absence) of the dc bus ground, as well as the quantity and configuration of blocking diodes, fuses, surge suppressors, and switches provided in the branch circuit terminal box.

An ungrounded dc bus, as illustrated in Figure 3-5(a), has the advantage that a short circuit requires two concurrent ground faults. The principal disadvantage is the possibility of static charges building up on the dc bus, resulting in dangerously high voltages to ground. Static buildup may be reduced by inherent leakage resistance or limited by surge suppressors. It is likely that large PV systems will be operated with grounded dc busses. One method of providing this ground, commonly used in existing PV system designs, is to ground one pole, as illustrated in Figure 3-5(b). While
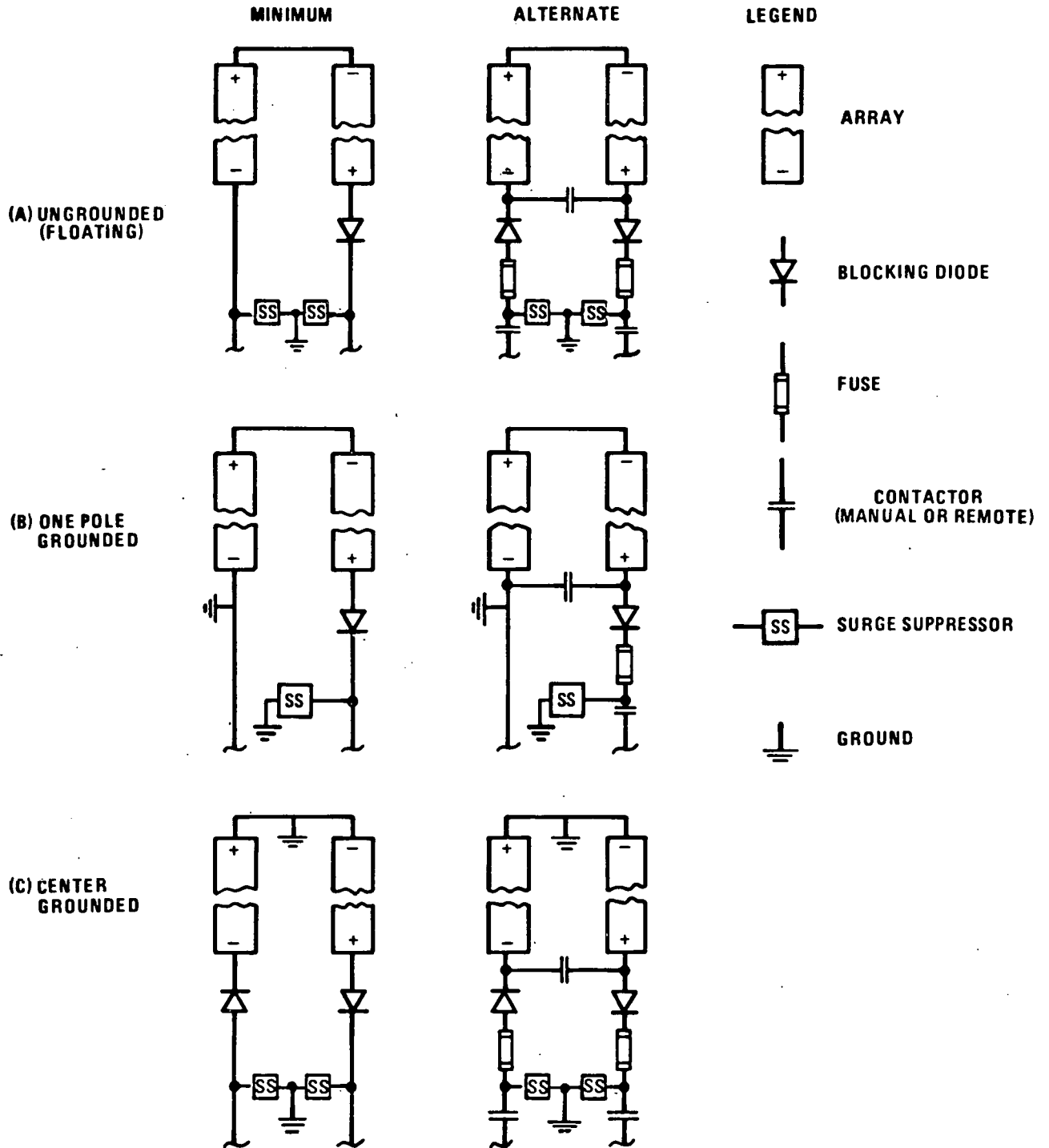
Figure 3-5 Possible DC Wiring Subsystem Configurations

this method provides a grounded bus, it has the disadvantage of causing the encapsulating system of the modules located near the opposite pole to be stressed by the full system voltage. The implications of increased electrical stress on module cost and long-time performance are discussed further in Section 5.1.2. Locating the ground at the center of the dc bus, as illustrated in Figure 3-5(c), eliminates this disadvantage by ensuring that, under normal operation, each module is stressed by not more than one half of the dc system voltage. Except for the possible implications with regard to module encapsulation requirements, the location of the dc ground does not significantly affect the results of the design tradeoff and optimization analyses reported herein.

The requirements for blocking diodes and fuses may also be affected by the location of the dc ground, and/or by system design philosophy. For example, many existing PV system designs provide fuses in series with the blocking diodes at each branch circuit, as illustrated in Figure 3-5. It would appear that such fuses are provided as a backup in the event of diode failure. Future experience may reveal this to be an unncessarily conservative design practice. However, the overall costs and, especially, the cost variations of these devices are generally not significant for the range of currents and voltages evaluated in this study.

Figure 3-5 also indicates the presence of transient surge suppressors in the branch circuit terminal box. These suppressors are provided to protect the solar cells and module encapsulation systems from potentially damaging high voltage spikes on the dc bus, resulting from lightning strikes, converter commutation failures, or other sources. While not well defined at this time, the requirements (and costs) of the surge

suppressors could be affected by dc voltage level, or other aspects of system configuration. This is discussed further in Section 3.5.

Another aspect of system design that could be affected by dc voltage level is the shorting and isolating switches, as illustrated in Figure 3-5, that are often provided in many present PV system designs. These switches are provided to facilitate maintenance and testing, while providing maximum personnel protection and operating flexibility. However, for large high power, high voltage installations the costs of such equipment could become excessive. This is illustrated in Table 3-5 (Ref. 3-9), which illustrates the costs (1978 dollars) for dc switches and contactors at various dc voltage ratings. In the interest of attaining acceptable energy costs, the need for routine array maintenance must be minimized. Therefore, the need to provide such switches at each branch circuit must be carefully assessed, especially for the larger systems. Additional operating experience is necessary to justify these needs. Perhaps other less costly methods of providing the required operating flexibility, such as mechanically removable bus links and portable grounding/shorting switches, will be acceptable.

Construction Methods. Tradeoff analyses are also required with regard to several of the more standard aspects of dc wiring design. These include:

- The number of parallel branch circuits per feeder
- The use of copper versus aluminum conductors
- The physical size of the conductor in relation to the current loading.

These factors are discussed and evaluated in subsequent subsections.

Table 3-5

DC Power Devices Survey

DISCONNECT SWITCH				CONTACTOR			
DESCRIPTION		SURVEYED SUPPLIER		DESCRIPTION		SURVEYED SUPPLIER	
MANUALLY OPERATED, NON-FUSIBLE, NON-LOAD BREAK, TWO POLE, SINGLE THROW, ENCLOSED UNIT		H.K. PORTER CO., MYERS SAFETY SWITCH CO., SQUARE D, PRINGLE, SIEMENS		CURRENT INTERRUPTING, TWO POLE, N. OPEN CONTACT, SINGLE THROW, OPEN TYPE, AC/DC OPERATED		WESTINGHOUSE, GOULD, ALLEN-BRADLEY, SQUARE D, SIEMENS	

MAX. VOLTAGE RANGE (Vdc)	AMPERE RATING (AMPS)	COST (1) PER UNIT ($)	MAX. VOLTAGE RANGE (Vdc)	AMPERE RATING (AMPS)	COST (1) PER UNIT ($)
125	15-60	20-35	125	20-45	100-235
	70-100	35-80		90-135	210-420
				15-60	190-450
250	15-60	8-15		70-100	400-500
	70-100	15-25		175-225	600-700
	175-225	28-35		250-400	800-1300
	250-400	70-80		450-600	900-1380
	450-600	100-180		800	2100
	800	250			
	1200-2000	260-350	250	1200-2000	2800-3000
440	400	98	600	15-100	230-320
				200-600	300-650
				800	900
				1200	1400
600	600	407		1600	2050
650	250	260(2)		3000	2100
				4000	2500
750	15-100	15-45			
	200-600	50-450			
	800	600			
	1200	1400			
1000	1600	1460			
	3500	2430			
	5000	3645	1000	1250	856
1300	110	110(2)			
1500	800-1200	2500-3000			
	2000-4000	3150-3480			
	6000-9000	3500-4000	1500	400	1128
4000	600	2400			
	1200	3000			
	4000	9500			

NOTES:

(1) 1978 PRICES
(2) WITHOUT ENCLOSURE

A system designer also has the option to employ either overhead or underground construction to install the dc conductors. The advantages of using overhead dc conductors might include:

- Lower first costs

- Some degree of protection for the arrays against direct lightning strikes

- Relatively easy location and repair of faults.

However, overhead dc conductors also present some potentially significant disadvantages, including:

- Clearance requirements necessary for personnel safety and vehicle access

- Possible shadowing of arrays by utility poles

- Increased susceptibility to wind, ice, and other weather damage

- Increased susceptibility to lightning strikes that may require overhead ground wires and may also increase the solar cell and module encapsulation surge protection requirements.

For locations having relatively good soil conditions (i.e., amenable to the digging of trenches), it may be cost effective to adopt the underground approach to realize its advantages.

For purposes of this evaluation, it was decided to use underground, direct buried conductors as the baseline approach. Trenching costs were based on the use of ladder-type trenching equipment and are for medium clay soil conditions. Other soil conditions might affect costs to some degree. However, it will be shown that by using this equipment the trenching costs are not a significant component of the total dc wiring subsystem costs.

Of course, extreme soil conditions, such as solid rock, could have an impact. However, the effect of these conditions on array support structure foundation costs would have more significant implications and would likely render such locations unattractive for photovoltaic power systems, especially for large systems.

3.2.3   Parametric Analyses

This subsection presents the results of parametric analyses conducted to identify first costs, I^2R energy losses, and total equivalent costs for the selected range of subsystem parameters and design alternatives.

Computer Programs. During this study, several computer programs were developed to analyze the wide range of selected parameters. These programs are reviewed here briefly.

Subfield layouts, conductor sizes, wiring first costs, and energy losses were calculated (for underground direct buried conductors) using a program referred to as Photovoltaic Layout Evaluation And Subsystem Economics (PLEASE). Figure 3-6 illustrates the output of a typical run for a vertical axis array subfield. As shown in the figure, the program permits the specification of key design parameters. The > sign is the computer prompt to enter a value for the indicated parameter and in this case does not mean greater than. Physical dimensions are expressed in meters.

The program first calculates the branch circuit dimensions and the locations of all branch circuit terminals. The latter are represented by the x and y coordinates, as shown in Figure 3-6. These coordinates are expressed in meters and are referenced to a corner of the array subfield.

ENTER 1 FOR FLAT PLATE, 2 FOR HOR. AXIS CON. , 3 FOR VERTICAL AXIS CON.? >3
 ENTER 1 FOR PARAMETRIC ANALYSIS, 2 FOR SPECIF DESIGN ANALYSISENTER ZEREO (0) TO STOP? >2
ENTER 1 FOR FIRST COSTS, 2 FOR LOSSES, 3 FOR OP. POINT MISMTCH? >1
ENTER 1 FOR COPPER CONDUCTORS, 2 FOR ALUMINUM CONDUCTORS? >1
ENTER WIRE SIZING FACTOR? >1
ENTER INTER-ARRAY WIRE STUB-UF LENGTH? >3
ENTER NUMBER OF PARALLEL BRANCH CIRCUITS PER FEEDER? >1
ENTER NAME OF INSOLATION DATA FILE? >ins
ENTER ARRAY SPACING? >1
ENTER BRANCH CIRCUIT ROAD WIDTH? >3
ENTER SUBFIELD ROAD WIDTH? >5
ENTER APETURE PACKING FACTOR?   >.25
ENTER ARRAY DIAMETER? >25
ENTER ARRAY EFFICIENCY? >15
ENTER ARRAY VOLTAGE? >250
ENTER SUBFIELD VOLTAGE? >2500
ENTER NUMBER OF BRANCH CIRCUITS PER SUBFIELD? >16

SUBFIELD LAYOUT

BC#	X-COORD.	Y-COORD.	CONN. NODE	NODE AMPS	WIRE SIZE	DISTANCE
1	129.5	35.01666	17	73.611795	4	179.54998
2	129.5	85.53332	17	73.611795	4	129.03332
3	129.5	136.04998	17	73.611795	4	78.516661
4	129.5	186.56664	17	73.611795	4	28
5	116.5	214.56664	17	73.611795	4	38
6	116.5	265.0833	17	73.611795	4	88.516659
7	116.5	315.59996	17	73.611795	4	139.03332
8	116.5	366.11662	17	73.611795	4	189.54998
9	172.5	35.01666	17	73.611795	4	197.54998
10	172.5	85.53332	17	73.611795	4	147.03332
11	172.5	136.04998	17	73.611795	4	96.516661
12	172.5	186.56664	17	73.611795	4	46
13	159.5	214.56664	17	73.611795	4	30
14	159.5	265.0833	17	73.611795	4	80.516659
15	159.5	315.59996	17	73.611795	4	131.03332
16	159.5	366.11662	17	73.611795	4	181.54998
17	142	202.06664	0	1177.7887		0

COST BREAKDOWN (DOLLARS PER SUBFIELD)

ARRAY TRENCH	FEEDER TRENCH	ARRAY CABLE	ARRAY TERMS.	FEEDER CABLE	FEEDER TERMS.	TOTAL
6656	1009.8638	12784.64	3384	9378.7404	676.79997	34682.043

DESIGN CASE SUMMARY

ARRAY DIA. (M)	ARRAY EFF. (%)	ARRAY VOLTS	SUBFD VOLTS	BRAN CKTS	POWER (KW)	COST (MILS /W)
25	15	250	2500	16	2944	12

(a) 1 BRANCH CIRCUIT PER PCU FEEDER

SUBFIELD LAYOUT

BC#	X-COORD.	Y-COORD.	CONN. NODE	NODE AMPS	WIRE SIZE	DISTANCE
1	129.5	35.01666	2	73.611795	4	50.516661
2	129.5	85.53332	3	147.22359	1/0	50.516661
3	129.5	136.04998	4	220.83539	4/0	50.516661
4	129.5	186.56664	17	294.44718	350	28
5	116.5	214.56664	17	294.44718	350	38
6	116.5	265.0833	5	220.83539	4/0	50.516659
7	116.5	315.59996	6	147.22359	1/0	50.516663
8	116.5	366.11662	7	73.611795	4	50.516659
9	172.5	35.01666	10	73.611795	4	50.516661
10	172.5	85.53332	11	147.22359	1/0	50.516661
11	172.5	136.04998	12	220.83539	4/0	50.516661
12	172.5	186.56664	17	294.44718	350	46
13	159.5	214.56664	17	294.44718	350	39
14	159.5	265.0833	13	220.83539	4/0	50.516659
15	159.5	315.59996	14	147.22359	1/0	50.516663
16	159.5	366.11662	15	73.611795	4	50.516659
17	142	202.06664	0	1177.7887		0

COST BREAKDOWN (DOLLARS PER SUBFIELD)

ARRAY TRENCH	FEEDER TRENCH	ARRAY CABLE	ARRAY TERMS.	FEEDER CABLE	FEEDER TERMS.	TOTAL
6656	1009.8638	12784.64	3384	11304.1	1938.8799	37877.483

DESIGN CASE SUMMARY

ARRAY DIA. (M)	ARRAY EFF. (%)	ARRAY VOLTS	SUBFD VOLTS	BRAN CKTS	POWER (KW)	COST (MILS /W)
25	15	250	2500	16	2944	13

(b) 4 PARALLEL BRANCH CIRCUITS PER PCU FEEDER

Figure 3-6 Typical PLEASE Output - Layout and Costs

The program then identifies the location to which each set of branch circuit dc terminals is electrically connected (connection node). This will be the PCU, if each branch circuit is wired individually, as illustrated in Figure 3-6(a). Alternately, if several branch circuits are wired in parallel, the connection point might be another branch circuit node, as illustrated in Figure 3-6(b). The program next calculates the current flowing between connection points (at rated operating conditions), sizes the wires, and calculates the physical distance between the connected points (i.e., between sets of branch circuit terminals or between the PCU and a branch circuit). The field layouts and wire routings in Figure 3-6 are shown graphically in Figure 3-7.

PLEASE uses the field layout and wire size data to calculate installed costs for the dc wiring subsystem. Unit material and installation costs used in the calculations are based on standard construction costs data references, as discussed in Section 1.4. These data were supplemented and refined using Bechtel's in-house construction costs data base.

The cost information generated by PLEASE is also illustrated in Figure 3-6. As shown, the program calculates the direct costs for trenching (and backfilling), cable, and terminations. The total cost therefore represents the direct field costs for all wire, terminations, and installation labor necessary to interconnect the individual arrays into branch circuits, and to connect the branch circuit dc power output terminals to the PCU. The total costs are also calculated and presented in terms of mills/Wp.
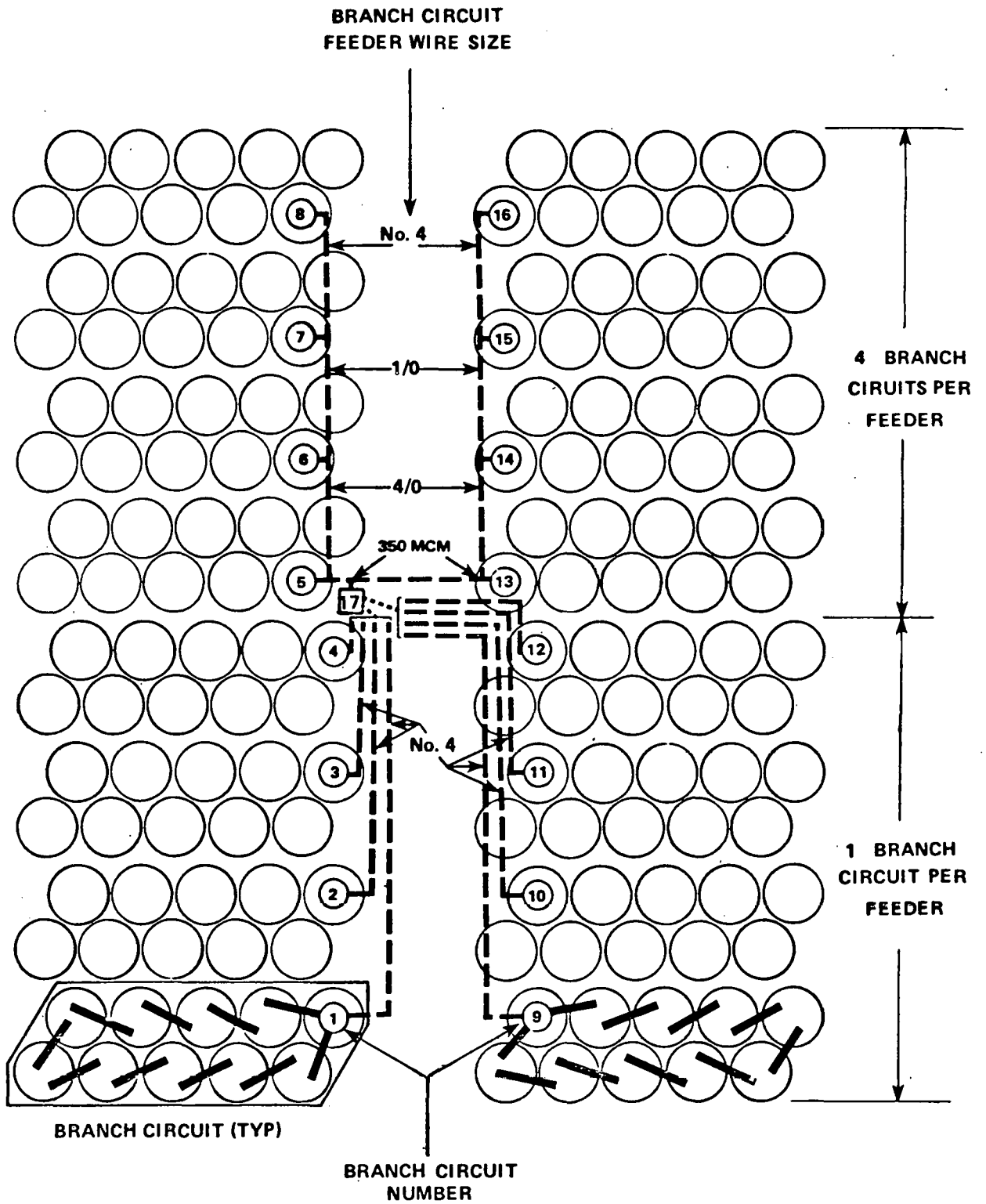
Figure 3-7 Typical PLEASE Generated Subfield Layout

By repeating this process for various combinations of subfield voltage level and number of branch circuits, a matrix of cost data can be generated spanning the desired range of subfield power and voltage levels. This is illustrated in Figure 3-8. The figure was produced using a second program called PLOT. PLOT reads the cost data generated by PLEASE for each design case analyzed. The data are sorted, formatted, and sent to a printer. PLOT also contains a curve fitting routine that converts the cost versus power data into an equivalent cost versus subfield voltage format. This is illustrated in Figure 3-9.

The process is then repeated, for different values of array voltage, to generate a family of plots representing dc wiring subsystem costs for alternate combinations of array and subfield voltage levels, at various subfield power levels.

These data are then analyzed by a third program called MINCOST. MINCOST evaluates the cost data generated by PLEASE for the specified range of array voltages, subfield voltages, and subfield power levels. MINCOST can be used to identify either the lowest cost configuration for each power level over the entire range of array and subfield voltages or the lowest cost configuration for each power level at a specified subfield voltage level. The latter is illustrated in Figure 3-10 for a 2500 volt subfield.

Finally, by repeating the analysis for other values of array size and array efficiency, as well as for copper and aluminum conductors, various wire sizing factors, and numbers of parallel branch circuits per feeder, the full range of design parameters can be evaluated. By varying other input
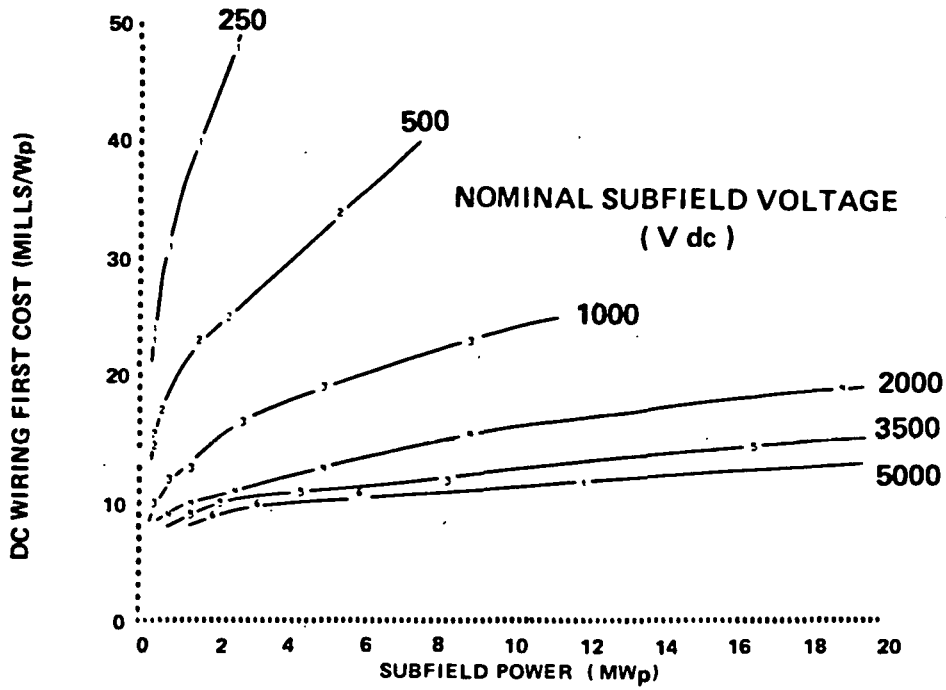
Figure 3 - 8   Typical PLOT Output - Cost versus Subfield Power
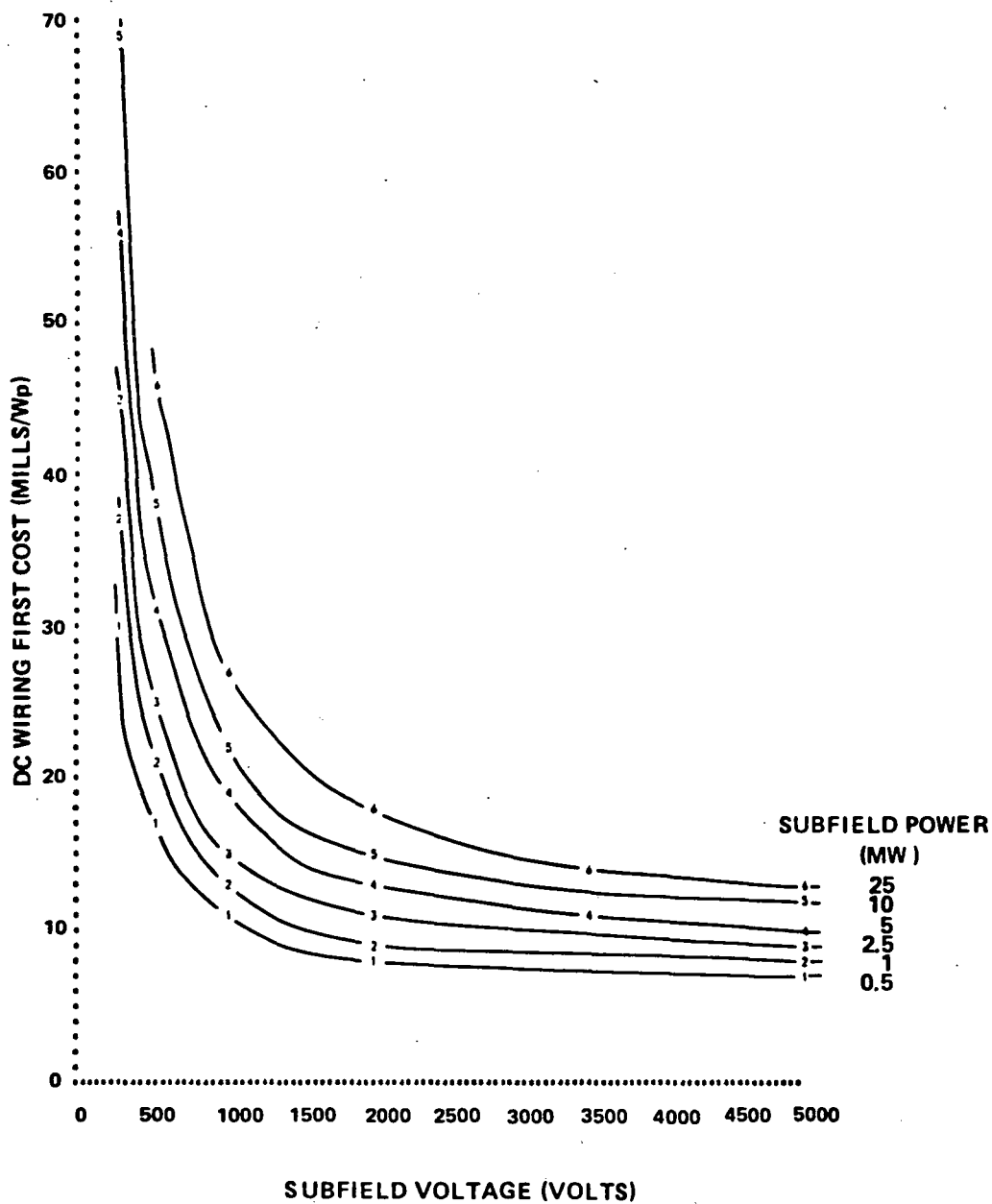
Figure 3 - 9 Typical PLOT Output - Cost Versus Subfield Voltage

```
ENTER "NONE" TO STOP? >cost1
ENTER MAX. SUBFIELD VOLTAGE (500-5000 VOLTS)? >2500

11581
ARRAY ARRAY SUBFD COND WIRE // ARRAY SUBFD COST
SIZE  EFF.  POWER TYPE SIZE BR  VOLTS VOLTS (MILLS
 (M)   (%)   (KW)       (%) CKT              /W)


25.0  15    455  CU   100   1   250  2500    7.8
25.0  15   1000  CU   100   1   250  2500    9.1
25.0  15   2200  CU   100   1   250  2500   10.6
25.0  15   4840  CU   100   1   250  2500   12.3
25.0  15  10648  CU   100   1   250  2500   14.4
25.0  15  23426  CU   100   1   250  2500   16.7
```

Figure 3-10 Typical MINCOST Output

```
ENTER 1 FOR FLAT PLATE, 2 FOR HOR. AXIS CON. , 3 FOR VERTICAL AXIS CON.? >3
 ENTER 1 FOR PARAMETRIC ANALYSIS, 2 FOR SPECIF DESIGN ANALYSISENTER ZERO (0) TO STOP? >2
ENTER 1 FOR FIRST COSTS, 2 FOR LOSSES, 3 FOR OP. POINT MISMTCH? >2
ENTER 1 FOR COPPER CONDUCTORS, 2 FOR ALUMINUM CONDUCTORS? >1
ENTER WIRE SIZING FACTOR? >1
ENTER INTER-ARRAY WIRE STUB-UP LENGTH? >3
ENTER NUMBER OF PARALLEL BRANCH CIRCUITS PER FEEDER? >1
ENTER NAME OF INSOLATION DATA FILE? >ins
ENTER ARRAY SPACING? >1
ENTER BRANCH CIRCUIT ROAD WIDTH? >3
ENTER SUBFIELD ROAD WIDTH? >5
ENTER APETURE PACKING FACTOR?   >.25
ENTER ARRAY DIAMETER? >25
ENTER ARRAY EFFICIENCY? >15
ENTER ARRAY VOLTAGE? >250
ENTER SUBFIELD VOLTAGE? >2500
ENTER NUMBER OF BRANCH CIRCUITS PER SUBFIELD? >16

ARRAY ARRAY ARRAY SUBFD POWER GROSS  TOTAL  PEAK BC PEAK FLD
DIA.  EFF. VOLTS VOLTS        ENERGY LOSSES LOSS    LOSS
 (M)  (%)                (KW) (MWH)   (%)    (%)     (%)
  25   15   250  2500    2944   311   1.1    1.7     1.4
PEAK FIELD POWER LOSS/YEARLY FIELD ENERGY LOSS= .82809299
```

Figure 3-11   Typical PLEASE Output - I^{2}R Losses

parameters, such as array spacing and road width, their effects can also be assessed.

The PLEASE program can also be used to calculate I^2R power and energy losses for each subfield configuration.

This is accomplished using the same layout and wire sizing data presented in Figure 3-6. However, rather than using this data to calculate first costs, when operating in the loss mode, PLEASE uses the data to calculate the electrical resistance between each set of connected nodes. Then, using hourly insolation data, PLEASE simulates one year of system operation. Array power levels and output currents are calculated, along with I^2R energy losses occurring between each set of connected nodes, during each hour of simulated operation. Typical results of this analysis are illustrated in Figure 3-11. As shown, the program determines the total yearly dc wiring subsystem energy loss, expressed as a percent of total array output. The peak branch circuit power loss, that is, the maximum instantaneous power loss occurring in any single branch circuit feeder, is also presented along with the peak power loss for the entire subfield dc wiring subsystem.

It can be seen that the peak power losses are larger than the yearly energy loss. This occurs because the magnitude of the loss in any system component is proportional to that component's electrical resistance and the square of the load current. Component resistance is essentially constant, being determined during initial system design. The magnitude of the load current, however, varies both hourly and seasonally in proportion to insolation. The peak power loss for any system design occurs at the time of maximum insolation and, hence, maximum current. Energy loss at a specific power level is

3-38

proportional to the square of the ratio between the magnitudes of the operating and peak power point currents. For example, losses at one half peak rated power output are 25% of those at full rated output. The energy loss on a yearly basis is determined by integrating the instantaneous power loss over the yearly operating cycle.

During the course of these evaluations, it was observed that for a specific yearly insolation profile the ratio between peak field power loss and yearly energy loss is essentially constant. Therefore, once this ratio has been determined for a given profile (e.g., the typical yearly direct normal insolation profile in Albuquerque), energy losses for any specific subfield layout and wiring design can be evaluated by simply calculating the peak field power loss.

To simplify the analysis of dc wiring subsystems, losses were determined using theoretical (per ASHRAE) insolation data representing 12 days (the 15th day of each month) of operation, calculated for a site latitude of 35°.

Results of the parametric analyses are presented in the next two subsections, for vertical and horizontal axis arrays, respectively. The baseline data are for subsystems designed to meet the following criteria:

- Costs are based on underground (direct buried) copper conductors.

- Conductors are sized for 100% loading, as allowed by the National Electric Code (1978), based on array peak power output.

- One branch circuit per converter feeder.

This was done to simplify the presentation and to minimize obscuring of

significant cost drivers (e.g., subfield voltage and power levels).

The effects of secondary parameters, are then discussed including:

- Copper versus aluminum conductors
- Conductor size versus peak current
- Number of parallel branch circuits per converter feeder.

Unless otherwise indicated, all first costs are presented in terms of 1980 dollars and include material and installation labor for all field-installed dc wire and terminations. The economic values of I^2R energy losses are based on equivalent area related replacement costs of $1.00/Wp (1980$), as discussed in Section 1.4.

Vertical Axis Array Subfields. For a specific vertical axis array size and efficiency, array dc terminal voltage affects the design of the dc wiring system by determining the nominal array dc output current; and, for a given system dc voltage, determining the number of series-connected arrays required to form a branch circuit. The effect of these factors on dc wiring subsystem first costs is illustrated in Figure 3-12 for a 5000 kWp subfield composed of 25m diameter, 15% efficient vertical axis arrays. As shown in the figure, for subfield voltages in the range of 500-5000 Vdc, minimum costs are obtained for an array terminal voltage of about 250 Vdc. Optimum voltages for the three vertical axis array sizes evaluated in this study are summarized in Table 3-6.
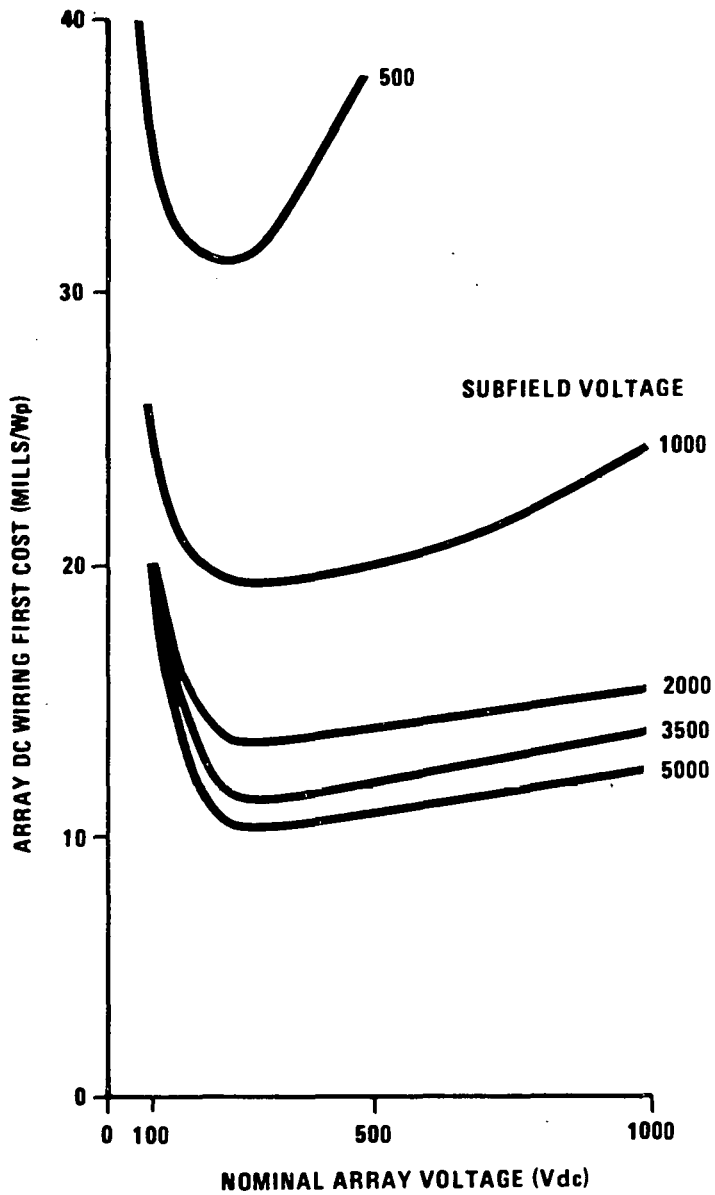
ARRAY DC WIRING FIRST COST (MILLS/Wp)

40

500

30

SUBFIELD VOLTAGE

1000

20

2000

3500

5000

10

0

0 100   500   1000

NOMINAL ARRAY VOLTAGE (Vdc)

COSTS INCLUDE MATERIAL AND
INSTALLATION LABOR FOR ALL FIELD
INSTALLED DC WIRE AND CORRESPONDING
TERMINATIONS

- 25 METER DIAMETER ARRAY NOMINAL 15 %
  EFFICIENCY (NOMINAL ARRAY PEAK
  POWER = 18 KW)

- 5000 KWp SUBFIELD

- COSTS ARE BASED ON UNDERGROUND DIRECT
  BURIED COPPER CONDUCTORS

- CONDUCTORS ARE SIZED FOR 100% LOADING,
  AS ALLOWED BY THE NATIONAL ELECTRIC
  CODE, BASED ON ARRAY PEAK POWER OUTPUT

- 1 BRANCH CIRCUIT PER CONVERTER FEEDER

Figure 3-12 Dc Wiring Costs Versus Vertical Axis Array Voltage

Table 3-6

OPTIMUM VERTICAL AXIS ARRAY VOLTAGES

Array Diameter (m)	Array Voltage (Vdc)
10	100
25	250
45	500

In addition to array size, array efficiency also influences optimum array voltage, with increasing efficiency tending to favor slightly higher voltage levels. However, unless otherwise indicated, the remainder of data presented in this subsection are based on the array voltages listed in Table 3-6.

First costs and I^2R energy losses for 25m diameter, 15% efficient vertical axis array subfields are presented in Figure 3-13, as a function of subfield voltage, for various subfield power levels. As shown, both costs and losses decrease with increasing voltage. However, the rate of decrease becomes relatively small for voltage levels above about 1000-2000 Vdc. It can also be seen that for a specific subfield voltage level, costs and losses increase with increasing subfield peak power level. This occurs because, as branch circuits are added to increase the subfield power level, their dc terminals are located farther and farther from the PCU. Therefore, although the power output of each additional branch circuit is the same as the last, branch circuit feeders become longer, thereby increasing the marginal cost of addition. This effect can be ameliorated, to some extent, by increasing the subfield dc voltage level.
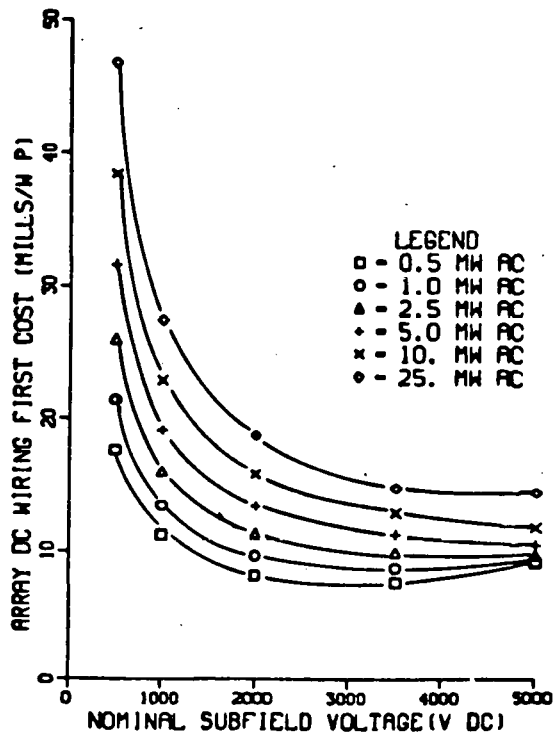
(a) FIRST COSTS
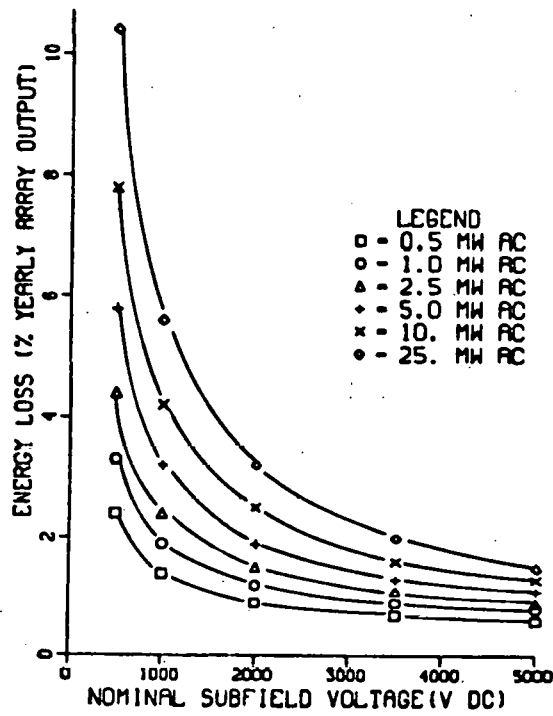
(b) ENERGY LOSSES

Figure 3-13 Vertical Axis Array Dc Wiring First Costs and I^2R Energy Losses - 25 Meter Diameter, 15 Percent Efficiency

3-43

As might be expected, in terms of dc wiring subsystem costs, larger subfields tend to favor somewhat higher voltage levels. However, selection of optimum dc subfield voltage requires consideration of other factors, including power conditioner and module encapsulation system costs. This is discussed further in Section 5.

Total equivalent costs (first costs plus the equivalent value of the I^2R energy losses) are presented in Figure 3-14 for 25m diameter arrays operating at efficiencies of 10, 15 and 20 percent.

First costs and I^2R energy losses for 10m diameter - 15% efficient arrays are presented in Figure 3-15. Figure 3-16 presents total equivalent costs for 10m diameter arrays operating at efficiencies of 10, 15, and 20%. First costs and I^2R energy losses, as well as total equivalent costs for 45m diameter arrays, are presented in Figures 3-17 and 3-18, respectively.

The breakdown of dc wiring first costs components, in terms of percent contribution for cable trench, inter-array wiring and terminations, and converter feeder cable and terminations is illustrated in Figure 3-19. The data are for 25m diameter, 15% efficient vertical axis arrays.

Horizontal Axis Array Subfields. As discussed in Section 3.1.1, horizontal axis array voltage is generally not constrained by inherent array design characteristics and is proportional to array length. Therefore, array voltage can be specified by the system designer to meet specific system requirements. For purposes of this study, horizontal axis array voltages were set at one half of the subfield dc voltage level. Branch circuits consist of two arrays, wired in series, as illustrated in Figure 3-2.
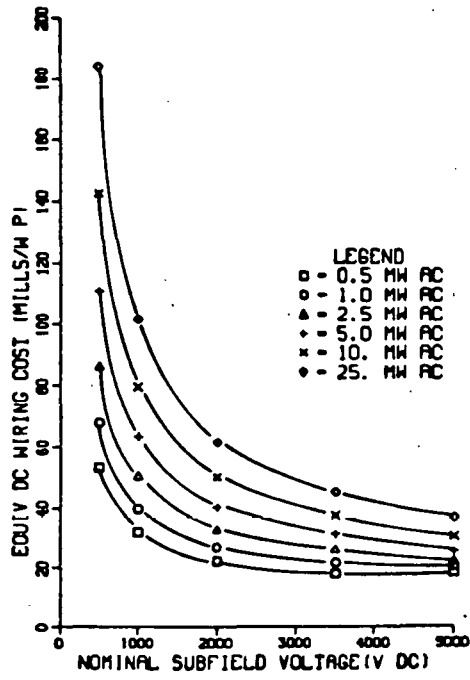
(a) 10 PERCENT EFFICIENCY
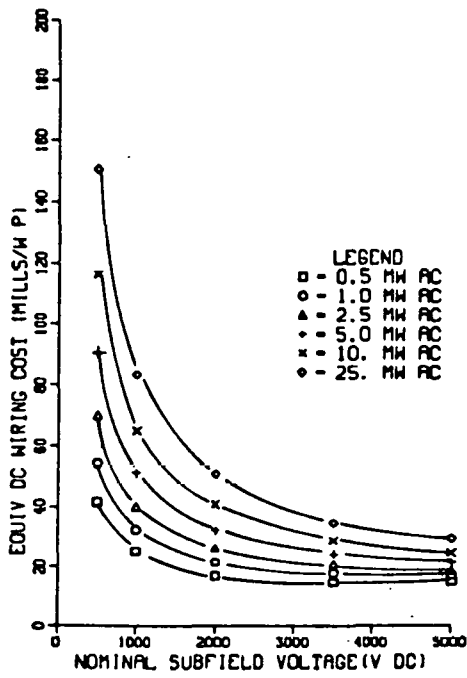
(b) 15 PERCENT EFFICIENCY
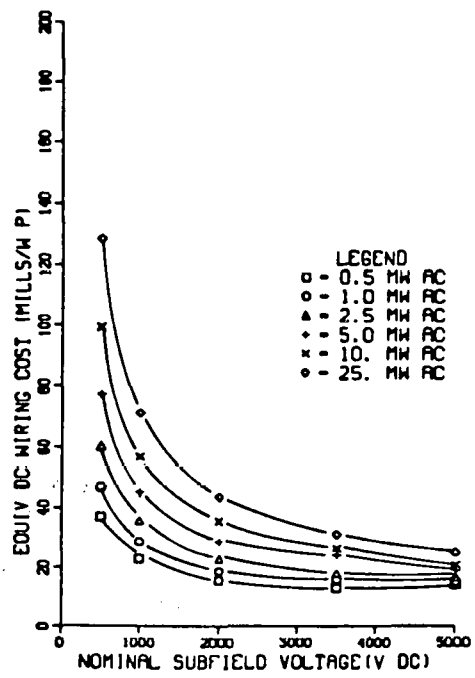
(c) 20 PERCENT EFFICIENCY

Figure 3-14 Vertical Axis Dc Wiring Equivalent Costs - 25 Meter Diameter
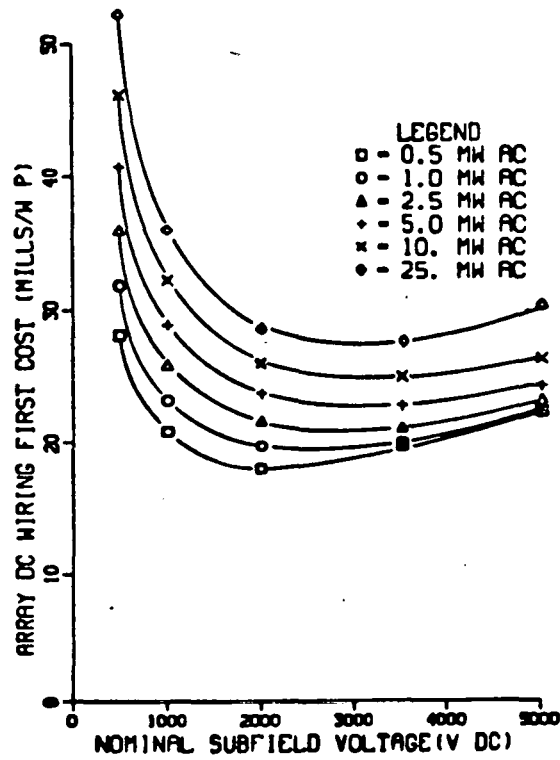
(a) FIRST COSTS
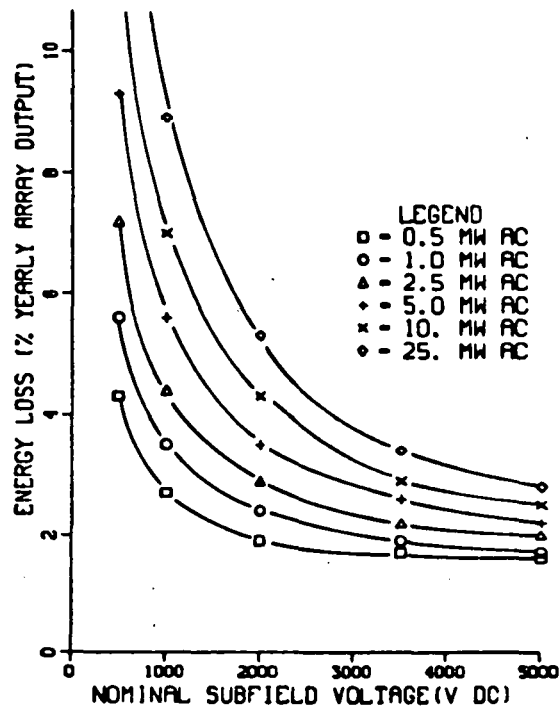
(b) ENERGY LOSSES

Figure 3-15 Vertical Axis Array Dc Wiring First Costs and I^2R Energy Losses - 10 Meter Diameter, 15 Percent Efficiency

3-46
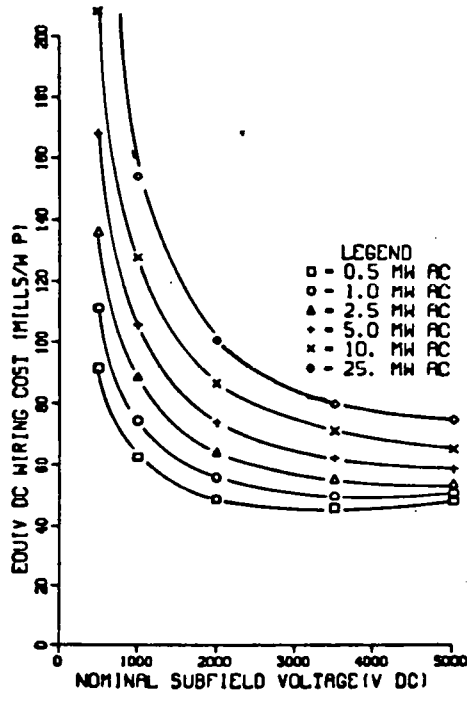
(a) 10 PERCENT EFFICIENCY
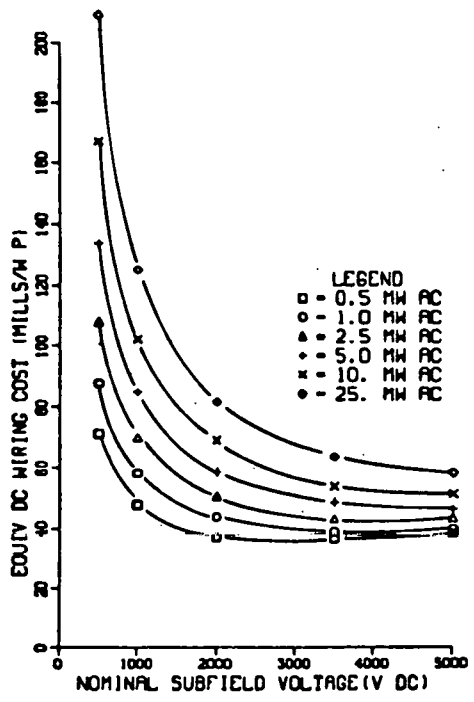
(b) 15 PERCENT EFFICIENCY
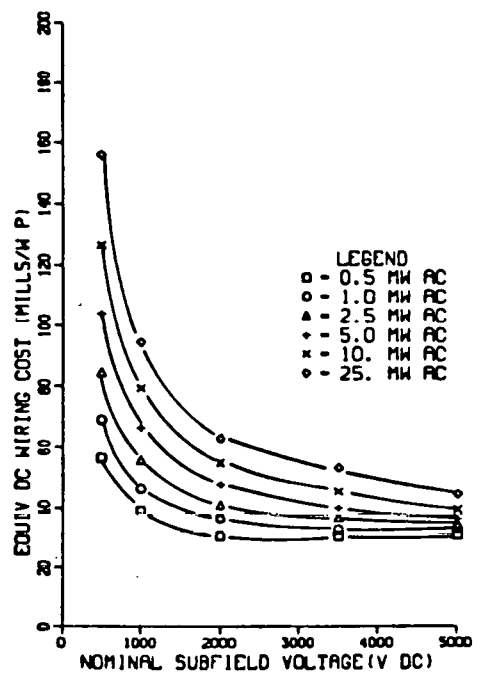
(c) 20 PERCENT EFFICIENCY

Figure 3-16 Vertical Axis Array Dc Wiring Equivalent Costs - 10 Meter Diameter

3-47
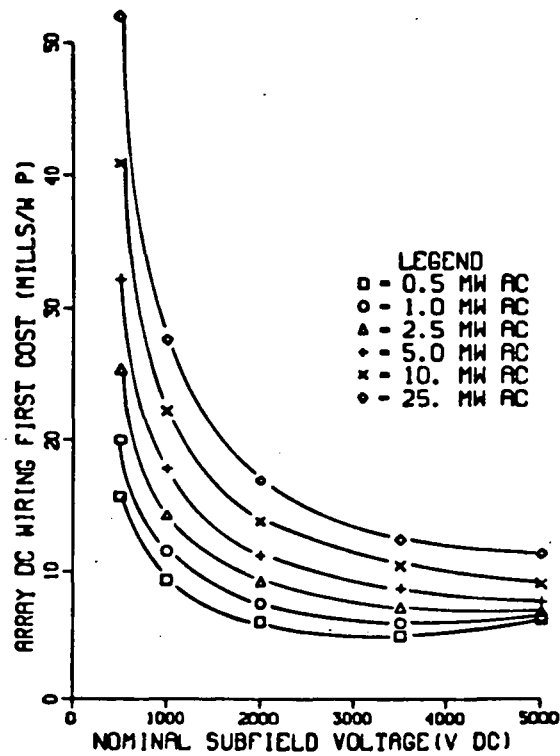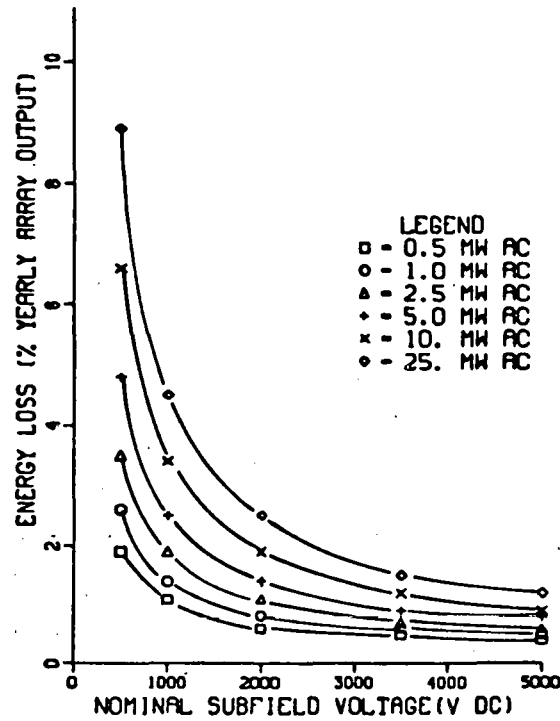
(a) FIRST COSTS

(b) ENERGY LOSSES

Figure 3-17 Vertical Axis Array Dc Wiring First Costs and I^2R Energy Losses - 45 Meter Diameter, 15 Percent Efficiency
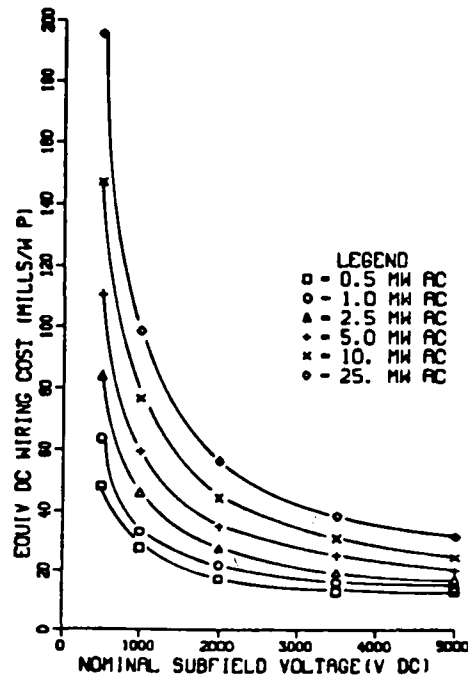
(a) 10 PERCENT EFFICIENCY
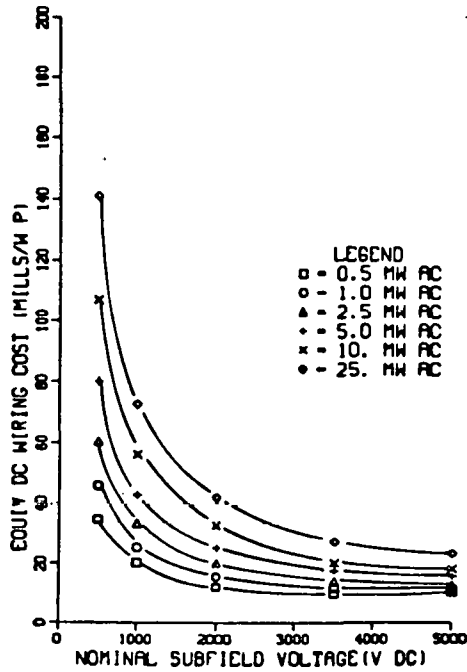
(b) 15 PERCENT EFFICIENCY
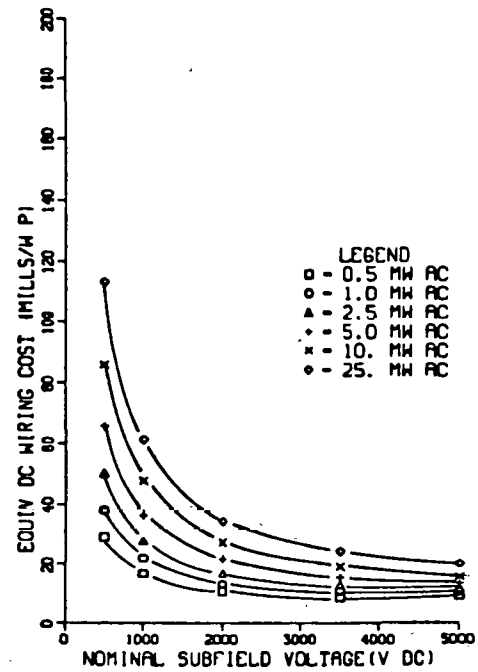
(c) 20 PERCENT EFFICIENCY

Figure 3-18 Vertical Axis Array Dc Wiring Equivalent Costs - 45 Meter Diameter
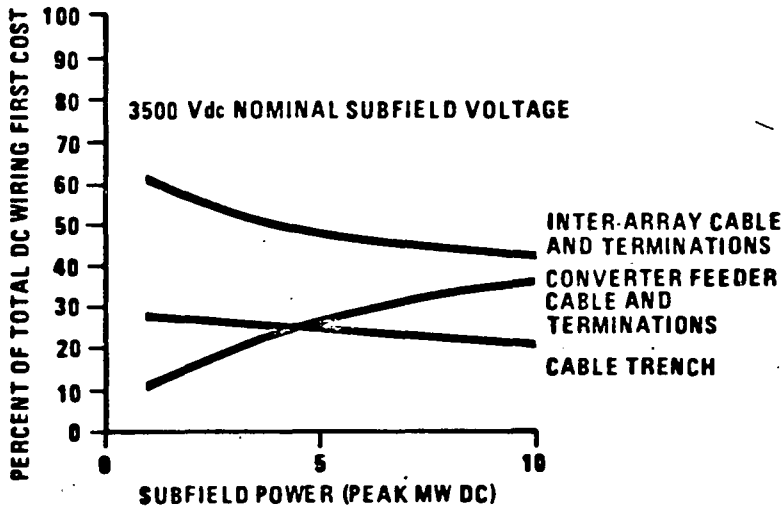
(a)

- COSTS INCLUDE MATERIAL AND INSTALLATION LABOR FOR ALL FIELD INSTALLED DC WIRE AND CORRESPONDING TERMINATIONS

- 25 METER DIAMETER ARRAY NOMINAL 15% EFFICIENCY (NOMINAL ARRAY PEAK POWER = 18 KW)

- COSTS ARE BASED ON UNDERGROUND, DIRECT BURIED COPPER-CONDUCTORS

- CONDUCTORS ARE SIZED FOR 100% LOADING, AS ALLOWED BY THE NATIONAL ELECTRIC CODE, BASED ON ARRAY PEAK POWER OUTPUT

- 1 BRANCH CIRCUIT PER CONVERTER FEEDER
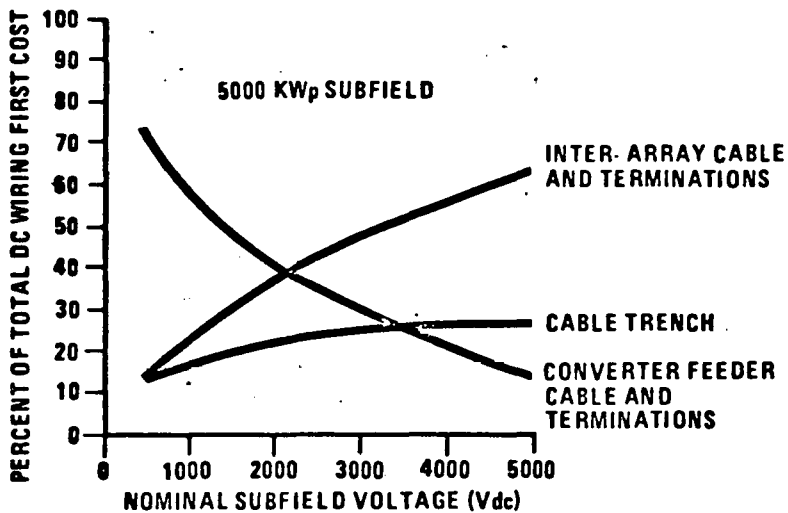
(b)

Figure 3-19 Vertical Axis Array DC Wiring First Cost Breakdown

Subfield voltages in the range of 500 to 5000 Vdc (array voltages of 250-2500 Vdc) result in array lengths in the range of 44 to 444m.

First costs and I^2R energy losses for 2.4m slant height, 13% efficient horizontal axis array subfields are presented in Figure 3-20, as a function of subfield voltage, for various subfield power levels. In general, the trends are the same as observed for the vertical axis subfields. However, both first costs and losses tend to be lower when compared to equivalent size (power) vertical axis array subfields. This is a direct result of the decreased quantity of field-installed wiring necessary to series connect individual horizontal axis arrays into branch circuits. Also, the knees of the curves tend to occur at somewhat lower subfield voltages.

Total equivalent costs (first costs plus the equivalent value of the I^2R energy losses) are presented in Figure 3-21 for 2.4m slant height arrays operating at 10, 13, and 16 % efficiencies.

First costs and I^2R energy losses for 1.2m slant height, 15% efficiency arrays are presented in Figure 3-22. Figure 3-23 presents total equivalent costs for 1.2m slant height arrays operating at efficiencies of 10, 13, and 16%. First costs and losses, as well as total equivalent costs for 4.8m slant height arrays, are presented in Figures 3-24 and 3-25, respectively.

Copper versus Aluminum Conductors. Both copper and aluminum conductors are commonly used in commercial, industrial, and utility power system applications, particularly at voltage levels above 600 volts. Although copper is a somewhat better conductor than aluminum, thereby requiring
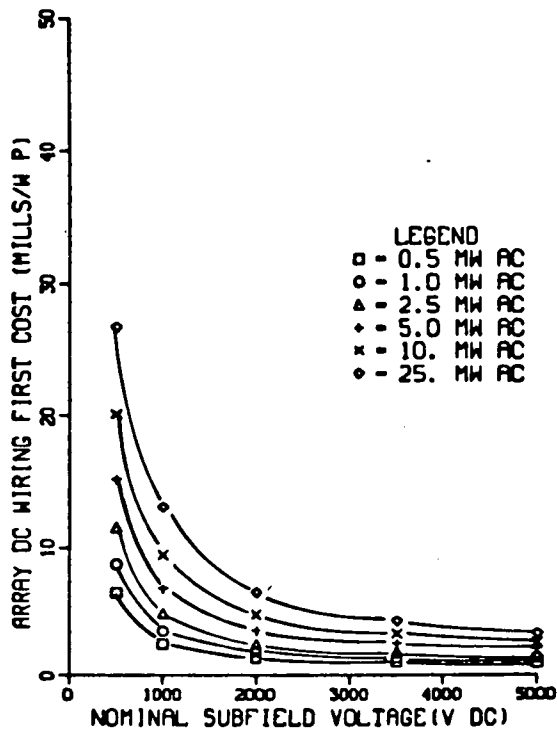
(a) FIRST COSTS
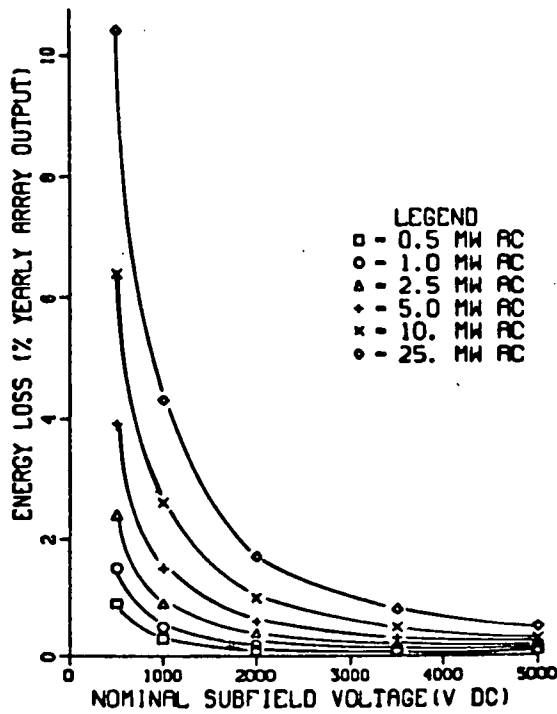
(b) ENERGY LOSSES

Figure 3-20 Horizontal Axis Array Dc Wiring First Costs and I^2R Energy Losses - 2.4 Meter Aperture Width, 13 Percent Efficiency
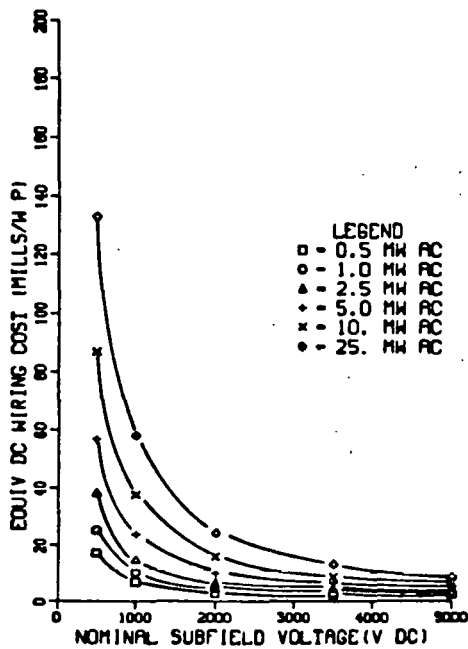
(a) 10 PERCENT EFFICIENCY
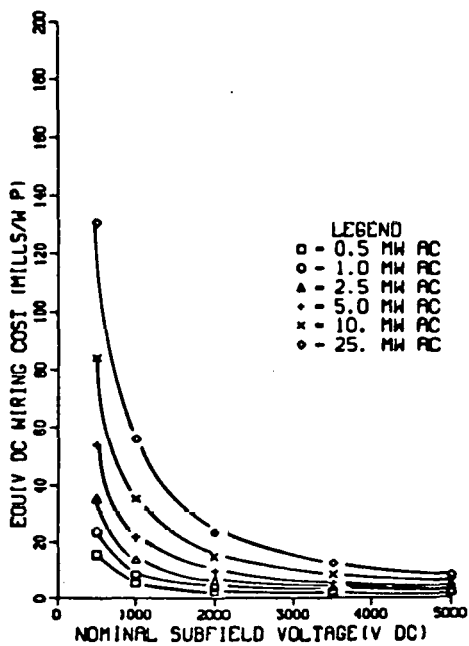
(b) 13 PERCENT EFFICIENCY
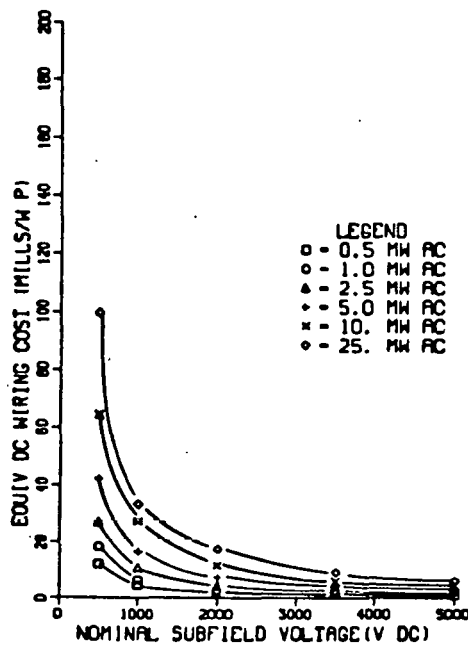
(c) 16 PERCENT EFFICIENCY

Figure 3-21 Horizontal Axis Array Dc Wiring Equivalent Costs - 2.4 Meter Aperture Width
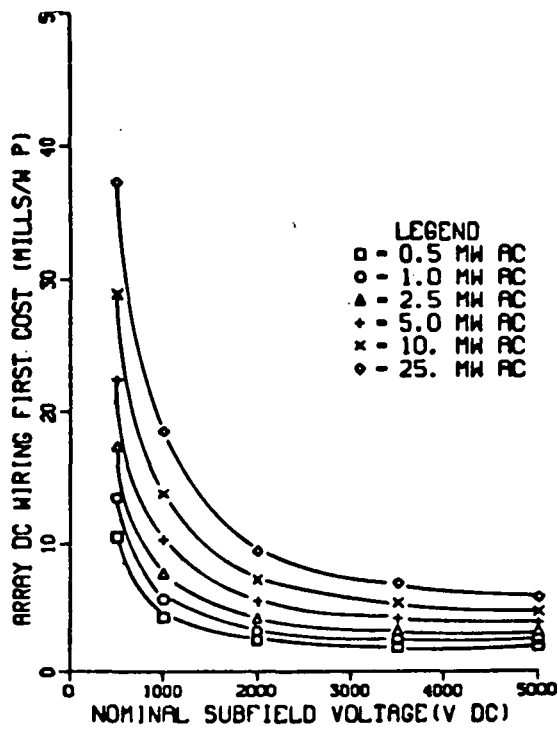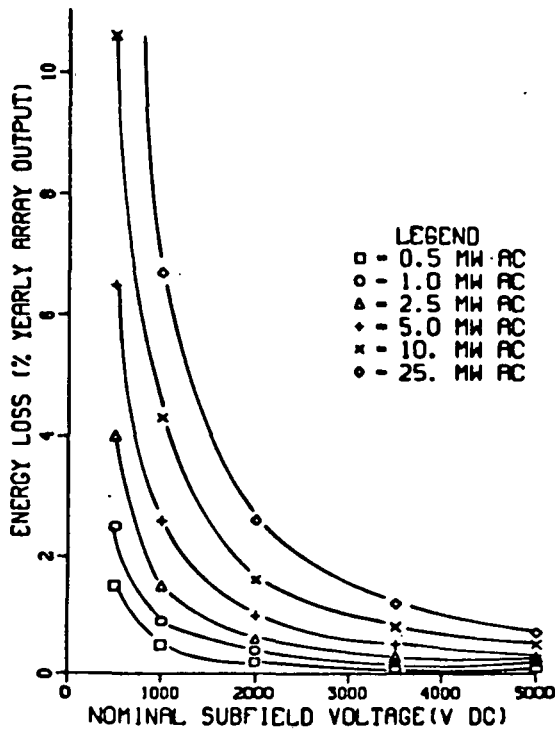
(a) FIRST COSTS

(b) ENERGY LOSSES

Figure 3-22 Horizontal Axis Array Dc Wiring First Costs and I^2R Energy Losses - 1.2 Meter Aperture Width, 13 Percent Efficiency
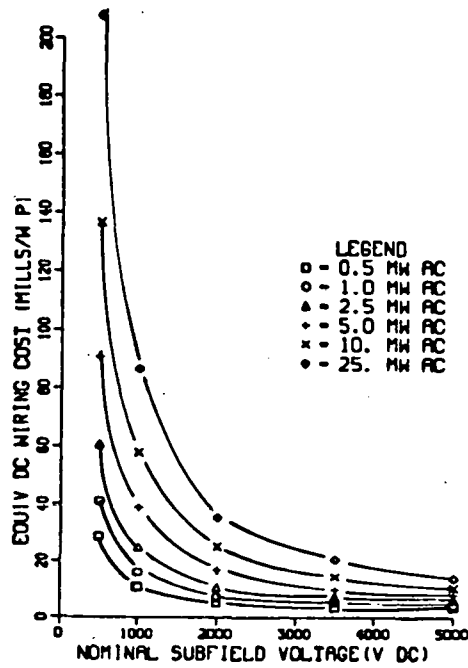
(a) 10 PERCENT EFFICIENCY
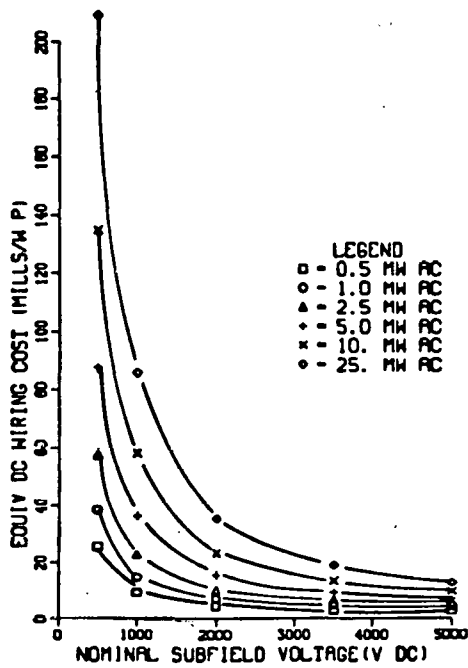
(b) 13 PERCENT EFFICIENCY
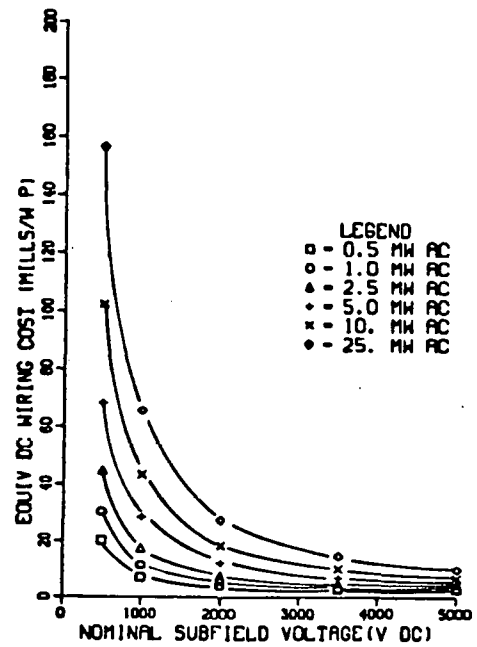
(c) 16 PERCENT EFFICIENCY

Figure 3-23 Horizontal Axis Array Dc Wiring Equivalent Costs - 1.2 Meter Aperture Width
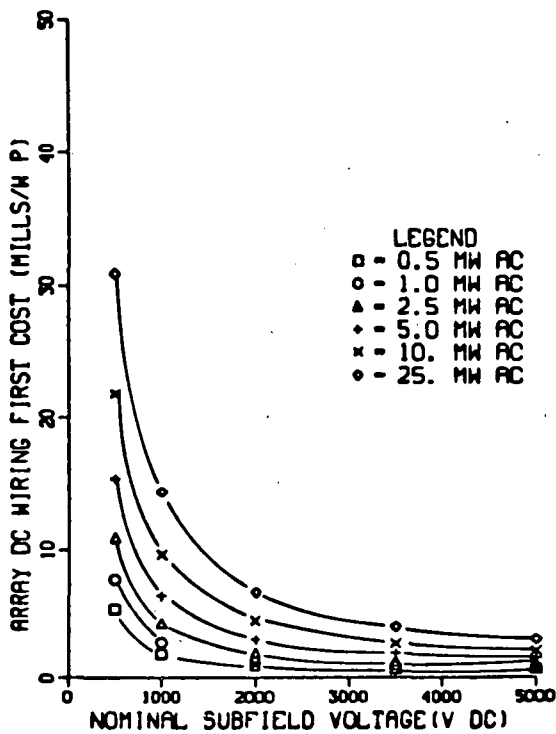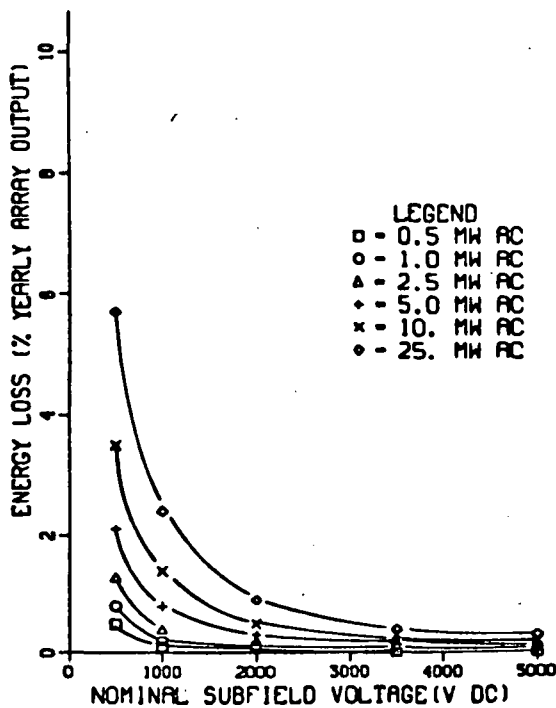
(a) FIRST COSTS

(b) ENERGY LOSSES

Figure 3-24 Horizontal Axis Array Dc Wiring First Costs and I^2R Energy Losses - 4.8 Meter Aperture Width, 13 Percent Efficiency
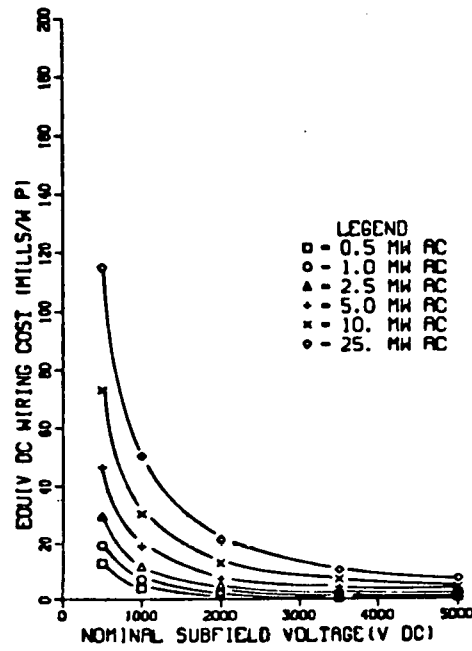
(a) 10 PERCENT EFFICIENCY
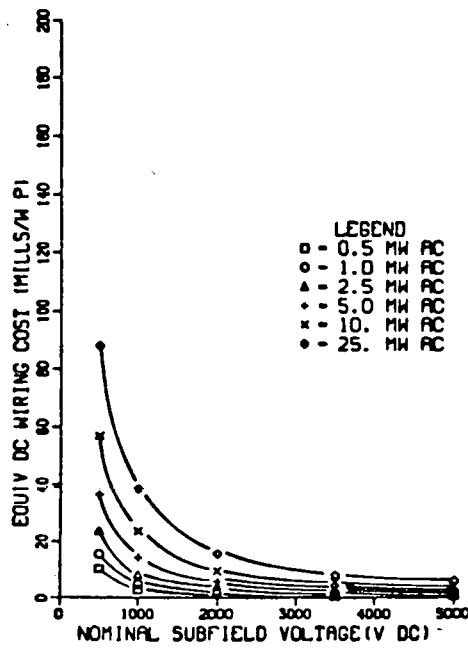
(b) 13 PERCENT EFFICIENCY
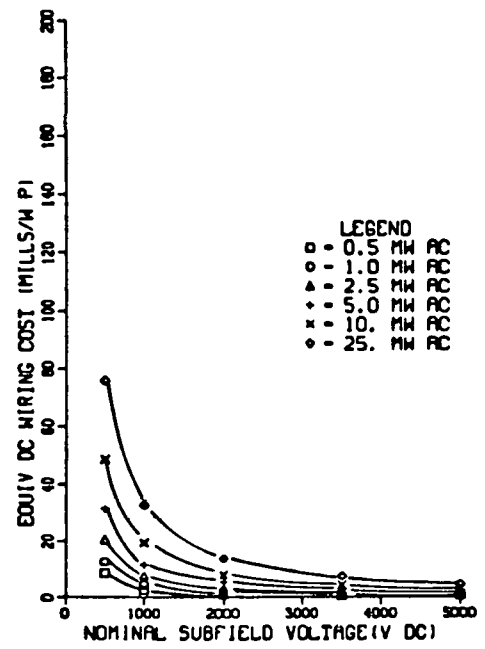
(c) 16 PERCENT EFFICIENCY

Figure 3-25 Horizontal Axis Array Dc Wiring Equivalent Costs - 4.8 Meter Aperture Width

larger aluminum conductors than equivalently rated copper conductors, circuits using aluminum conductors generally result in lower installed costs. This is due to the cost differential between copper and aluminum. Therefore, the results of any installed cost comparison are dependent on the relative costs of the materials at the time of the evaluation. The costs of aluminum cable (material only) used in this study ranged from approximately 1/2 to 1/4 of the costs for equivalent physically sized copper cables. For example, the costs for 600 Vac, #4 AWG single conductors were $1,200 and $425/1000m for copper and aluminum conductors, respectively.

However, I^2R energy losses for aluminum conductor circuits can be slightly larger than those for copper conductor circuits of equivalent current carrying capacity. Therefore, on a life cycle costs basis, the selection of optimum conductor type should consider both the first costs, at the time of installation, and the value of the energy losses.

First costs, I^2R energy losses, and total equivalent costs are presented in Figures 3-26 (a), (b), and (c), respectively, for a 5000 kWp subfield consisting of 25m diameter -15% efficient vertical axis arrays using both copper and aluminum conductors. Figure 3-26(a) indicates that aluminum conductors result in slightly lower first costs for subfield voltages in the range of 500 to 5,000 Vdc. However, Figure 3-26(b) indicates that I^2R energy losses are slightly lower for the copper conductors over the same subfield voltage range. A comparison of total equivalent costs, illustrated in Figure 3-26(c), reveals that for this example there are no significant economic differences between the two options.
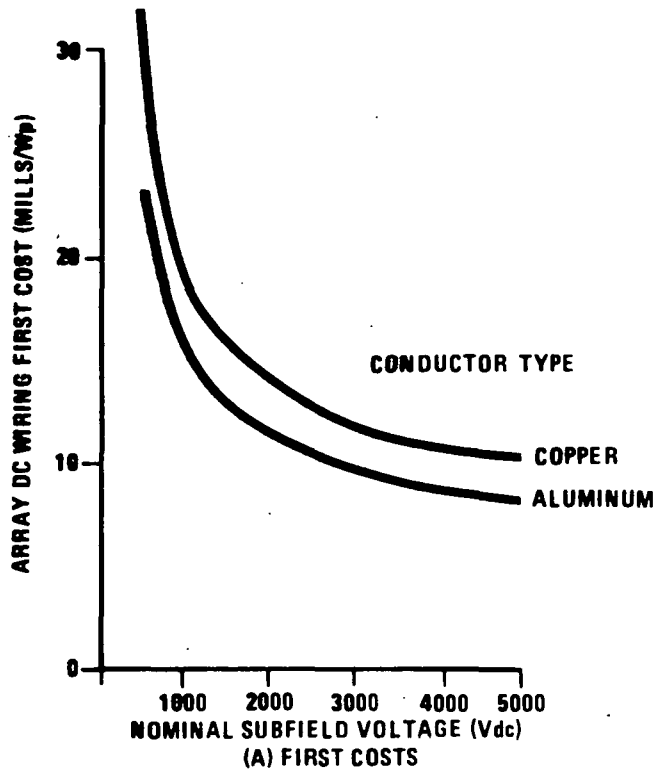
- 25 METER DIAMETER ARRAY NOMINAL 15 % EFFICIENCY (NOMINAL ARRAY PEAK POWER = 18 KW)

- 5000 KWp SUBFIELD

- COSTS ARE BASED ON UNDERGROUND, DIRECT BURIED CONDUCTORS

- CONDUCTORS ARE SIZED FOR 100% LOADING, AS ALLOWED BY THE NATIONAL ELECTRIC CODE, BASED ON ARRAY PEAK POWER OUTPUT

- 1 BRANCH CIRCUIT PER CONVERTER FEEDER
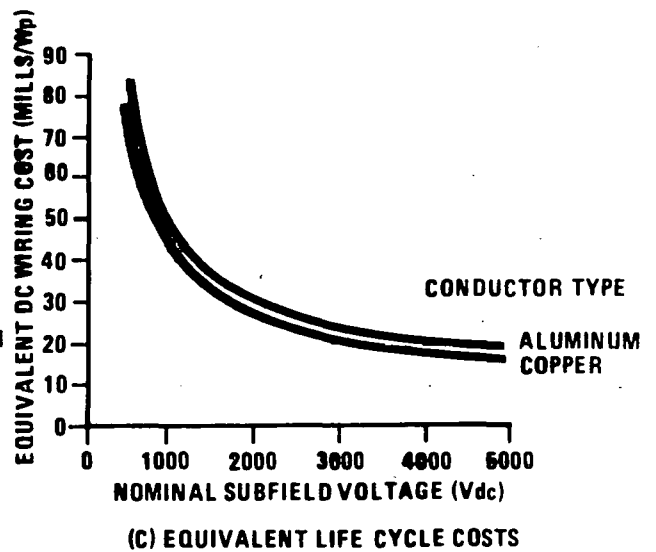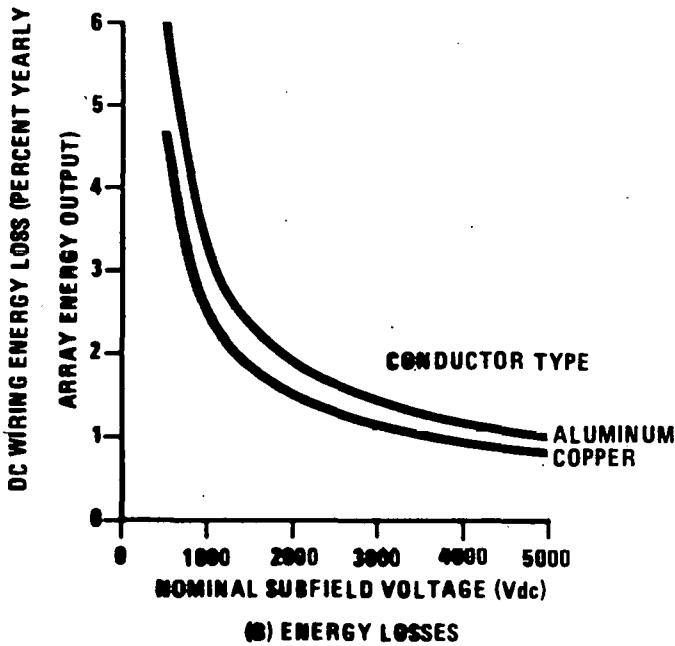
Figure 3-26 Effect of Conductor Type on DC Wiring Costs and I^2R Energy Losses

Of course, changes in array type, array efficiency, the value of the energy losses, or the relative costs of copper and aluminum could result in a more clear-cut advantage for one or the other of the conductor types. This demonstrates the need to perform this type of tradeoff analysis during the detailed design of specific PV systems.

Conductor Size. A similar tradeoff between first costs and energy losses can be made with regard to the size of the conductor selected and the peak operating current of the circuit. For example, installing oversized conductors increases the first costs of the installation but reduces the I^2R energy losses. This tradeoff is illustrated in Figure 3-27, for a 5000 kWp subfield consisting of 25m diameter, 15% efficient vertical axis arrays, using copper conductors. Figure 3-27(a) presents first costs as a function of subfield dc voltage for several conductor loading factors. The loading factor is defined as the ratio between the actual peak operating current and the maximum full load current allowed by the National Electric Code (NEC). For example, a loading factor of 75% indicates that the conductor will not be loaded to more than 75% of its rated full load current, and is therefore oversized with regard to compliance with the code. As indicated in Figure 3-27(a) and (b), oversized conductors result in higher first costs, but reduced I^2R energy losses. Total equivalent costs are compared in Figure 3-27(c), which shows that using a 75% loading factor results in a slight economic advantage. Figure 3-28 presents the results of this trade-off for horizontal axis arrays. An economic advantage for oversizing conductors is indicated but it is not significant within the accuracy of the study. Similar results are observed for aluminum conductors, as well as for other array types and efficiencies. Again, changes in study parameters
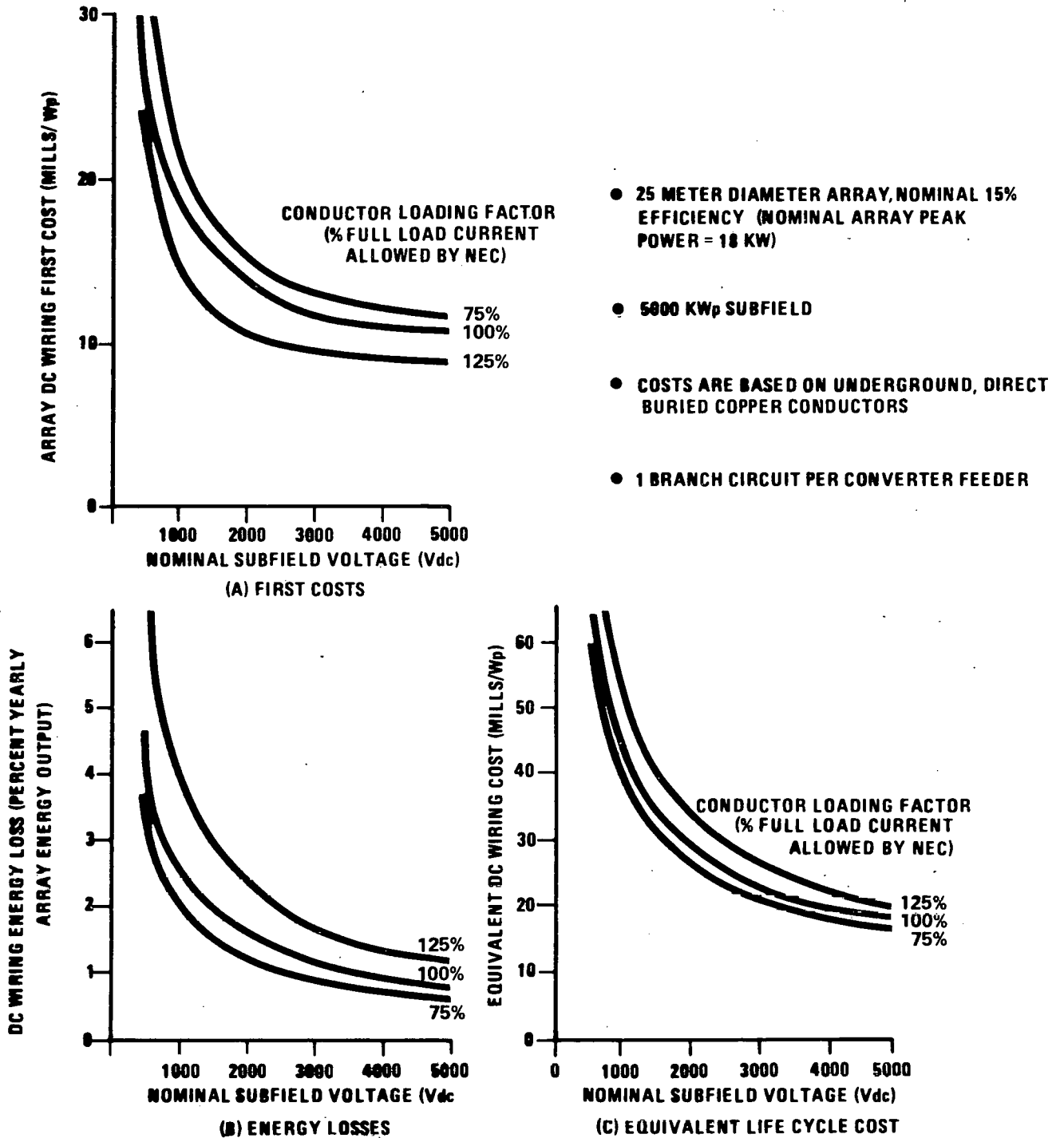
Figure 3-27 Effect of Wire Size on Dc Wiring Costs and I²R Energy Losses
for Vertical Axis Arrays

.(particularly the value of the energy losses) can affect the optimum configuration for specific PV system applications.

It can also be inferred from the data in Figure 3-27(c) that should the NEC or other safety codes require that array conductors be sized for maximum expected short circuit current, rather than maximum peak power point current, this could likely be accommodated without economic penalty.

Parallel Branch Circuits. In the preceding analysis it was assumed that each branch circuit within the subfield was connected to the power conditioning unit (PCU) via an individual feeder circuit, as illustrated by Figure 3-6(a). It is also possible to collect the power outputs of several branch circuits onto a common feeder circuit, as illustrated in Figure 3-6(b). This latter approach requires fewer higher current capacity circuits to be routed and terminated at the (PCU). The feeder circuit is tapped at each branch circuit, using a field-installed rubber insulated crimp type tap assembly. Taps of this kind are commonly used by the utility industry to provide service taps off of direct buried secondary distribution circuits, at voltages of up to 600 Vac. Discussions with a manufacturer of this type of equipment indicated that modification of these taps for operation in the range of dc voltages proposed in this study could be accomplished by simply increasing the thickness of the insulating rubber cover. In large quantities, the cost impact of this modification should be minor.

The effect of the number of parallel branch circuits per feeder on dc wiring first cost is illustrated in Figure 3-29 for both horizontal and vertical axis arrays. As can be seen, there may be an optimum for given
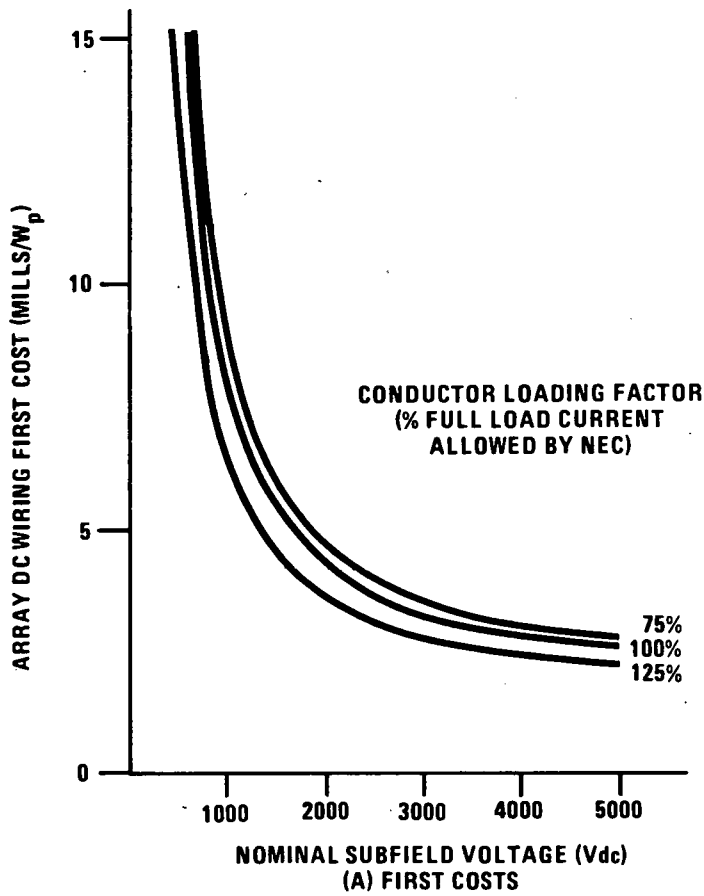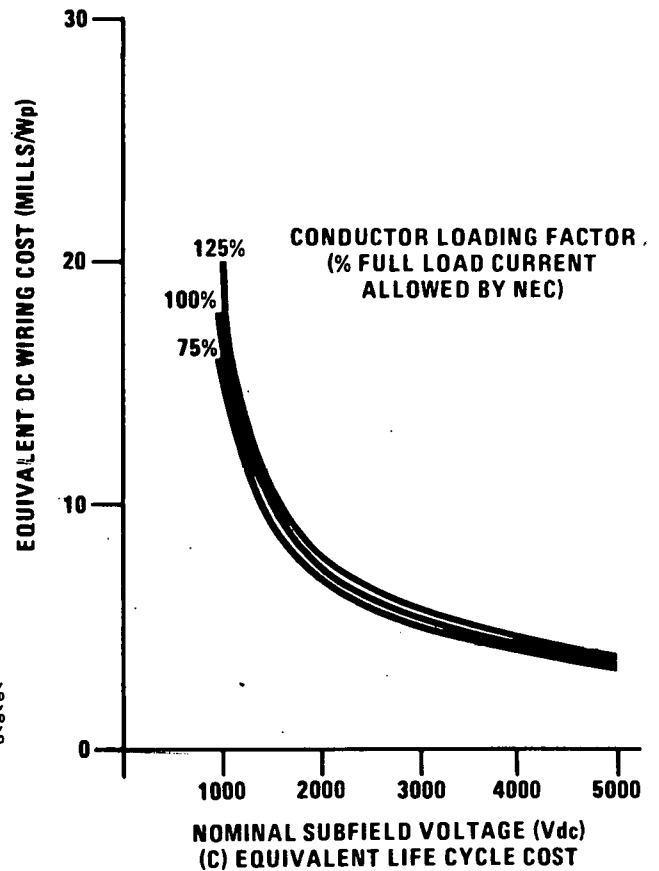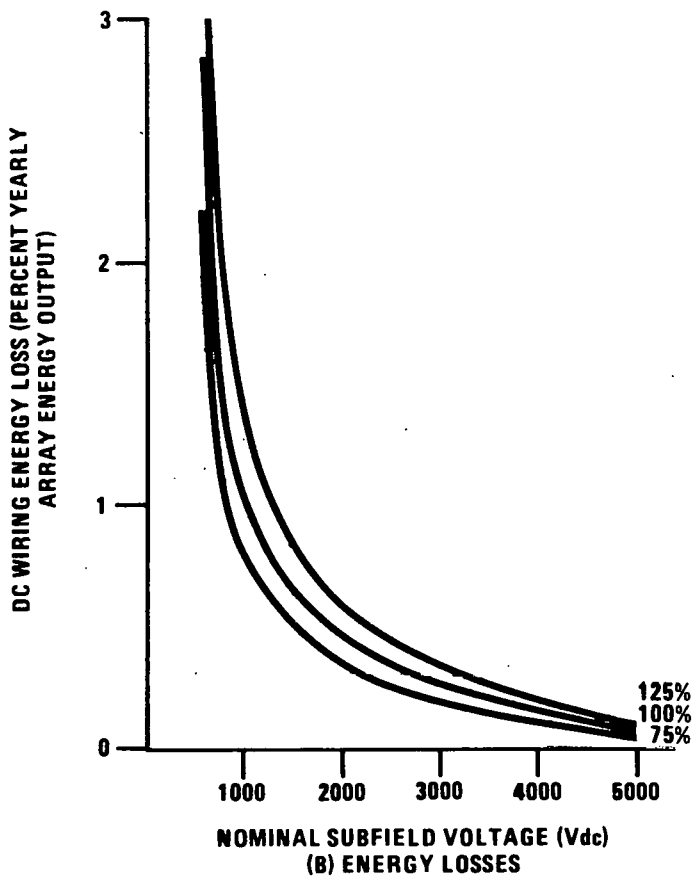
Figure 3-28 Effect of Wire Size on Dc Wiring Costs and I_2R Energy Losses for Horizontal Axis Arrays

3-63

HORIZONTAL AXIS ARRAYS
13 PERCENT EFFICIENT
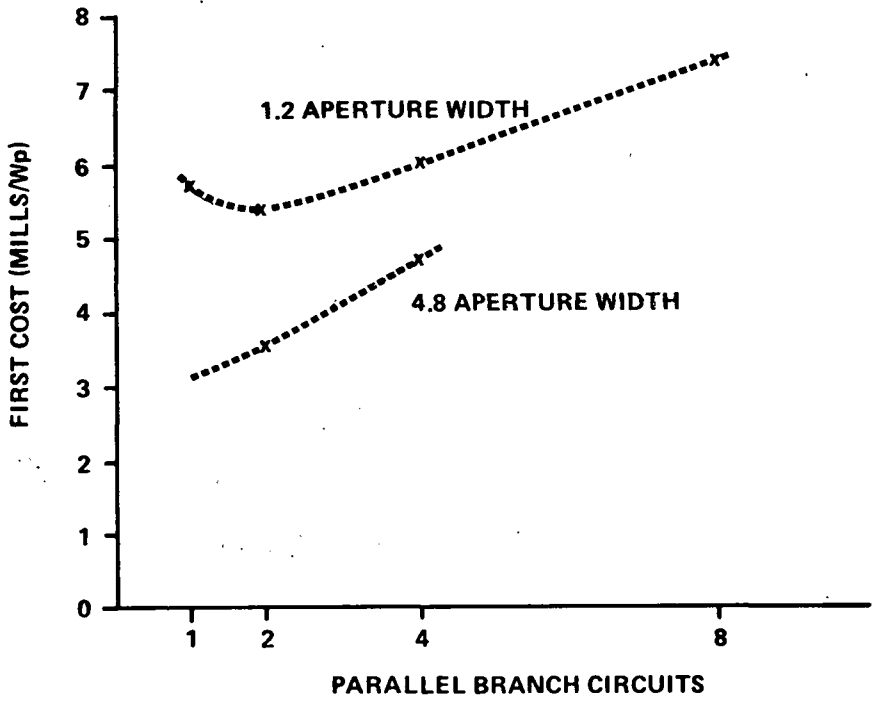
5000 kWp Subfield
2000 Vdc Subfield Voltage

Cost are Based on Undergroud
Direct Buried Copper Conductors
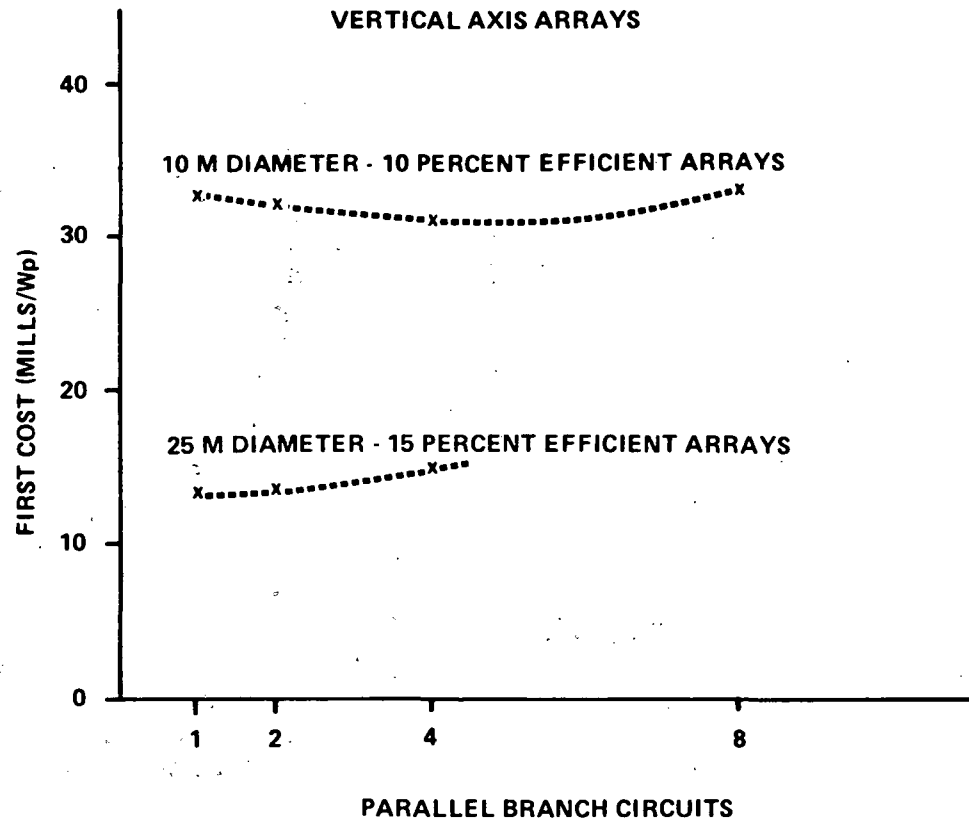
Figure 3-29 Effect of Parallel Branch Circuits on Dc Wiring Cost

3-64

array and subfield parameters but the variation is not large compared to effects produced by other parameters. It should be noted that the upper set of curves (horizontal axis arrays) have a more expanded scale than the lower set of curves (vertical axis arrays).

3.3 AC POWER COLLECTION WIRING

The ac power collection subsystem collects the electrical output(s) of the PCU(s) for delivery to the PV system load. For this study, the PCU is assumed to include transformers, circuit breakers, filters, power factor correction capacitors (if necessary), and other equipment required to deliver ac power of acceptable quality to the ac power collection subsystem. These requirements are discussed further in Section 4.

If the PV system consists of a single subfield, the ac power collection subsystem is simply the connection between the PCU and the load. The design of this link will be governed by PCU power rating, load characteristics (e.g., voltage level), and, possibly, the physical distance between the PV system and the load. If, however, the PV system consists of several array subfields, the ac power collection subsystem must gather the outputs of the individual PCUs, scattered throughout the array field, to a central location. The point of collection may either be the load distribution center or, in the case of a utility central station, the point of connection with the utility grid.

In many ways, the ac power collection subsystem resembles a conventional utility primary distribution system in reverse: collecting power from dispersed points of generation rather than distributing power to dispersed loads.

3.3.1 Design Requirements

The design requirements placed on the ac power collection subsystem are similar to those previously described for the dc wiring. The subsystem must accomplish power collection in an efficient and cost effective manner, maintain equipment and personnel safety during both normal operation and upset conditions, and minimize interference with regard to array shadowing and access for maintenance vehicles.

Normal design practices (e.g., Refs. 3-7, 3-10, and 3-11) should be followed with regard to equipment current and voltage ratings, overcurrent protection, grounding and lightning protection, and other aspects of system design.

The scope of the ac power collection subsystem is illustrated in Figure 3-30. Included in the subsystem are the connections to the PCU ac power output terminals, power cable, central collection busses, and circuit breakers. For purposes of this study, step-up transformers and/or other central switchyard equipment necessary to interface the ac power collection subsystem with the load are not included. These requirements are application specific and will generally not affect the results of the ac power collection subsytem design tradeoff and optimization analysis.

3.3.2 Design Alternatives

Design alternatives with regard to the ac power collection subsystem are primarily concerned with the selection of the ac voltage level and the use of either underground or overhead construction.

For this study, nominal ac voltage levels of 15, 35, and 69 kv were investigated. These are standard utility distribution voltage levels, for which design standards and commercially available equipment are well established.

TO LOAD INTERFACE

AC POWER COLLECTION SUBSYSTEM

CIRCUIT BREAKER (TYPICAL)

AC COLLECTION
BUS

PCU
(TYPICAL)

AC POWER
COLLECTION WIRING
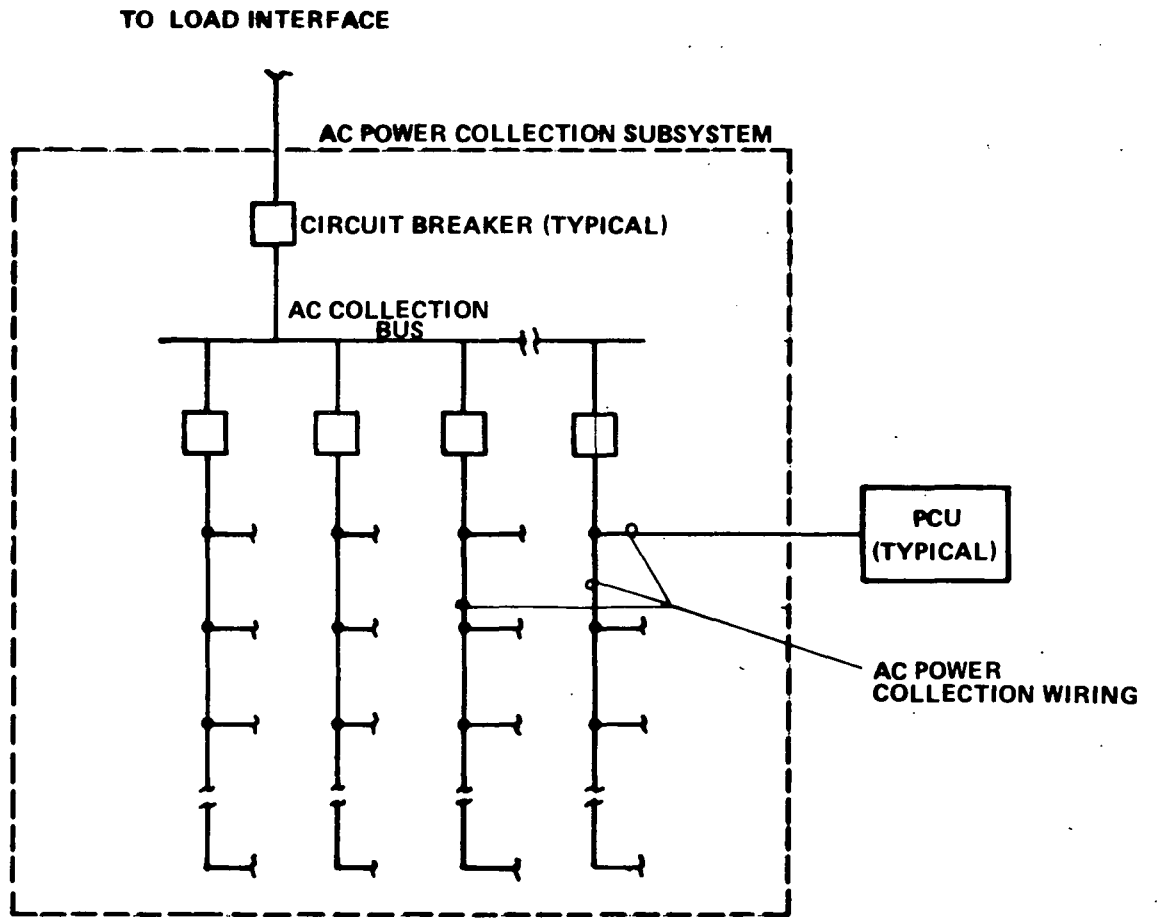
Figure 3-30 Ac Power Collection Subsystem

The tradeoff between overhead and underground construction generally involves consideration of the same factors (including cost, maintenance accessibility, safety clearances, array shadowing, and lightning susceptibility) as discussed in Section 3.2 for the dc wiring subsystem. It is unlikely that wiring construction types would be mixed. That is to say, if underground construction were used for the dc wiring, then underground construction would likely also be used for the ac power collection subsystem.

3.3.3 Parametric Analysis

In addition to voltage level and construction type, the design and cost of the ac power collection subsystem are also affected by both the array field power density and the array subfield (PCU) peak power rating.

For a given array field peak power rating, the field power density determines the lengths of the ac power collection circuits. This can affect both subsystem costs and the optimum ac voltage level. These effects can be evaluated independently of specific array characteristics (e.g., vertical versus horizontal axis arrays). A review of the range of power densities presented in Table 3-4 resulted in the selection of 100, 200, and 400 kWp/acre for investigation in this study.

The PCU peak power rating also affects the ac power collection subsystem design and cost by influencing collection feeder layout and the required number of terminations. For this portion of the study, PCU peak ac power ratings of 1, 5 and 10MW were evaluated.

First Costs. The estimated first costs (material and installation labor) for the ac power collection subsystem are presented for field power
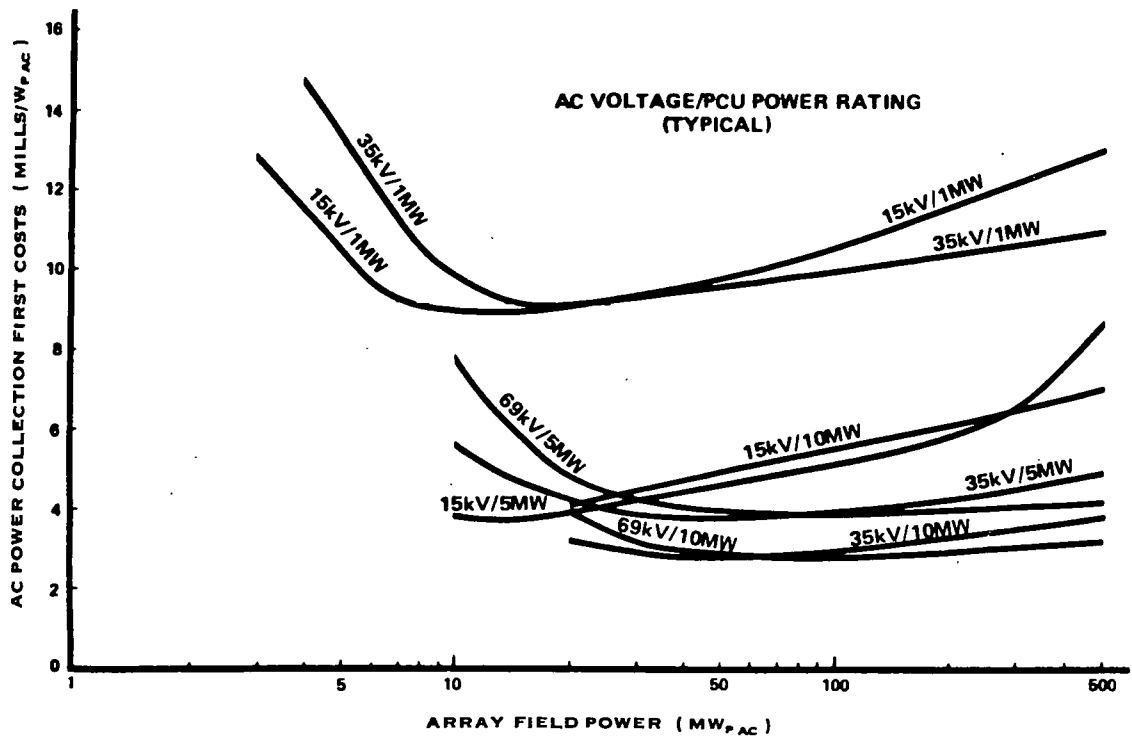
a) OVERHEAD
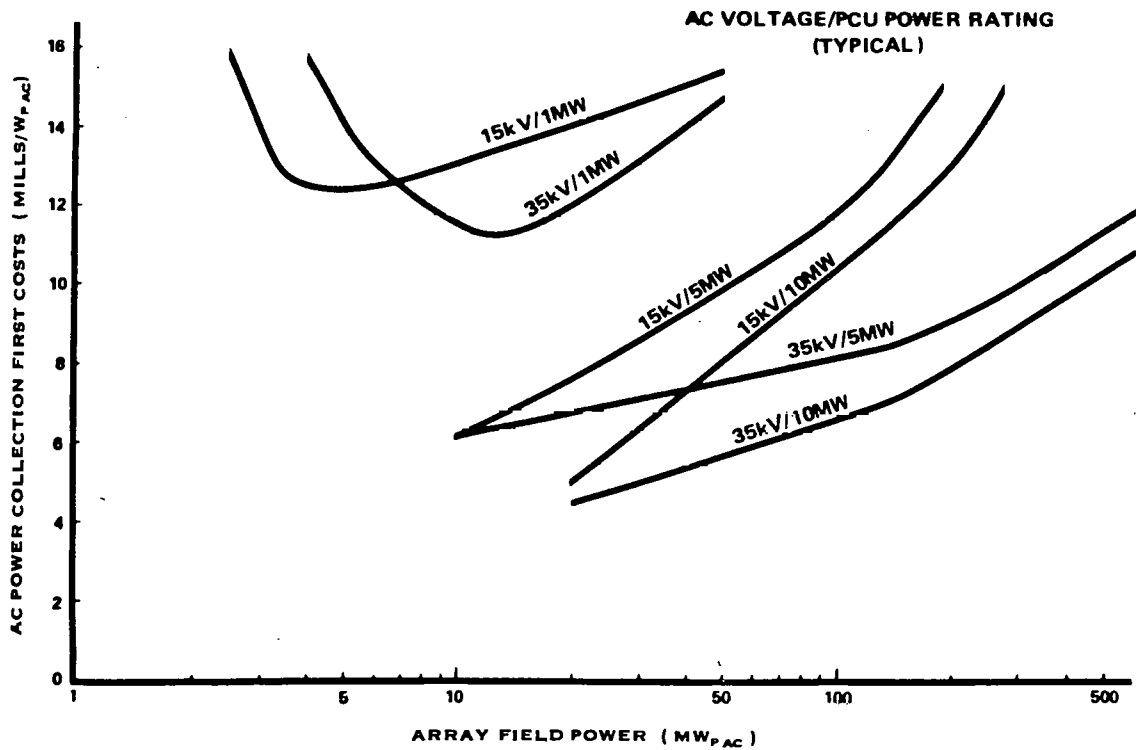
b) UNDERGROUND

Figure 3-31 Ac Power Collection System Costs - 100 kW$_p$/Acre Power Density
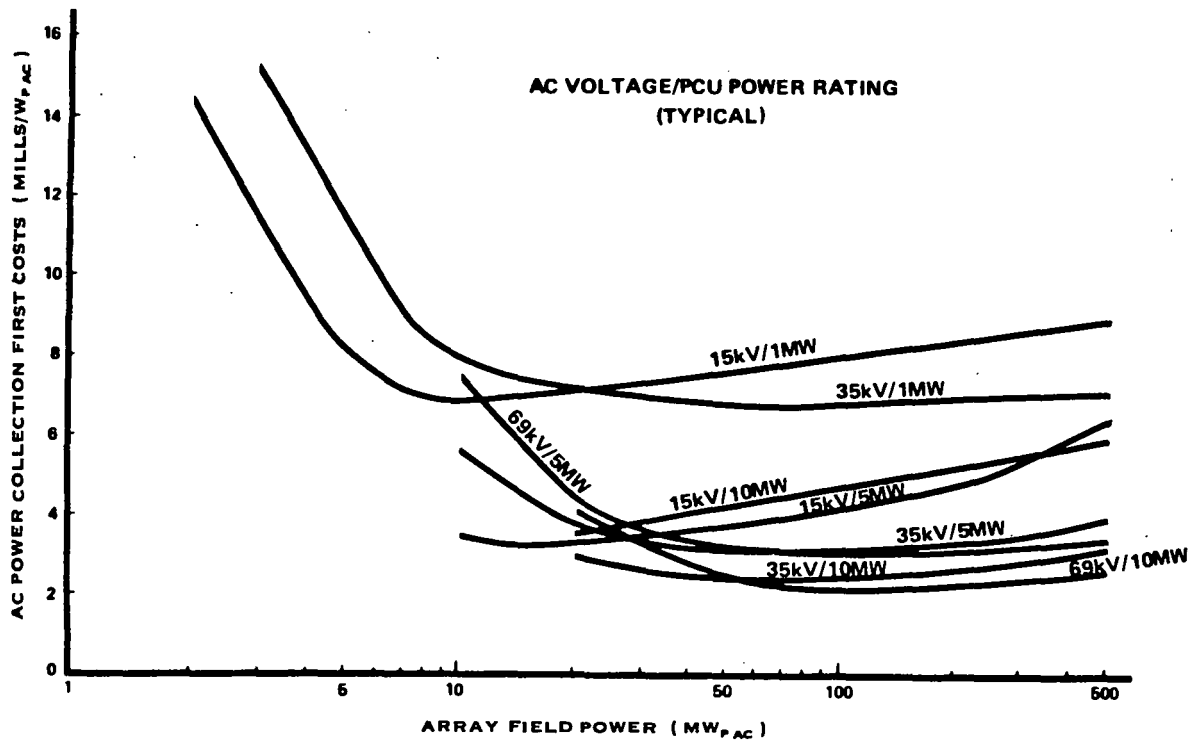
a) OVERHEAD
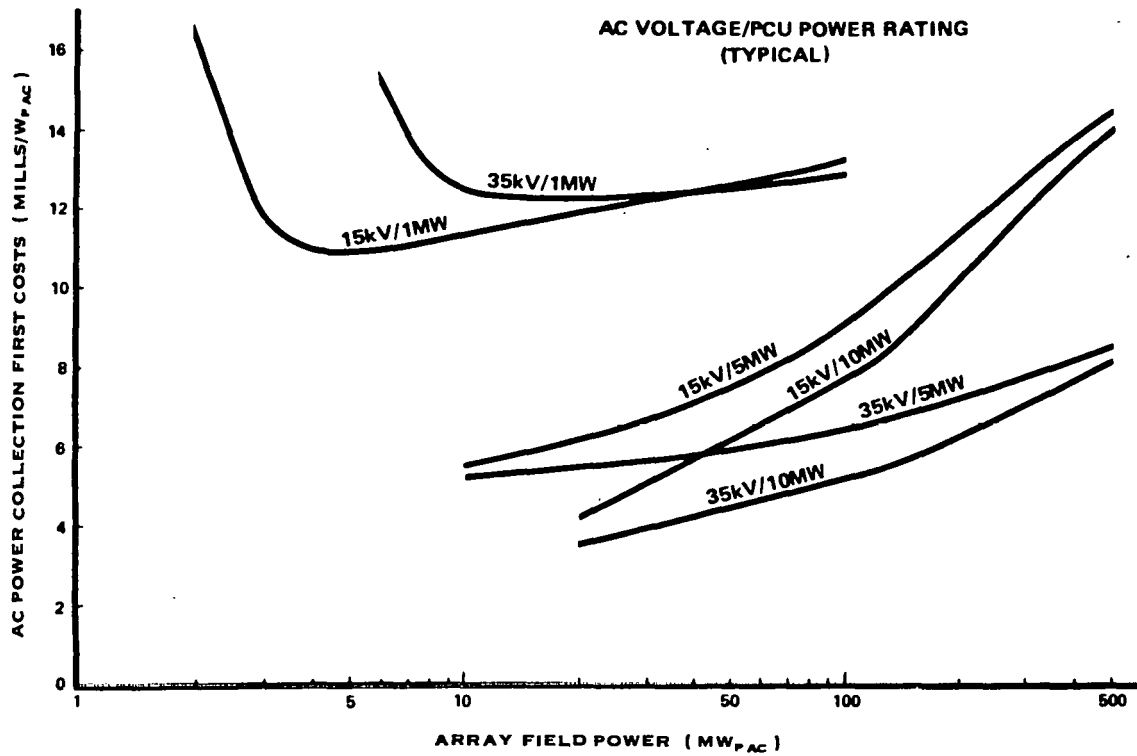
b) UNDERGROUND

Figure 3-32 Ac Power Collection System Costs - 200 kW$_p$/Acre Power Density

a) OVERHEAD
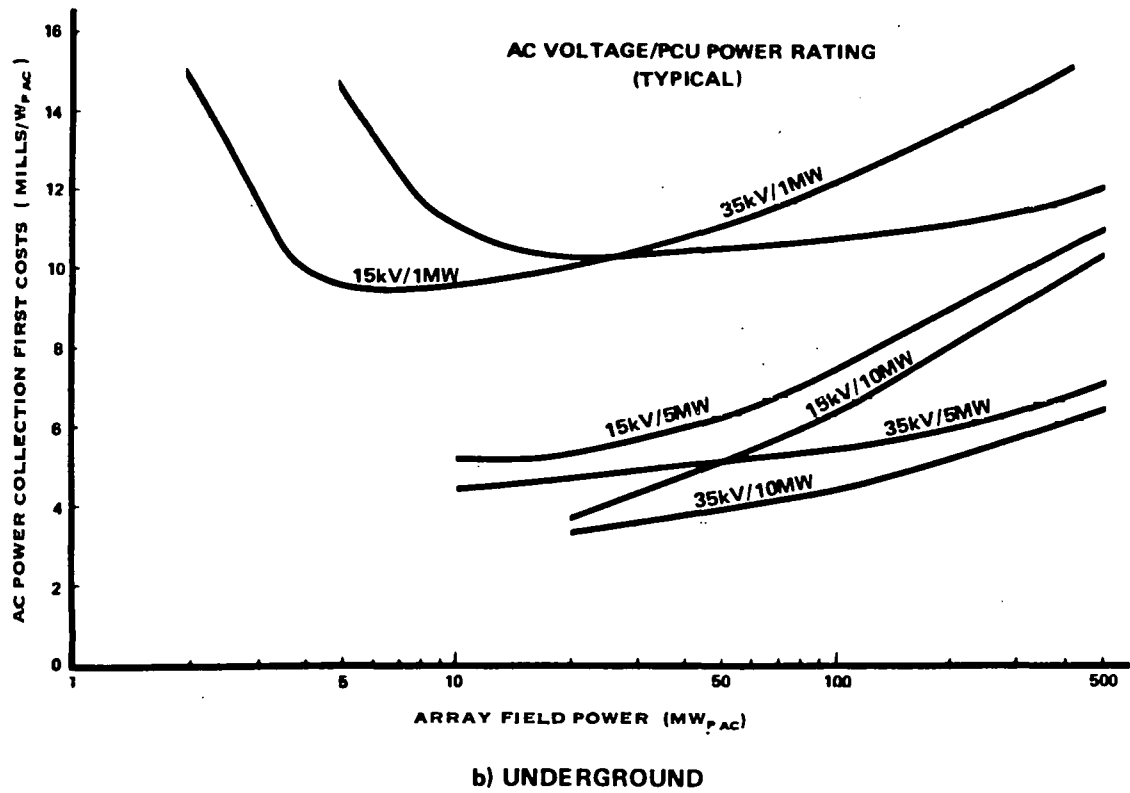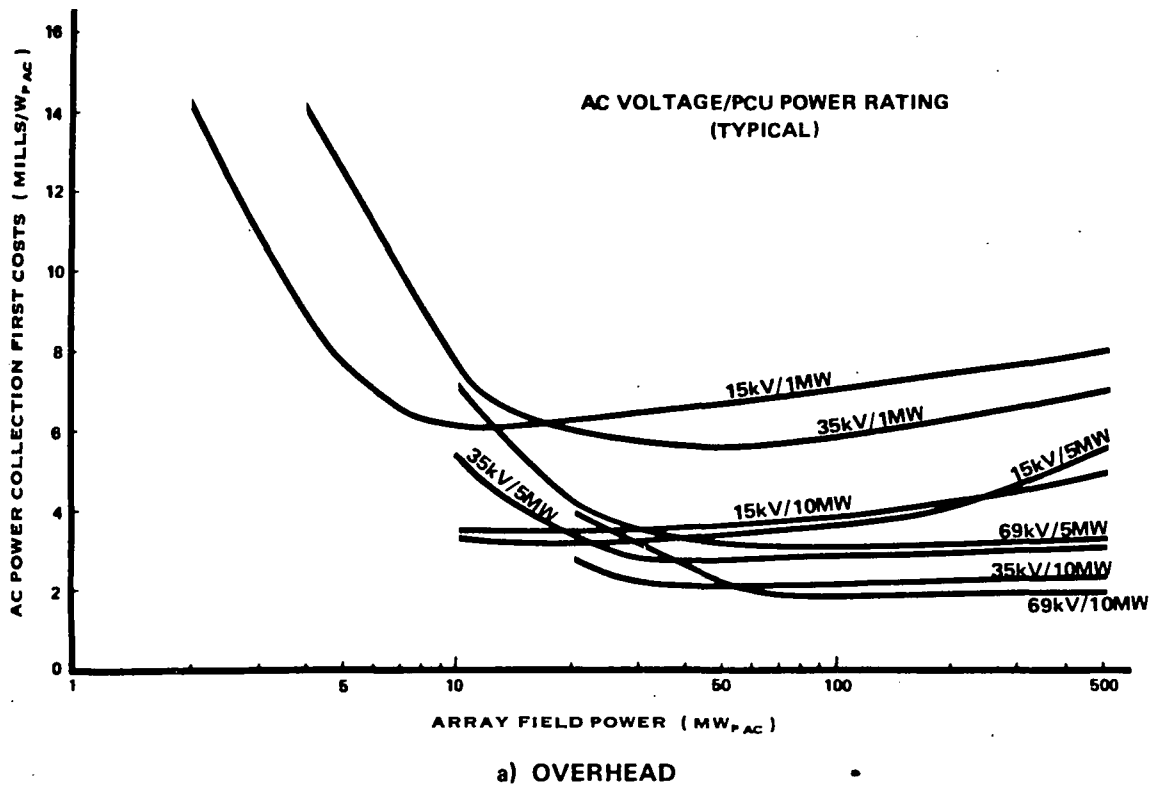
b) UNDERGROUND

Figure 3-33   Ac Power Collection System Costs - 400 kW$_p$/Acre Power Density

densities of 100, 200 and 400 kWp/acre in Figures 3-31, 3-32, and 3-33, respectively. The figures illustrate the costs for both overhead and underground construction as a function of array field (PV system) peak power rating, for various combinations of ac collection voltage and PCU (subfield) peak power rating.

It can be seen that, in general, overhead construction has somewhat lower first costs than equivalent capacity underground installations. However, the differences are relatively small, especially at higher field power densities. Further, the cost of the ac power collection subsystem is also relatively small (on the order of 2 to 10 mills/Wp) compared to the total plant costs of 1100 to 1800 mills/Wp (per the PV program goals). Several other general trends can also be observed from the data, as follows:

- Costs decrease for increasing array field power density.

- Within the range of ac voltage levels and PCU power ratings evaluated, costs tend to decrease with both increasing voltage and subfield (PCU) power ratings.

- Except at relatively low system power levels ($\leq$ 10 MWp), cost per watt increases with increasing system (array field) power level.

It should be noted that the costs presented in Figures 3-31, 3-32, and 3-33 do not account for the potential effects of ac voltage level on PCU costs. In general, the cost impact on PCU output transformers and circuit breakers would be minor within the range of 15 to 69kV. However, the commercial availability of required wire sizes at the desired voltage should be verified in performing a detailed design.

However, one area of potential impact (not investigated in the present study) could be the cost of harmonic filters and power factor correction

capacitors, if these are required for a particular application and/or PCU design.

Energy Losses. Energy losses (I^2R losses) in the ac power collection subsystem are small, and do not significantly affect the selection of optimum voltage levels. Losses generally decrease with increasing ac voltage level, and, for a fixed voltage level, increase with increasing array field power level. Also, losses may be slightly higher for overhead wiring due to higher allowable conductor current ratings (based on thermal considerations).

For the array field peak power and power density levels evaluated in this study, energy losses are less than one half of one percent for all practical ac voltage levels.

3.4   GROUNDING

The purposes of a grounding system generally include:

- Protection of personnel and equipment against dangerous voltages

- Provision of a path to the earth for lightning, switching surges and static charges, as well as for system neutral currents

- Provision of a system reference for instrumentation and relaying systems.

This section discusses several aspects of the application of grounding systems in PV power plants. While useful cost relationships and design considerations are identified, it was beyond the scope of this study to develop a manual on how to design safe grounding systems for PV power plants.

3.4.1 Design Requirements

Specific design requirements are presently not well defined, especially for large PV systems. This results from uncertainties with regard to both the required levels of protection, and the nature of specific system configurations. An example of the latter is a plant using the JPL postulated array structure/ foundation approach of buried plates. It is possible to construct the structures and plates of wood and use plastic substrate modules. Similarly, the MBAssociates approach uses concrete. In such cases there is nothing to ground (except one pole or the center of the dc bus). If in the JPL approach, the buried plates and structure are metal, the conducting plates could form an adequate ground system in many cases, with little need to bury additional conductors. Similarly, for many vertical axis arrays, simply connecting the array structures together with a buried bare wire might form an adequate ground system. The conditions for this are discussed in Section 3.4.3.

Typical grounding systems often use a low resistance path to earth to accomplish the general requirements previously listed. However, a low resistance ground is not sufficient to ensure a safe and adequate ground system. One criterion presently used in electrical plant design is to have acceptably low potentials in areas accessible by plant personnel. Methods of accomplishing this are outlined in IEEE Standard 80 (Ref. 3-12). This standard is generally applicable to plant and substation design for alternating currents and has several shortcomings for use in the dc portion of photovoltaic power systems. Unfortunately, little detailed information exists on grounding for large area dc systems. Thus, IEEE 80 is used in this study to provide indications of the impacts of grounding system design.

Additionally, it is generally required to have ground system conductors buried below the frost line at the site. This is because frozen soil has a significantly higher resistance. Such depths are also required for buried foundations for structural reasons.

3.4.2 Design Alternatives

Grounding for small systems is commonly accomplished by driving a conducting rod into the soil. Metal pipes, metal foundation piers (bare or concrete encased), or similar conductors in contact with the earth are often used in forming a ground system. As system size increases, the ground may comprise a multiplicity of driven rods tied together by a horizontal grid of conductors. For large systems, the buried grid of horizontal conductors (mesh) is often sufficient to establish a suitable ground and the vertical driven rods become superfluous. This will generally be the case in larger photo-voltaic power plants, although ground rods may still be added at selected locations. Also, mesh size may be decreased at some interior regions subject to high currents or where instrumentation shielding is required.

For photovoltaic power systems, a ground is required for the dc, PCU, ac substation, and instrumentation subsystems. Except for the first item (the dc subsystem and arrays), existing standard practice is generally adequate to design the ground system. Accommodating these requirements will not be a significant cost factor. However, little related industry experience exists from which specific design criteria for the array field can be obtained. Thus, standard practice is applied.

This design leads to bonding all of the metal array structures together

with a grid of buried conductors. For purposes of design example, number 2 AWG bare copper conductors buried 18 inches deep are used as a baseline. It will be shown that for large plants and low soil resistance, this grid alone will likely produce an adequate ground system.

3.4.3   Parametric Analysis

The major parameters relating to ground system design include:

- Soil resistivity
- Plant size
- Array Type
- Array size
- Array efficiency.

These parameters may generally be considered as input conditions and are not particularly subject to optimization. Subfield size is not among the list of parameters because for a given plant size the entire grounding grid would be bonded together to form one large grid. There is no advantage and some disadvantage to having a multiplicity of smaller grids each associated with an array subfield.

The generally accepted design criteria for substation design (per IEEE 80) is to have a mesh potential less than 1000 volts. This potential is the maximum potential between any point on the surface of the soil within the mesh and a grounded object. This voltage applies to shock hazards of not less than 0.03 seconds duration and may be subject to further interpretation of what currents are dangerous for exposures significantly less than 0.03 seconds.

The major shortcoming of IEEE 80 is that it assumes all points on the conductor grid (mesh) to be at the same potential. This seems to neglect surge impedance, which may be an order of magnitude higher than calculated by the methodology outlined.

For purposes of illustration, a maximum fault current of 20 kA is used. This is typical of a direct lightning strike.

The mesh potential for a field of vertical axis arrays is shown in Figure 3-34. As can be seen, for 100 ohm-meter soil resistivity, the grid used to bond the array structures together is sufficient to keep the mesh potential below 1000 volts for plant sizes above 10 MW. The figure also shows that for a given plant size, the mesh potential decreases with decreasing array diameter and efficiency. This is because more copper wire is required to bond the larger number of smaller or less efficient arrays needed to achieve a given power level. For large plant sizes, simply bonding the array structures together results in a very low mesh potential even without ground rods or consideration of the contribution made by foundation metal in contact with the soil.

Mesh potential and ground resistance vary linearly with soil resistivity. This parameter is an essentially unadjustable input for the plant site selected and can vary over several orders of magnitude. Typical values for several soil types are shown in Table 3-7 (Ref. 3-13). The effect of soil resistivity on ground system cost is shown in Figure 3-35. The horizontal line segment in this figure shows the normalized cost for bonding together 25m diameter, 15% efficient arrays as a function of plant size. The
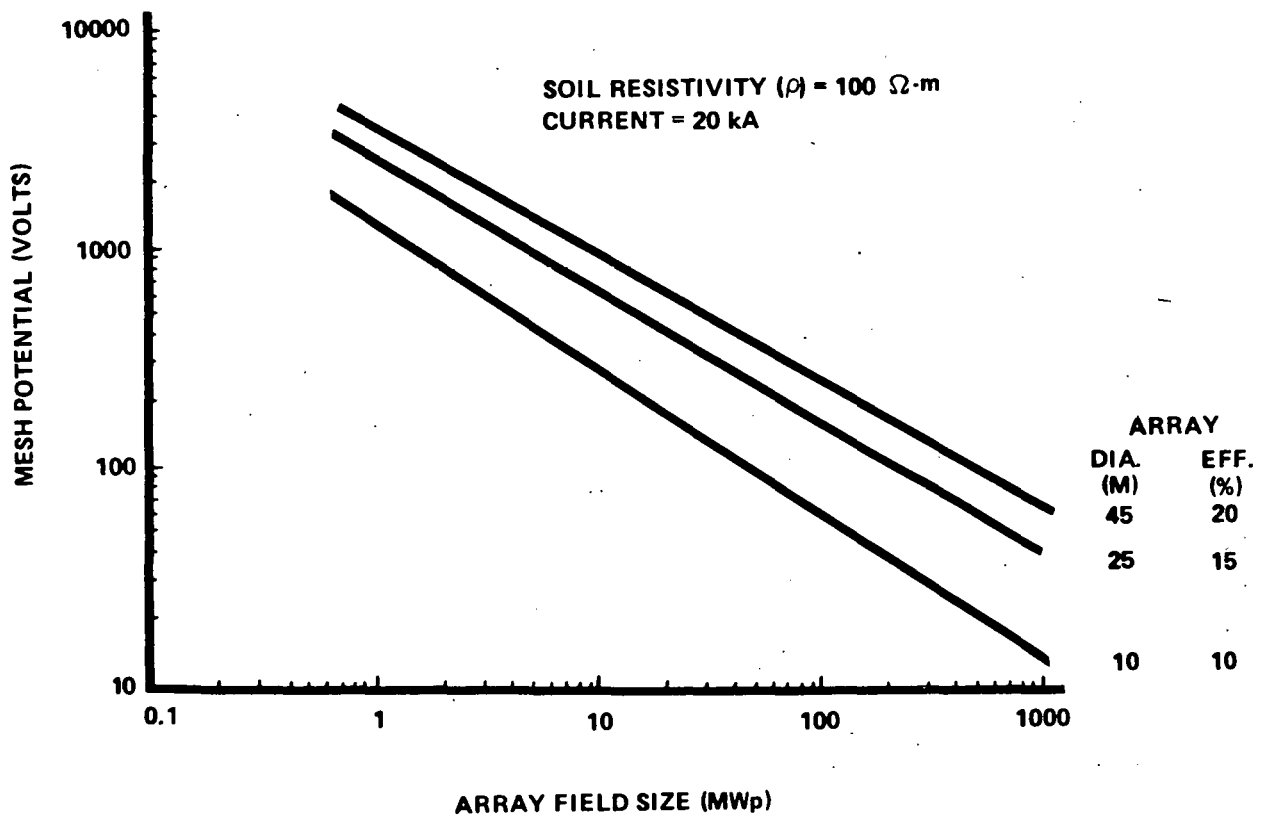
Figure 3-34 Mesh Potential versus Vertical Axis Array Field Size

Table 3-7

SOIL RESISTIVITIES

Soil Type	Resistivity (ohm-meter)		
	Minimum	Average	Maximum
Surface soils, loam, etc	1	--	5
Clay, shale, loam	2	40	200
Limestones	5	--	4,000
Clay, shale with sand and gravel	10	150	1,000
Sandstones	20	--	2,000
Decomposed gneisses	50	--	500
Granites, basalts, etc	--	10,000	--
Flat areas, marshes, woods (typical of Louisiana)	2	100	--
Pastures, hills, forests (typical of the Northeast)	--	200	--
Rocky soil, steep hills (typical of New England)	10	500	1,000
Sandy, dry, flat (typical of coastal areas)	300	500	5,000

Source: Ref. 3-13
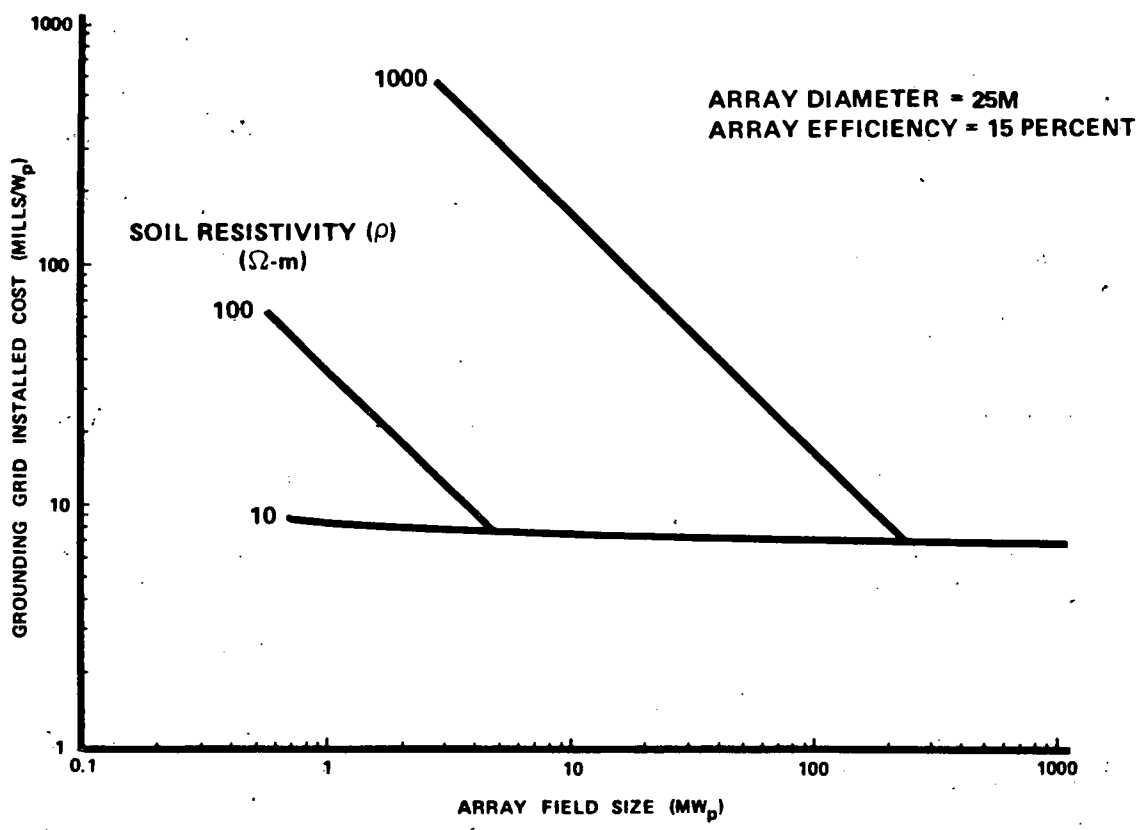
Figure 3-35 Effect of Soil Resistivity on Vertical Axis Array Grounding Costs

3-80

inclined line segments show the cost of a ground system wherein sufficient copper is added to keep the mesh potential below 1000 volts, with soil resistance as a parameter. Although all of the designs with costs shown by the horizontal line segment have mesh potentials below 1000 volts, the mesh potentials for larger plants may be well below 1000 volts (see Figure 3-34). Thus, the level of personnel safety provided is not uniform for these designs.

The effect of array diameter on grounding subsystem cost is shown in Figure 3-36. The horizontal line segments show the cost for simply bonding the array structures together. The inclined line segments show costs where copper must be added to that required for array bonding to keep the mesh potential below 1000 volts.

Similarly, Figure 3-37 shows the effects of array efficiency on grounding costs for vertical axis arrays.

In the cases where additional wire (over that needed to bond the arrays) is used, the reduction in ground resistance produced by the array foundation is neglected. This contribution can be significant for driven metal piles or concrete pile foundations with electrically bonded rebar cages. There would be no contribution to lowering ground resistance for wooden or concrete piles or similar nonconductive foundation types. Thus, the costs shown in Figures 3-35 through 3-37 might be considered an upper bound.

Grounding system design requirements for horizontal axis arrays are less well defined than for vertical axis arrays. In part, this is because horizontal axis arrays in the same row may be bonded together above the soil at
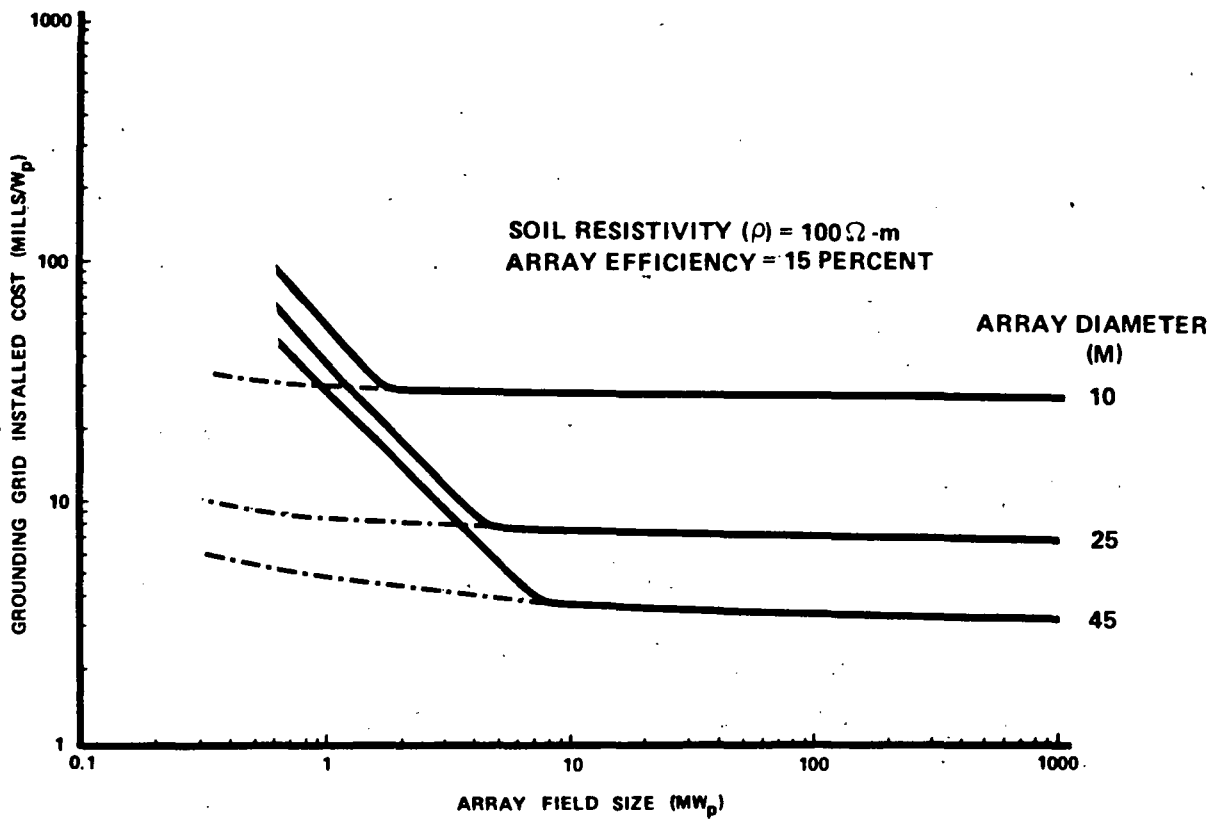
Figure 3-36 Effect of Array Size on Vertical Axis Array Field Grounding Costs
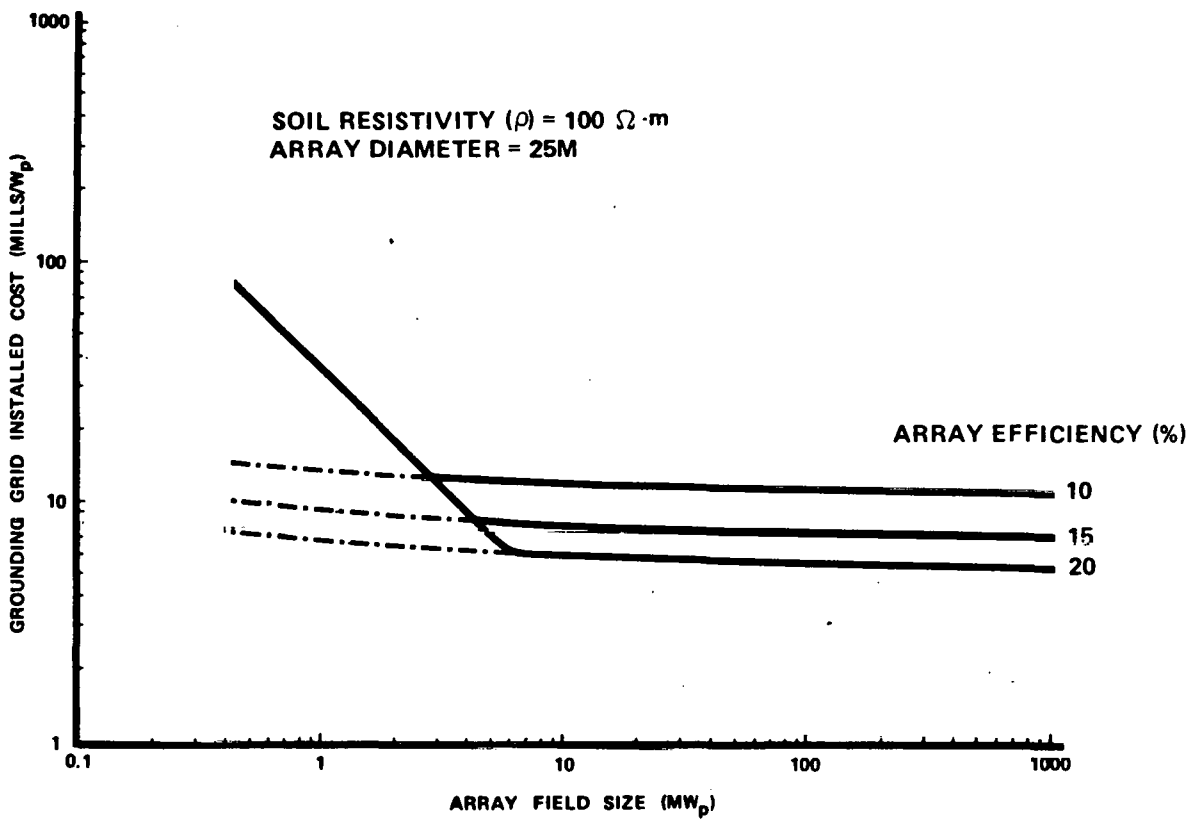
Figure 3-37 Effect of Array Efficiency on Vertical Axis Array Field Grounding Costs

their extremities. For example, torque tube array designs (see Section 6.2.1) may have adjacent tubes connected by a ground strap. Such above-the-soil connections do not contribute to ground resistance in the same way as buried bare copper wire used to connect vertical axis arrays.

For purposes of illustration, the costs for a horizontal axis array grounding system were estimated. The array structure has a 20-foot span. As for the vertical axis cases, additional copper wire is buried as needed to keep the mesh potential below 1000 volts. The results, presented in Figure 3-38 through 3-40, show curves with similar characteristic inflection points at low power levels where additional wire is used.

As shown in Figure 3-38, increasing soil resistance increases costs at lower power array fields in the same general manner as for vertical axis arrays. However, the inflection points occur at lower power levels. This can be partially attributed to the size and lower efficiency of the horizontal axis array selected for study.

The effects of array size (i.e., slant height) and efficiency on grounding system costs are shown in Figures 3-39 and 3-40 respectively. As for vertical axis arrays, horizontal axis array grounding system costs decrease with increasing array size and efficiency.

Although specific guidelines and designs have not been established, several general conclusions can be derived from the above analyses, as follows:

- There is no advantage to having separate grounding grid systems for each array subfield. Thus, ground systems design cannot be optimized as a function of subfield parameters.

3-84
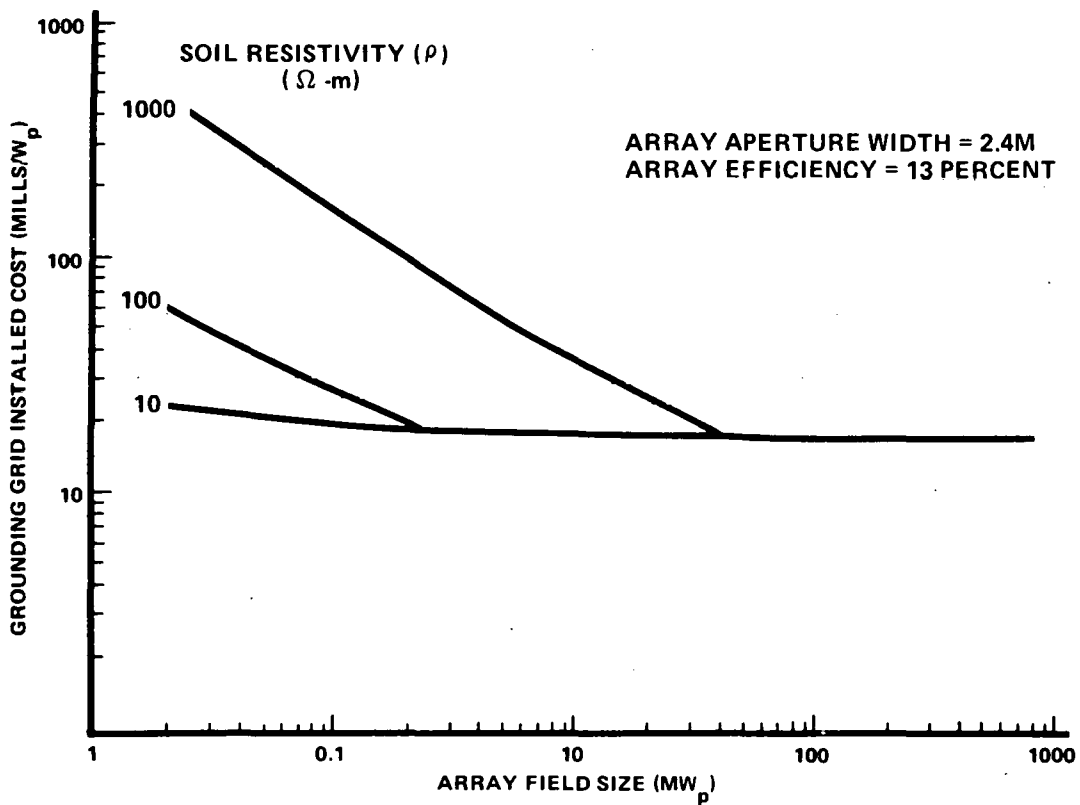
Figure 3-38 Effect of Soil Resistivity on Horizontal Axis Array Grounding Costs
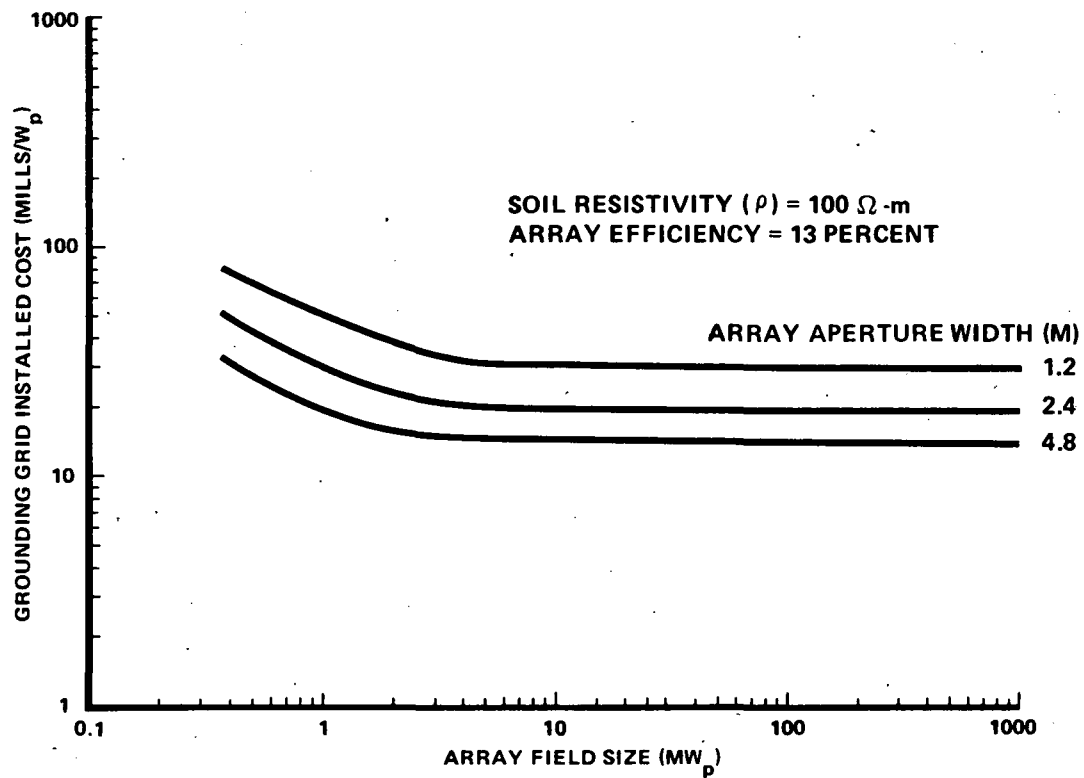
Figure 3-39 Effect of Array Size on Horizontal Axis Array Field Grounding Costs
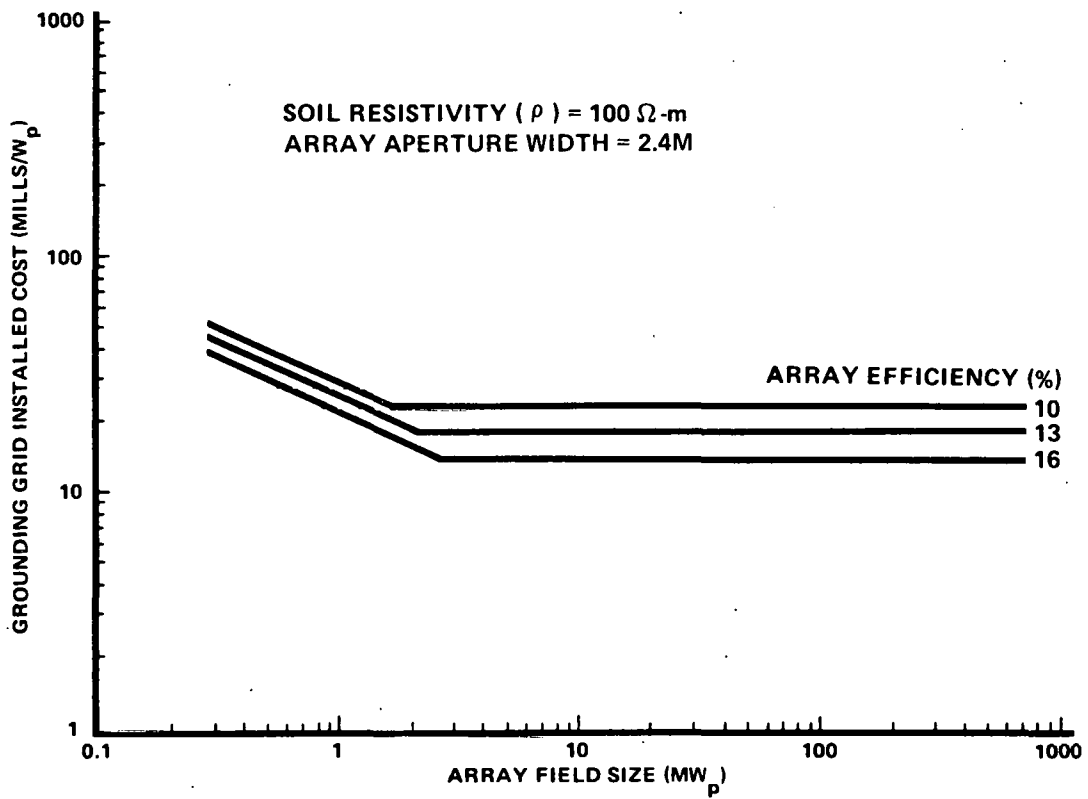
Figure 3-40 Effect of Array Efficiency on Horizontal Axis Array Field Grounding Costs

- Grounding system costs are a strong function of parameters which are not subject to optimization (i.e., site and plant input specification parameters). Soil resistivity can vary over several orders of magnitude and can cause order-of-magnitude variation in grounding system costs, with decreasing soil resistivity decreasing cost (or increasing level of protection). Increasing plant size (peak power rating) tends to result in lower cost or increased level of protection.

- For vertical axis arrays, simply bonding the array structures together with a buried bare wire grid can form an adequate grounding system (depending on soil resistivity, plant and array sizes, and array efficiency). Structures together will likely not produce an adequate ground and additional wire would have to be used.

- Further study is needed to evolve specific design criteria for the grounding system in the array field portion of photovoltaic power systems.

It is assumed that the ground wire network is buried over the power and other wiring in the same trenches and thereby offers a significant degree of shielding from lightning surges for these subsystems. Overhead wiring would require a similar network of ground-connected wires above the power and other wiring to offer the same degree of shielding. An additional buried network of wire would still be required to form the ground system to which the overhead shield wires are connected. This significant added cost must be considered in trading off underground versus overhead wiring approaches designed to the same level of protection.

3.5   LIGHTNING AND SURGE PROTECTION

The primary functions of the lightning and surge protection subsystems in a photovoltaic power plant are to protect the plant equipment and maintain its integrity under conditions of lightning and other surges. These subsystems also serve to protect personnel and aid in safely dissipating lightning energy.

3.5.1 Design Requirements

There are several possible sources of surges in the dc portion of photovoltaic plants, including lightning and surges from the PCU (either generated or fed through from the utility lines). Surges in the ac portion of the plant may be due to PCU operation, PF correction, or similar switching surges, as well as lightning or other surges on the utility lines. Any of the above may also cause surges to appear in the instrumentation and control systems. Surge protection in ac and instrumentation systems can be accomplished by application of existing standard techniques. However, the dc subsystem is somewhat unique and is therefore addressed in this section. Further, the magnitude of lightning related surges, compared with other surges, makes lightning protection a dominant design criteria.

Lightning is a discharge of thousands of amps through an ionized air channel between clouds and earth (or other clouds) and is caused by potentials of several million volts. The strokes have very rapid risetimes (20 kA/ microsecond) and each event may actually comprise several strokes separated by a fraction of a second. Several damage-causing effects may result:

- A direct hit can melt equipment or structures due to resistive heating by large currents.

- Magnetic fields produced by the large currents and short risetimes can induce voltages and currents in arrays or equipment.

- The lightning current flowing in the soil can be resistively coupled into arrays or structures.

- Coupled currents may be large enough to damage equipment.

- Similarly, potential differences may puncture insulation on arrays or wiring.

Capacitive coupling to the lightning stroke itself seems to be negligible. However, capacitive coupling between solar cells and the array structure can be significant. Photocurrents due to the lightning flash seem to be insignificant (Refs. 3-8 and 3-14).

The probability of a photovoltaic plant being struck by lightning is a site-dependent variable. The number of thunderstorm days per year (isokeraunic level) is shown by the map in Figure 3-41 (Ref. 3-15). Similar maps can be found in other references (e.g., 3-13, 3-16 and 3-17). There is general but not exact agreement among these various data sources. It has also been shown that the probability of a lightning stroke reaching the ground decreases with increasing latitude. Taking both of these factors (location and latitude) into account indicates that the probability of a lightning strike varies over more than a 20:1 range across the U.S. In general, large plant sites (> several km^2) can reasonably be expected to be hit by several lightning strikes per year. Comparing maps of isokeraunic and insolation levels shows that sites with high levels of insolation (e.g. the southwest) also often have high levels of lightning activity. Thus, there is a valid reason to consider the effects of lightning in photovoltaic plant design.

3.5.2 Design Alternatives
Several methods of providing lightning and surge protection are currently available. Generally, lightning protection may include dissipative and shielding techniques. The dissipative approach involves installing an overhead array of wires with sharp points (similar to barbed wire for fences) and connecting the wire to a suitable ground. Static charges are slowly leaked off (dissipated) from the myriad of points, thereby reducing the static charge
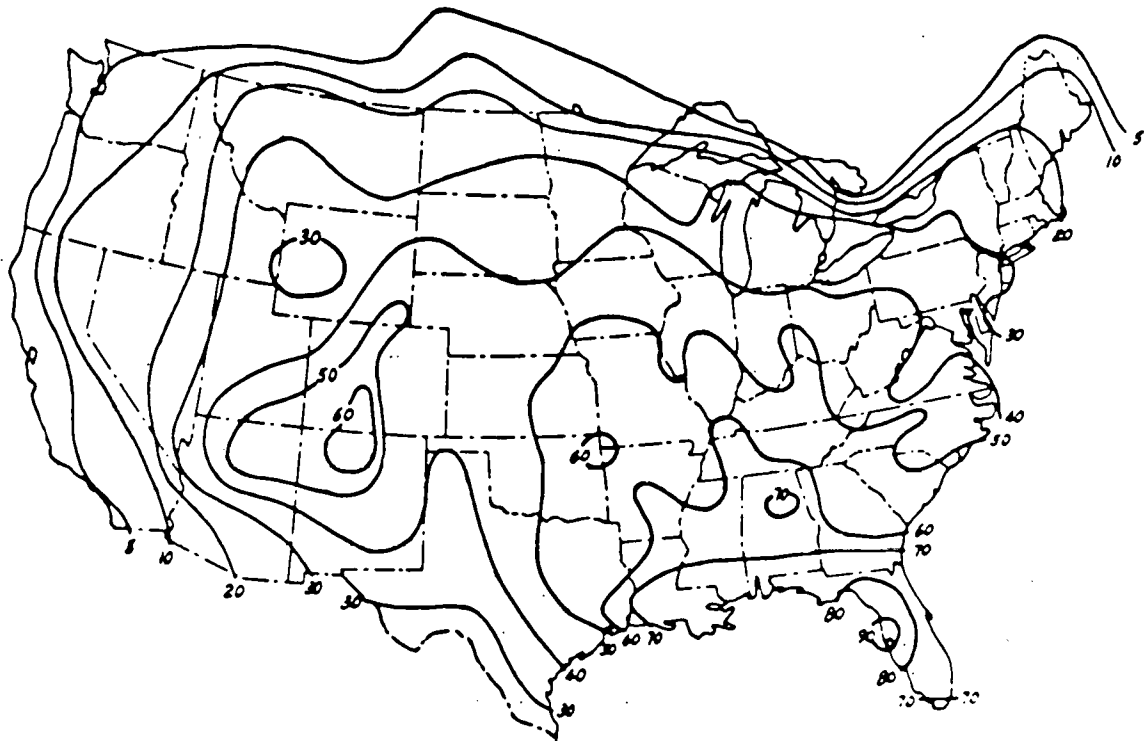
Figure 3-41 Annual Isokeraunic Map of the United States

buildup between the clouds and earth or protected structure. Previous work by Bechtel (Ref. 3-18) indicated that such systems might cost on the order of $3500 to $7000 per acre. This translates to approximately $0.01 to $0.06 per peak watt, depending on array size and efficiency. The dissipation approach is newer and less frequently used than shielding techniques.

Shielding techniques involve use of a conductor to intercept lightning strokes and conduct them to ground. Both masts and overhead wires are used to protect areas beneath them. The area of protection is approximately a 35 degree cone for a mast and an inverted "V" shaped trough for wires. This approach would require a rather extensive network of masts or overhead wires to protect a large photovoltaic power plant. Although not specifically estimated, it is expected that these costs would be on the same order of magnitude as those for the dissipative approach.

There are several drawbacks to the above approaches. Both require extensive overhead wiring and/or masts or support poles. Support poles or large masts can cause significant shadowing and would tend to interfere with installation and maintenance operations. Further, the shielding approach will cause large electromagnetic and conductive surges when conducting lightning currents to ground, and thus require additional surge protection equipment to prevent or minimize array damage. On the other hand, it is possible to install such surge protection equipment without lightning masts or overhead wires and occasionally repair the few arrays damaged by a direct lightning stroke.

The principal function of surge protection equipment is to prevent excessive voltages from occurring between the wiring, the module encapsulation, and the array structures; to prevent excessive surge currents from flowing

through the wiring; and to safely conduct lightning or other surge currents to ground. Protection of ac lines is routinely accomplished with commercially available devices and application of existing design techniques. Most of the available devices depend on zero-crossings in the alternating current sine wave to extinguish after operation (e.g., spark gaps). Thus, protection of the dc bus in photovoltaic power systems requires special consideration. Several devices are available that may be applicable to accomplish the surge protection function for the dc bus. These devices include generic zener and other diodes, nonlinear resistors (varistors), and specially designed spark gap devices. All of these devices are similar in that their resistance dramatically decreases in a nonlinear manner with increasing applied voltage. The characteristics, performance, and descriptions of such surge protectors are discussed in Ref. 3-15, as well as in manufacturers' literature, and are not repeated in this study. The characteristics and costs of any given generic type of surge protection device vary with manufacturer and with models from the same manufacturer. A detailed analysis of surge protectors for all array types, system voltages, and other parameters is beyond the scope of this study. A large number of potentially suitable devices is commercially available from several manufacturers. Several are designed for dc application in the voltage range being evaluated. The cost of such devices does not appear to be a very strong function of system voltage. Rather, cost is a function of the surge energy the device can withstand and/or the peak surge current it must conduct. This is illustrated in Figure 3-42.

As can be seen in the figure, higher energy dissipation generally implies higher costs. The costs in the figure are for metal oxide varistor surge

suppressors from several manufacturers. The line segments represent a series of devices at a constant voltage. The range of voltages is from 350 to 8500 volts. The costs are for large volume purchase and are the selling price, not installed costs. It is anticipated that such protection devices would be least expensive when installed in array junction boxes (or at module terminals) in the array manufacturer's factory.

Cost also varies with purchase quantity, as illustrated (generally) by Figure 3-43.

3.5.3   Parametric Analysis

As mentioned, the wide variety of protective devices, array types, and system voltages precludes a detailed analysis of all possible configurations. Based on previous work by Bechtel and others, a metal oxide varistor was selected for further analysis in this study.

Varistors are available for the voltage range addressed in this report. Selection of a particular device is governed by estimates of the maximum surge current to be conducted. Based on work in several studies, a device with a 5,000 amp peak surge current capability was selected for purposes of example. This device should be able to handle a majority of surges, except for direct hits by lightning. The cost impact of this device is shown by Figure 3-44 for vertical axis arrays. The dashed lines illustrate the costs for locating two varistors at each branch circuit terminal box (between each dc pole and ground), as shown in Figure 3-5(a). Costs for a system with one pole grounded, as shown in Figure 3-5(b), would be half that shown. The solid lines in the figure represent the cost of locating a varistor at each array (i.e., at intermediate points along the dc bus) in addition to
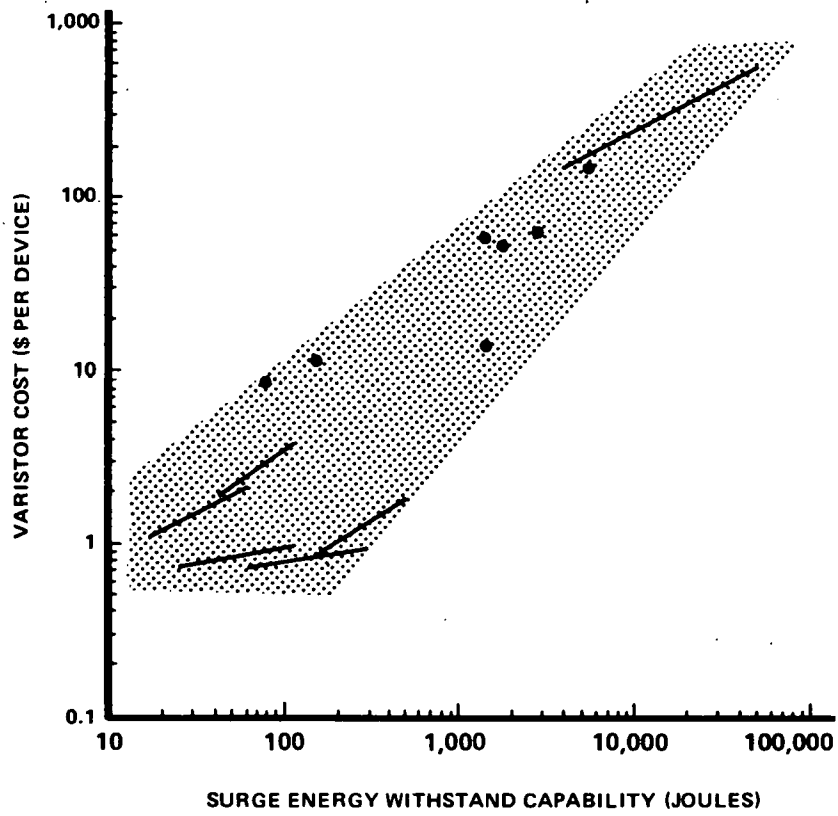
Figure 3-42 Varistor Cost versus Surge Withstand Capability
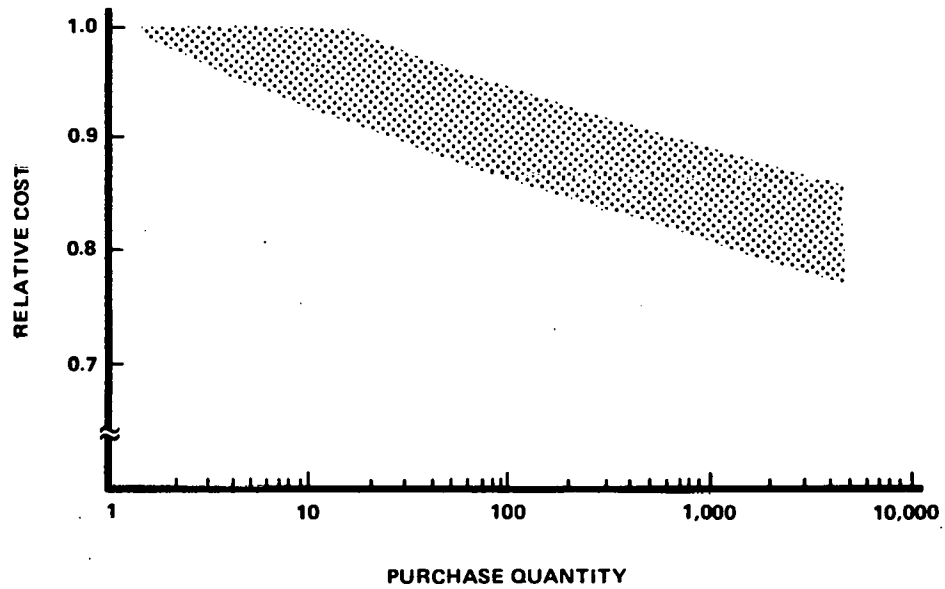
Figure 3-43 Relative Varistor Cost versus Purchase Quantity

the two located at the branch circuit terminal box. Figure 3-45 shows a similar set of curves for horizontal axis arrays, with a 20-foot span.

The costs shown are (large volume) purchase prices, not installed costs. All other array efficiencies and sizes considered are bounded by the curves shown. The cost of protecting against direct strikes (i.e., if overhead dc power collection wiring were used) would increase the costs shown by a factor of about 15 (using a commercially available device).

It can be seen from the data in Figures 3-44 and 3-45 that the cost for locating one varistor at each array is relatively constant for a given array size and efficiency, and that the costs of only providing two varistors per branch circuit vary inversely with branch circuit power. However, the level of protection is not the same in the two approaches. This is also true for the case of one device per array. The object of the surge suppressor is to protect expensive equipment (e.g., the arrays and/or cells). In comparing alternatives, the level of protection should be constant (or at least a parameter). The constant should reflect the dollar amount of equipment protected, not the number of items protected. That is to say, the protection should be applied to fixed power (e.g., 50 kWp) and not on a per array basis, where value varies with array size and efficiency.

Where and how many surge protectors to install requires an analysis of the surge-causing lightning effects (Ref. 3-14) and specific array design configurations. An analysis of this type was attempted, as a part of this study, for horizontal axis, fixed-tilt arrays, but proved to be too complex to be completed within the scope of the present study.
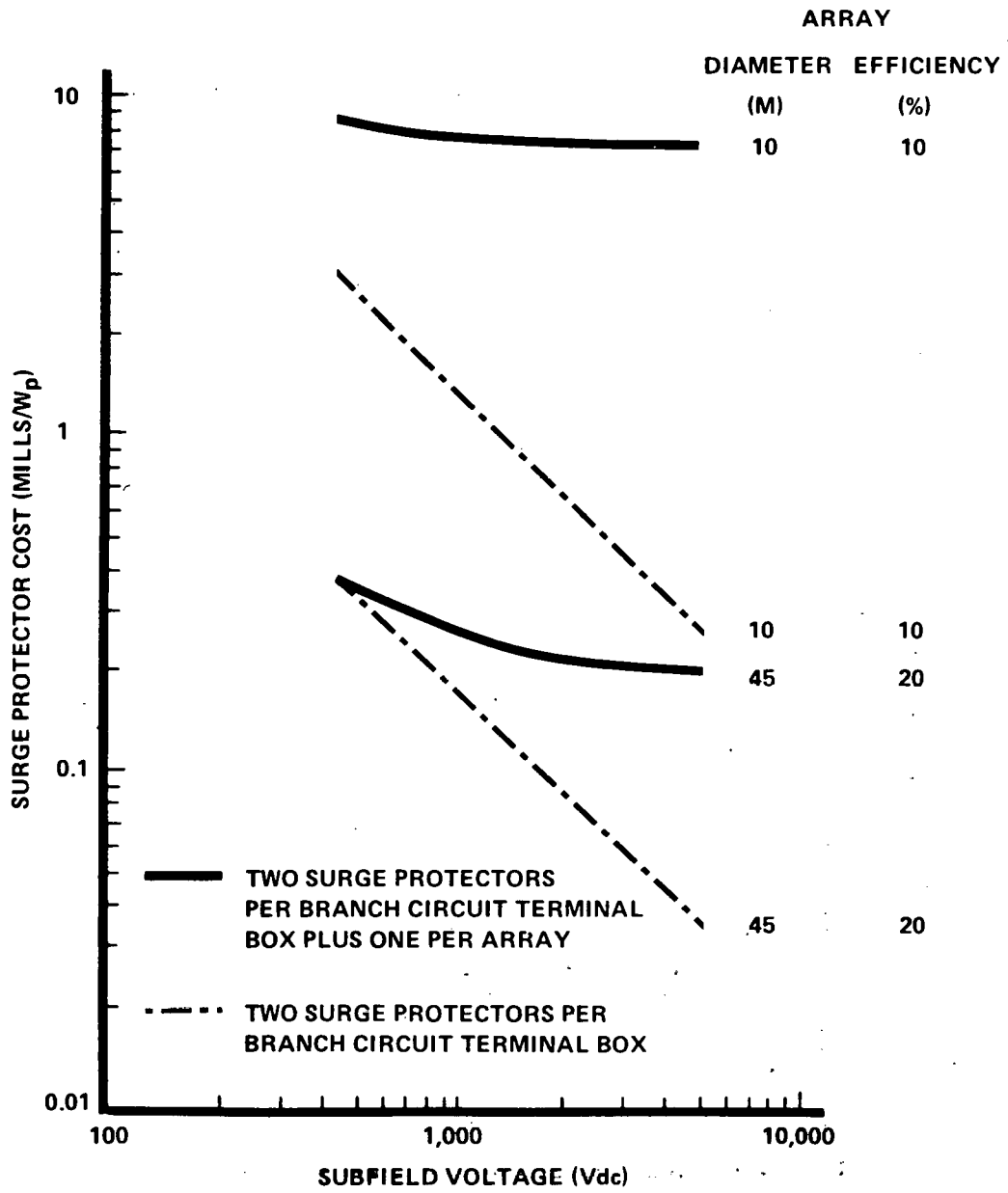
Figure 3-44 Surge Protector Costs Versus Vertical Axis Array Subfield Voltage
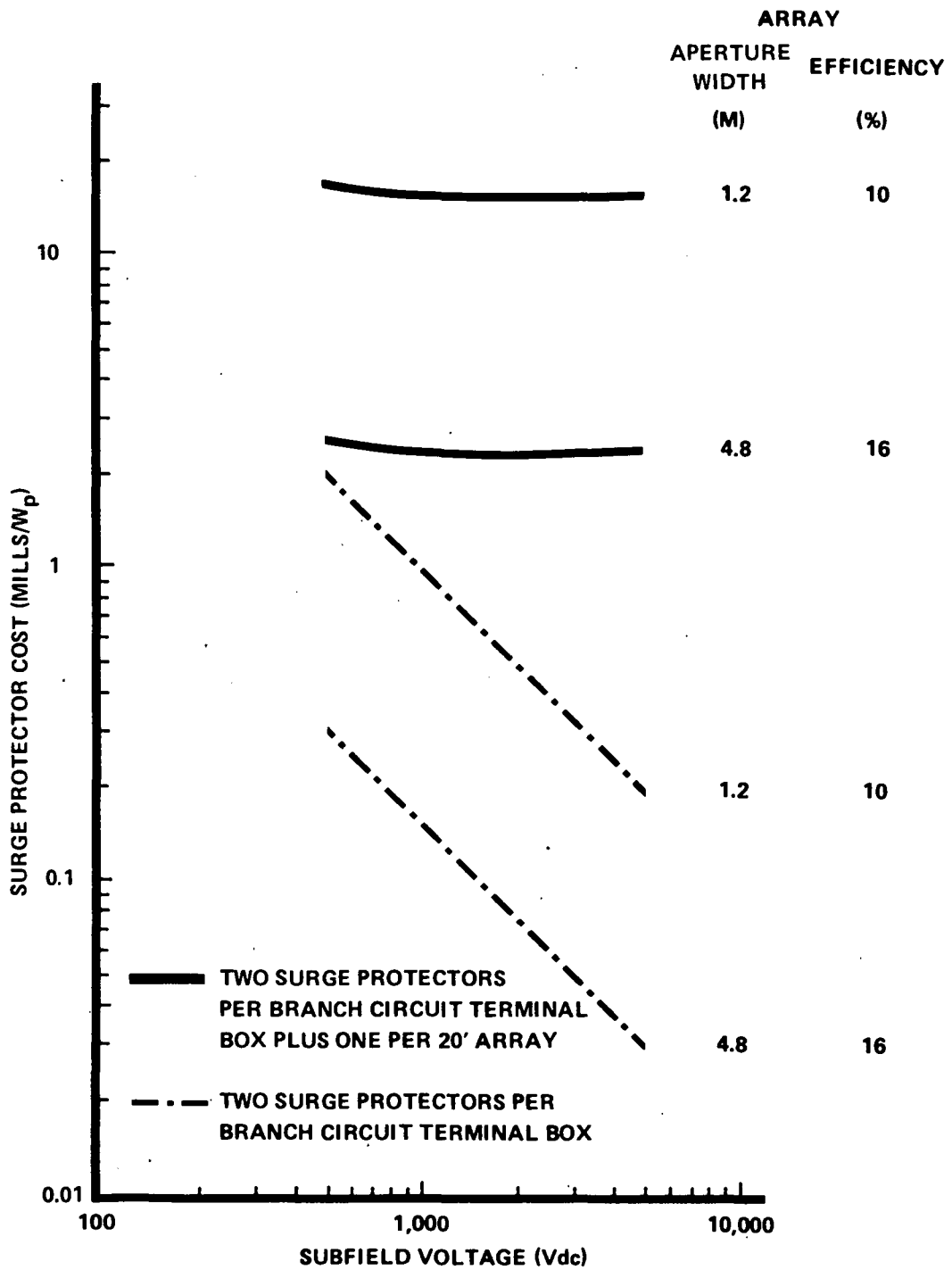
Figure 3-45 Surge Protector Costs Versus Horizontal Axis Array Subfield Voltage

Preliminary results of that analysis indicated that:

- Both radiated and conducted surges should be considered simultaneously.

- Conducted surges require analysis of current available to be conducted from the ground into the array structure, and not just the ground potential caused by conductive surge currents.

- In addition to other parameters, cell-to-ground capacity should be considered. This factor combined with bus and structure inductance can lead to oscillations.

- Traveling wave and time delay effects should be considered in large plants.

- The major factor in protecting modules is the instantaneous voltage across module dielectric insulating materials.

- Ac systems are adequately protected by use of commercially available surge suppressors and prevailing design practice.

- A variety of surge protection devices suitable for dc applications is commercially available in the 500 to 5000 volt range from several manufacturers.

- The cost of such devices is a strong function of their energy withstanding capability and a moderately weak function of voltage.

- Surge protection cannot likely be optimized as a function of subfield size and should not be optimized as a function of subfield voltage (since this leads to poor and perhaps inadequate protection).

- Further analysis is required to define criteria as to acceptable levels of protection (e.g., dollar loss per year due to lightning versus life cycle costs of surge protection).

- Correspondingly, further analysis is required to determine the size and location of surge protective devices within the dc power subsystem.

3.6   CONTROL, INSTRUMENTATION, AND AUXILIARY POWER WIRING

The requirements for control, instrumentation, and auxiliary power wiring are

significantly affected by specific array design characteristics and, to a

lesser extent, by application specific factors. Where required, the field installed wiring necessary for these functions could likely be installed in conjunction with the dc power collection wiring.

Previous studies (e.g., Ref. 3-18) indicate that costs may be in the range of $0.01 to $0.02 per peak watt for ac array tracking power wiring subsystems and $0.01 per peak watt for instrumentation and array control wiring subsystems. It is likely that these costs would be affected by array diameter, array efficiency, and other system specific characteristics in a manner similar to that discussed in Section 3.2 for the dc wiring subsystem.

Due to the array and application specific nature of these subsystems, they were not addressed in detail during this study. Identification of design requirements and subsystem optimization studies should be conducted during the detailed design of specific photovoltaic power systems.

3.7   INSTALLATION COST REDUCTION TECHNIQUES

The data presented in the previous subsections generally indicate that, for optimized designs, the costs for the field-installed wiring subsystems will be an acceptably small percentage of total plant costs. However, additional cost reductions may also be obtained by the application of appropriate fabrication and installation techniques. Such techniques can result in overall system cost savings by reducing the amount of installation labor required in the field, and by improving labor productivity.

Installation cost reduction techniques can be broadly grouped into two categories:

- Factory prefabrication
- Field installation.

3.7.1   Factory Prefabrication

One method of reducing installation costs is to maximize the use of
factory prefabrication and assembly techniques. The cost of factory
labor can be significantly less than the cost to accomplish the
same tasks in the field using construction labor. For example, a
recent study (Ref. 3-2) of module electrical termination design requirements
used rates of $9.70 and $19.15/hr for factory and field labor, respectively.
In addition, factory settings are generally more amenable to the use of
automated equipment (e.g., wire crimping machines) than is an outdoor
construction site.

Finally, various characteristics of field construction, such as weather
variability and the physical distances that must be traveled to accomplish
repetitive construction operations in place, generally result in reduced
labor productivity.

Various components of the field installed wiring subsystems, such as array
and branch circuit dc wiring and branch circuit terminal boxes, should be
amenable to factory prefabrication.

For example, the dc wiring subsystem cost breakdown presented in Figure 3-6(a)
indicates that the field costs for terminating the array and branch circuit
dc wiring conductors is about 12% of the total installed cost of the wiring.
Approximately 85% of this cost is for the labor required to strip the
conductors, crimp the terminal lugs, and bolt the connections. Therefore,

cost reductions could potentially be realized by precutting and stripping the wires, and crimping the terminal lugs in a factory.

Similarly, diodes, fuses, switches, surge suppressors, and other equipment could be factory-preassembled into branch circuit terminal boxes prior to shipment to the field for installation on the arrays.

3.7.2 Field Installation

The cost of installing the wiring subsystems can be 50%, or more, of the total subsystem costs discussed in the preceding subsections. The principal installation cost component for these baseline scenarios is the cost of the labor necessary to install and terminate the wires. Therefore, efforts to reduce the installation costs should logically focus on techniques that reduce field labor requirements and/or increase field labor productivity.

The applicability and cost effectiveness of such techniques are often influenced by application specific factors, such as array design and soil characteristics. For example, the baseline scenarios postulated during this study use underground, direct buried conductors installed in open trenches. Digging the trenches is accomplished using ladder-type trenching equipment. An alternate technique would be to use a cable plow. The use of a cable plow can result in an installation at the desired grade, with a minimum effort and with little disruption to the surrounding area. Installation rates of up to 76 meters per minute are possible (Ref. 3-19). However, a recent survey (Ref. 3-20) indicated that during 1978 and 1979, only about 5.5% of the underground residential distribution (URD) cable installed by U.S. electric utilities was plowed in. The remainder was

installed in trenches (of which approximately 90% was direct buried).
Reasons for the limited use of plowing include the variability of soil
conditions and the relative lack of maneuverability required in many
applications, such as cable installation in residential subdivisions.

The use of cable plows for photovoltaic power system wiring installation
could have economic advantages, especially if the wiring is installed prior
to array foundation and support structure installation. However, design-
specific requirements, such as the need to install numerous, relatively
short, wire lengths to interconnect vertical axis arrays might negate any
potential cost savings. Also, where many branch circuit feeders are routed
in parallel to the PCU, especially in a large subfield, the digging of a single
trench might result in a more economic installation than would the plowing
of numerous individual circuits.

The use of labor reducing subsystem components and hardware can also result
in installation cost reductions. An example of this approach is the use of
innovative, mechanically fastened connectors to replace the exothermic welding
process conventionally used to interconnect grounding grid conductors (Ref.
3-21). These connectors can be installed in any type of weather using
standard tools. A field comparison between the two connection methods,
conducted by an electric utility company, revealed a 65% decrease in instal-
lation costs using the mechanical connector (Ref. 3-21).

A third method of reducing installation costs, and one that should be given
careful and thorough evaluation during detailed system design, is the inte-
grated design and construction of the various subsystems. For example, if
underground dc wiring conductors were installed in trenches, it would be

logical (as well as technically advantageous) to overlay the grounding grid

conductors in the same trenches, wherever possible. It may also be possible,

depending on array support structure design characteristics, to install

a part or all of the wiring in array support structure foundation excavations.

Section 4

POWER CONDITIONING EQUIPMENT

Most PV systems require some type of interface between the array dc output
terminals and the load to provide voltage matching, dc/ac inversion, or
other power conditioning functions. For this study the power conditioning
subsystem, sometimes referred to as the power conditioning unit (PCU),
is defined to include all equipment necessary to receive the dc power
outputs of all branch circuit feeders and deliver ac power of acceptable
quality to the PV system load.

This section presents the results of a study, performed by United Tech-
nologies Corporation (United) under subcontract to Bechtel, to assess
dc to ac power conditioning equipment for use in solar photovoltaic
power systems. United provided parametric cost and efficiency data for
megawatt-scale power conditioning equipment for a range of dc voltages
and power levels relevant to the other portions of this study. In
addition, studies were performed to determine the effects of dc voltage
window and the use of dc up-converters on power conditioning subsystem
cost and efficiency. A technical assessment of line-commutated versus
self-commutated converters was also made. Further details of PCU char-
acteristics are also presented in the appendix.

Where possible, existing sources of information regarding power conditioning
equipment were used. In addition, a number of existing United proprietary
computer programs were used to estimate PCU design requirements, costs,
and efficiencies.

Cost estimates were based on component costs determined during a previous United study, EPRI RP841-1 (Ref. 4-1), corrected to 1980 dollars. In addition, it was specified that the power conditioning equipment shall:

- Be for mature, large-volume production (100 units/year), without development costs

- Be suitable for connection to groups of photovoltaic arrays with typical I-V (current versus voltage) curves

- Include a maximum power tracking capability

- Not inject disruptive levels of ripple current into the arrays (ripple $\leq$ 5% rms)

- Provide an output voltage of 34kv, 3 phase

- Be capable of operation with multiple units connected in parallel on the ac side

- Include all appropriate control and protective equipment and/or subsystems

- Have an ouput compatible with proposed utility standards and operate in parallel with utility lines (THD $\leq$ 5% fundamental, per Ref. 4-2)

- Either deliver power at unity power factor over the entire operating range, or include power factor correction equipment that will maintain unity power factor at the utility interface.

A technology basis year of 1986 (e.g., to establish thyristor and other component performance characteristics) was chosen to reflect the probable time of early application of large, solar photovoltaic power systems on utility grids.

Unless otherwise noted, system efficiency was calculated at the nominal dc voltage for both full- and part-load, where nominal voltage is the midpoint of the voltage window. Voltage window is the ratio of maximum to minimum operating dc voltage.

Selling price estimates include all equipment required for the PCU. A 50% markup (Ref. 4-3) over manufacturing costs (parts and labor) was used for all components except:

- Self-commutated converters: output transformer
- Line-commutated converters: output transformer, harmonic filters, and power factor corrrection equipments.

It is assumed that these nonmarked up components would be purchased directly by the utility or company installing the solar power system, rather than being furnished by the converter manufacturer, but their costs are included in the PCU selling price. Changes in these assumptions can, of course, affect estimated selling prices (e.g., if the markup were higher or lower), as well as economic comparisons between line- and self-commutated converters (e.g., if output transformers, harmonic filters, and power factor correction capacitors were also procured and marked up by the PCU manufacturer). Estimates of PCU installation costs are presented in Section A.10 of the appendix.

The remainder of this subsection presents:

- A parametric analysis of selling price and efficiency for both line- and self-commutated converters over a range of dc voltage and power levels
- A parametric analysis of the effect of dc voltage window on PCU selling price and efficiency

- An investigation of the effects on selling price and efficiency of using dc-dc up-converters between the branch circuit feeders and the dc-ac converters

- A comparative assessment of line- and self-commutated converters for use in PV power systems.

4.1   PCU COST AND EFFICIENCY VERSUS DC VOLTAGE AND POWER

Dc voltage and power ratings can affect PCU selling price in terms of dollars per peak kilowatt, as well as PCU full- and part-load efficiencies. Therefore, to facilitate identification of optimum array subfield dc voltage and power levels, cost and efficiency data were generated for the range of PCU dc voltage and power levels illustrated in Table 4-1.

Appropriate converter system configurations, covering the entire parameter range, were selected using both self-commutated inverter (SCI) and line-commutated inverter (LCI) technologies.

It should be noted that the PCU power ratings listed in Table 4-1 are presented in terms of ac power output at full load (and unity power factor). Therefore, full-load dc input power ratings for specific designs will be somewhat higher, the actual value depending on full-load efficiency.

As shown in the table, PCU ac power ratings ranging from 1 to 25MW and nominal dc voltages ranging from 600 to 5000 volts (depending on PCU power rating) were investigated. As a baseline, a voltage window of 1.5 was selected, where the nominal dc voltage represents the midpoint of the operating voltage range. The voltage window is defined as the ratio of maximum to minimum operating voltage. For example, a value of 1.5 and $V_{dc(nominal)}$ = 1000 volts yields a range of $V_{dc(min)}$ = 800 volts to

Table 4-1

PCU DC VOLTAGE AND POWER LEVELS

Case Number	P_{ac}(MW)	V_{dc}(nominal)	V_{dc}(min)	V_{dc}(max)
1	1.0	600	480	720
2	1.0	1250	1000	1500
3	1.0	2000	1600	2400
4	2.5	1000	800	1200
5	2.5	2000	1600	2400
6	2.5	5000	4000	6000
7	5.0	1000	800	1200
8	5.0	2000	1600	2400
9	5.0	5000	4000	6000
10	10.0	1500	1200	1800
11	10.0	2500	2000	3000
12	10.0	5000	4000	6000
13	25.0	3750	3000	4500
14	25.0	5000	4000	6000

$V_{dc(max)}$ = 1200 volts. Effects of decreasing the voltage window are discussed in Section 4.2.

The SCI design used in the analyses is based on United's advanced high-frequency bridge, which is presently under development (Refs. 4-4 and 4-5). This converter provides full four-quadrant operation. It delivers full-rated real power at unity power factor (PF = 1.0), hence no PF correction is required. It requires no filters, since harmonics are controlled in the bridge by pulse-width modulation (PWM) high-frequency switching. It uses a utility substation type transformer. A block diagram showing the system configuration is presented in Figure 4-1. Several aspects of the system design vary over the study matrix; two important variables are:

- The number of bridges in parallel, based on power rating and dc voltage

- The number of main thyristors in series, based on dc voltage

Semiconductors used for the SCI converters were assumed to have the following ratings:

1) <u>Main thyristors for SCI converters</u>

- Forward blocking voltage = 2500 volts
- Forward current = 1500 amperes rms
- Turn-off time = 60 microseconds
- Chip diameter = 77 mm
- Maximum power dissipation = 2000 watts
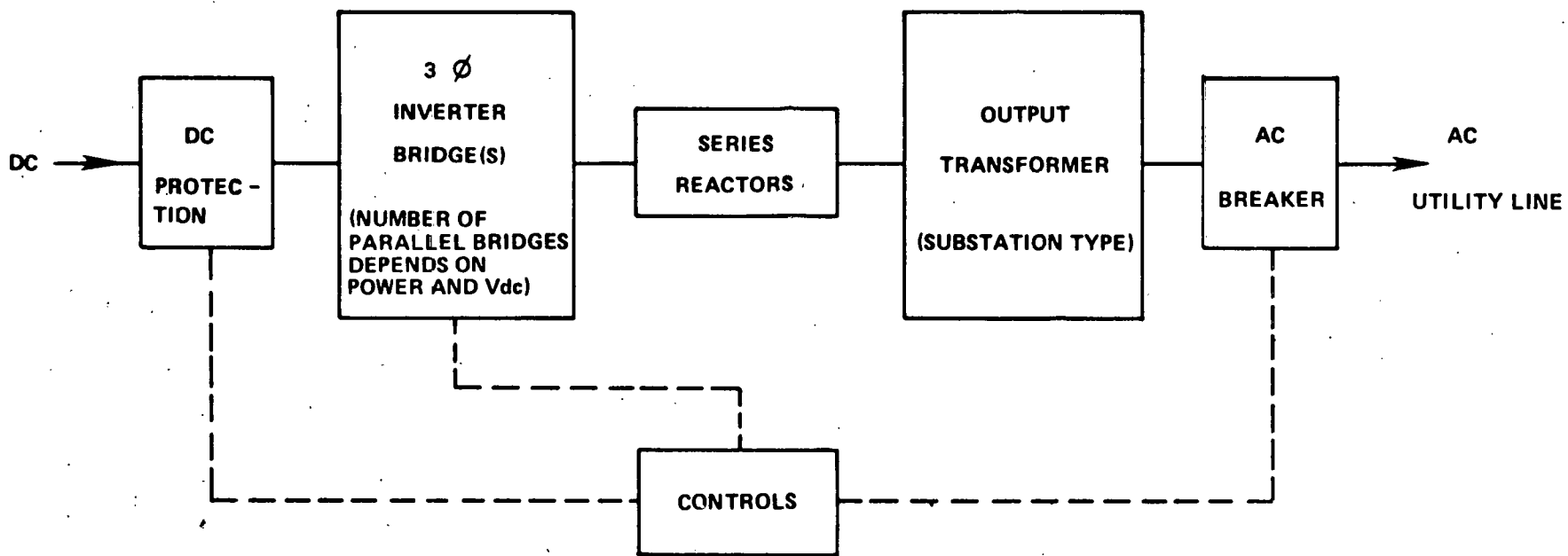
Figure 4-1 SCI System Configuration

2) <u>Commutation thyristors for SCI converters</u>

- Forward blocking voltage = 1500 volts
- Forward current = 1000 amperes rms
- Turn-off time = 50 microseconds
- Chip diameter = 53 mm
- Maximum power dissipation = 1500 watts

LCI designs are of the Graetz bridge type, with the number of bridges in series and/or parallel varied according to power and voltage level. A twelve-pulse configuration was used to minimize the harmonic filtration requirements, except for the lower-power systems, where a single 6-pulse bridge would suffice to handle the power. In these cases, it was assumed that the cost of adding 5th/7th harmonic filters was not as great as the cost of an added bridge and more complex controls and output transformer. Figure 4-2 shows a typical 12-pulse LCI system configuration. Solar photovoltaic applications of LCI converters are described in more detail in Refs. 4-6 and 4-7, and LCI system analysis is discussed in Refs. 4-8 and 4-9. The following assumptions were used regarding main thyristors (SCR's) for the LCI converters:

1) <u>Main thyristors for lower-power LCI converters</u>

- Forward blocking voltage = 3000 volts
- Forward current = 1000 amperes rms
- Chip diameter = 53 mm
- Maximum power dissipation = 1500 watts
- Turn-off time = 150 microseconds

2) <u>Main thyristors for higher-power LCI converters</u>

- Forward blocking voltage = 3000 volts
- Forward current = 1500 amperes rms
- Chip diameter = 77 mm
- Maximum power dissipation = 2000 watts
- Turn-off time = 250 microseconds
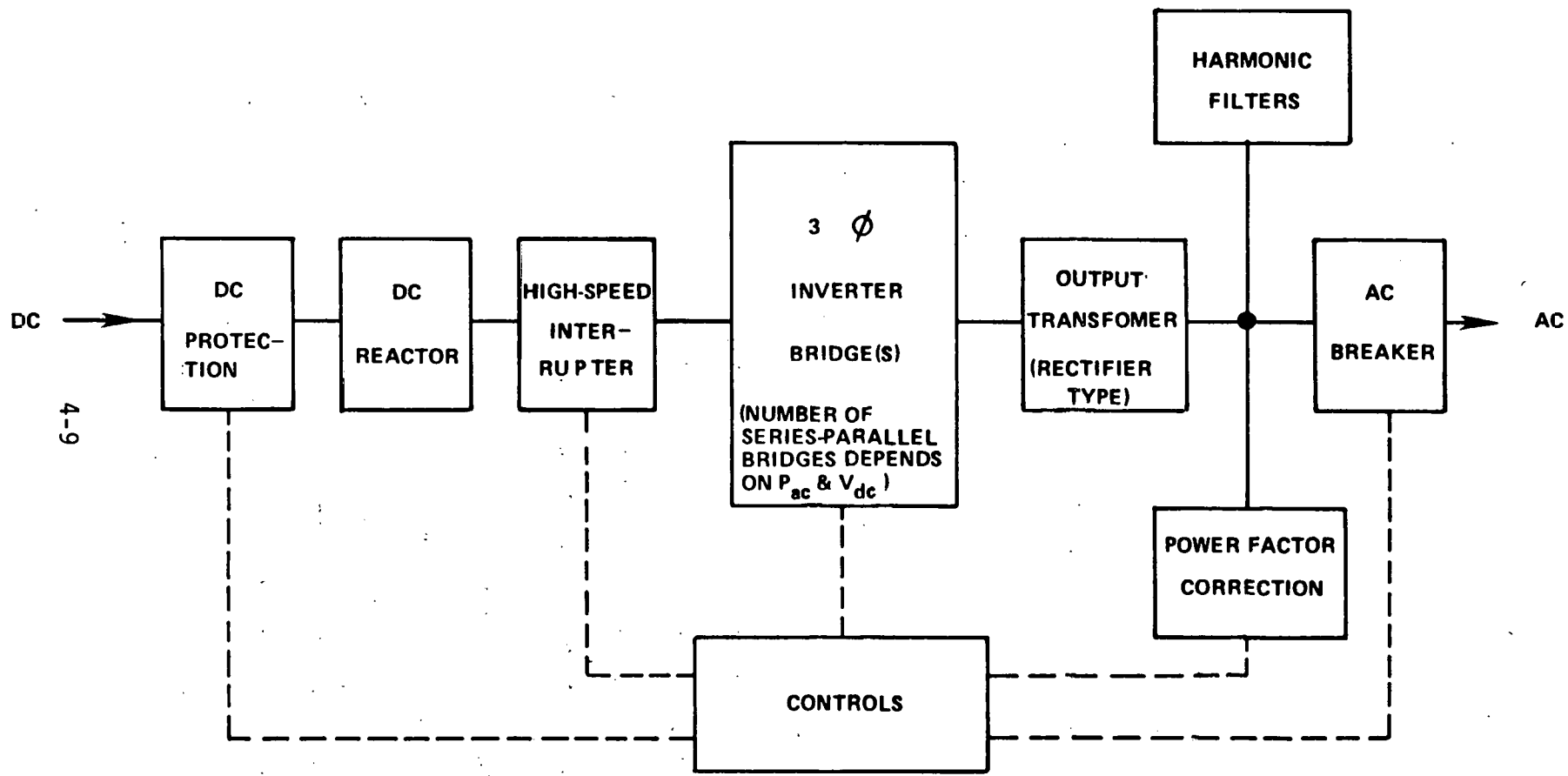
Figure 4-2 LCI System Configuration

Using the above assumptions and design parameters, United's converter design and evaluation computer programs were used to generate PCU design requirements, costs, and efficiencies. Where necessary, hand calculations were used to supplement the computer analysis.

Cost estimates were based on EPRI RP841-1 data (Ref. 4-1), which was expressed in 1977 dollars. This was converted to 1980 dollars, assuming constant 8% inflation per year for 3 years. Thus,

$$1980 \ \$ = 1977 \ \$ \times (1.08)^3 = 1977 \ \$ \times 1.26$$

Converter system efficiency was evaluated by first determining losses for all system components. Then, system efficiency was calculated as follows:

$$\text{SYSTEM EFFICIENCY (\%)} = 100 \times \frac{P_{ac}}{P_{ac} + \text{component losses}}$$

4.1.1 PCU Selling Price

Estimated selling prices, for the range of PCU parameters listed in Table 4-1, are presented in Table 4-2 for both SCI and LCI systems. The prices are expressed in ranges to account for variations in design specifics, component costs, and other uncertainties.

It can be seen that, for equivalently designed systems, the SCI converters are 15% to 20% less costly than the LCI converters over most of the study matrix, except for the 1MW, 600 $V_{dc(nom)}$ systems, which are about equal in cost. This overall cost difference is primarily attributed to the LCI system requirements for PF correction, harmonic filters, larger rectifier-type output transformers, and static bypass (emergency commutation)

Table 4-2

SCI - LCI PRICE COMPARISON

Case	P_{ac} (MW)	$V_{dc(nom)}$ (volts)	SCI System Cost (1980$/kW) Min	Max	LCI System Cost (1980$/kW) Min	Max
1	1.0	600	85	94	87	96
2	1.0	1250	75	83	91	100
3	1.0	2000	83	92	94	104
4	2.5	1000	60	66	77	86
5	2.5	2000	72	79	78	86
6	2.5	5000	73	81	82	90
7	5.0	1000	51	55	61	67
8	5.0	2000	52	57	59	65
9	5.0	5000	49	54	60	66
10	10.0	1500	45	50	51	57
11	10.0	2500	43	48	52	57
12	10.0	5000	44	49	51	56
13	25.0	3750	36	40	46	51
14	25.0	5000	33	36	47	52

Notes:
● Selling prices are for production quantities of 100 units per year

● 1.5 voltage window designs

● The above prices do not include the costs to install the PCU. It is estimated that these costs are $9.7/kW for the SCI and $16.3/kW for LCI for 10MWac, 2000 V dc units. Installation cost details and comparisons of these two types of PCU are presented in the Appendix.

switches. The total costs of these items more than offset the lower costs of the LCI bridges, resulting in higher LCI system costs.

The relative contribution of power factor correction capacitors and harmonic filters to the total LCI system selling price is illustrated in Table 4-3. The table also illustrates the cost contributions of bridges and magnetics for both SCI and LCI systems.

Of course, if increased harmonics (>5% THD) and/or operation at less than unity power factor were acceptable, these requirements, and LCI costs, would decrease somewhat. However, utility interface requirements, in terms of power factor and harmonic content, are not well defined at this time. It is reasonable to expect that, as significant levels of PV market penetration (as well as batteries, fuel cells, and other dc power sources) are attained, PCUs will be required to provide relatively high quality output power.

Of primary interest to this parametric study are the following general observations common to both SCI and LCI converters:

- Specific cost ($/kW) decreases as power level increases.

- In general, specific cost for a given power level is relatively constant over the range of dc voltages studied (except for the 1MW cases).

These trends are illustrated in Figures 4-3 and 4-4, which present converter costs (the midpoints of the ranges presented in Table 4-2) as a function of nominal dc voltage for SCI and LCI systems, respectively. In general, the decrease in cost with increased power level is predominantly due to

Table 4-3

PCU PRICE BREAKDOWN

PCU Element	Percent of Total System Selling Price	
	LCI	SCI
Bridges, controls, protection, wiring	24-32	46-60
Magnetics	38-47	40-54
PF correction and harmonic filters	24-43	--
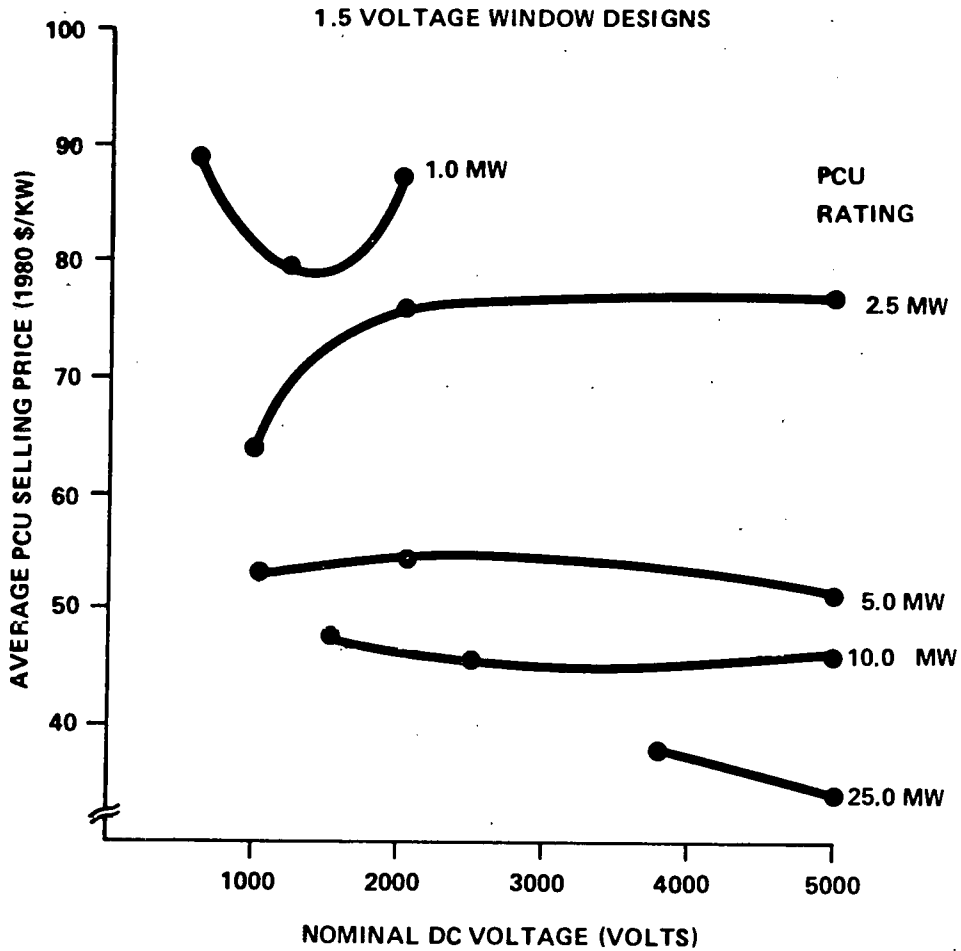
Figure 4-3 Average PCU Selling Price - SCI Systems

1.5 VOLTAGE WINDOW DESIGNS
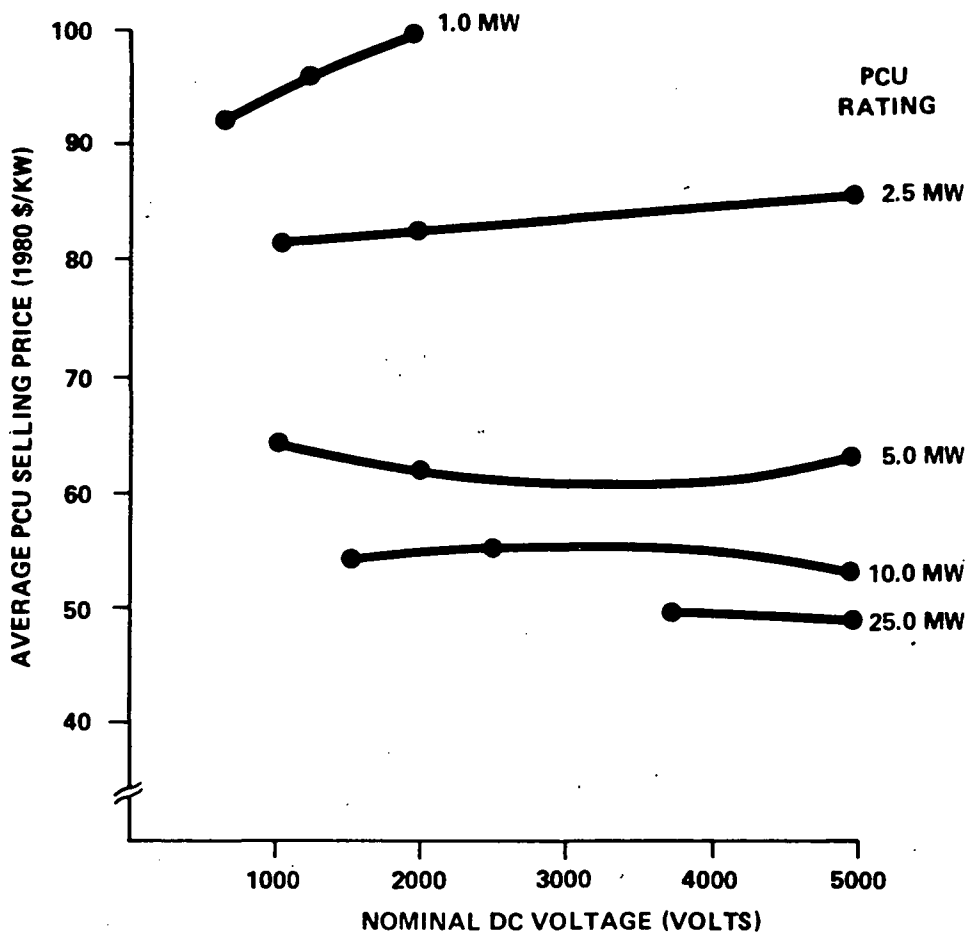
Figure 4-4 Average PCU Selling Price - LCI Systems

the same economies of scale that apply to almost all other electrical devices, since these converters are really modules of such equipment. The relative lack of variation with voltage is due to the somewhat narrow range selected (i.e., 600 - 5000 Vdc). If this range were wider, costs might tend to increase at either end due to the additional copper (and more parallel bridges) required at the lower voltages (due to higher currents), and the additional insulation (as well as more series bridges or semiconductors) required at higher voltages. These conclusions are generally supported by Reference 4-10.

4.1.2 PCU Efficiency

Loss and efficiency data were generated for all of the SCI and LCI converter systems in the study matrix. The calculated full- and quarter-load PCU efficiencies are presented in Table 4-4 for both SCI and LCI systems. LCI system data is presented as a range to account for possible variations in the designs of the harmonic filters and PF correction equipment. Since the designs of these components are somewhat site specific it was felt that losses (and hence efficiencies) should reflect the range of probable minimum to maximum component requirements. The mean value of the range of harmonic filter losses used (0.4% of rated power) is similar to the value used in the EPRI RP390-1 study (Ref. 4-10). The range of PF correction equipment losses used (0.5 to 1.0 watts/kVAR) is typical for the utility industry.

Breakdowns of the losses by major components are presented in Table 4-5 for all 14 SCI systems and in Table 4-6 for the LCI systems. These tables illustrate one of the generic differences between SCI and LCI inverters.

Table 4-4

PCU EFFICIENCY SUMMARY

Case	System Rating			PCU[1] Efficiency (Percent)					
	Power	Voltage[2]		Full Load			Quarter Load		
	MWpac	Vdc	SCI	LCI[3]			SCI	LCI[3]	
				Min	Max			Min	Max
1	1	600	95.7	95.5	96.7		94.2	93.4	96.0
2	1	1250	95.8	95.6	96.9		91.2	93.4	96.0
3	1	2000	95.6	95.6	96.8		90.7	93.2	95.7
4	2.5	1000	96.2	95.5	96.8		94.8	93.4	96.0
5	2.5	2000	95.7	95.7	96.9		93.7	93.4	96.0
6	2.5	5000	94.7	95.1	96.3		86.8	91.9	94.4
7	5	1000	96.7	96.1	96.7		95.9	94.6	95.9
8	5	2000	96.3	96.3	96.9		94.9	94.8	96.0
9	5	5000	95.1	96.5	97.1		88.5	94.7	96.0
10	10	1500	96.8	96.2	96.8		96.1	94.7	96.0
11	10	2500	96.8	96.3	96.9		96.0	94.7	96.0
12	10	5000	95.8	96.5	97.1		93.7	94.9	96.1
13	25	3750	96.7	96.4	97.0		96.0	94.8	96.1
14	25	5000	96.7	96.5	97.1		95.8	94.8	96.0

1) 1.5 Voltage Window Designs
2) Nominal dc voltage
3) Range of losses presented for power factor correction capacitors and harmonic filters represents uncertainty regarding site specific utility interface requirements

Table 4-5

SCI SYSTEM LOSSES

Case	Losses (kW)							
	Full Load				Quarter Load			
	Bridges	Magnetics	Auxiliary	TOTAL	Bridges	Magnetics	Auxiliary	TOTAL
1	20.9	14.6	9.0	44.4	7.6	5.2	2.5	15.3
2	20.8	14.5	9.0	44.3	16.4	5.2	2.5	24.1
3	22.3	14.5	9.0	45.8	17.9	5.2	2.5	25.6
4	41.1	36.3	22.5	99.9	15.2	13.1	6.3	35.6
5	54.0	36.3	22.5	112.8	22.8	13.1	6.3	41.2
6	82.1	36.3	22.5	140.9	75.6	13.1	6.3	95.0
7	55.3	72.5	45.0	172.8	14.5	26.3	12.5	53.2
8	76.8	72.5	45.0	194.3	28.6	26.3	12.5	67.3
9	140.9	72.5	45.0	258.4	124.2	26.3	12.5	162.9
10	94.8	145.0	90.0	329.8	23.7	52.5	25.0	101.2
11	91.4	145.0	90.0	326.4	25.4	52.5	25.0	102.9
12	208.5	145.0	90.0	443.5	91.9	52.5	25.0	169.4
13	258.3	362.5	225.0	845.8	64.6	131.3	62.5	258.3
14	276.5	362.5	225.0	864.0	80.5	131.3	62.5	274.2

Table 4-6

LCI SYSTEM LOSSES

Case	Losses (kW)													
	Full Load							Quarter Load						
				PF Corr. & Filters		TOTAL					PF Corr & Filters		TOTAL	
	Bridges	Magnetics	Auxiliary	Min	Max	Min	Max	Bridges	Magnetics	Auxiliary	Min	Max	Min	Max
1	6.2	17.0	9.0	1.7	15.1	33.9	47.3	1.1	6.0	2.5	0.8	8.1	10.4	17.6
2	5.8	15.6	9.0	1.7	15.1	32.1	45.5	1.2	5.9	2.5	0.8	8.1	10.4	17.6
3	6.6	15.3	9.0	1.7	15.1	32.6	46.1	1.9	5.9	2.5	0.8	8.1	11.1	18.3
4	17.2	39.0	22.5	4.2	37.8	82.9	116.6	2.8	14.7	6.3	2.1	20.2	25.9	43.9
5	15.0	37.6	22.5	4.2	37.8	79.3	112.9	3.3	14.6	6.3	2.1	20.2	26.3	44.3
6	32.4	36.6	22.5	4.2	37.8	95.6	129.2	14.4	14.5	6.3	2.1	20.2	37.2	55.3
7	34.4	82.4	45.0	8.4	40.6	170.2	202.4	5.7	31.1	12.5	4.2	21.6	53.5	70.8
8	34.4	74.3	45.0	8.4	40.6	162.2	194.4	5.7	29.1	12.5	4.2	21.6	51.5	68.8
9	26.2	71.4	45.0	8.4	40.6	150.9	183.1	6.8	28.9	12.5	4.2	21.6	52.5	69.8
10	50.3	178.0	90.0	16.8	81.2	335.1	399.5	8.0	63.0	25.0	8.4	43.1	104.5	139.2
11	44.2	164.8	90.0	16.8	81.2	315.7	380.1	9.5	62.2	25.0	8.4	43.1	105.1	139.8
12	44.2	143.9	90.0	16.8	81.2	294.8	359.2	9.5	57.9	25.0	8.4	43.1	100.8	135.5
13	102.2	394.3	225.0	42.0	203.0	763.5	924.5	16.9	154.5	62.5	21.0	107.8	254.9	341.6
14	112.9	372.7	225.0	42.0	203.0	752.6	913.6	22.3	153.1	62.5	21.0	107.8	258.9	345.7

Note: Range of losses presented for power factor correction capacitors and harmonic filters represents uncertainty regarding site-specific utility interface requirements

The SCI inverter bridge is more complex and has higher losses than an LCI bridge but the SCI inverter avoids losses in power factor correction capacitors and filters. Examination of the system efficiencies shows a number of interesting points. These will be discussed briefly in the following paragraphs.

All of the SCI and LCI systems exhibit lower efficiencies at quarter load than at full load. Also the difference between full- and quarter-load efficiencies increases with increased dc voltage. This is the result of fixed losses present in both converter systems - that is, certain losses are independent of load, as shown in Table 4-7. Also, some of these losses increase with increased dc voltage, hence the larger gap at higher dc voltages.

In general, high power systems exhibit slightly greater efficiencies than low power sytems. This trend is because at a fixed dc voltage many of the fixed losses mentioned above increase at a slower rate than the power rating of converters. Thus these losses, when expressed as a percentage of delivered power, tend to decrease somewhat as system power rating increases. For a given power rating, SCI converter efficiency decreases at both full and quarter load as the dc voltage increases. This can be explained as follows: Commutation losses and snubber losses increase with dc voltage, primarily due to the larger amounts of energy stored and released (and hence dissipated) by the circuit's capacitors ($F = 1/2\ CV^2$). Of course, load losses per component decrease with increased dc voltage, since they are conduction losses ($P = I^2R$), and the load current required for a given power output decreases as the voltage increases. However, the

Table 4-7

COMPONENTS CONTRIBUTING TO CONVERTER SYSTEM FIXED LOSSES

<u>SCI Converters</u>

- Commutation circuits (and related switching losses)

- Power semiconductor snubbers

- Magnetic cores

- Bridge cooling fans

- Controls

<u>LCI Converters</u>

- Power semiconductor snubbers

- Magnetic cores

- Harmonic filters (fundamental losses)

- PF correction (to some degree)

- Bridge cooling fans

- Controls

commutation losses increase with increased dc voltage at a faster rate than the per-component load losses decrease. Therefore, SCI converter efficiency decreases with increased dc voltage for fixed power ratings. It is important to note that this effect is far more pronounced for quarter-load operation than it is for full-load operation because at quarter-load, fixed losses are proportionately greater than load losses. In fact, within the accuracy of this study, SCI full-load efficiency is constant with dc voltage.

Except for the lower power ratings (2.5MW and below), LCI converter system efficiencies show a somewhat different trend: efficiency increases slightly with increasing dc voltage for fixed power levels. As described above, power semiconductor snubber losses increase as the dc voltage increases, and higher-voltage rated LCI converters have more power semiconductors in series. However, the decrease in load losses (due to decreased load current) at the higher voltages tends to more than offset the purely voltage-related losses. Thus, LCI converter efficiency increases slightly with increased dc voltage for both full- and quarter-load operation. Again, within the accuracy of this study, it is appropriate to note that the higher-power LCI system efficiencies are almost constant over the range of dc voltages investigated.

In the lower power ratings (1.0MW and 2.5MW), the LCI converter efficiency trends are more like those of the SCI converters, decreasing with increasing dc voltage. This is because the voltage-dependent losses are a higher proportion of the total loss than the load (current-dependent) losses. Therefore, at higher dc voltages, the increase in snubber losses is

greater than the decrease in load losses, and the system efficiency is lower.

A comparison of SCI versus LCI system efficiencies over the study matrix indicates that for most cases SCI efficiencies are comparable to LCI efficiencies at full and quarter load. That is, SCI efficiencies fall within the range of the minimum to maximum LCI efficiencies. The exceptions are the higher-voltage cases (5000 V_{dc}) where the LCI systems' mimimum efficiency estimates are somewhat higher (by at least 1%) than the SCI system efficiencies. This difference is likely to be reduced in the future, since SCI converter efficency at higher voltages is expected to increase by at least 1% with the development of semiconductors having greater blocking voltages and shorter turnoff times.

4.2   PCU VOLTAGE WINDOW STUDY

The objective of this investigation was to determine the effect of voltage window on converter system cost and efficiency. Earlier investigations (Ref. 4-1) have indicated a trend toward greater efficiency and lower specific cost ($/kW) for lower voltage windows. This study attempted to further quantify these differences. Based on a review of the dc wiring subsystem study, discussed in Section 3.2, and the cost and efficiency data presented in Section 4.1, it was decided that both SCI and LCI systems rated at 5MW 2000 volts dc would be evaluated for voltage windows of 1.1 and 1.3. Table 4-8 shows the resulting voltage ranges (minimum to maximum) and compares them with the 1.5 voltage window converter operating range.

Table 4-8

DC VOLTAGE RANGES FOR VARIOUS VOLTAGE
WINDOW CONVERTER DESIGNS

Voltage Window	Nominal Voltage	Minimum Voltage	Maximum Voltage
1.1	2000	1905	2095
1.3	2000	1740	2260
1.5	2000	1600	2400
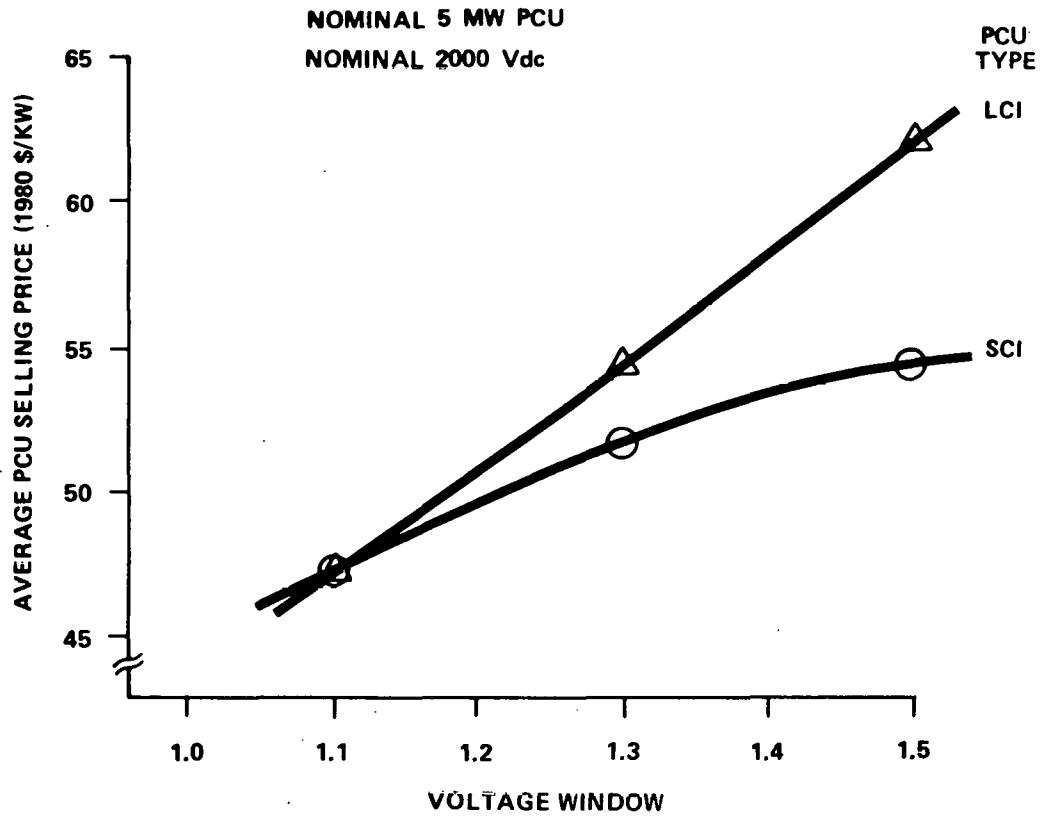
Figure 4-5 Average PCU Selling Price vs. DC Voltage Window

All other assumptions regarding the design and operation of these reduced voltage window converters are identical to those stated in Section 4.1. The same computer programs used to generate the data presented in Section 4.1 were employed to evaluate costs and efficiencies for 1.1 and 1.3 voltage window converters.

The estimated average selling prices for the SCI and LCI systems, as a function of voltage window, are presented in Figure 4-5.

Because they are designed to operate over narrower voltage ranges, the reduced voltage window converters tend to cost less and be more efficient than the 1.5 voltage window systems. Two factors are primarily responsible for these differences:

- Decreased maximum dc voltage, hence:

    - decreased voltage ratings of equipment (decreased cost)

    - decreased fixed losses (increased efficiency).

- Increased minimum dc voltage, which decreases the bridge currents, hence:

    - decreased current ratings of equipment (decreased cost)

    - decreased conduction losses (increased efficiency)

    - smaller commutation circuits for SCI systems (decreased cost and increased efficiency)

    - smaller dc reactors for LCI systems (decreased cost and increased efficiency).

In addition, the narrower dc voltage range benefits the LCI systems by increasing the power factor (PF) at which it can operate. This allows a decrease in the ratings of PF correction equipment and the output transformer.

Selling price estimates, cost breakdowns, and efficiency estimates are presented in Table 4-9 for the SCI and LCI systems. Decreasing bridge costs are the greatest factor causing SCI system costs to decrease as voltage window decreases. For LCI systems, the decreased costs for dc reactors, transformers, and PF correction equipment are responsible for decreased system costs. For SCI systems, the 1.3 voltage window system price is 5% lower, and the 1.1 voltage window system price is 15% lower than the 1.5 voltage window design. LCI systems for 1.3 and 1.1 voltage windows are 11% and 24% lower than the 1.5 voltage window selling price. It can be seen from this data, and from Figure 4-5, that the LCI selling price shows a more marked decrease with decreased voltage window. In fact, the SCI and LCI system selling prices are estimated to be nearly equal for the 1.1 voltage window design.

Efficiency trends also indicate the desirability of operating converters over narrower dc voltage windows. Both full- and quarter-load efficiencies for SCI and LCI converters increase for the lower voltage window designs by more than 0.5% for the 1.1 voltage window designs. The effects are approximately equal for both converter types, as seen in Table 4-9. In general, SCI system efficiency still falls within the range of minimum to maximum LCI system efficiencies.

Based on these results, it can be seen that the design of both SCI and LCI converters for operation over narrower voltage windows can both reduce system cost and increase system efficiency. Other studies, such as Reference 4-1, have shown similar findings.

Table 4-9

PCU VOLTAGE WINDOW STUDY SUMMARY
(Nominal 5MW, 2,000Vdc Systems)

| PCU Type | Voltage Window | Selling Price ($/kW) | Price Breakdown (Percent of Total Price) | | | Efficiency (Percent)[1] | |
			Bridges, Controls, Protection and Wiring	Magnetics	Pf Correction and Harmonic Filters	Full Load	Quarter Load
SCI	1.5	55	53	47	-	96.3	94.9
SCI	1.3	52	51	49	-	96.5	95.2
SCI	1.1	47	47	53	-	96.9	95.7
LCI	1.5	62	27	42	31	96.3 - 96.9	94.8 - 96.0
LCI	1.3	55	29	41	30	96.7 - 97.3	95.2 - 96.5
LCI	1.1	47	30	42	28	96.9 - 97.5	95.4 - 96.7

1) Range represents loss differences in power factor correction capacitors and harmonic filters resulting from site-specific utility interface requirements

4.3   DC UP-CONVERTER STUDY

The objective of this portion of the study was to investigate the effects on power conditioning subsystem cost and efficiency of using subfield-located dc up-converters between the solar arrays and a centrally located dc-to-ac converter. Such an arrangement would:

- Regulate the dc voltage at the converter input; hence, a lower voltage window converter could be used

- Step up the array output voltage, with the result of decreasing the dc bus copper requirements (decreased cost and losses) plus permitting the use of a smaller number of larger power-rated converters for the site.

In Section 4.1 of this report, it was shown that converters with higher power ratings are generally less expensive and more efficient. In Section 4.2 it was shown that a narrower voltage window also improves cost and

efficiency. Therefore, this section presents cost and efficiency estimates for combination dc-dc up-converter and unity voltage window dc-ac converter systems, in order to assess the concept.

Bechtel and United agreed upon the following assumptions for this part of the study:

- A large central converter, not HVDC, would be studied; 25MW power level was chosen

- Both SCI and LCI central dc-ac converters would be investigated

- Dc-dc up-converters would be nominally rated 5MW

- Dc input to the up-converters would be 1000 volts

- Dc output of the up-converters would be 3000 to 5000 volts.

Results of the voltage window study (Section 4.2) were used to estimate cost and efficiency of 25MW SCI and LCI converters having a 1.0 voltage window. Two up-converter designs were evaluated. One type of up-converter design (hence cost and efficiency data) was based on boost-regulator equipment designed by United for a previous program (Ref. 4-3). The other up-converter is a conventional inverter-transformer-rectifier (ITR) type dc-dc converter; its cost and efficiency were based on components used previously in the parametric study. These were incorporated into the two system schemes illustrated in Figures 4-6 and 4-7. System cost and efficiency were estimated for each scheme, using both SCI and LCI converters.

The estimated costs and efficiencies for the two schemes are presented in

Table 4-10. In general, the boost-regulator systems (Scheme 1) are considerably less expensive (by 40%) than the ITR up-converter systems (Scheme 2). However, the efficiency of the ITR up-converter systems are 4 percentage points greater than that of the boost-regulator systems at full load, and 1 percentage point greater at quarter load. These results are relatively independent of which central converter type (SCI or LCI) is used with the up-converter. Therefore, a clear-cut choice of up-converter type would depend on which factor is more important: initial cost (purchase price) or operating costs (energy losses).

The attractiveness of using dc up-converters in (large) PV power systems is discussed further in Section 5.

Table 4-10

DC UP-CONVERTER STUDY SUMMARY

SYSTEM NO.	COMPONENT	COST ($/kW) SCI	LCI	EFFICIENCY (PERCENT) FULL LOAD	QUARTER LOAD
1	DC Up-converter	12	12	94	94
	DC to AC Converter	30	35	97.6	97
	TOTAL	42	47	91.7	91.2
2	DC Up-converter				
	Inverter	23	23	99	99
	Transformer	5	5	99.9	99.9
	Rectifier	10	10	99.2	98
	DC to AC Converter	30	35	97.6	97
	TOTAL	68	73	95.6	92.2

ARRAY SUBFIELDS

DC UP—CONVERTERS (BOOST REGULATORS)

DC TO AC CONVERTER

1000 Vdc — 6.25 MWp

1000 Vdc — 6.25 MWp

1000 Vdc — 6.25 MWp

1000 Vdc — 6.25 MWp

3750 Vdc

NOMINAL 25 MWp
NOMINAL 3750 Vdc
1.0 VOLTAGE WINDOW
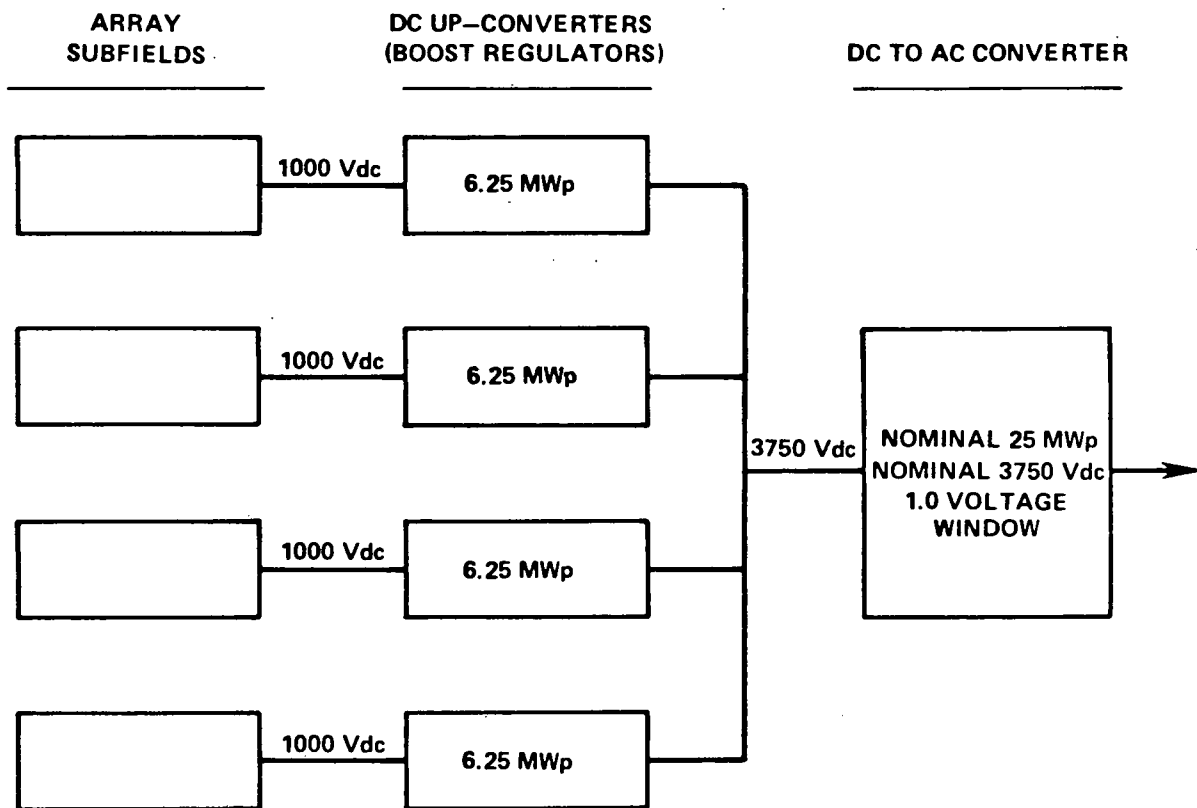
Figure 4—6 Dc Up - Converter System Configuration — Scheme I

ARRAY
SUBFIELDS

DC UP-CONVERTERS
(INVERTER—TRANSFORMER
RECTIFIER)

DC TO AC
CONVERTER

1000 Vdc   5MWp

1000 Vdc   5MWp

1000 Vdc   5MWp

1000 Vdc   5MWp

1000 Vdc   5MWp

5000 Vdc

NOMINAL 25 MWp
NOMINAL 5000 Vdc
1.0 VOLTAGE WINDOW

AC
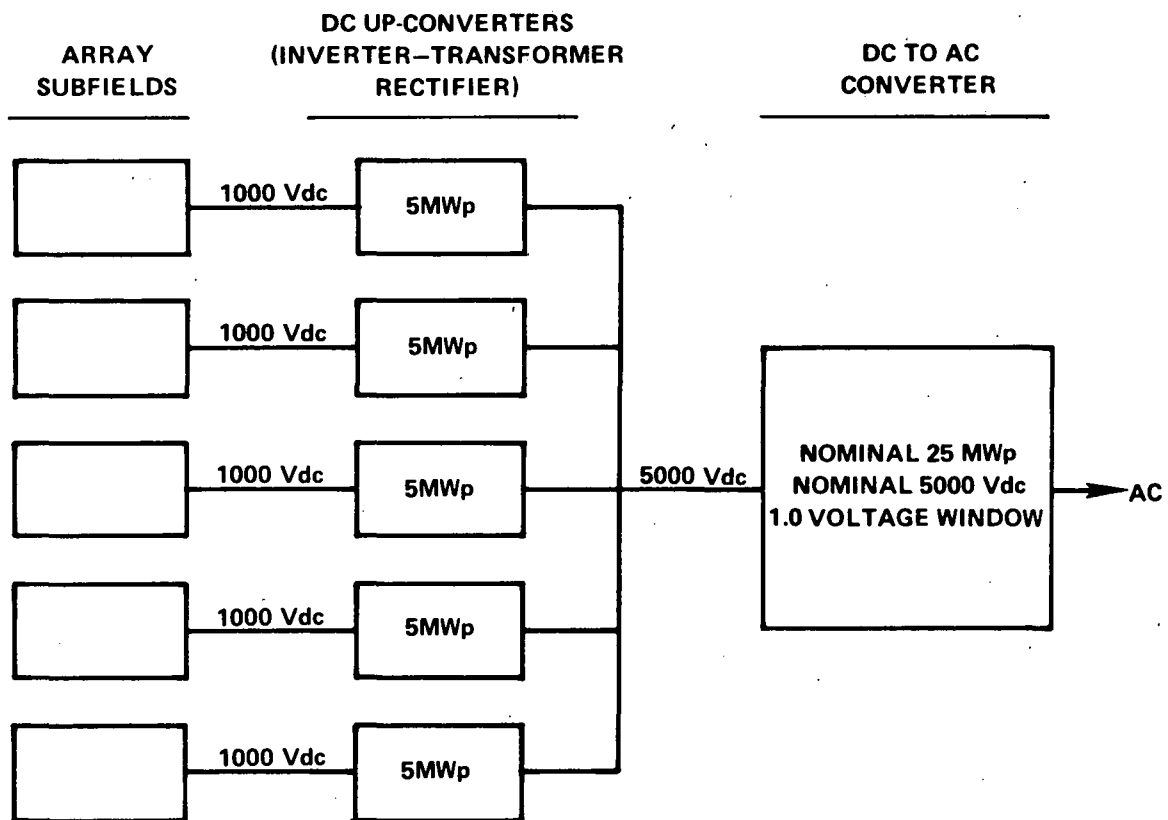
Figure 4-7 Dc Up-Converter System Configuration— Scheme II

4.4   ASSESSMENT OF SCI VERSUS LCI SYSTEM TECHNOLOGIES

Selection of appropriate PCU technology with regard to line versus self-commutated systems for use in large photovoltaic power systems requires evaluation of both economic and technical considerations. Comparisons between SCI and LCI converters often state that LCI systems are less costly and more efficient. However, these comparisons frequently ignore the fact that when an LCI system is designed to meet the same requirements and have operational capabilities similar to an SCI system, cost and efficiency differences may change drastically (Ref. 4-11). In addition, SCI converters have long been recognized as promising greater potential for improvement in cost and efficiency due to technological advances, especially in the area of semiconductor devices (Refs. 4-11 and 4-12).

This subsection presents a comparison of LCI and SCI systems, with regard to:

- First cost and operating efficiency

- Technical operating characteristics.

It is assumed throughout the following discussion that the SCI and LCI systems to be compared are designed to meet identical dc and ac interface specifications (for example, both systems must deliver rated power at unity power factor, and dc ripple and ac harmonic injection limits are the same).

4.4.1 First Costs and Operating Efficiency

Results of the parametric study discussed in Section 4.1.1 indicate that, except for the low power levels (approximately 1MW), SCI converters are 15% to 20% less expensive than LCI systems. However, the voltage window study reported in Section 4.2 suggests that this gap decreases for narrower voltage window designs and that LCI and SCI system costs may be nearly equal for 1.1 voltage window converters.

Also, SCI systems usually have fewer separate pieces of equipment to handle and connect (no filters or PF correction equipment); hence, they are likely to cost less to install than LCI systems.

Based on the data presented in Section 4.1.2, it can be seen that the full- and part-load operating efficiencies of the two converter types are also comparable, except at the highest dc voltages (5000 volts), where LCI systems exhibit slightly higher efficiencies.

It should be pointed out that the scope of this study did not permit detailed design and optimization of the entire matrix of PCU configurations reported in this study. In addition, design optimizations were not conducted with regard to the tradeoffs between PCU first costs and operating efficiency, particularly for low load operation.

In general, based on the data presented in Sections 4.1.1 and 4.1.2, there does not appear to be a distinct economic advantage for either of the two technologies. This is further illustrated in Section 5.1.1, which presents and compares total equivalent PCU costs. Therefore,

although further detailed investigation of PCU first costs and operating efficiencies is warranted, it appears that the selection of appropriate PCU technology will be influenced by factors such as technical operating characteristics.

4.4.2 Technical Operating Characteristics

Differences in design and operating principles between the LCI and SCI systems result in variations with regard to operating characteristics. In general, the SCI system provides a greater degree of flexibility with regard to several aspects of PV system design and operation. These differences are reviewed here briefly.

Reactive Energy and Power Factor. LCI systems may require substantial power factor correction (either switched capacitors or static VAR generators) to enable them to operate at unity power factor or control the exchange of reactive power (VARs) with the utility. However, the SCI system has the inherent capability to control VAR flow, and it operates at unity power factory without any additional PF correction equipment.

Harmonics. The SCI system allows better control over generated harmonics (through the use of PWM high-frequency switching); ac filters are generally not necessary. Harmonic filters for the LCI converter are often site specific designs; they must account for utility system characteristics at the point of application to ensure their proper operation and to avoid network resonance problems.

Output Transformer. LCI systems require larger, more expensive rectifier-type transformers than equivalently rated SCI systems. LCI transformers

are larger because they must carry reactive power (since the LCI bridge operates at less than unity power factor) and harmonic currents. Although the impact of these effects on the transformer may be reduced by placing the PF correction and harmonic filters on the low-voltage (converter) side of the transformer, the size and costs of the filter and PF correction components would increase. In any case, the LCI system transformer requires added bracing for the higher magnitude of fault currents that can flow (SCI systems use ac reactors that eliminate this requirement).

Protection from Utility Voltage Transients. LCI converter bridges, and therefore their power semiconductors, are subject to higher magnitudes of voltage transients passed through the output transformer from the utility line from capacitor bank switching, lightning, etc. Therefore, very large voltage safety factors (ratio of SCR string blocking voltage rating to peak line voltage) must be employed to ensure the semiconductors can survive these transients (Ref. 4-4). This increases bridge costs and losses. In SCI converters, the bridge semiconductors are isolated from utility line transients by the ac reactors. These reactors also cause the SCI system to be less likely to suffer commutation failure due to utility voltage disturbances. The SCI semiconductors are subject to voltage transients generated within the converter bridge; these are more easily controlled than utility line transients. Therefore, SCI converters may be designed with voltage safety factors of approximately 1.4 to 1.8 which are much lower than the factors of 2 to 3 required in LCI converters (Ref. 4-13).

Fault Characteristics. SCI converters can generally ride through faults more easily and are less likely than LCI systems to allow fault currents to flow from the dc source or the utility (Ref. 4-14).

4-34

Application Flexibility. SCI converters have a greater degree of flexibility than LCI converters, in that:

- SCI systems can be more easily adapted for stand-alone operation (Refs. 4-4, 4-11 and 4-14)

- SCI systems can be useful for static VAR control, even without a dc source (Refs. 4-4, 4-11 and 4-14)

- SCI systems can be easily adapted for use in systems employing battery storage, since they inherently have the capability of fast power reversal (Ref. 4-1) without using additional equipment. If an LCI system is to be used for battery charge/discharge operation, it requires reversal switchgear for dc polarity switching.

4.4.3 Summary

A clear-cut economic advantage for either LCI or SCI system cannot be identified based on the results of this study. Additional study is required to better define application-specific design requirements and associated PCU costs, especially for the LCI systems. Also, full- and part-load operating efficiencies need to be better defined to facilitate the calculation and comparison of total equivalent PCU costs.

Aside from cost and efficiency (economic) considerations, certain technical characteristics, including power factor control and harmonics injection into the ac power system, may affect the selection of appropriate PCU technology. In this respect, the SCI system has some potentially significant advantages, especially for large individual PV systems and/or for significant levels of PV penetration on a utility system.

It does not appear necessary or prudent at the present time to select one or the other of these technologies as being more appropriate for use in large PV applications. Rather, the performance of similar systems (e.g., Refs. 4-13 and 4-15) currently being designed, built, and installed for use with storage batteries, fuel cells, and other dc power sources should be closely monitored. At the same time, the design aspects of these systems that are either unique or of special interest to photovoltaic system applications, such as dc input filters, narrow voltage window, peak power tracking (or other special control requirements) and low load operating efficiencies, should also be investigated.

Subsequent to the completion of the above described work, a follow-on contract was awarded to further analyze LCI and SCI operational characteristics and estimate installation costs. These results are presented and summarized separately in the appendix.

Section 5

DESIGN TRADEOFFS AND OPTIMIZATION

The preceding two sections have presented data illustrating the effects
of various parameters on the first costs and operating characteristics of
the field-installed wiring and PCU subsystems. These data are useful in
determining optimum subsystem configurations. However, the identification
of optimum system design parameters requires consideration of the interactions
between the various subsystems as well as the effects of application
specific factors.

This section presents an analysis of these tradeoffs with regard to:

- Dc power collection subsystem

- Array spacing.

5.1   DC POWER COLLECTION SUBSYSTEM

The optimum dc power collection subsystem configuration, including the
PCU, is that which results in the minimum total cost per unit of annual
energy production. Tradeoffs in this area include evaluation of:

- Total equivalent PCU costs

- Total equivalent dc subsystem costs

- PCU voltage window

- Total equivalent dc up-converter costs

5.1.1   Total Equivalent PCU Costs

As indicated in Section 4.1, all PCU design configurations are less than 100% efficient. Therefore, a certain percentage of the dc energy generated by the solar arrays is lost in the PCU. Losses occur due to several sources, including I^2R heating, control, and other auxiliary power requirements, as well as factors such as commutation losses or losses in harmonic filters and power factor correction capacitors. To compare the various PCU design alternatives, it is necessary to evaluate their net energy efficiencies so that the total equivalent PCU costs (first costs plus the value of the losses) can be identified.

PCU Net Energy Efficiency. For a given PCU design, instantaneous efficiency is a function of the percent of full load at which the PCU is operated. This is shown in Figure 5-1, which illustrates the effects of part-load operation on PCU efficiencies for both SCI and LCI systems, nominally rated at 5MW, 2000Vdc, and a 1.5 voltage window. In general, efficiencies remain relatively high for both inverter types, down to about 10 or 20% of full load. At operating power levels below this range, efficiencies fall off rapidly as the fixed losses begin to dominate.

It should be pointed out that the low load efficiency data presented in Figure 5-1 may be somewhat lower than would be the case for actual systems. This resulted primarily from an over estimation of certain no-load losses, including auxiliary equipment and transformer no-load losses. For example, the 10% load efficiencies presented in Figure 5-1 are about 77 and 86% for SCI and LCI systems, respectively. However, subsequent evaluation of the no-load losses revealed that the 10% efficiencies might actually
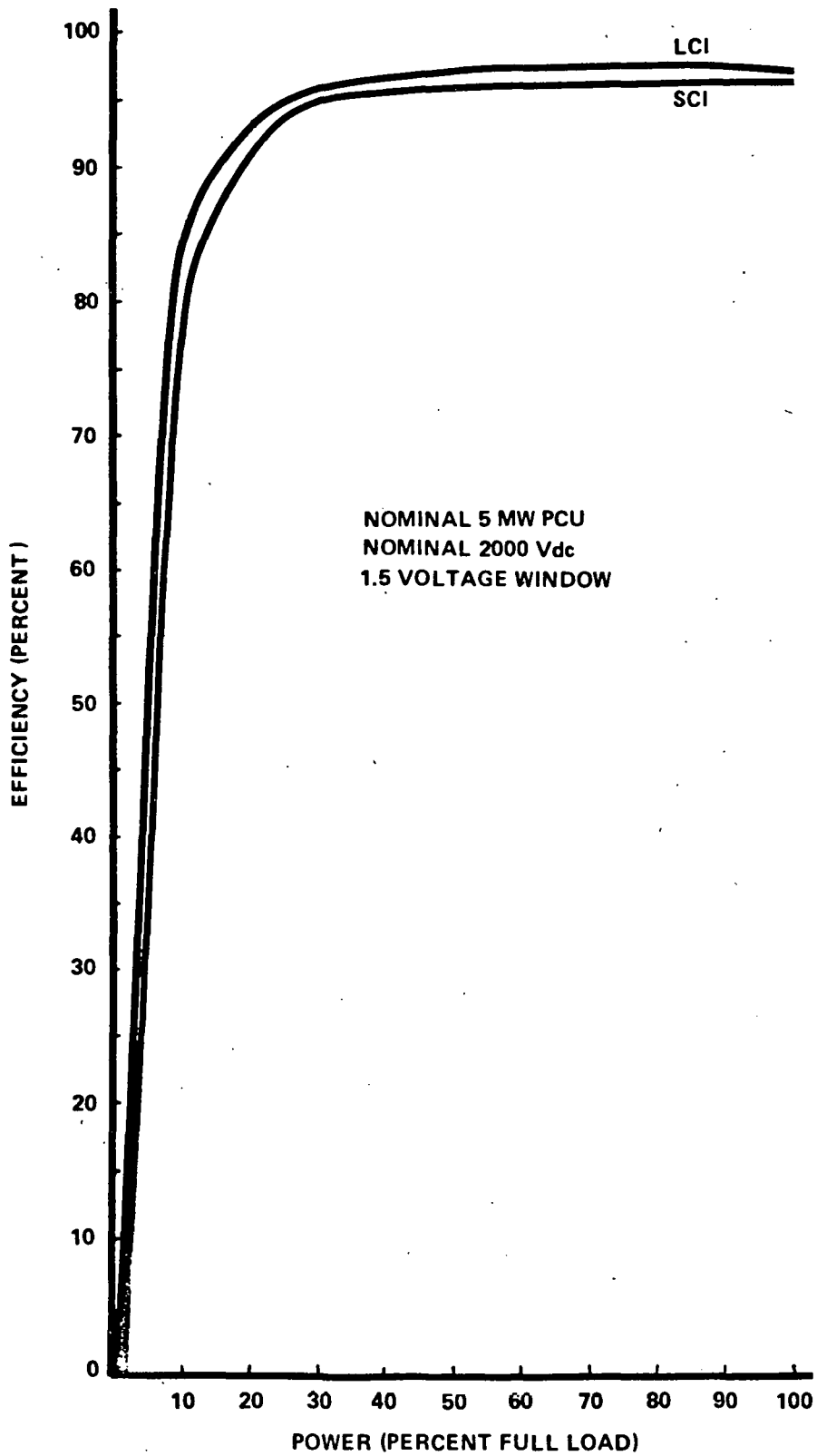
Figure 5-1 Typical PCU Efficiency Profiles

be on the order of 90% for both systems. Unfortunately, this was not discovered in time to permit recalculation of the results presented in this subsection. In general, this is not likely to affect the results of the tradeoff analysis. Net PCU energy efficiencies would increase slightly for all PCU configurations investigated in this study.

Since the available insolation, hence array output, varies during both the diurnal and yearly operating cycles, it is necessary to identify the amount of energy that is processed by the PCU at each power level. For purposes of this study, this was accomplished by evaluating SOLMET typical meterological year (TMY) insolation data for three representative geographic locations: Albuquerque, Boston, and Miami. Based on these data, Figure 5-2 presents the total yearly incident energy (kWh/m^2) as a function of power level (W/m^2), for fixed, latitude-tilted flat-plate arrays and for two axis tracking arrays, in each of the three geographic locations. Several observations can be made regarding the data in the figure. It can of course be seen that different locations receive different amounts of annual insolation. More importantly for the present analysis is the fact that the percent of total energy received at each power level can vary between locations. For example, based on the data in Figure 5-2(a), fixed, latitude-tilted arrays located in Boston receive about 8% of their total yearly insolation at power levels less than or equal to only 10% of the peak power level. Similar arrays located in Albuquerque would receive only about 3% of their total insolation at or below the 10% power level. This implies that the net PCU energy efficiencies may be lower for a system located in Boston for a similar system located in Albuquerque.
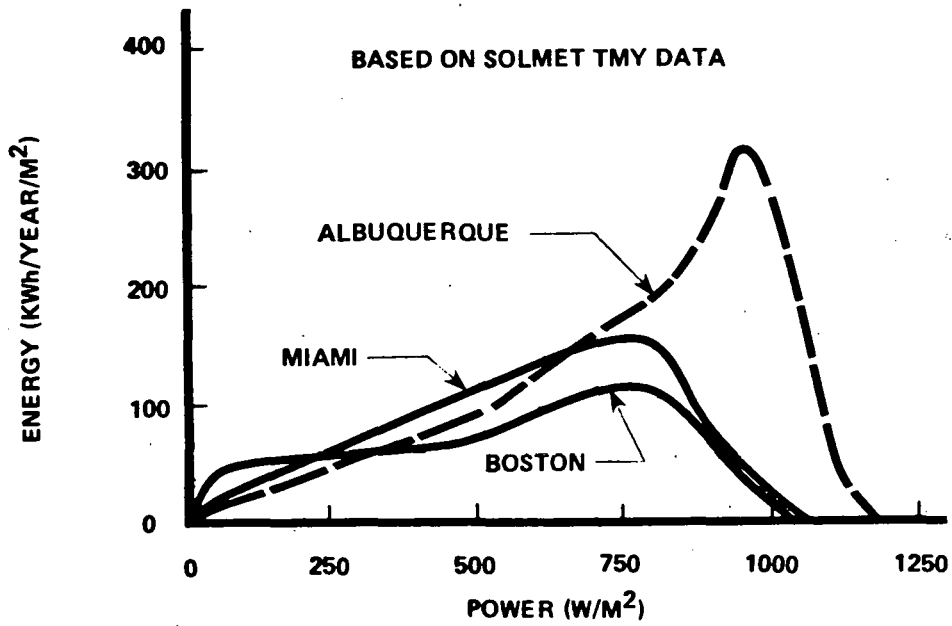
(a) FIXED LATITUDE TILTED FLAT PLATE ARRAYS
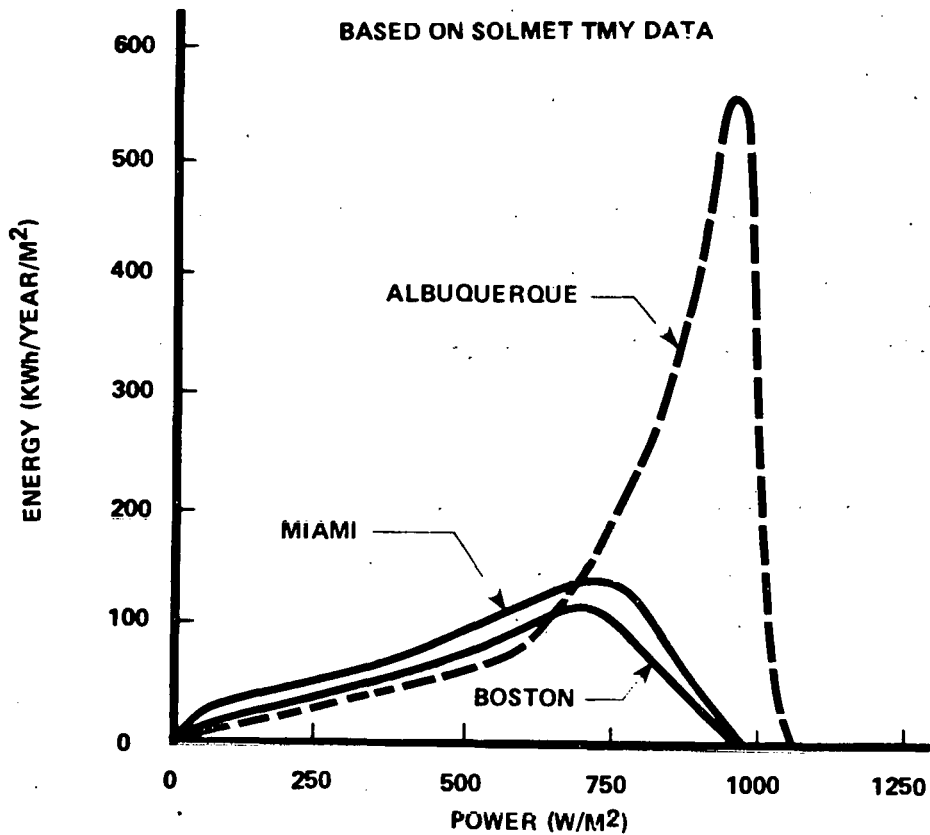
(b) TWO AXIS TRACKING ARRAYS

Figure 5-2 Yearly Insolation Profiles

The amount of energy received at or near the peak power level can also vary. For example, based on the data in Figure 5-2(a), fixed latitude-tilted flat-plate arrays located in Albuquerque receive about 3% of their total yearly insolation at power levels above 90% of peak power. Similar arrays located in Boston would receive less than 1% of their total insolation above 90% of peak power. This suggests that it may not be economically desirable to size the PCU for peak array power output and that a tradeoff exists between the PCU peak power rating and the array peak power output. Specifically, the cost savings of providing a PCU rated at less than the array peak power output can be compared to the equivalent value of the energy lost during periods when the array peak power output would be greater than the PCU rating. It should be noted that not all available energy is lost by operating the array off of its peak power point; only the difference between the PCU full-load rating and the array peak power point is lost. An additional potential benefit of undersizing the inverter is to increase the yearly operating time at higher percentages of full load, thereby improving the net energy efficiency.

Assessment of these tradeoffs, for the relatively large number of PCU configurations presented in Section 4, was facilitated by the use of a short computer program called PCUOPT.

PCUOPT combines the insolation data presented in Figure 5-2 with the PCU part-load efficiency data, such as illustrated in Figure 5-1, to calculate yearly net energy efficiencies for various ratios of PCU to array peak

power rating. The output of PCUOPT is illustrated graphically in Figures 5-3(a) and 5-3(b) for fixed, latitude-tilted and two axis tracking arrays, respectively. Figure 5-3 illustrates the differences in net energy efficiencies occurring between different locations, as well as the differences that can occur between different array types at the same location. Also indicated is the fact that for the 5MW, 2000Vdc, 1.5 voltage window designs, LCI systems generally result in slightly higher net energy efficiencies. The actual differences are somewhat affected by array type and location. Finally, Figure 5-3 illustrates that a maximum net energy efficiency is achieved for a certain ratio between PCU and array peak power (at 1 kW/m^2 insolation) ratings. Again, the specific value is affected by array type and location.

Maximum net energy efficiencies for the full range of PCU voltage and power levels (at a 1.5 voltage window) are presented in Figures 5-4, 5-5, and 5-6 for PV systems located in Albuquerque, Boston, and Miami, respectively. Net energy efficiencies for each location are presented as a function of subfield peak power (at 1 kW/m^2 insolation) for both fixed, latitude-tilted flat-plate and two axis tracking arrays, using both LCI and SCI systems with various nominal dc voltage levels. The data indicate that net PCU efficiency generally increases with increasing power and/or dc voltage levels. This is particularly evident for the SCI designs. It should be remembered that the data in Figures 5-4, 5-5, and 5-6 are based on efficiencies for PCU designs with a 1.5 voltage window.

NOMINAL 5 MW PCU
NOMINAL 2000 Vdc
1.5 VOLTAGE WINDOW

LCI
SCI

96

95

94

93

92

91

NET PCU ENERGY EFFICIENCY (PERCENT)

ALBUQUERQUE

MIAMI

ALBUQUERQUE

BOSTON

MIAMI

BOSTON

80

100

120

INVERTER RATING (PERCENT ARRAY PEAK POWER AT 1 kW/m^2 INSOLATION)
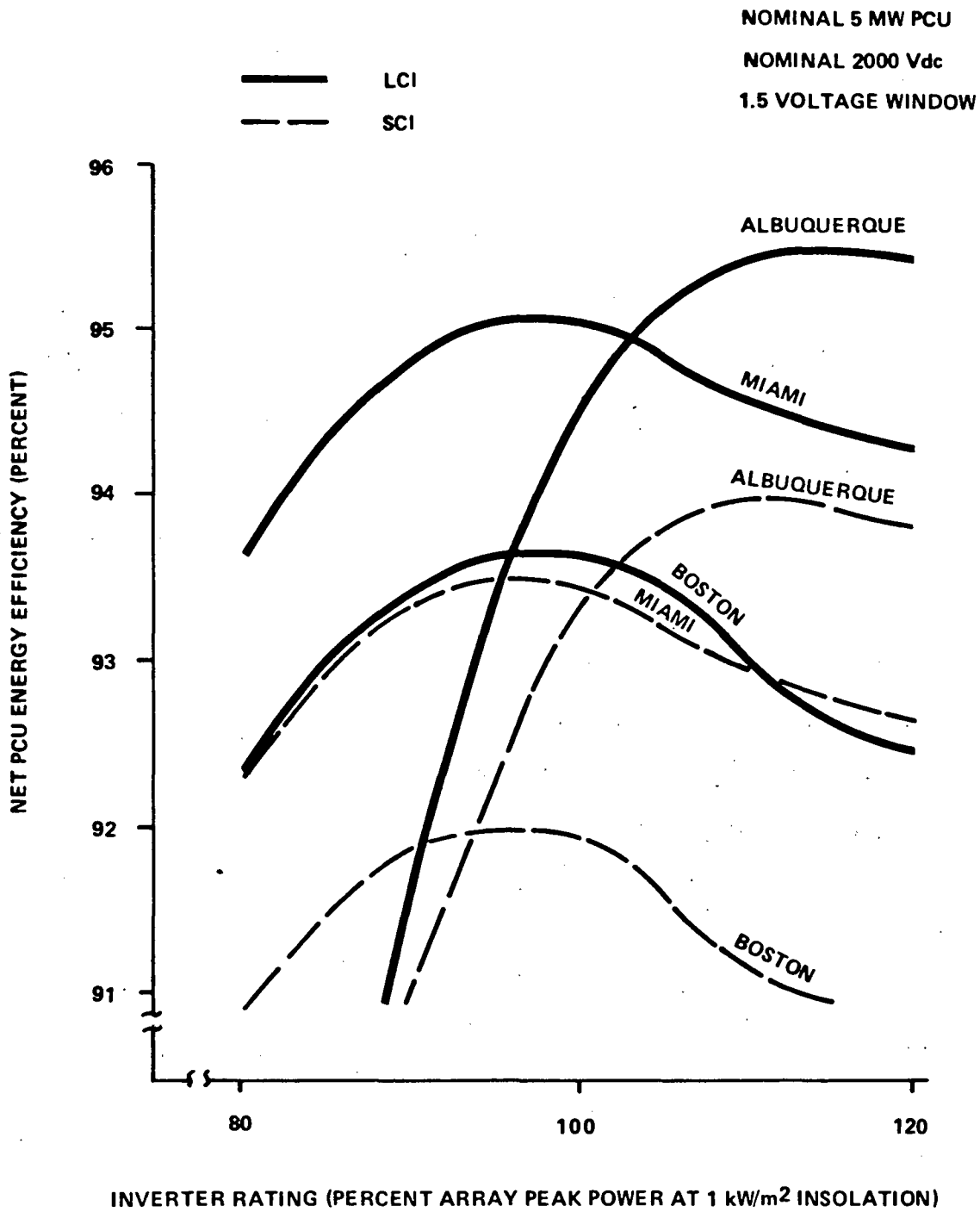
Figure 5-3 (a) Typical Net PCU Energy Efficiency - Flat Plate Arrays
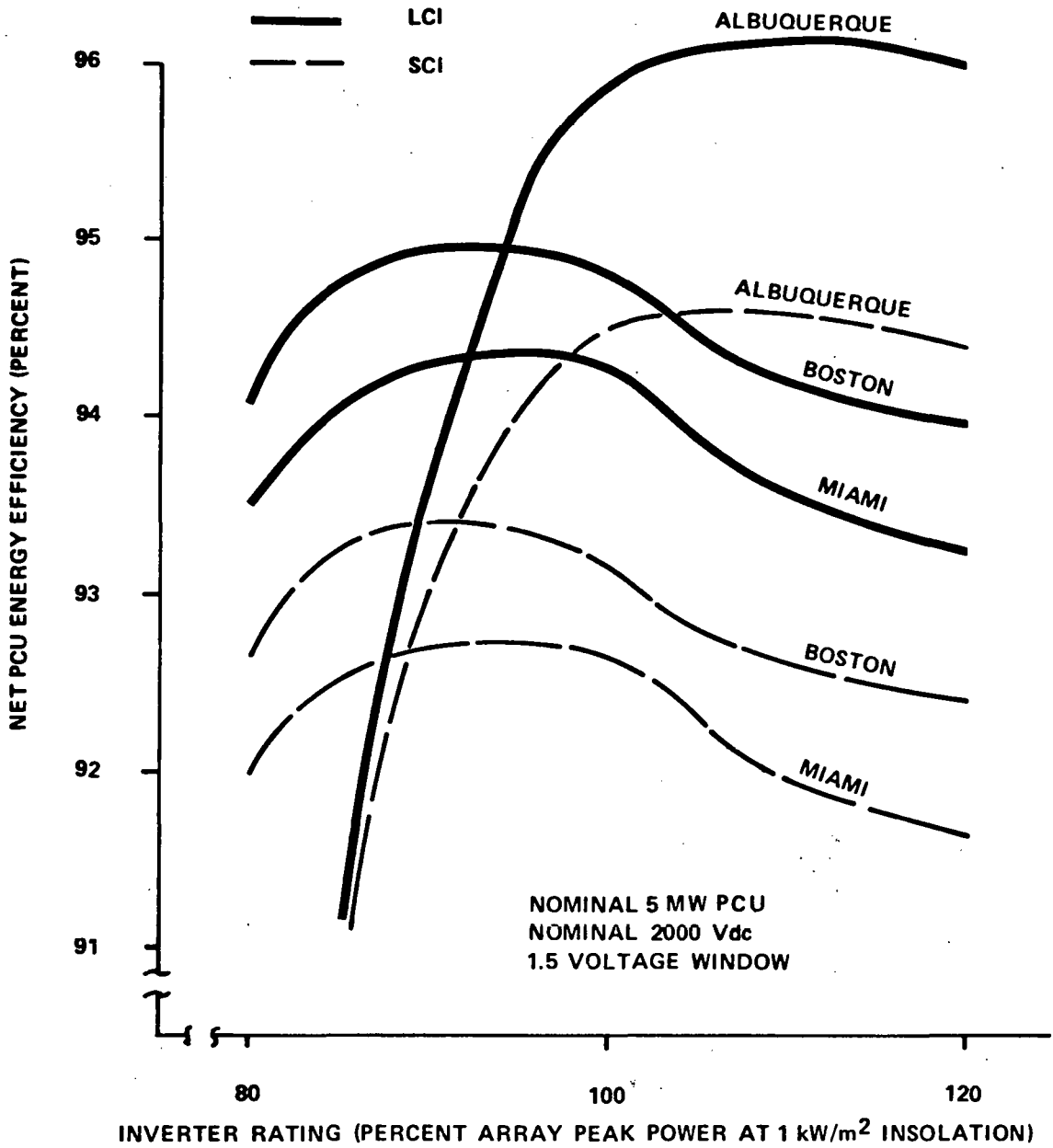
Figure 5-3 (b) Typical Net PCU Energy Efficiency - Two Axis Tracking Arrays

LCI   SCI

1.5 VOLTAGE WINDOW

FIXED
FLAT
PLATE
ARRAYS

TWO
AXIS
TRACKING
ARRAYS
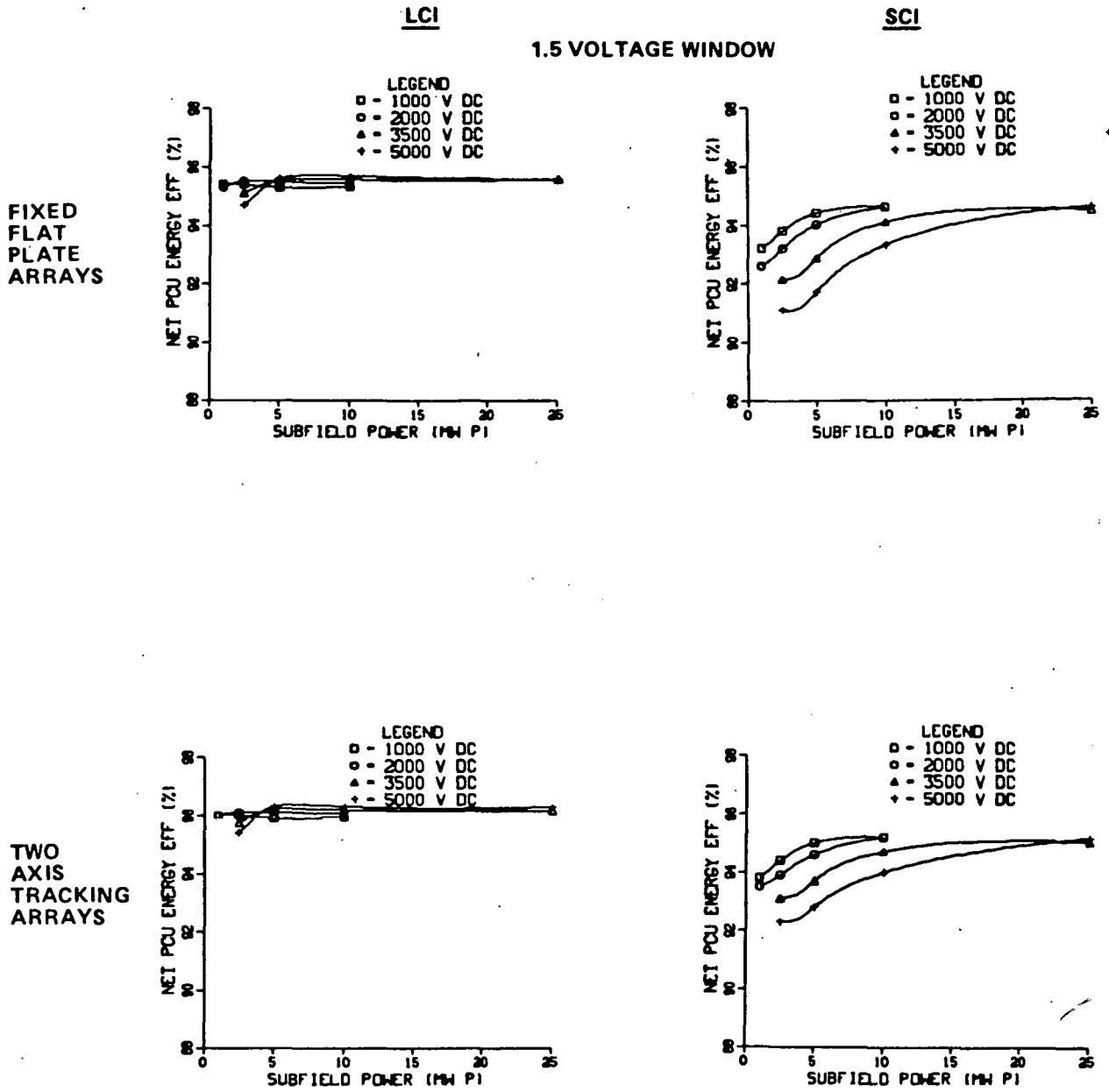
Figure 5-4 Net PCU Energy Efficiency - Albuquerque

LCI

SCI

1.5 VOLTAGE WINDOW

FIXED FLAT PLATE ARRAYS

TWO AXIS TRACKING ARRAYS
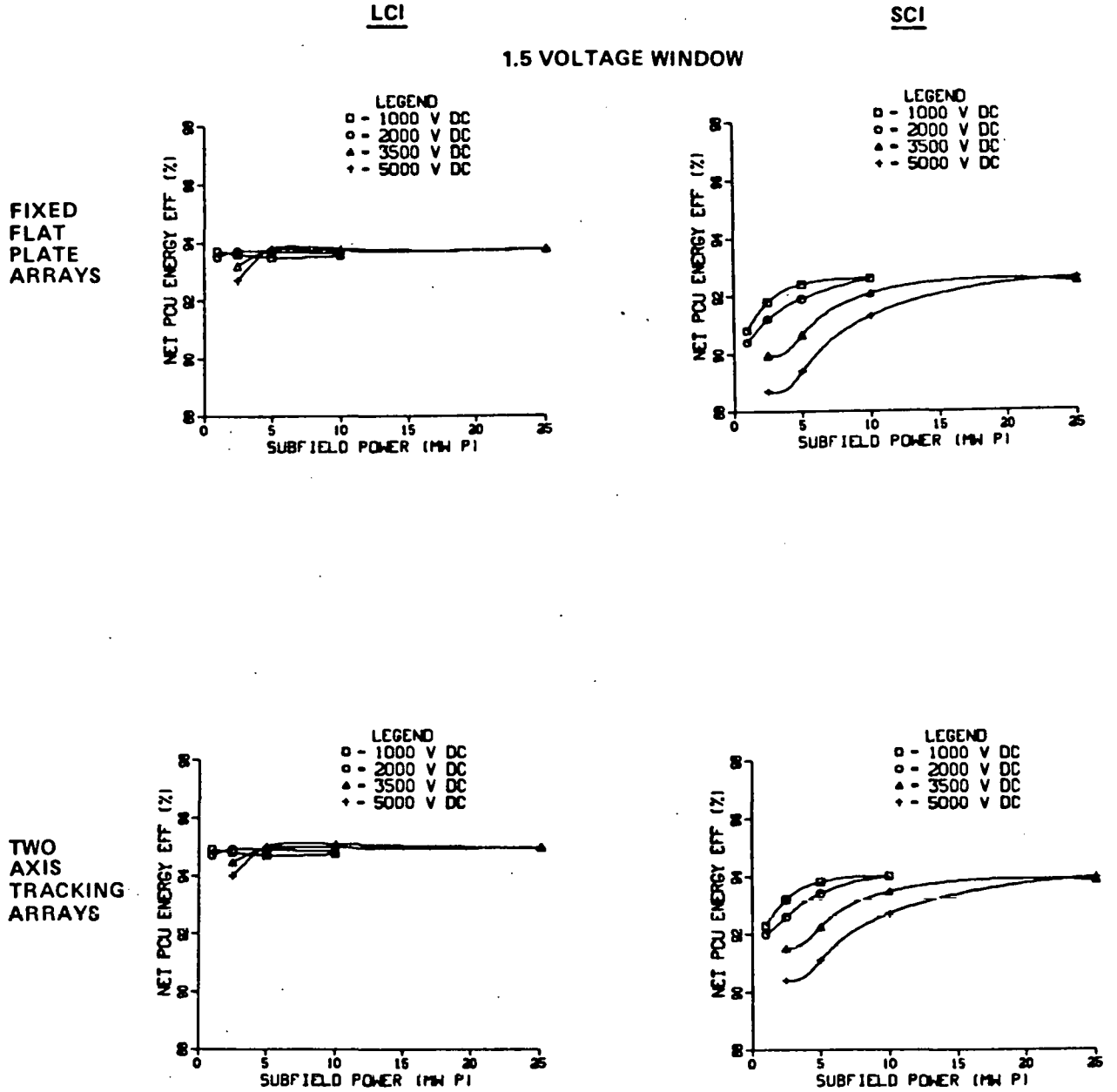
Figure 5-5 Net PCU Energy Efficiency - Boston

SCI

1.5 VOLTAGE WINDOW

FIXED
FLAT
PLATE
ARRAYS

TWO
AXIS
TRACKING
ARRAYS
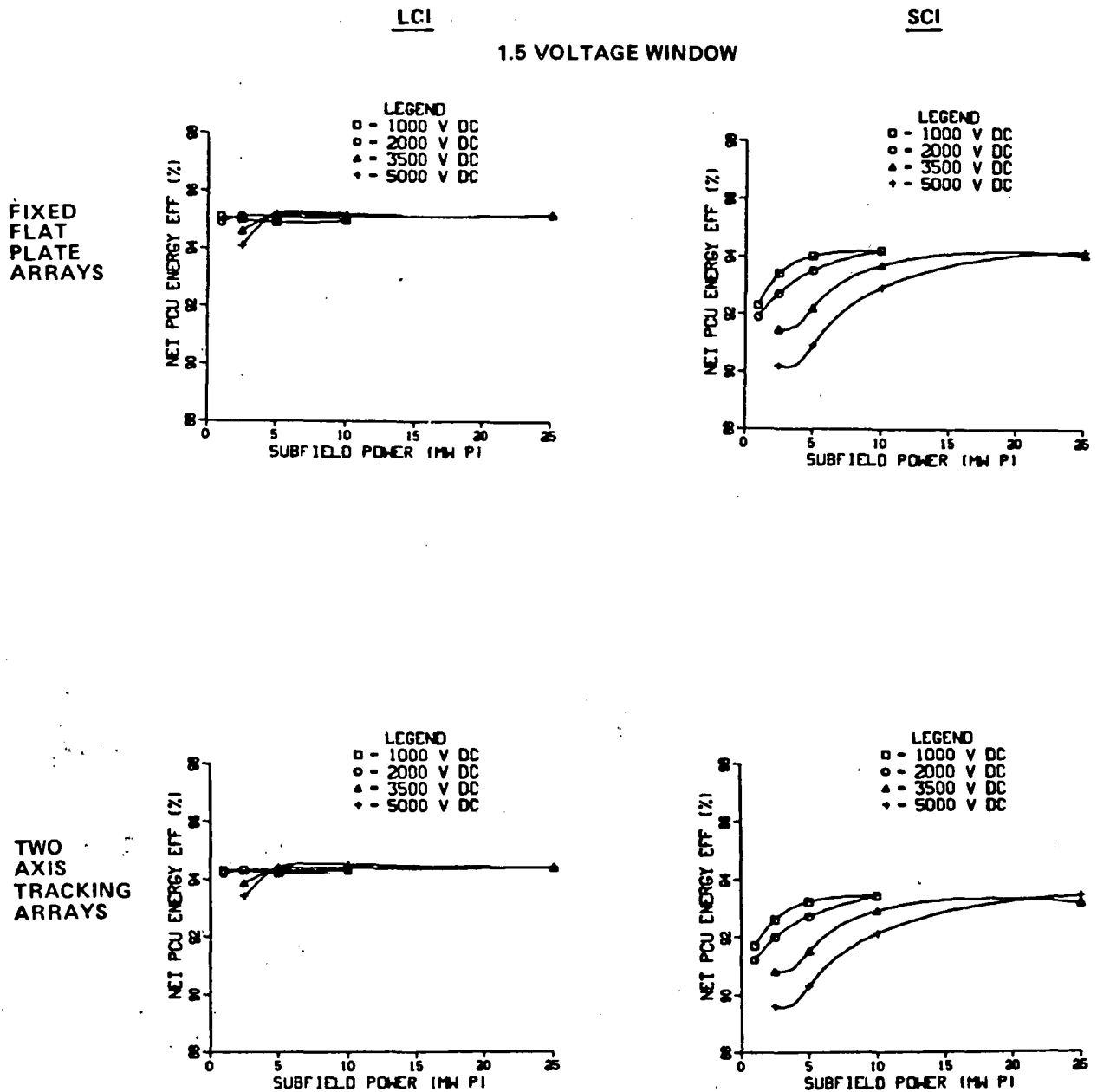
Figure 5-6 Net PCU Energy Efficiency - Miami

Narrower voltage windows will result in improved net energy efficiencies, especially at the lower power and voltage levels. This is discussed further in Section 5.1.3.

Equivalent Costs. In addition to net energy efficiency, PCUOPT calculates the total equivalent PCU cost by combining PCU first costs for each ratio of PCU to array peak power rating (at 1 kW/m^2 insolation) with the equivalent value of the energy losses at that point. The equivalent value of the losses is determined using the methodology discussed in Section 1.4. Figures 5-7(a) and 5-7(b) illustrate the total equivalent costs calculated for the system configurations represented in Figures 5-3(a) and 5-3(b). Costs are presented in terms of mills per peak watt of array output at the maximum peak power point (i.e., the array rather than the PCU maximum power rating). As shown, a minimum total equivalent cost exists for each combination of array type, PCU type, and location. Since PCU cost, in terms of $/Wp of array output, decreases in direct proportion with the ratio between PCU and array peak power ratings, minimum total equivalent costs tend to occur at slightly lower ratios than do maximum energy efficiencies.

Minimum total equivalent costs for the full range of PCU voltage and power levels are presented in Figures 5-8, 5-9, and 5-10 for photovoltaic systems located in Albuquerque, Boston, and Miami. The differences attributable to array type, PCU type, and system location are again evident. Several general trends can also be observed:

- Costs decrease with increasing subfield (and PCU) power level.

5-13
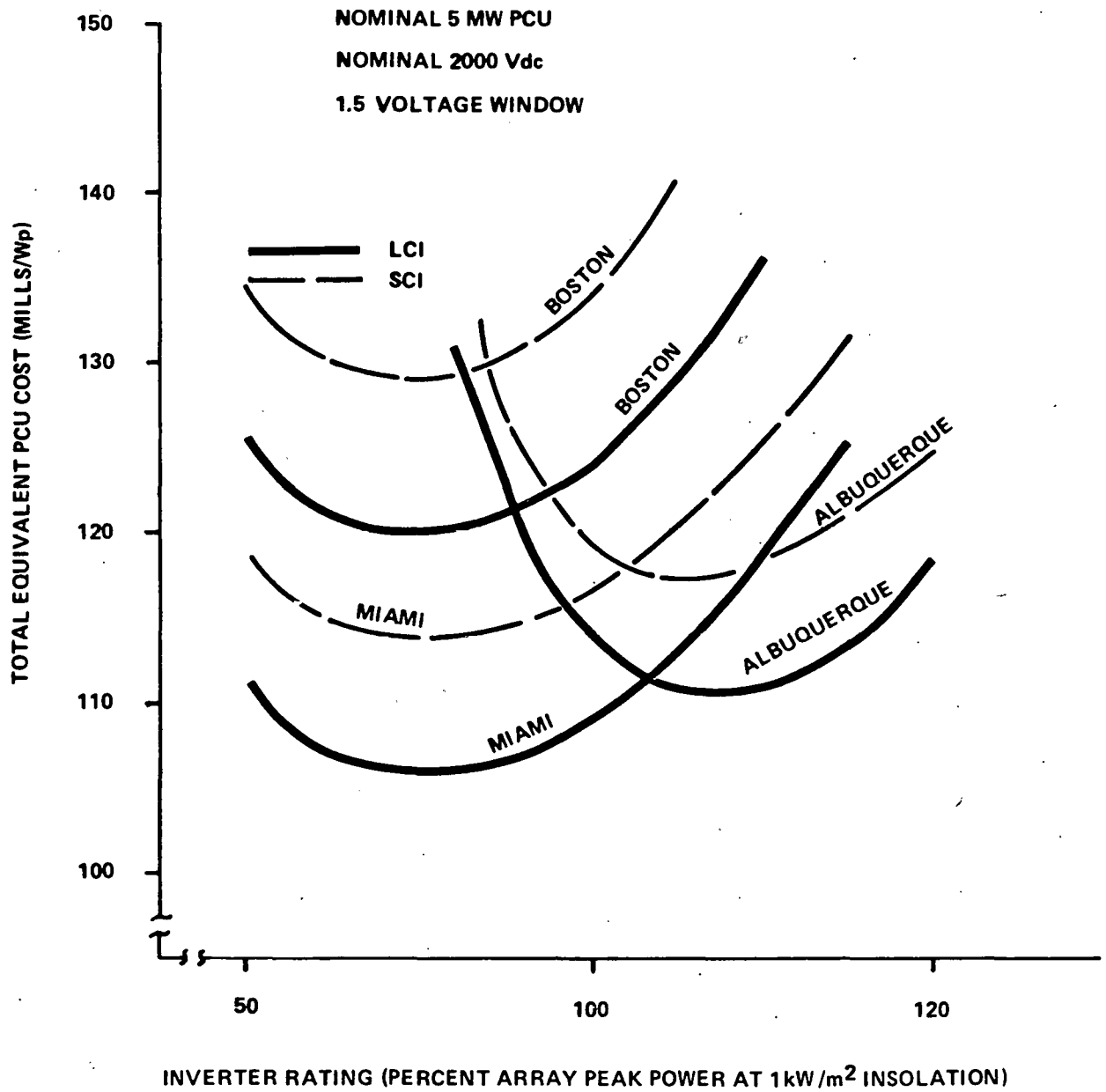
Figure 5-7 (a) Typical Total Equivalent PCU Costs - Flat Plate Arrays
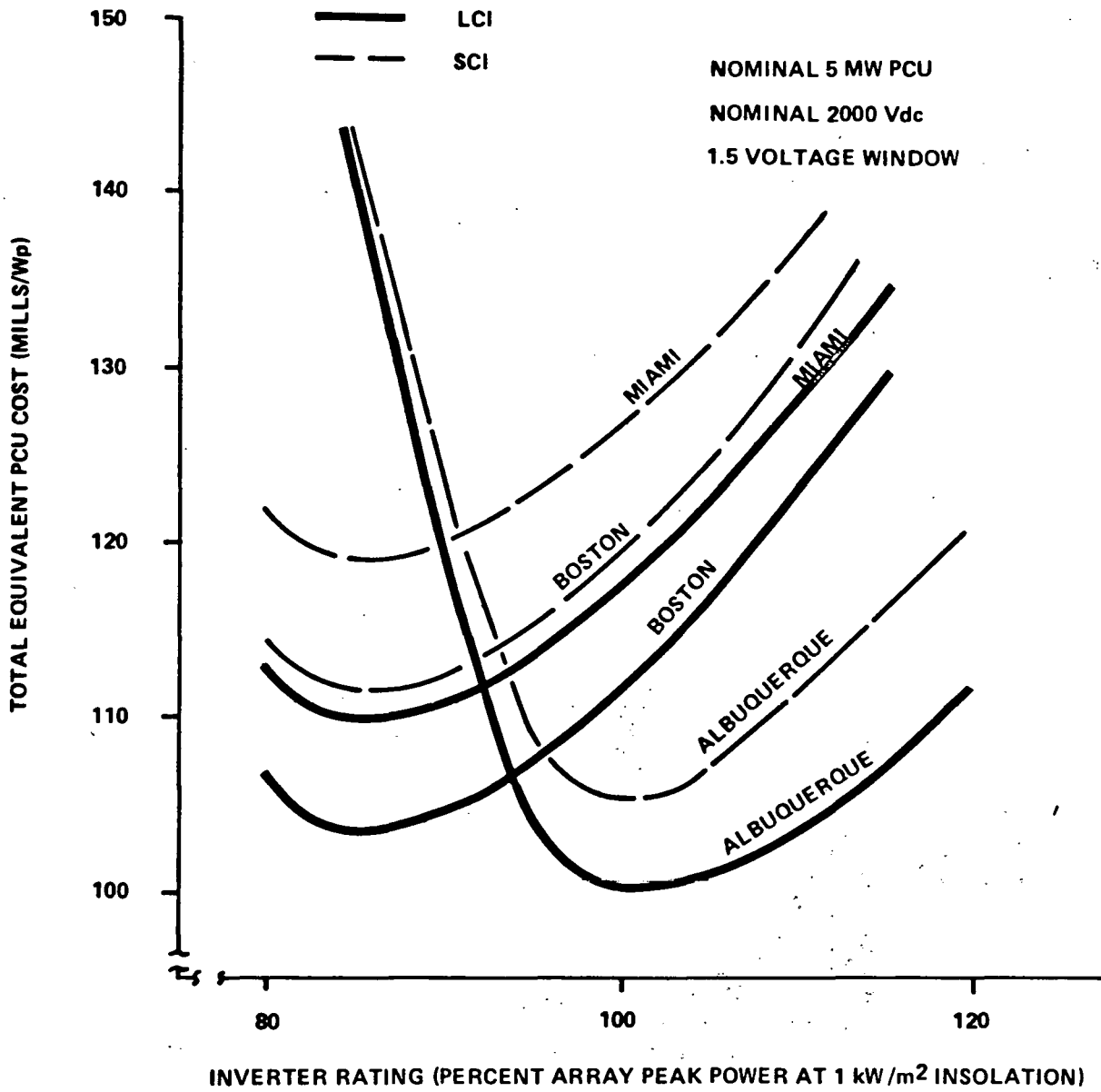
Figure 5-7 (b) Typical Total Equivalent PCU Costs - Two Axis Tracking Arrays

1.5 VOLTAGE WINDOW

FIXED
FLAT
PLATE
ARRAYS
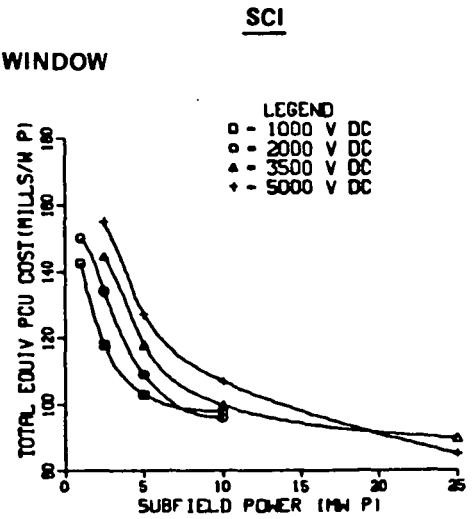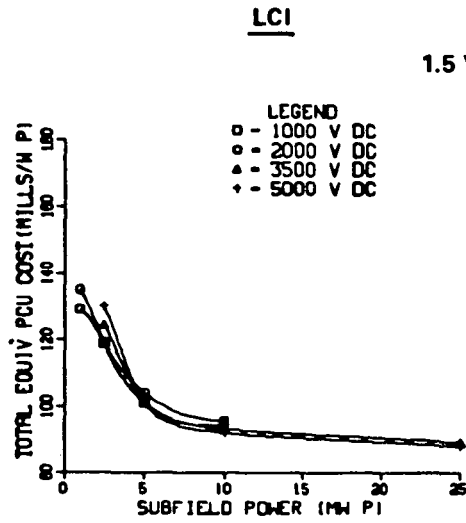
TWO
AXIS
TRACKING
ARRAYS
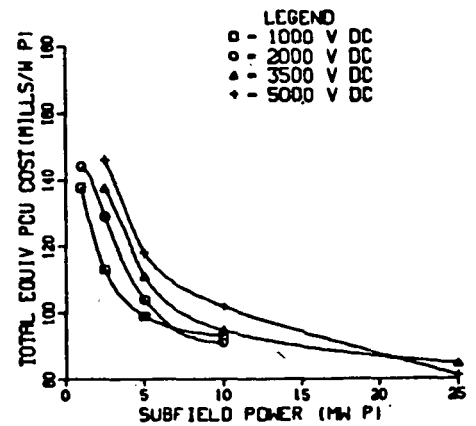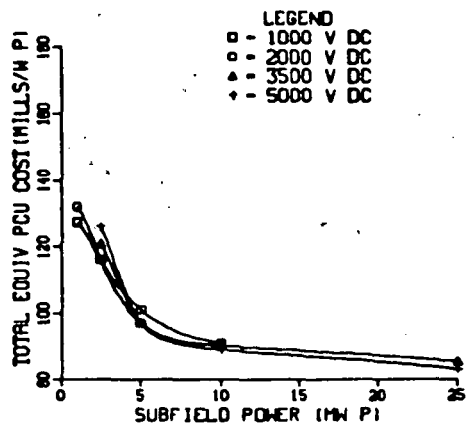
Figure 5-8 Total Equivalent PCU Cost - Albuquerque
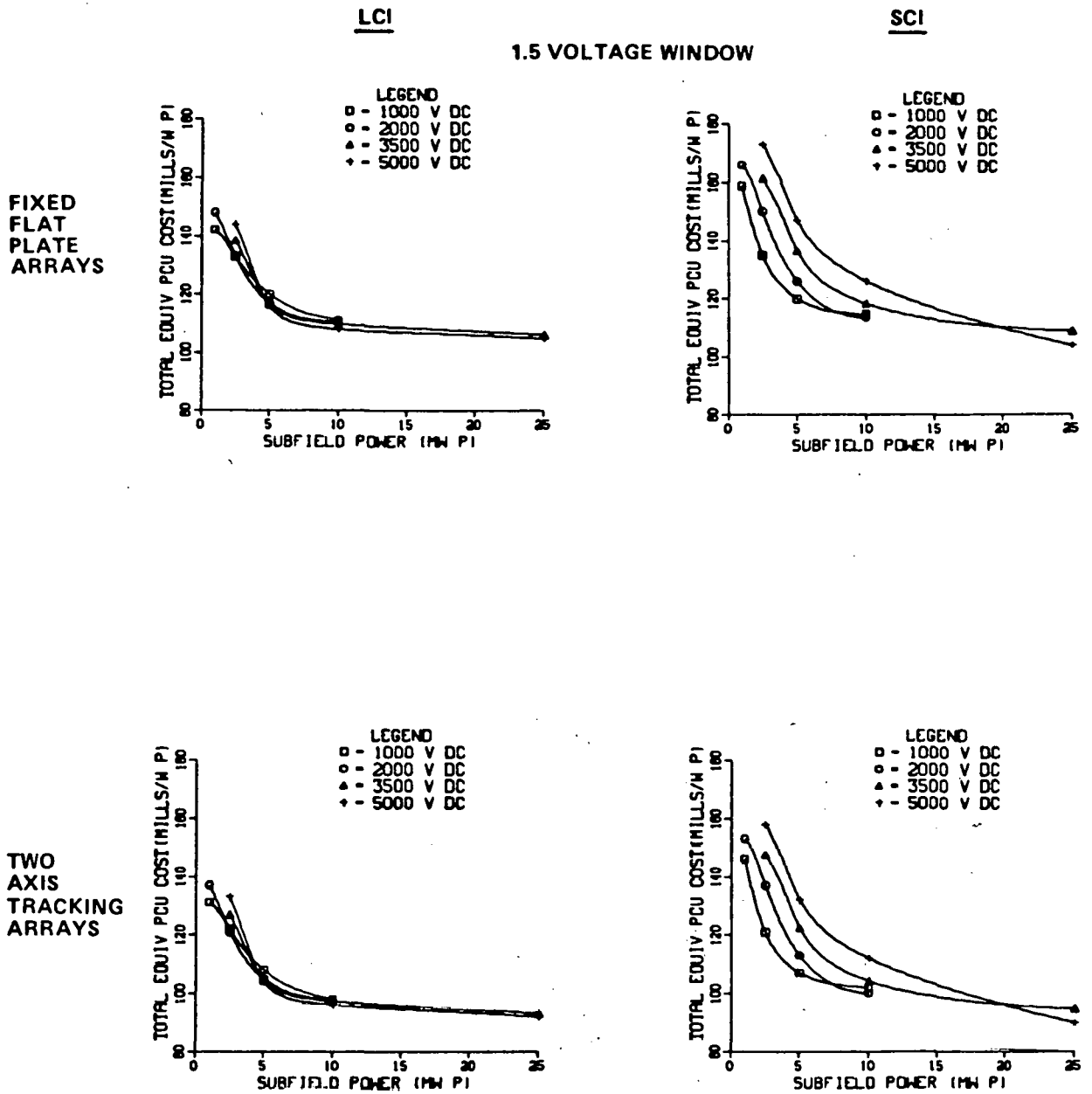
Figure 5-9 Total Equivalent PCU Costs - Boston

Figure 5-10 Total Equivalent PCU Costs - Miami

- Costs decrease significantly up to about 5MW. Above 5MW, costs generally continue to decrease, but at a slower rate.

- For the LCI systems, total equivalent cost is not significantly affected by dc voltage level, within the range of 1000 to 5000 Vdc.

- For the SCI systems, (1.5 voltage window) costs tend to increase slightly, especially at the lower power levels, with increasing dc voltage level.

5.1.2   Total Equivalent Dc Subsystem Costs

In addition to total equivalent PCU costs, several other factors influence the selection of optimum (low cost) dc subsystem configurations. For example, although equivalent PCU costs tend to decrease with increasing power levels, the equivalent dc wiring costs tend to increase. This implies that for a given dc voltage there is an optimum power level that results in the lowest combined total of PCU and dc wiring costs. This is illustrated in Figures 5-11, 5-12, and 5-13, which present the total equivalent PCU and dc wiring costs for PV systems located in Albuquerque, Boston, and Miami. The PCU costs are those shown in Figures 5-8, 5-9, and 5-10. Wiring costs for the flat-plate arrays represent 2.4m slant height, 13% efficient arrays, as illustrated in Figure 3-21(b). Wiring costs for the two axis tracking arrays represent 25m diameter, 15% efficient arrays, as illustrated in Figure 3-14(b).

It can be seen from the data presented in Figures 5-11, 5-12, and 5-13 that at the 1000 and 2000 Vdc levels, cost minima occur in the area of about 5MW peak subfield power. At the higher voltage levels, costs generally continue to decrease, although at a slower rate (particularly for the LCI systems).
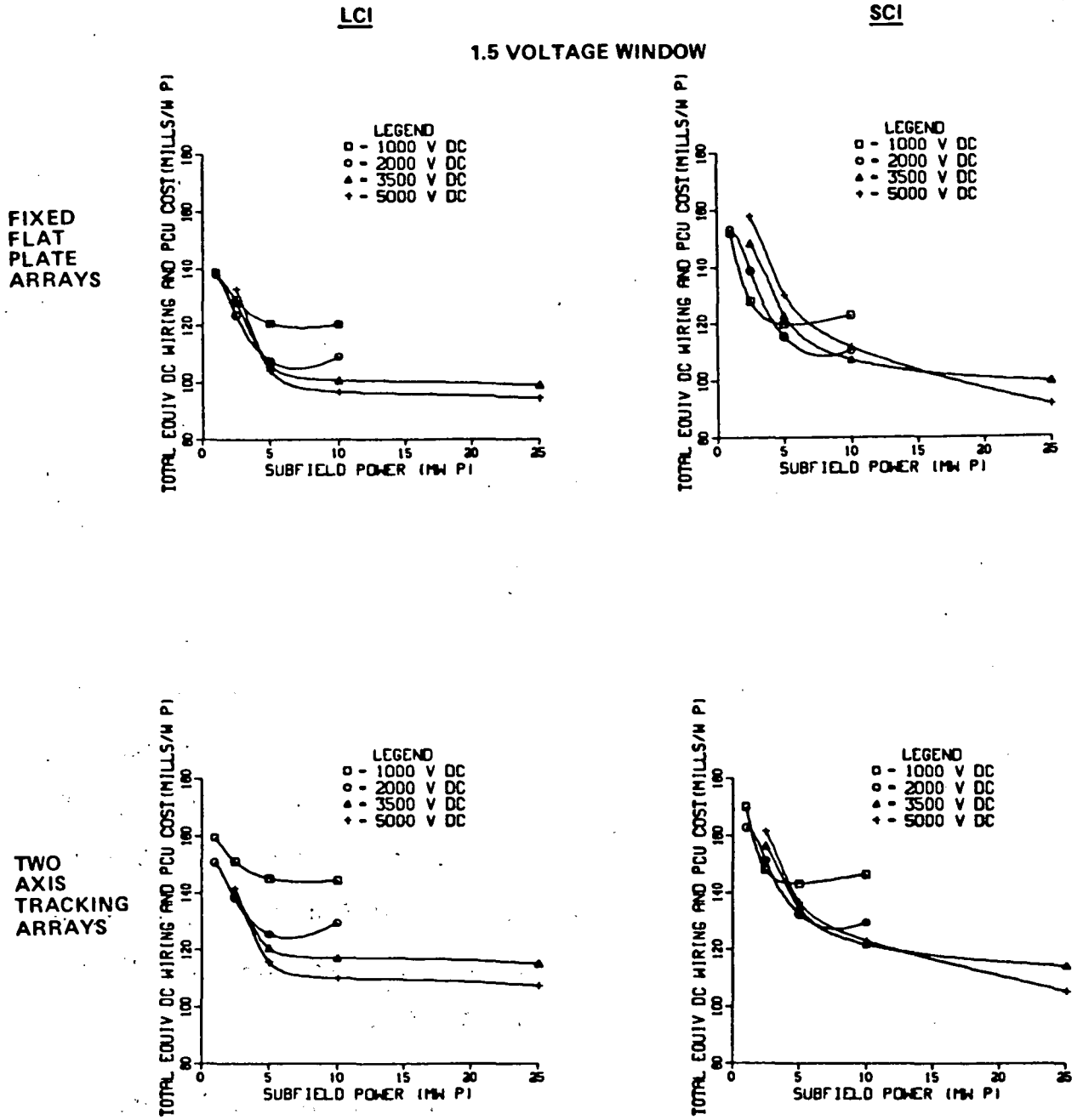
Figure 5-11 Total Equivalent Dc Wiring and PCU Costs - Albuquerque
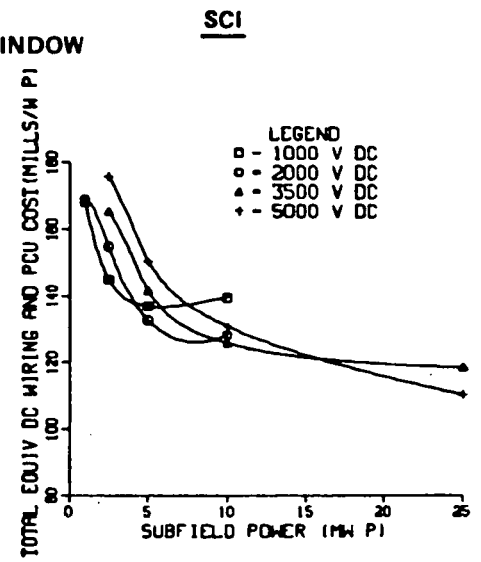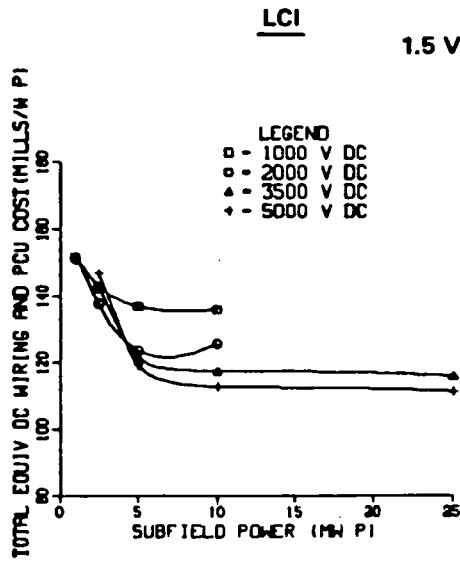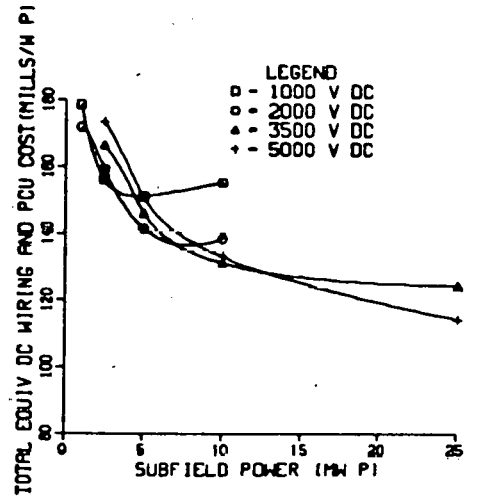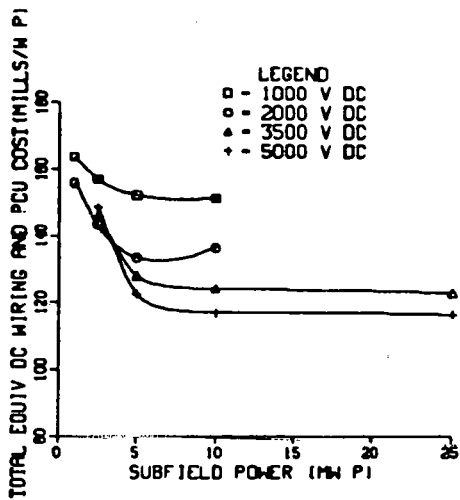
Figure 5-12 Total Equivalent Dc Wiring and PCU Costs - Boston
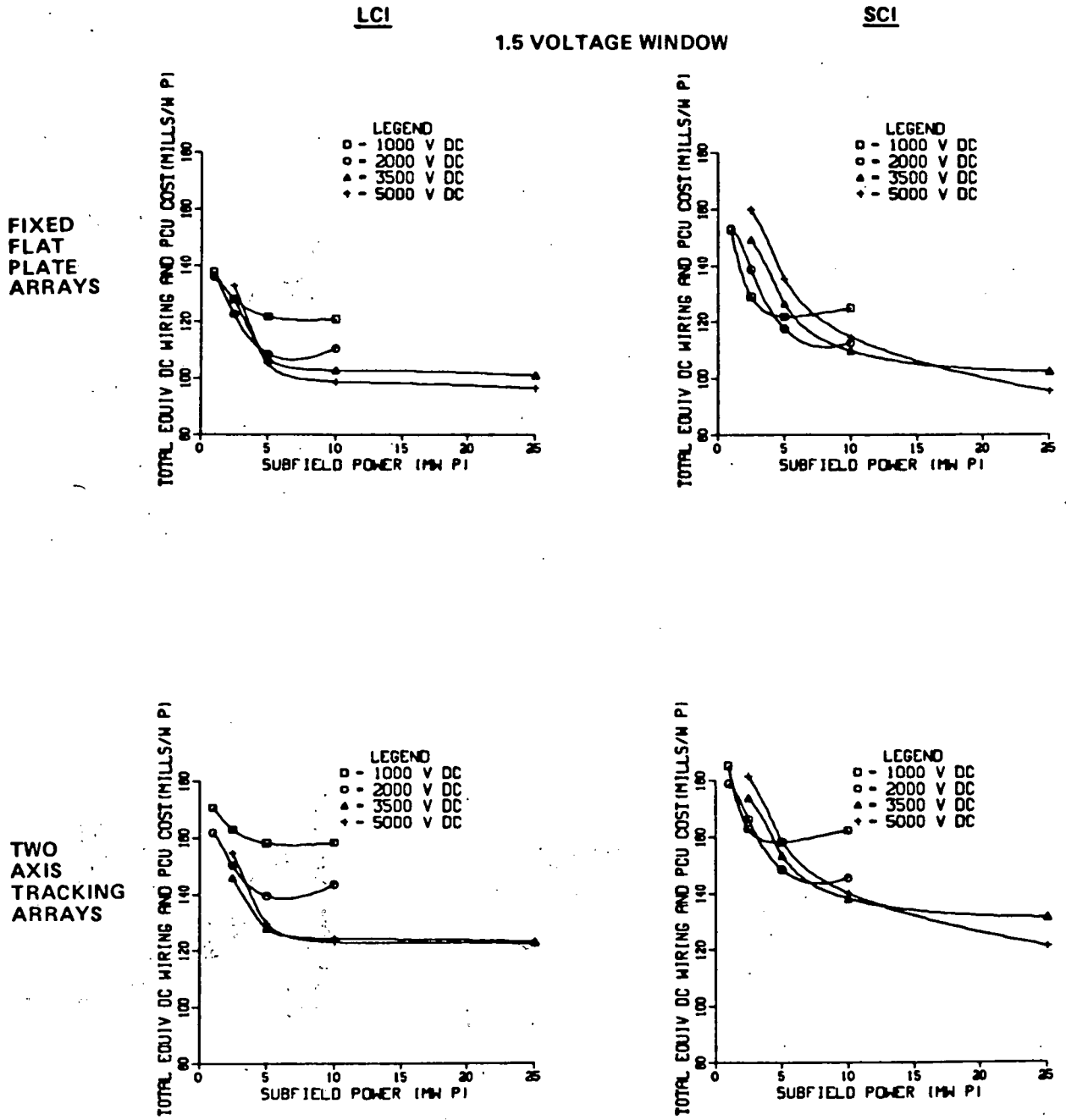
Figure 5-13 Total Equivalent Dc Wiring and PCU Costs - Miami

Although it may be tempting to draw conclusions regarding optimum subfield power and dc voltage levels based on the data presented in Figures 5-11, 5-12, and 5-13, the prudent system designer would be wise to consider several other factors. One of these factors, which is sometimes overlooked in analyses of this type, is the need for the solar cell encapsulation system to maintain acceptable electrical insulating properties throughout the life of the array. That is, the encapsulation system, in addition to providing mechanical and physical protection for the solar cells, must also serve as an electrical insulator to maintain proper system operation and safeguard personnel. Increasing system voltage levels will result in increased electrical stress on the encapsulation system. Above a certain voltage level, it may become necessary to add additional encapsulation material thickness at increased cost and possibly decreased module performance to prevent premature electrical failure.

A previous study conducted by Bechtel (Ref. 5-1) indicated that insufficient information presently exists regarding the long time electrical performance of module encapsulating materials under actual operating conditions. Therefore, it is not possible to determine, with any confidence, the design requirements for a specific module as a function of system voltage level. Neither can assessments be made of the long time voltage performance capabilities of existing or proposed module designs. However, other encapsulation system design considerations, such as requirements for low cost, as well as high thermal and optical conductivities, will influence module designers to employ thin layers of encapsulation. It may be reasonable to expect that additional module costs may be incurred if the

modules must be capable of long time operation at 5000, 3500, or even 2000 Vdc. This will tend to move the minimum cost points presented in Figures 5-11, 5-12, and 5-13 to the left (lower dc voltages). Although, as previously discussed, the requirements for dc disconnect switches, surge arrestors, and other dc equipment are not well defined at this time, their costs may also result in lower optimum voltage levels, especially for the larger systems.

In general, the results of this study appear to indicate that there is relatively little incentive at this time to postulate array subfield designs with ratings much above about 5MW and 2000 Vdc.

5.1.3   PCU Voltage Window

It is well known that the peak power point voltage of a solar cell varies with temperature and, to a much lesser extent, with insolation. Converting the maximum amount of solar energy available requires that a cell (array, branch circuit, etc) be continually operated at its maximum power point voltage. Historically, it has been assumed that lowest life cycle energy costs accompany extraction of maximum available solar energy. This assumption neglects the fact that a PCU's cost and efficiency will vary with voltage window (as discussed in Section 4.2). In this study, the effect of voltage window on array output was determined and subsequently combined with PCU characteristics to assess the effects of voltage window on system optimization. The approach used was to mathematically model a solar cell and, using computer simulations, compare the energy outputs for continuous operation at the maximum power point voltage with the energy output for operation over a range of voltage windows for a typical yearly cycle of varying temperature and insolation.

The voltage-current and power characteristics of the cell model are illustrated in Figure 5-14 for two temperatures. These characteristics are within a few percent of measured data for actual cells.

The basis for the analysis is further illustrated in Figure 5-15, which is an enlargement of the maximum power region of Figure 5-14. As can be seen, at $1kW/m^2$ and a cell temperature range of 28 to 60°C, the voltage window is 1.17:1. Narrowing the voltage window to 1.07:1 reduces the maximum power by 1%.

A computer program was used to calculate annual energy loss in terms of array dc output as a function of voltage window and the center voltage of the voltage window. The results are shown in Figure 5-16. These results are for:

- The cell characteristics shown in Figure 5-14
  (0.7 fill factor)

- JPL's flat-plate module thermal characteristics
  (Tcell = Tair + 0.3 x insolation) (Ref. 5-2)

- Albuquerque daily air temperature profiles

- Theoretical insolation (cloudless days)

- Modeling one day per month.

The solid curves in Figure 5-16 show the percent of maximum available array energy obtained for the parametric set of voltage windows centered at the dc voltage level indicated on the absicssa. The dashed line shows the cumulative percentage of maximum power collected as a function of maximum power point voltage for an infinitely wide voltage window.
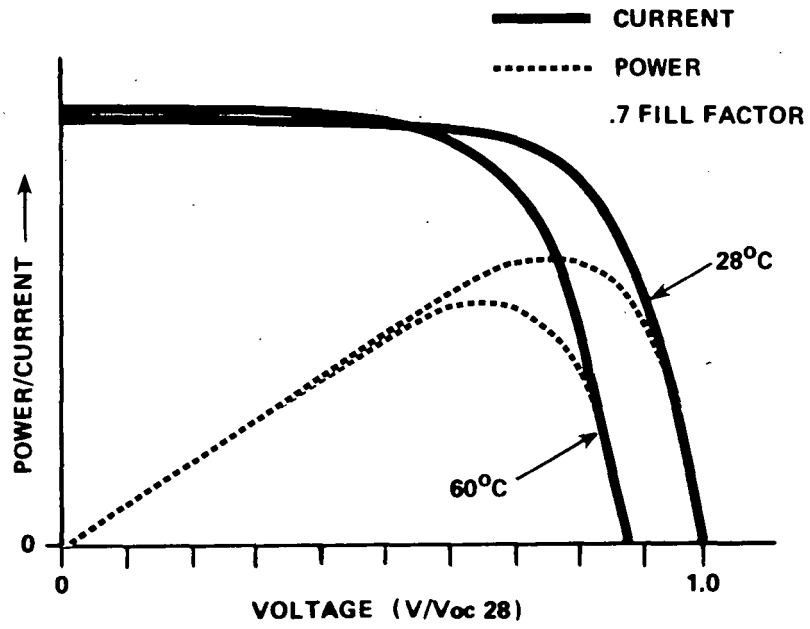
Figure 5- 14   Solar Cell Model Characteristics
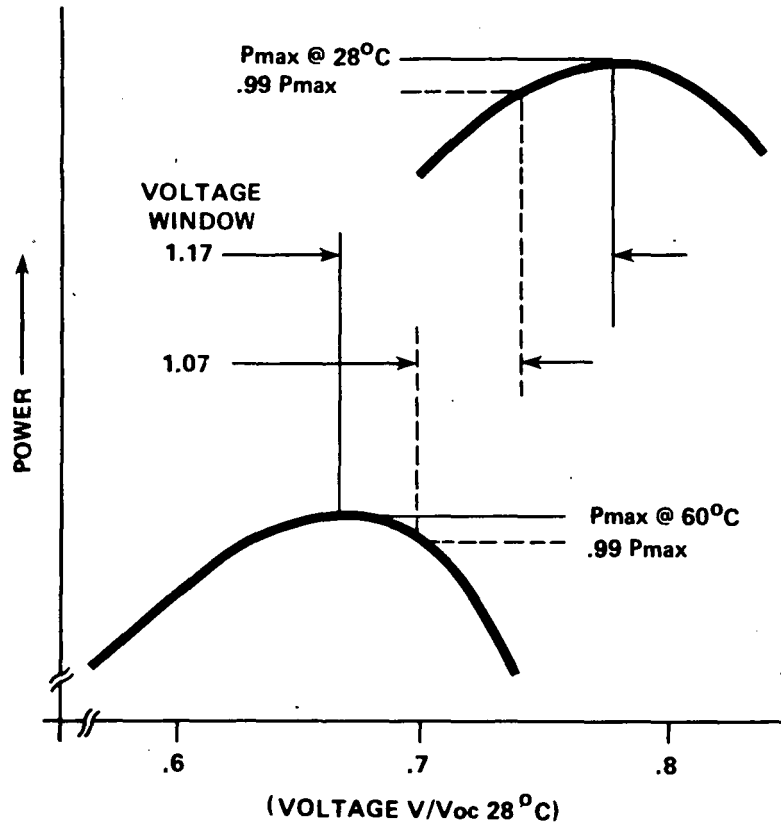
Figure 5-15 Effect of Voltage Window on Peak Power Point Operation
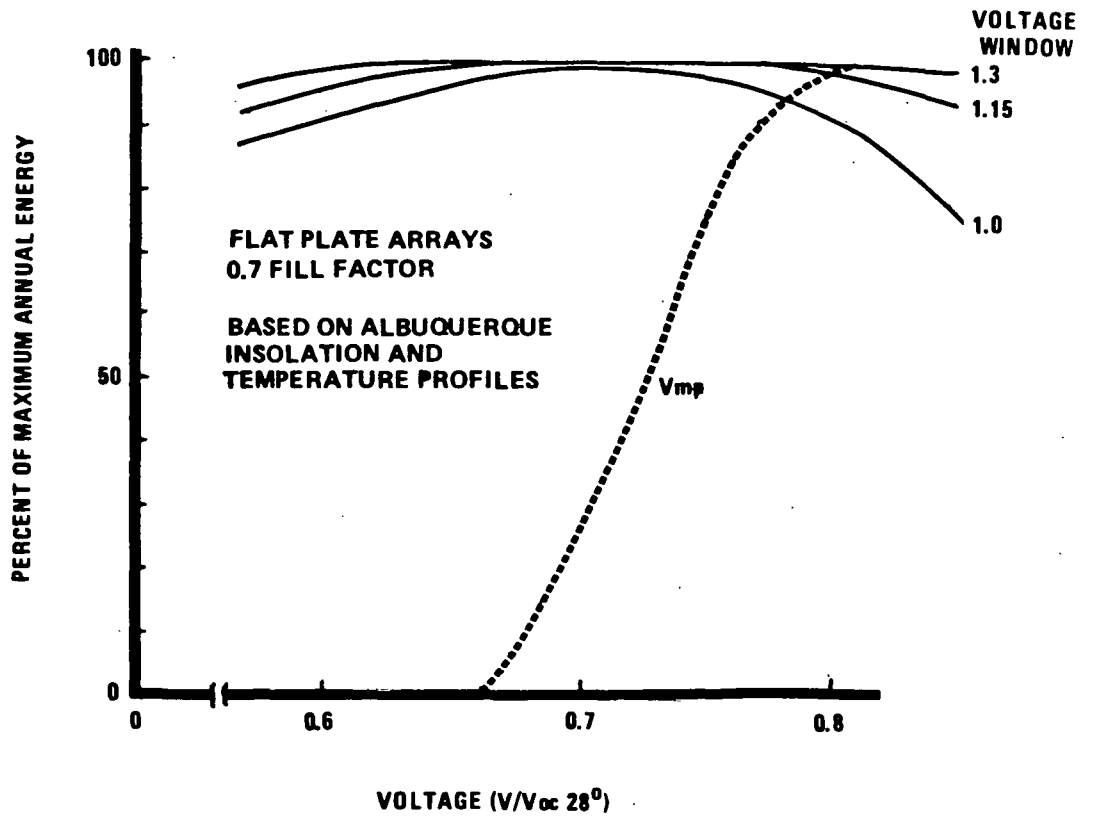
Figure 5-16 Effect of Voltage Window on Flat Plate Array Energy Collection

It can be seen from the figure that for a properly selected range of center voltage, no energy is lost for voltage windows $\geq$ 1.15:1. Further, relatively little energy is lost for operation at a single voltage (voltage window = 1.0:1).

The above procedures were repeated for several cities selected to represent a range of variations in daily and seasonal air temperature profiles. The results are shown in Figure 5-17. In each case, the optimum center voltage for the voltage window is plotted. Two cell fill factors (0.7 and 0.6) were used. These are expected to be representative of the fill factors for large arrays containing many interconnected cells.

The data in Figure 5-17 indicate that if the center voltage is properly selected, the required voltage window may not be as wide as previous studies have assumed. For example, a voltage window of 1.1 would result in the collection of more than 99.5% of the maximum power point energy for all cases illustrated in Figure 5-17. A second item shown by the data is that lower fill factor cells or branch circuits can tolerate narrower voltage windows for a given loss in annual energy. In general, it was observed that for a given percentage of energy loss, sites with large temperature variations require wider voltage windows and slightly lower center voltages. Further optimization efforts should consider actual meteorological data (temperature and insolation), measured voltage-current characteristics for large arrays and multiple branch circuits, and measured thermal responses of the modules being evaluated.

To provide a comparison between the effects of PCU voltage window on array output energy and total PCU equivalent costs, PCUOPT was used to
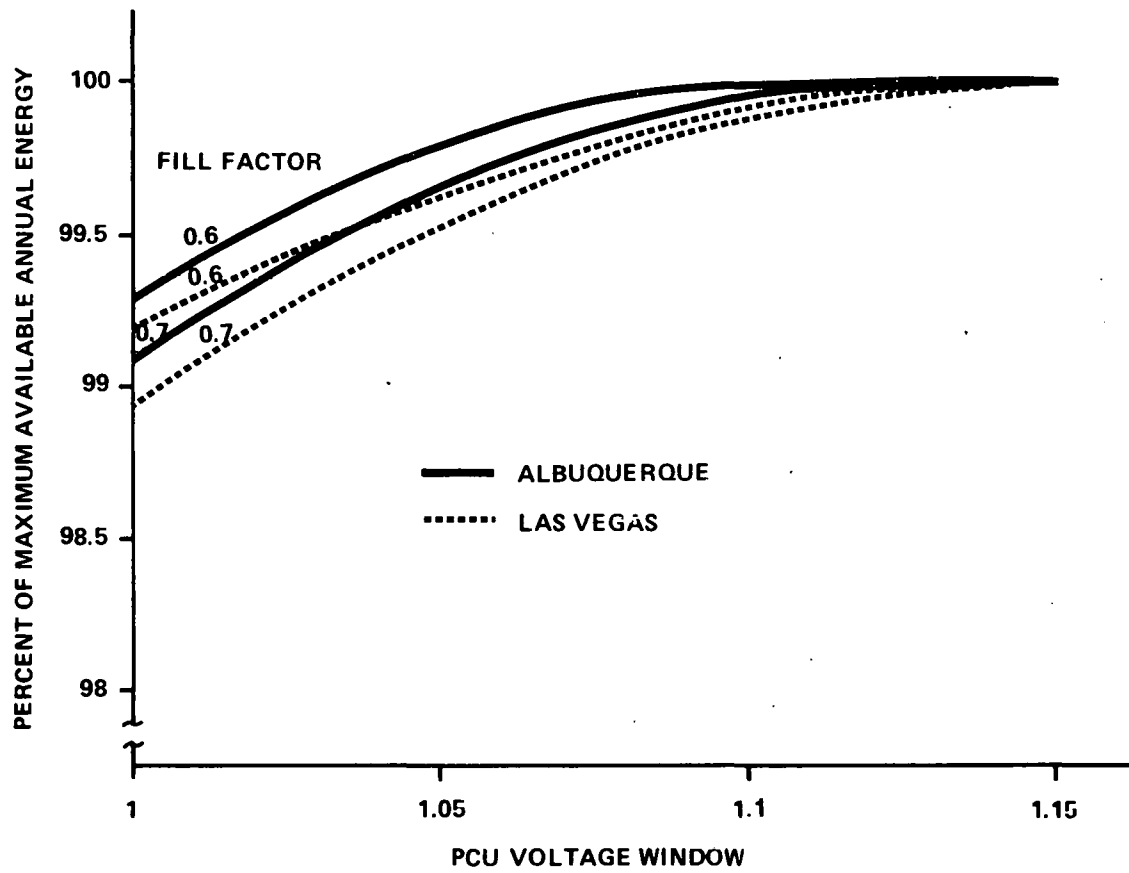
Figure 5-17 Effect of PCU Voltage Window on Annual Energy Collection

calculate total equivalent costs using the PCU voltage window cost and efficiency data presented in Section 4.3. The results are illustrated in Figure 5-18, which presents total equivalent PCU and dc wiring costs as a function of voltage window for fixed flat-plate and two axis tracking arrays, using both LCI and SCI systems. The data are for nominal 5MW, 2000 Vdc subfields. These data do not account for energy losses that would occur for PCU voltage windows narrower than the ideal voltage window, as illustrated in Figure 5-17. However, it can be seen that for both SCI and LCI systems, significant reductions in total equivalent costs occur as the voltage windows become smaller. Comparison of the equivalent cost data in Figure 5-18 with the energy loss data presented in Figure 5-17 indicates that voltage windows as narrow as 1.1 may be acceptable in many locations.

However, a word of caution is in order regarding the stability of the photovoltaic array peak power point voltage during the life of the system. That is, cell failures, changing cell characteristics, changes in module thermal performance, or other aging factors may result in a gradual shifting of peak power point voltages. In general, insufficient long time array performance data is presently available to assess the magnitudes of such changes (if any). If relatively large changes occur, the selection of too narrow a PCU voltage window could result in unacceptable performance degradation as the system ages.

5.1.4 Total Equivalent Dc Up-Converter Costs

The potential advantages of using in-field dc up-converters to interface between relatively low voltage (e.g., 1000 Vdc) branch circuits and higher voltage (e.g., 5000 Vdc) centrally located inverters were discussed in
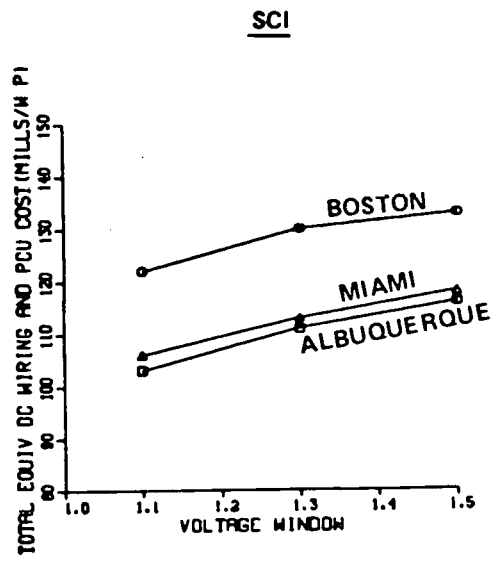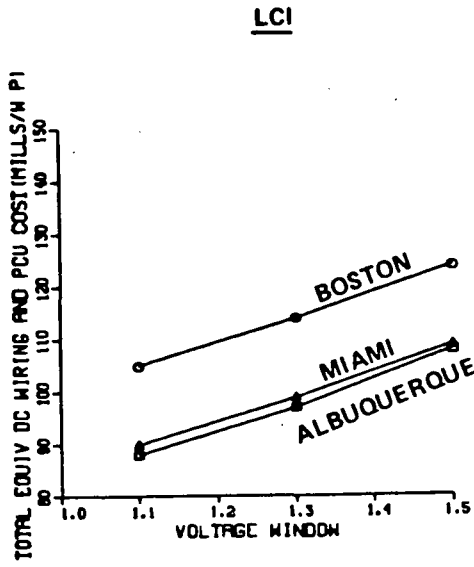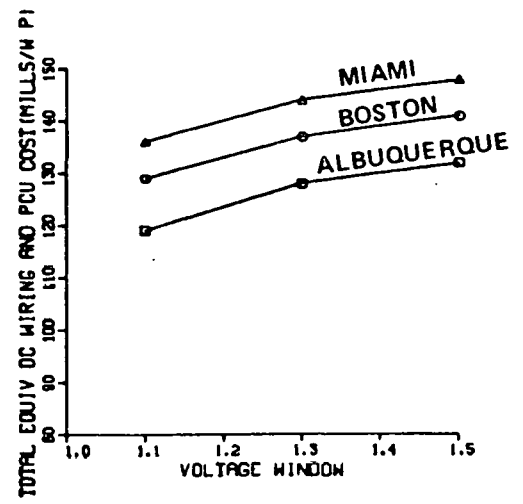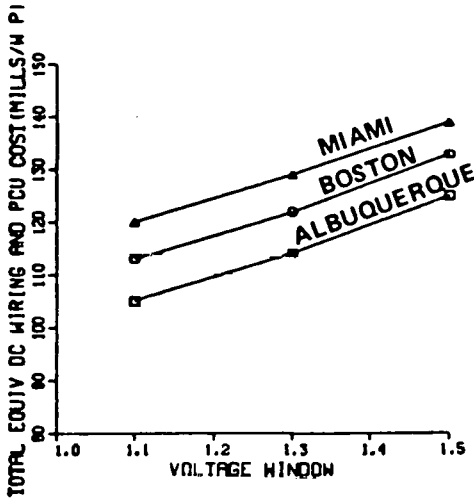
Figure 5-18   Effect of Voltage Window on Dc Wiring and PCU Equivalent Costs

Section 4.3. First costs and efficiency data for two schemes using alternate dc up-converter technologies were also presented in Section 4.3.

To assess the economic attractiveness of using dc up-converters, it is necessary to compare the total equivalent costs (first costs and the value of the energy losses) for otherwise equivalent photovoltaic power systems, both with and without in-field up-converters. The total equivalent costs for the two up-converter schemes are presented in Table 5-1. Based on the data presented in the table, the use of in-field dc up-converters does not appear to be cost effective (at least for the system configurations evaluated in this study).

5.2   ARRAY SPACING

The spacing provided between adjacent array structures is a tradeoff between access requirements, shadowing losses, the cost of land, wiring, and other subsystems affected by the spacing distance. This subsection examines these tradeoffs with regard to:

- Fixed, latitude-tilted flat plate arrays

- Vertical axis arrays

5.2.1   Flat Plate Arrays

Shadowing losses for flat-plate arrays are dependent on interarray spacing and weather in several ways, as illustated in Figure 5-19. First, adjacent structures may block the direct component of sunlight (i.e., cast a shadow). This effect depends on the angle of the sun (time of day and year), array geometry, and interarray spacing. Secondly, adjacent structures

Table 5-1

DC UP-CONVERTER TOTAL EQUIVALENT COST COMPARISON

LOCATION	ARRAY TYPE	TOTAL EQUIVALENT COSTS (Mills/Wp)					
		LCI UP-CONVERTER SCHEME			SCI UP-CONVERTER SCHEME		
		NONE(1)	I(2)	II(3)	NONE(1)	I(2)	II(3)
Albuquerque	Flat Plate	104	134	132	103	138	127
Albuquerque	Two Axis	101	131	128	99	134	121
Boston	Flat Plate	120	148	147	120	154	142
Boston	Two Axis	108	137	135	107	142	130
Miami	Flat Plate	105	135	133	105	139	128
Miami	Two Axis	114	143	142	114	148	137

1) Nominal 5MW, 1000 Vdc, 1.5 Voltage Window PCU

2) 1000-3750 Vdc boost regulators - 25MW, 3750 Vdc, 1.0 Voltage Window PCU

3) 1000-5000 Vdc inverter - rectifier-transformer - 25MW, 5000 Vdc, 1.0 Voltage Window PCU

Figure 5-19 Shadowing of Fixed Flat Plate Arrays

SPACING FACTOR	INSOLATION (kwh/m²/year)	LOSS (%)
∞	1825	—
1.0	1777	2.6
0.75	1742	4.5

BASED ON TMY DATA FOR MIAMI
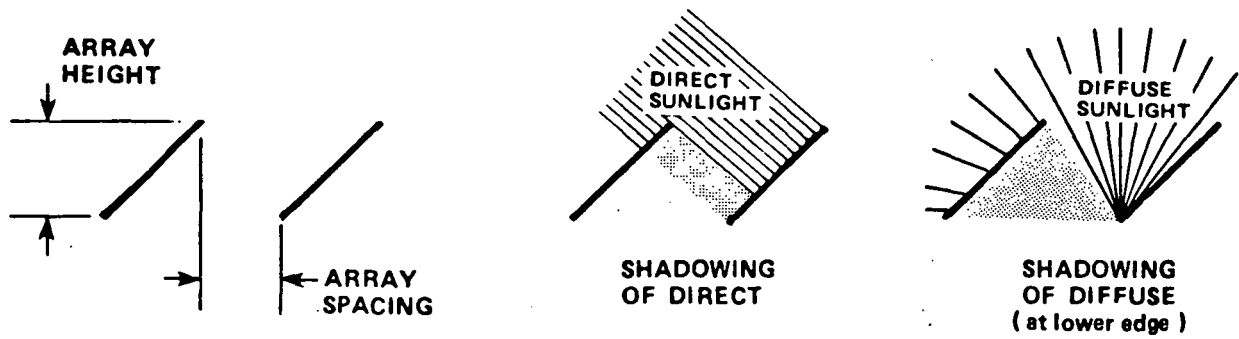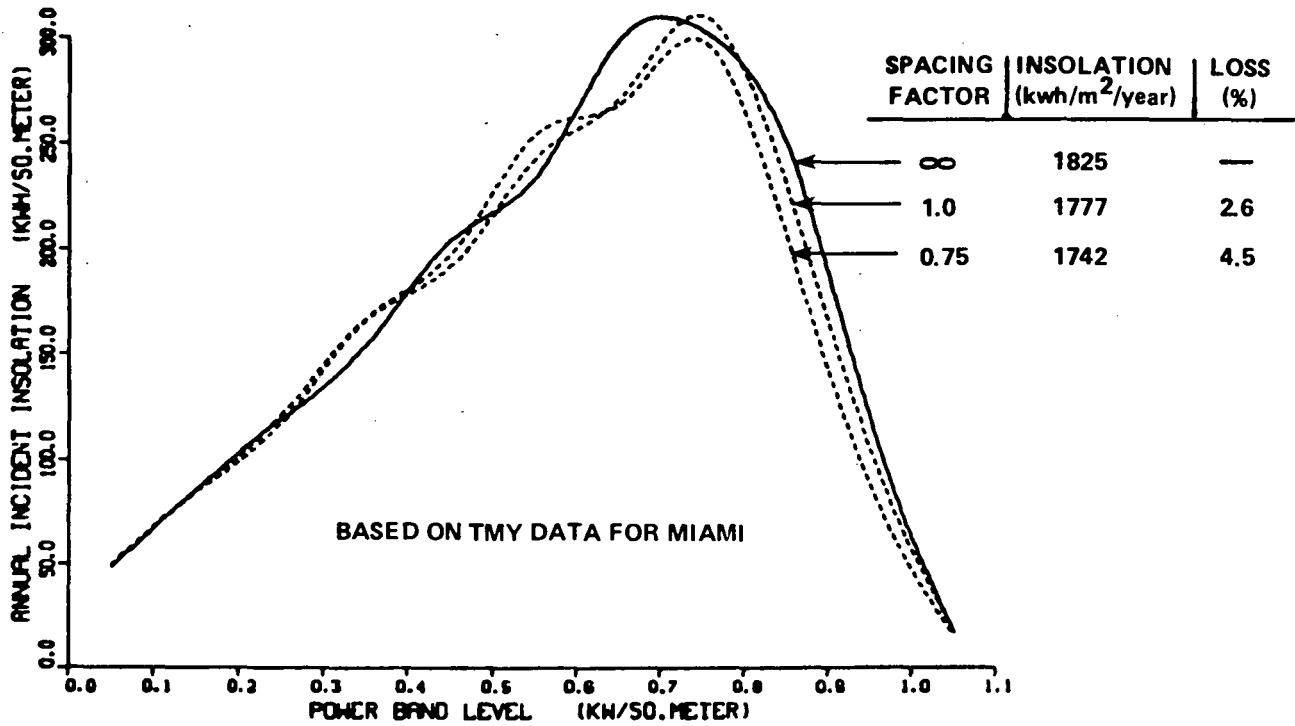
Figure 5-20 Effect of Flat Plate Array Spacing on Yearly Incident Insolation

5-34

can block a portion of the diffuse component of sunlight. The fraction of diffuse component blocked depends only on the array spacing and geometry. Thirdly, shadowing effects are weather dependent insofar as energy reduction depends on the relative amounts of direct and diffuse sunlight present. Since the angle of the sun depends on the site latitude (in addition to time of day and year), shadowing effects are also dependent on site latitude.

To determine the magnitude of the shadowing losses for specific locations and array geometries, the SOLMET TMY insolation data were modified, using an existing in-house computer program originally written to calculate theoretical insolation data. The program calculates the sun angle for each hour of yearly operation and calculates the amount of direct and diffuse insolation lost due to shadowing for a specified array geometry. Typical output data are illustrated in Figure 5-20 for several array spacings in Miami. Array spacing is given in terms of multiples of the vertical height of the array (spacing factor). Total yearly energy loss, along with the shifting of the power bands, as a function of array spacing is illustrated.

Figure 5-21 presents the percent of annual energy lost in Albuquerque, Boston, and Miami, as a function of array spacing based on the TMY data. Also shown are the losses based on theoretical insolation calculations for sites at corresponding latitudes. As can be seen, actual losses can be different (usually higher) than those calculated on a theoretical basis.
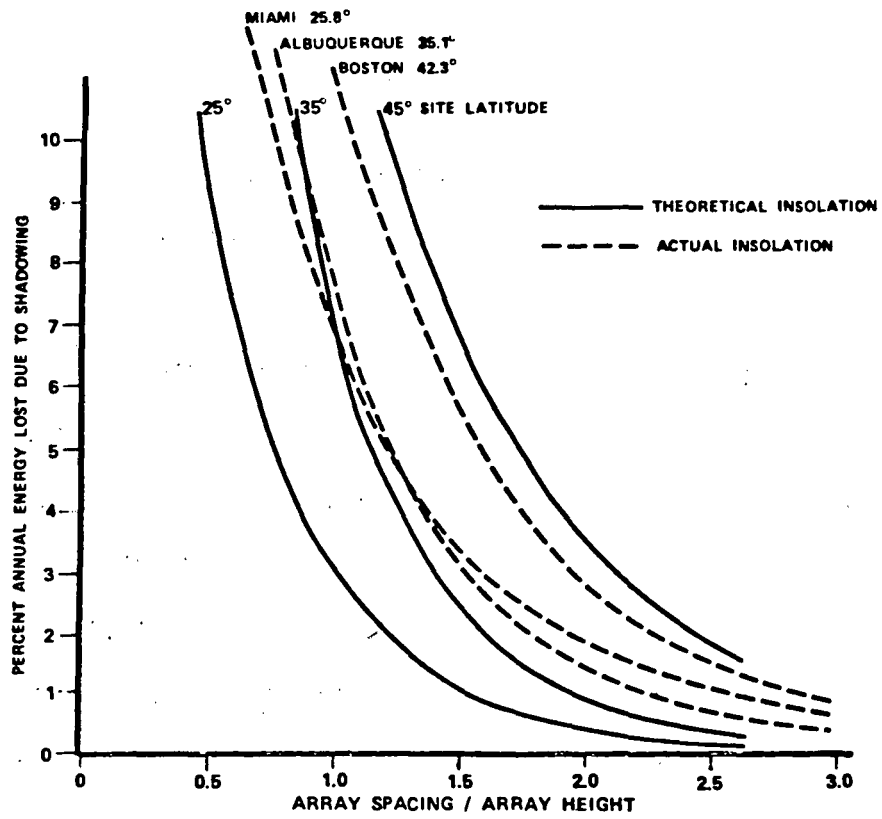
Figure 5-21 Fixed Flat Plate Array Shadowing Losses

The value of these losses can be compared with the costs of dc wiring and land, to identify optimum spacings.

The effect of fixed, latitude-tilted flat-plate array spacing on dc power collection wiring costs is illustrated in Figure 5-22. The data were generated using PLEASE, as described in Section 3.2, and represent total equivalent costs (first costs plus the value of the losses) for a nominal 5MW array subfield consisting of 2.4m slant height, 13% efficient arrays.

The relationship between the value of the shadowed energy losses, the dc wiring costs, and land costs (land acquisition and site preparation) is illustrated in Figure 5-23 for a 5MW, 2000 Vdc subfield located in Albuquerque and for a land cost of $1000/acre. The values of the shadowed energy losses are calculated based on the methodology described in Section 1.4. As shown, the subtotal of all spacing related costs is minimized for a spacing of about 2.5 times the array height.

Data for similar systems located in Boston and Miami are illustrated in Figures 5-24(a) and 5-24(b), respectively. The site dependence of optimum array spacing can be observed by comparison with the data in Figures 5-23 and 5-24. Of course, optimum array spacing is also influenced by subfield power and voltage levels, array size and efficiency, land cost, and the assumed value of the shadowed energy losses. However, the data in Figures 5-23 and 5-24 indicate that in some cases, optimum spacings may be larger than the nominal 1.5 times the array height often assumed in design studies.
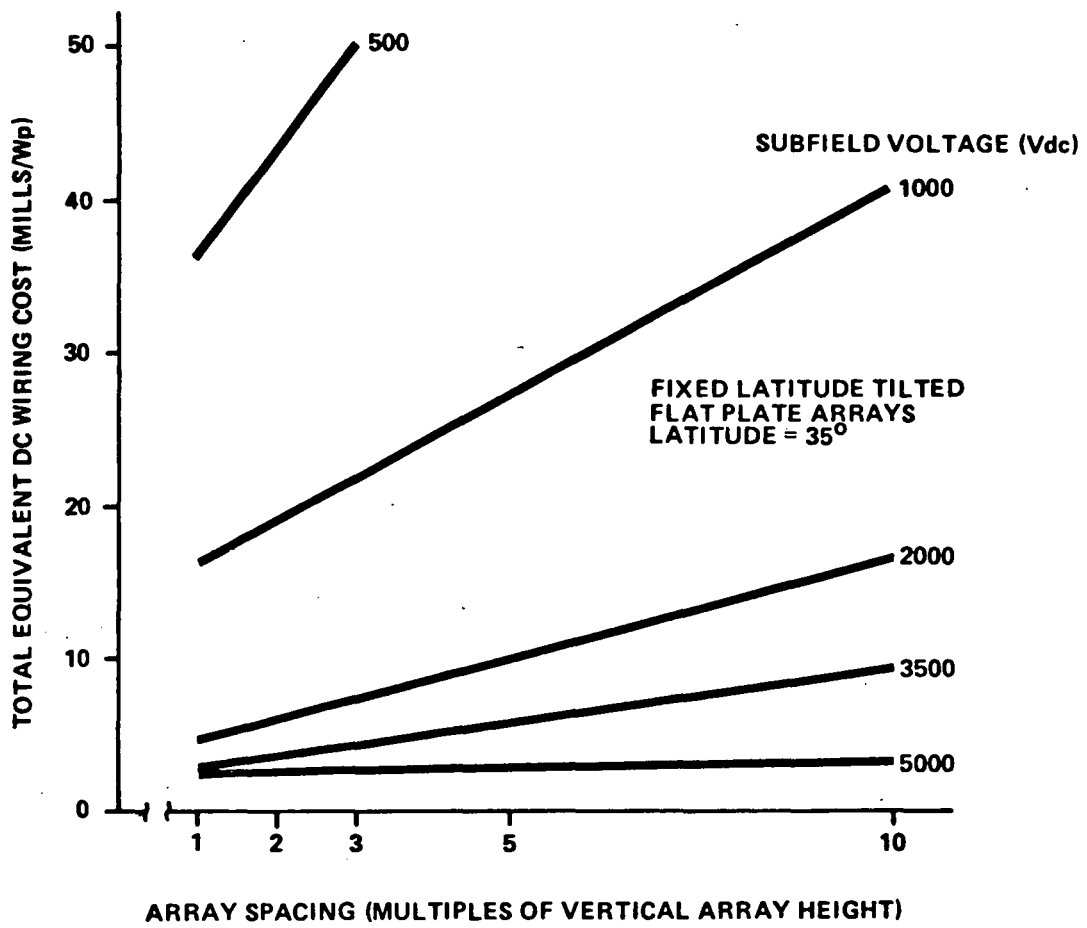
Figure 5-22 Effect of Flat Plate Array Spacing on Total Equivalent DC Wiring Costs

NOMINAL 5 MW$_p$ - 2000 V$_{dc}$ SUBFIELD

2.4 SLANT HEIGHT - 13 PERCENT EFFICIENT ARRAYS

LEGEND
□ = DC WIRING
○ = SHADOWED ENERGY LOSS
▲ = LAND (1000 $/ACRE)
+ = SPACING RELATED SUBTOTAL

MILLS/WATT

ARRAY SPACING FACTOR
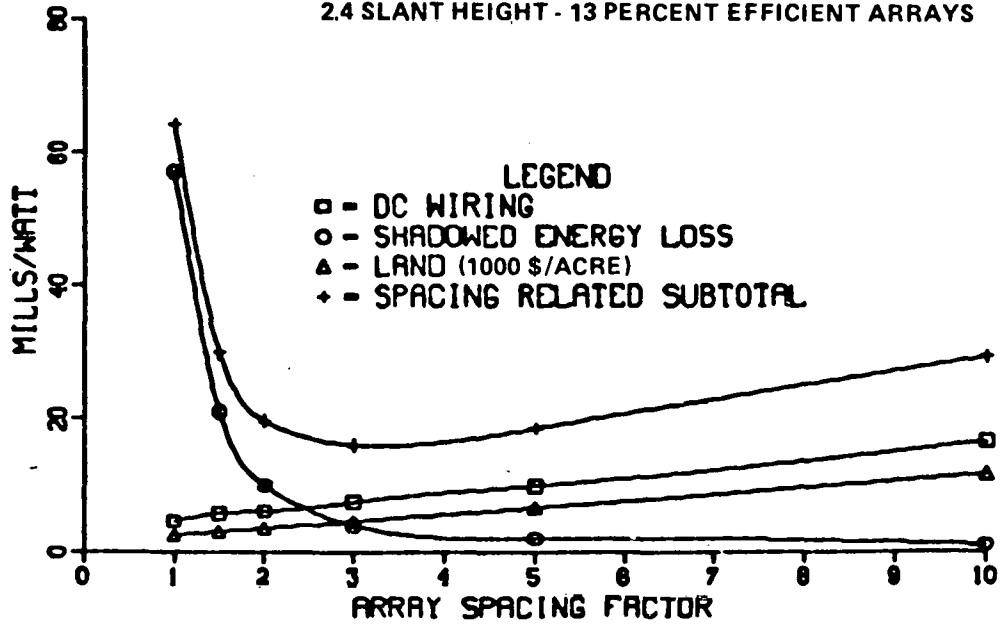
Figure 5-23 Cost Effect of Flat Plate Array Spacing - Albuquerque
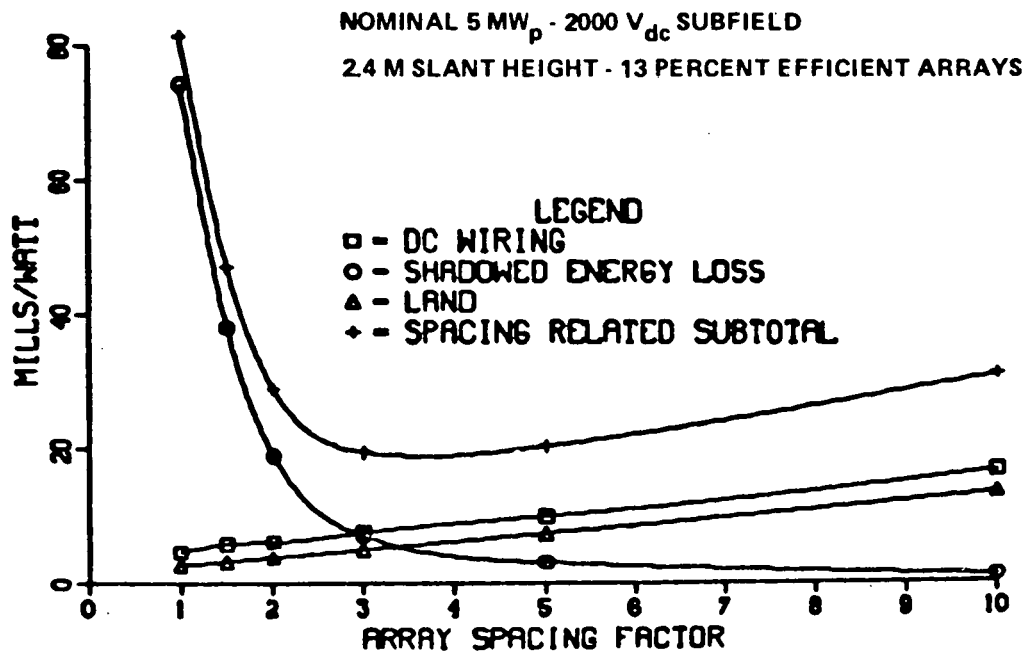
(a) BOSTON
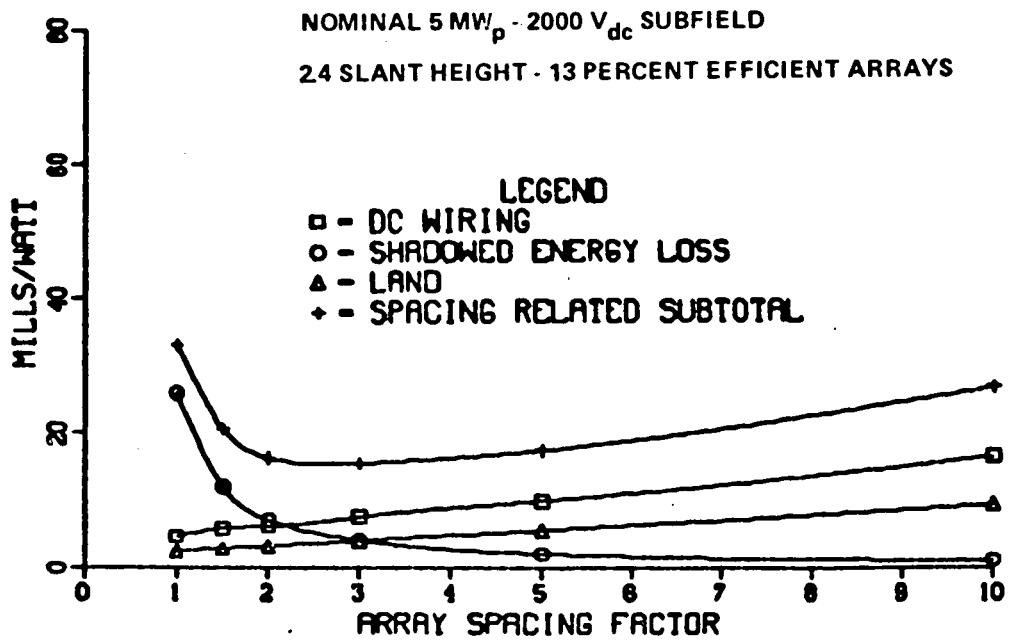
(b) MIAMI

Figure 5-24 Cost Effects of Flat Plate Array Spacing - Boston and Miami

5.2.2 Vertical Axis Arrays

Shadowing losses for vertical axis arrays, which generally incorporate concentrating collectors, are significantly affected by array geometry and other design-specific characteristics. Therefore, these losses were not evaluated during this study. However, the effect of array spacing (as defined in Figure 3-2) on total equivalent dc wiring costs is illustrated in Figure 5-25 for three array diameters. The data are for nominal 5MWp, 2000 Vdc subfields using 15% efficient arrays. As shown, cost increases are relatively small for the larger array sizes, but can become significant for small diameter arrays.
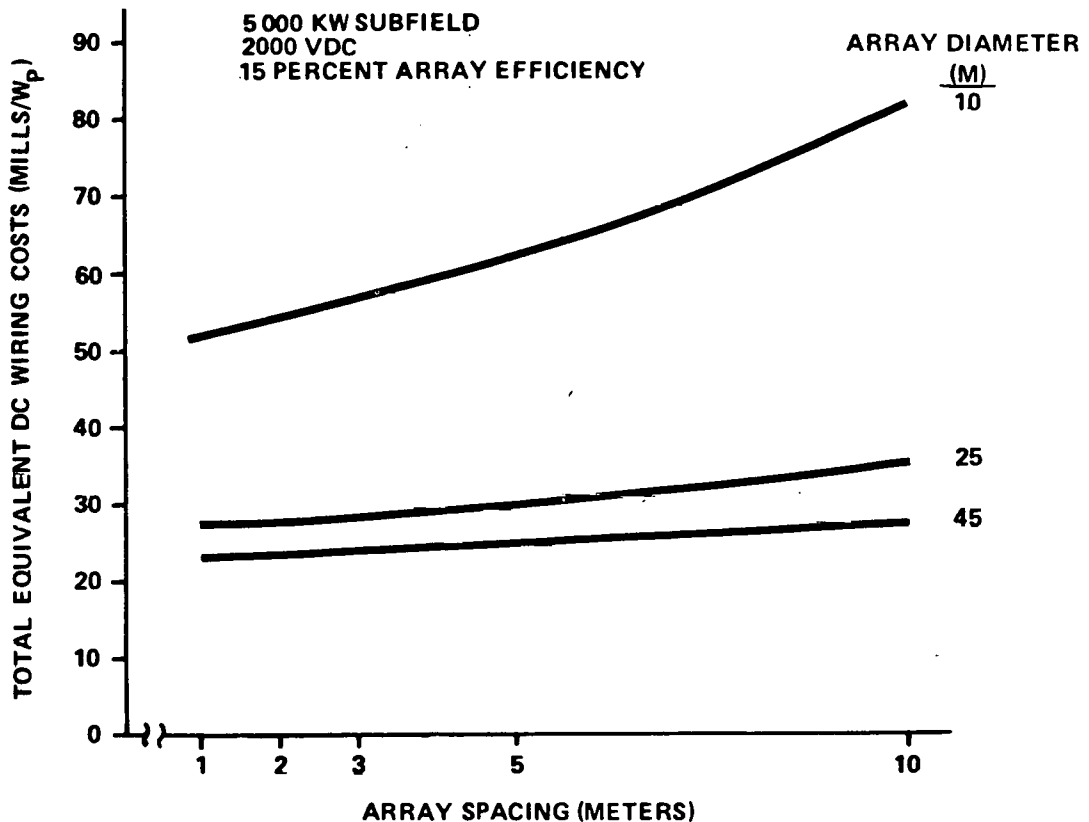
Figure 5-25 Effect of Vertical Axis Array Spacing on Total Equivalent Dc Wiring Costs

Section 6

ARRAY SUPPORT STRUCTURE CONSIDERATIONS

Previous studies have shown that array support structures can be significant contributors to photovoltaic balance of system (BOS) costs. This section discusses two aspects of array support structure design and installation. First, design considerations and requirements for mounting fixed, flat-plate arrays on flat-roofed commercial and industrial buildings are discussed. The second part of the section discusses installation techniques, including automation, which has the potential to reduce the total installed costs of large array fields.

Due to the predominant use of English units by the U.S. building and construction industries, English (rather than metric) units are used in this section.

6.1 ROOF-MOUNTED ARRAYS

Mounting photovoltaic arrays on building rooftops requires that consideration be given to the consequences of additional structural loadings imposed by the arrays, as well as other factors such as the need to maintain the watertight integrity of the roof membrane. These requirements are discussed with regard to:

- Flat roof construction types
- Building code review
- Design loads
- Array support structure design considerations

- Structural evaluation

- Support structure designs

- Analysis of promising support concepts.

The scope of this portion of the study was contractually limited to the investigation of flat-roofed buildings.

6.1.1   Flat-Roof Construction.Types

Various types of roof framing systems exist throughout the United States. From a material point of view, the most common roof systems installed on commercial or industrial buildings may be categorized as:

- Steel

- Concrete

- Wood.

Selection of a roofing system is based on several considerations that include:

- Span and load

- Aesthetics

- Climate

- Acoustical and thermal insulating properties

- Fire resistance

- Framing details such as attachments to supports, support of hung ceilings, ducts, light fixtures, piping, etc

- Diaphragm action required for transfer of lateral loads

- Cost of material, installation, finishing, and maintenance.

Table 6-1 lists the physical characteristics of several roof systems typically used on commercial and industrial buildings (Ref. 6-1).   The list of 18 roof

Table 6-1

ROOF FRAMING SYSTEMS
TYPICAL CHARACTERISTICS

Roof Type	Roof Type No.*	Physical Properties			Structural Properties	
					Recommended	
		Std. Thickness	Weight	Depth of System	Maximum Live Load	Span Range
		Inches	psf	Inches	psf	Feet
Wood Joist	1	4,6,8,10,12	5-8	4 to 12	40	20
Stressed Skin Panel	2	3 1/4,8 1/4	3-6	3 1/4-8 1/4	40	11-25
Steel Joist/Poured Gyp.	3	8 to 48	11-19	11 to 51	40	96
Steel Joist/Insul. Deck	4	2 to 3	6-8	9 1/2 - 51	40	96
Steel Beam/Precast Plank	5	2 to 3	14	8 to 15	40	15-25
Steel Deck/Insul. or Fill	6	3 5/8-7 1/4	6-24	3 5/8-7 1/4	40	9

* See Reference 6-1 for further details

Table 6-1 (cont'd)

ROOF FRAMING SYSTEMS
TYPICAL CHARACTERISTICS

Roof Type	Roof Type No.*	Physical Properties			Structural Properties	
					Recommended	
		Std. Thickness	Weight	Depth of System	Maximum Live Load	Span Range
		Inches	psf	Inches	psf	Feet
Long Span Steel Deck	7	1 1/2-7 1/2	2-11	1 1/2-7 1/2	40	33
Unit Masonry Planks	8	4,6,8,10	20-55	4 to 10	45	33
Precast Concrete Planks	9	4,6,8,10	40-75	4 to 10	40	15-50
Conc. Slab (one way)	10	3 to 10	50-125	3 to 10	60	25
Conc. Slab (two way)	11	6 to 10	75-125	6 to 10	60	10-30
Conc. Pan Joist	12	Std. Pans 6,8,10,12,14	39-76	8 to 17	60	20-34

*See Reference 6-1 for further details

Table 6-1 (cont'd)

ROOF FRAMING SYSTEMS
TYPICAL CHARACTERISTICS

Roof Type	Roof Type No.*	Physical Properties			Structural Properties	
		Std. Thickness	Weight	Depth of System	Recommended Maximum Live Load	Span Range
		Inches	psf	Inches	psf	Feet
Conc. Waffle Slab	13	Std. Pans 8,10,12,14	73-104	11 to 17	60	20-50
Conc. Flat Slab	14	6 to 10	75-150	6 to 12	60	15-30
Precast Conc. Dbl. Tee	15	8 to 24	35-54	8 to 24	60	15-75
Precast Conc. Single Tee	16	12 to 48	65-84	12 to 48	60	25-110
Composite Slab/Beam	17	3 1/2 to 6	35-70	3 1/2 to 6	60	35
Wood Truss	18	1/2	8-14	72 to 120	40	30-50

* See Reference 6-1 for further details

types in the table gives an indication of the wide variety of roof systems commonly used. Variations of these systems, exhibiting their own unique physical and structural properties as well as different fire ratings, are also commonly used. The extensive variety of roof systems does not fall easily into simple structural classifications. Consequently, roofs must be considered on a case-by-case basis when investigating array installation. All of the roof systems described in Table 6-1 could not be addressed within the scope of this study. Therefore, several representative roof systems were selected to demonstrate structural concerns for the installation of photovoltaic arrays on flat-roofed buildings.

Table 6-1 provides an indication of the self-weight (dead load) of typical roof systems. In general, steel and wood systems have weights varying between 2 to 24 psf, whereas the concrete roofs are much heavier, having a range of 20 to 150 psf. Therefore, the mounting of arrays on the average steel or wood roof is more likely to result in a significant percentage increase in dead load than for the typical concrete roof.

Steel roof systems are the most popular and comprise about 52% of all roofs used in commercial and industrial building construction. These systems are typically composed of steel joists, steel beams, or a steel deck normally topped with insulating fill, gypsum, or concrete. Steel joist systems are typically used in buildings where long spans (up to 100 ft) are necessary.

Two typical steel systems commonly found in commercial and industrial buildings are shown in Figure 6-1. The first is a steel joist/poured gypsum system which has bulb tees spanning between the joists with 1-inch

BULB T 24" OR 32" O.C.

1" FORMBOARD

2" GYPSUM

8" MIN

CEILING

4'-6'   SPACING

STEEL JOIST @ APPROX. 4'-6" C.C.
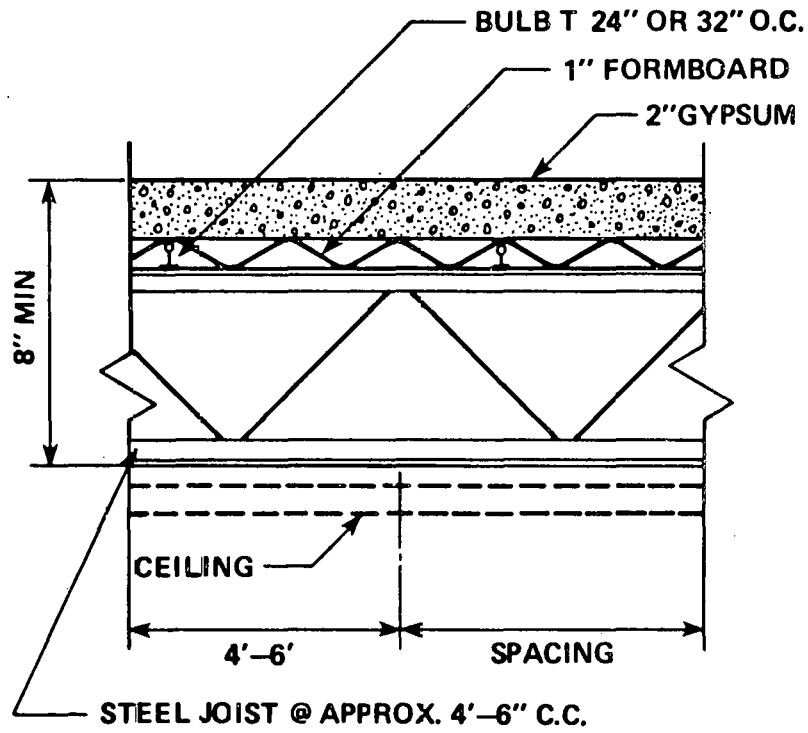
SPAN TO 96'
STEEL JOIST / POURED GYPSUM

RIGID INSULATION OR
INSUL. FILL

STEEL DECK

3 5/8" MIN

CEILING

BEAM OR JOIST
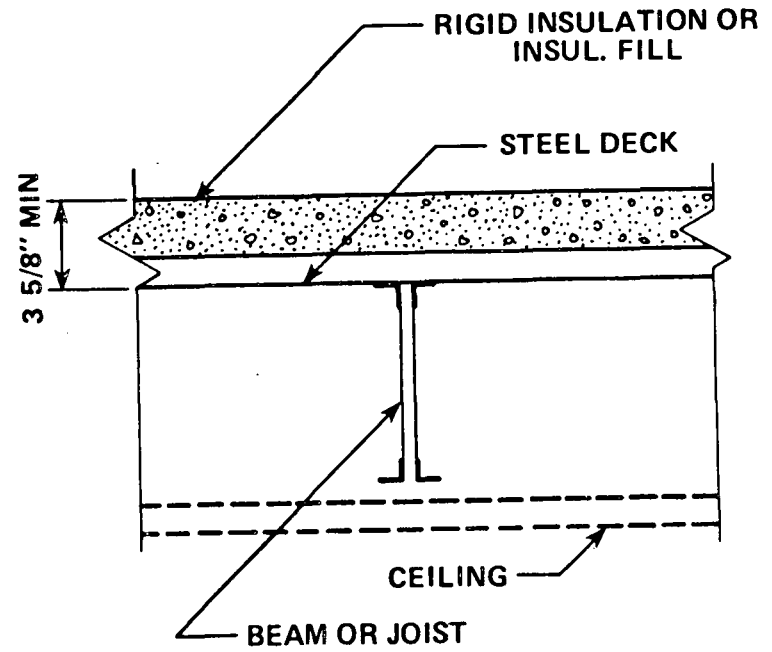
SPAN TO 10'
STEEL DECK/RIGID INSULATION

Figure 6-1 Typical Steel Industrial Roof Systems

fiberboard used as formwork for a poured-in-place gypsum layer. The second is a steel deck/rigid insulation system which uses a steel deck for diaphragm action and to serve as formwork for insulating fill.

Concrete systems, which include poured reinforced and precast/prestressed concrete, are also popular and comprise about 24% of the roofs used in industrial and commercial building construction. These systems are used where short-to-medium length ($\leq$ 50 ft) spans are needed. However, the precast concrete tee systems may be used to span lengths up to 100 ft. A concrete pan joist/waffle slab system commonly found in industrial buildings with span lengths up to 50 ft is shown in Figure 6-2.

Wood systems comprise about 15% of the roofs used in commercial and industrial building construction. These systems are used primarily in the western regions of the United States and may be utilized where relatively short span lengths (up to 25 ft) are needed. A typical wood joist roof system comprised of sawed lumber beams topped with plywood sheathing is shown in Figure 6-2.

In almost all climates provisions must be made for roof drainage. On the nominally flat roofs considered in this study, a slight pitch of the roof surface is usually included to facilitate drainage. This pitch may be as slight as 1%. When arrays are attached at an angle on a flat roof, the panels should be raised above the roof surface to allow for water drainage, to prevent ice dams, and, in some cases, to mitigate the creation of snow drifts between arrays.

In most cases the roof surface must be protected against penetration of

6-9

Figure 6—2 Typical Concrete and Wood Industrial Roof Systems

water. On flat roofs this will normally be accomplished by the use of a membrane. The most common is that consisting of multiple layers of felt mopped with tar and topped with gravel for protection during hot weather. Plastic membranes consisting of multiple layers of materials such as neoprene and Hypalon are sometimes useful for complex formed roofs and surfaces exposed to view. Sheets of tin, copper, lead, aluminum alloys, stainless steel, and galvanized or enameled steel may also be used. Maintaining the watertight integrity of the roof membrane can be a significant concern, especially for retrofit photovoltaic array installations. Most roofs are designed for a nominal amount of traffic, such as that occurring during construction, inspection after construction, and maintenance. Where higher loads are anticipated, walkways or duckboards may be used. This should be given consideration where solar array installations are contemplated. Roof areas that are used for promenades, terraces, sun decks, etc., will usually require a membrane protected by paving.

6.1.2 Building Code Review

Wide variations exist from state to state and between localities in the adoption and enforcement of building codes. In some instances, several states and localities enforce no general building code. On the other hand, states such as New York and some localities (particularly major cities such as New York, Chicago, and Los Angeles) have developed their own codes and standards. However, the majority of states, localities, and most major cities subscribe to or have adopted some variation of four model

building codes. These are:

- Uniform Building Code, 1979
- Standard Building Code, 1979
- Basic Building Code, 1978
- National Building Code, 1976.

The Uniform Building Code, issued by the International Conference of Building Officials, is generally subscribed to by the midwestern and northeastern regions of the United States. The Standard Building Code, sometimes referred to as the Southern Building Code, is issued by the Southern Building Code Congress International and is subscribed to primarily by the southern and southwestern regions. The Basic Building Code, issued by the Building Officials and Code Administrators, Inc., is subscribed to by the midwestern and north-eastern regions.

The remaining model code, the National Building Code, was developed from services provided by the American Insurance Association. No concise information could be gathered during this study that could identify which regions of the country subscribe to this particular code. Figure 6-3 (Ref. 6-2) is an aggregate map that shows the regions of the country that generally subscribe to or have adopted some variation of the model building codes.

Each model code group has a special committee (sometimes referred to as the Research Committee) to which unusual (outside present code) building permit requests may be referred by building regulatory officials. To assess the extent to which the model code groups and their Research Committees have addressed photovoltaic installations, various contacts were made during
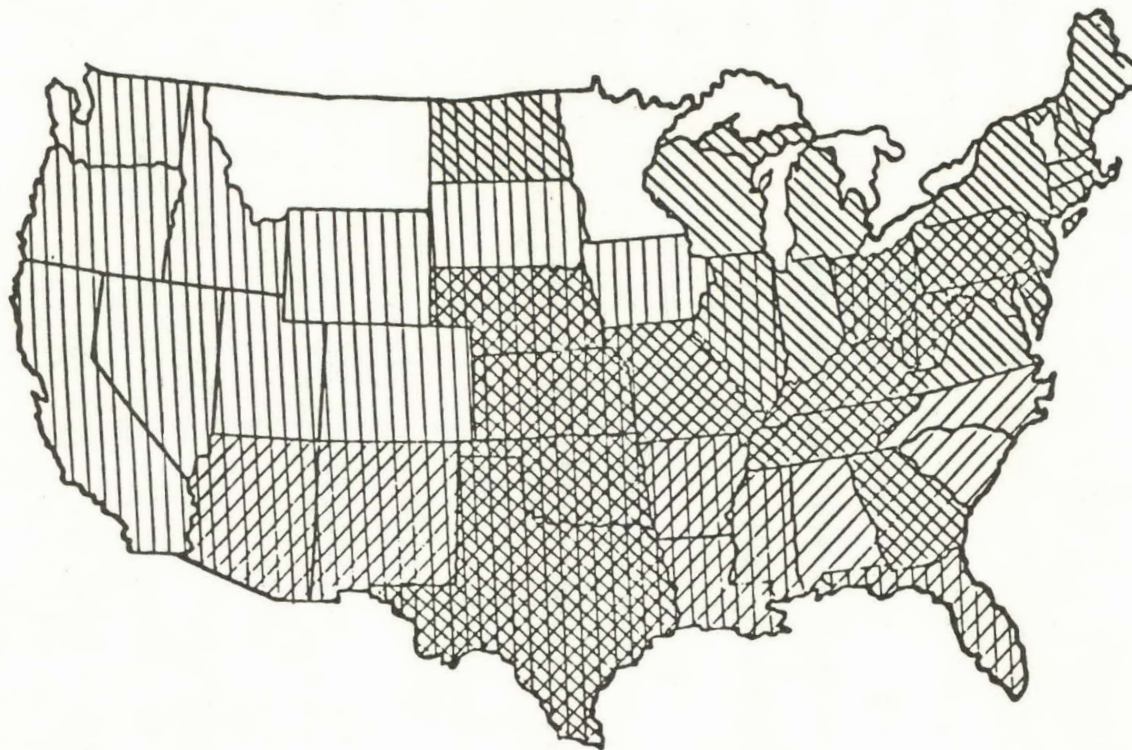
- BASIC BUILDING CODE
- STANDARD BUILDING CODE
- UNIFORM BUILDING CODE

TAKEN FROM REFERENCE 6-2

Figure 6–3   Utilization of Building Codes in the United States

this study, not only with each model code group, but also with organizations such as the Center for Building Technology of the National Bureau of Standards (NBS) and the Solar Energy Research Institute (SERI). These contacts revealed that the code groups have not directly addressed photovoltaic installations and generally showed little inclination to do so in the near future. At present these groups tend to handle the regulatory aspects of photovoltaic array installation by:

- Ignoring them altogether

- Treating photovoltaic installations like any other piece of equipment attached to a roof structure and letting existing codes and standards govern. (This causes building officials to rely upon their individual interpretation of the codes and standards in applying them to photovoltaic installations.)

- Classifying photovoltaic arrays into the same categories as solar thermal collectors and letting those codes or standards apply.

For example, several organizations and government agencies have already proposed standards for solar thermal collectors that have been adopted by states and municipalities in several areas. These include:

- HUD Intermediate Minimum Property Standards Supplement, 1979 Edition, prepared by the Department of Housing and Urban Development

- Uniform Solar Energy Code, 1979 Edition, prepared by the International Association of Plumbing and Mechanical Officials (IAPMO).

Even these standards, perhaps more properly referred to as manuals of accepted practice, fail to address the structural aspects of attaching solar thermal collectors to roof structures. Rather, they address the mechanical aspects of solar thermal collectors and define state-of-the-art procedures currently accepted by the industry.

Due to the variations within the model codes, an attempt was made to categorize those portions of the codes which might be interpreted as applying to new or retrofit array installations on building roofs. Three categories within the codes can be identified that pertain specifically to roof systems. These are:

- Roof construction
- Roof coverings
- Roof structures.

Roof Construction. Under the category of roof construction, the building codes are subdivided into a number of different subcategories. Among the four model codes, common subcategories are grouped and identified in Table 6-2, along with the corresponding clause numbers.

Codes also consider roof construction in light of the intended use of the building and varying impact on public safety. For example, a building used for assembly purposes (e.g., an auditorium), where public safety is involved, would be designed under greater scrutiny and have stricter fire regulations than a building used simply as a warehouse. Thus, a building official would likely express more concern about photovoltaic installations on structures of the former type. This would be particularly true for retrofit applications where the additional loadings might reduce the factor of safety in the structural design. Building officials would also be concerned over photovoltaic installations where the arrays contain materials that might pose a higher fire hazard than is accepted by code for the particular structure.

Table 6-2

MODEL CODE CATEGORIES RELATING TO ROOF CONSTRUCTION

ITEM	ICBO	SBCCI	BOCA	AInA
Classification a) Occupancy b) Fire Requirements	501 1701	401 601	202.0 214.0	300.2 700
Modifications	307	302	105,106	103.4
Loads	2305 2311 2312	1202,1203 7 1205,1206	710.0-712.0 714.0,716.0	904.2
Framing	2106(d) 2518(h)	1707	854	708
Drainage	2305(f) 3207	711	*	*
Insulation	3204	1707.4	823.4	802.4
Plastic Panels	5206	2604	1904.0	*

* No specific section of that code

ICBO - International Conference of Building Officials
        Uniform Building Code,1979
SBCCI - Southern Building Code Congress International
        Southern Building Code, 1979
BOCA - Building Officials and Code Administrators, Inc.
        Basic Building Code, 1978
AInA - American Insurance Association
        National Building Code, 1976

Loadings on roof structures may include wind, snow, earthquake, live loads, and wind pressures on exposed surfaces. Wind load provisions contained within the four building codes are based on the requirements or modifications of those given in the ANSI A58.1-1972 standard (Ref. 6-3). For retrofit installation of photovoltaic arrays, additional loadings would be imposed on the existing roof structure and would require a building official's judgment as to whether or not a structural reanalysis of the roof is warranted. Loadings imposed by photovoltaic arrays are discussed further in Section 6.1.3

Under the subcategory of framing, specifications are given pertaining to:

- Maximum allowable span length
- Maximum allowable stresses
- Maximum deflections
- Width and depth requirements of rafters
- Roof slope requirements.

Other items such as drainage requirements, specifically those pertaining to ponding on roof structures, would also need to be considered for the installation of photovoltaic arrays.

Roof Coverings. Table 6-3 indicates the sections of each code corresponding to roof coverings. Roof coverings are classified according to the severity of exposure to exterior fire and their ability to resist the spread of fire from surrounding buildings and structures. Also certain restrictions exist in the codes as to the extent an existing roof may be renewed or repaired.

Table 6-3

MODEL CODE CATEGORIES RELATING TO ROOF COVERINGS

ITEM	ICBO	SBCCI	BOCA	AInA
Roof Coverings	3201-3208	301.3(d), 706,1707.9	903.3, 926.0	530,802

Table 6-4

MODEL CODE CATEGORIES RELATING TO ROOF STRUCTURES

ITEM	ICBO	SBCCI	BOCA	AInA
Roof Structures	3601	*	925.0	807

* No specific section of that code

ICBO - International Conference of Building Officials
       Uniform Building Code, 1979
SBCCI - Southern Building Code Congress International
       Southern Building Code, 1979
BOCA - Building Officials and Code Administrators
       Basic Building Code, 1978
AInA - American Insurance Association
       National Building Code, 1976

Roof Structures. The corresponding sections of each model building code pertaining to roof structures are shown in Table 6-4. According to the codes, a roof structure is defined as any structure above the roof of any part of a building, or any bulkhead, tank, or other surface equipment that extends above the roof. Under this definition, photovoltaic arrays installed on the surface of a roof would most likely be categorized as roof structures even though the current codes do not explicitly define them as such.

Any structure or equipment installed on a roof must have a supporting framework capable of supporting all loads. The structure must be able to transfer the loads to the foundations or other permanent supports of the building.

6.1.3 Design Loads

When photovoltaic arrays are installed on the roof of a building, their influence on a variety of loadings must be considered. The most important loads to be considered include:

- Dead load
- Live load
- Snow load (sometimes considered a component of the live load)
- Wind load
- Seismic load.

As a part of this study, a survey was conducted of firms in the solar industry (primarily those involved with the design and installation of thermal collectors) to identify the methods and practices currently in use.

From the survey it was found that for large retrofit installations, most building inspectors require a structural reanalysis of a roof. Depending upon the location of the site, wind and/or snow loads are the most significant factors in determining if roofs are structurally adequate. Loadings due to solar installations are largely determined by an engineer's experience and judgment and his interpretation of present codes. The survey also revealed that, in some cases, building inspectors do not require a reanalysis of the roof if the dead load of the arrays is below certain arbitrarily set values.

The survey revealed inconsistencies in the manner in which loadings, especially wind and snow, are determined for roofs in retrofit installations.

Thus, before any standard procedures or recommendations concerning rooftop solar installations can be incorporated into the building codes, more research is needed to adequately define the loadings. Work continues in the general area of loadings, initiated at least in part by roof failures of stadiums and coliseums in the past few years that have been attributed mostly to uncertainties in the loads and to unanticipated loading combinations (Refs. 6-9 through 11). This work includes that of ANSI Committee A.58, the Model Code Groups, and the Center for Building Technology, National Bureau of Standards. It should be noted that a Draft Revision of the ANSI A.58 Standard is undergoing public review; a new edition is expected to be issued within the 1981-82 time frame.

Dead Load. The dead load of a structure is its self weight and is readily defined in all major building codes. In the solar industry, designers have

expressed concern that existing roof structures may be overstressed by the dead load of the collectors. Previous studies have indicated that photovoltaic arrays weigh approximately 3 to 4 psf of projected roof area (Ref. 6-4). When the weight of the support frame is added, the dead load of the entire photovoltaic array might be as much as 12 psf. However, when compared with the other loads, such as snow and wind loads, the dead weight of the collectors may be relatively small.

Live Load. The live load specified in most codes covers all structural loads except dead loads and lateral loads (from wind and earthquakes). Loads due to the required function of the structure as well as some possible environmental loads fall into this category. For example, live loads for industrial structures may typically be dominated by equipment weights or storage of materials, while live loads for the floor of an auditorium are dominated by loads due to occupancy. In the case of roofs, the live load is typically given as a minimum required loading for design. This must be checked and perhaps increased for loads due to roof top equipment and building machinery, maintenance requirements and personnel access and ponding of rainwater. Minimum live loads for slab roofs are normally in the range of 12 to 20 psf but can be as high as 100 psf if the roof is used as a sundeck or is available for public assembly (Ref. 6-3). Failure to prescribe adequate live loads has been known to lead to roof distress and failures such as after stacking heavy materials on a roof for intended maintenance.

Snow Load. Snow loads on roofs vary widely throughout the United States. For certain sections in the Western states, actual snow packs of over 700 psf have

been recorded (Ref. 6-5). Factors affecting snow accumulation on roofs include:

- Geographic aspects: local climate, latitude, elevation
- Roof geometry
- Site exposure
- Wind characteristics.

In addition, snowfall varies from year to year and either a mean recurrence interval must be established for design purposes or account should taken of the maximum recorded snow load for which data is available. Snow loads may be stipulated by the governing building code. In the absence of such a code or where the code's guidance appears inadequate for the special circumstances involved, snow loading for design purposes may be based on local historic records, or on the use of accepted snow load maps.

To establish a design snow load for a particular roof, it is necessary to have an estimate of the amount of snow that will settle on the ground in that vicinity. Roof snow loads are normally related to the ground snow loads, through a ground-to-roof conversion factor. For the design of both ordinary and multiple series roofs, either flat, pitched, or curved, a ground-to-roof conversion factor of 0.8 is specified in most codes.

Tilted arrays mounted on flat roofs pose particular potential problems in that they might tend to behave as snow fences, encouraging additional snow accumulations. Heavy snow loads may cause roof failure or otherwise damage the roof by causing excessive deflection and the breakage of bonds between insulation and membrane within the roofing composite. One method, presently

used for thermal collector installations to ensure against snow drifting, is to mount the arrays suitably clear of the roof surface. In this manner, snow removal may be aided by the wind rather than by maintenance personnel.

Some initial data exists, regarding the accumulation of snow and ice at solar thermal collector installations as well as exploratory work on design criteria (Ref. 6-7). However, this particular study is limited in that results are reported for only a small number of installations studied over only a part of one winter. In summary, work on the development of snow loading criteria for roof mounted array installations is at the exploratory stage and more research is needed to properly identify the effects of solar arrays on snow loads. Until such design criteria are developed and incorporated into existing codes and standards, the engineer must apply experience and judgment to predict how solar installations may affect normal snow loads on roofs.

Wind Load. Designing structures to resist wind loading is, like the analysis for snow loading, a complex engineering task. Considerable research has been conducted to evaluate wind effects on various structures. This has resulted in the establishment of design pressure coefficients that account for building shape and wind direction. In addition, extensive studies of basic wind velocities related to geographical locations have resulted in the development of detailed wind velocity maps for the United States. Other studies of surface resistance relative to the degree of land development and gust characteristics at a given location have provided a method for a refinement of the basic wind velocity and its effect on structures.

When photovoltaic arrays are mounted on roofs, the resulting wind loads on the arrays and roof structure are even more difficult to determine. Wind design criteria for roof-mounted arrays presently fall well short of the state of development of criteria for buildings having regular roof configurations. In general photovoltaic array installation will obstruct and modify the wind characteristics (pattern, velocity, and pressure) about a roof structure and therefore change its loads from those that would occur without the arrays. To what extent these changes are significant depends upon the particular location, orientation, and size of the photovoltaic installation. Only by extensive (and expensive) wind tunnel testing of the specific system configuration can the engineer develop a detailed understanding of its wind flow characteristics. For most engineering applications, however, a designer must look to generalized standards and codes and, consequently, somewhat conservative guidance as to wind loadings.

Current building codes have not incorporated wind loading criteria for roof-mounted photovoltaic arrays. However, codes and standards have included criteria for mounting other equipment and structures on roofs. For example, some solar installation firms use HUD's Intermediate Minimum Property Standard (Ref. 6-8) and mount structures to withstand at least 100 mph winds. The present lack of design criteria for roof-mounted photovoltaic arrays may lead building inspectors to apply these, perhaps overly conservative, design requirements to photovoltaic array installations, especially in the near term.

Seismic Loads. The typical building code approach (for example UBC) for the evaluation of seismic loads requires that static-equivalent lateral forces

be calculated at various elevations of the building, which are directly related to the vertical distribution of the weight of the structure. Adding photovoltaic arrays to the roof increases the weight at that elevation and modifies the lateral forces calculated by this simple approach. This could be used to estimate the array reaction forces on the roof structure. However, other than through this method, the building codes do not specifically deal with the seismic loads on roof-mounted arrays.

6.1.4 Array Support Structure Design Considerations

This section discusses some of the significant array support structure design considerations and options with regard to:

- Structural material
- Support location
- Roof penetration
- Design integration
- Installation.

On flat roofs, some type of framing system will generally be necessary to support and properly orient the photovoltaic panels. The framing system used to support the panels might consist of simple wide-flange and angle-steel sections or more complex steel or aluminum tubular space frames. Space frames are often suggested for arrays that span long distances. However, studies have shown that space frames are more expensive, more difficult to fabricate, and less available than conventional frame construction (Ref. 6-12).

Structural Materials. Potential materials for the fabrication of low-cost support structures for photovoltaic arrays include concrete, wood, aluminum, and steel.

6-24

Concrete was eliminated as a candidate material for this study due to its large material unit weight and its potential for overloading the roof.

Wood has the disadvantage of limitations on the lengths and shapes of structural members that can be purchased unless more expensive glue-lamination construction is employed. When regular wood members are called for in lengths greater than 16 ft, the unit price increases significantly. This implies the need for numerous roof penetrations for the vertical array supports. As will be shown in the following subsections, penetrations are a major cost driver. Although wood cannot be excluded as a candidate material, it was not considered further in this study.

Aluminum is light weight and can be easily fabricated into unusual structural shapes. However, aluminum is generally more costly than structural steel and may not be cost effective for large photovoltaic array installations. Although the high initial cost for aluminum may be somewhat offset by low life cycle maintenance costs and by aesthetic considerations, it was not considered further in this study.

Steel was considered to offer the greatest versatility over the other structural materials. It has a wide range of applications and is readily available from mills and warehouses in a variety of standardized shapes and forms. Many different fastening systems exist that allow the use of fast assembly operations. For these reasons, steel was selected as the most promising low-cost structural material for evaluation in this study.

Support Location. Two general methods can be used to transfer the array

loads to the building structure. These relate to where the reaction loads are carried as follows:

- Roof supports
- Wall supports.

By using roof supports, the array support structures are located over and supported by structural components of the roof system, such as the membrane, beams, or joists, much in the same manner as shown in Figure 6-4. With this method the array loadings must generally be distributed evenly over the entire roof system to prevent any localized overstress. However, insufficient margin in structural capacity may exist in the roof (especially for retrofit applications) to sustain the additional loadings. Therefore, some type of strengthening or reinforcing procedure might be required to structurally upgrade the roof; this normally cannot be performed without substantial expense.

The wall support method has the distinct advantage of distributing the loads only at vertical building members such as walls or columns. The wall approach, illustrated in Figure 6-5, distributes the array loads only at selected locations on the roof -- that is, directly above vertical building members. Thus, the array support structure may be required to span extremely long distances or even span the entire roof.

From the survey of solar (thermal) installation procedures, it was determined that most firms presently use the wall support method. For a given array size, the wall support approach also has the advantage of requiring fewer roof penetrations. The economic advantages of using the wall support
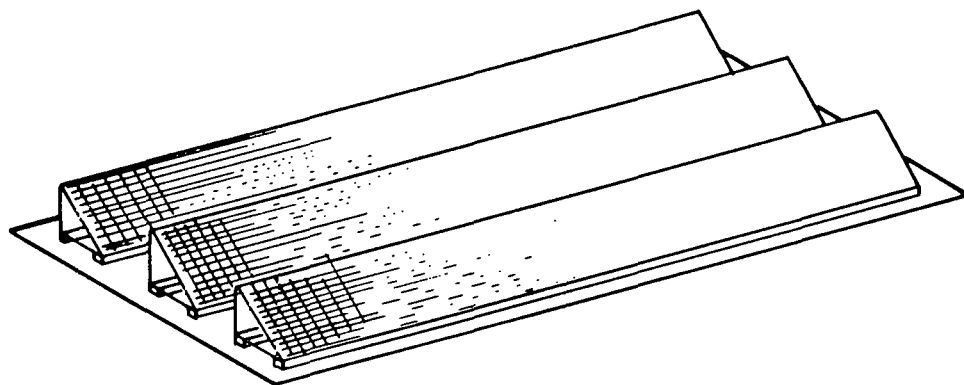
TYPICAL SUPPORT PADS WHICH
TRANSFER ARRAY LOADS DIRECTLY
INTO MINOR ROOF BEAMS OR JOISTS.
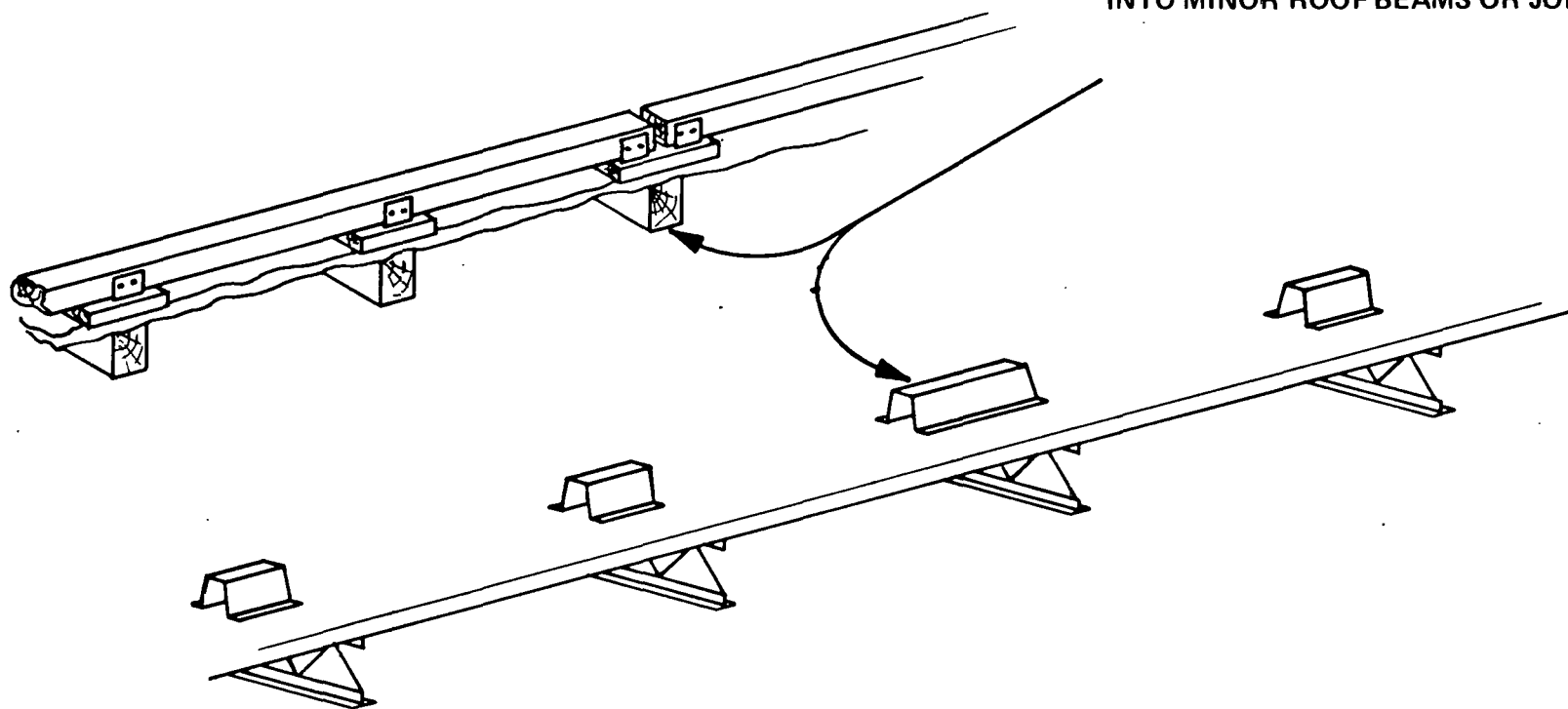
Figure 6–4 Roof-Support Method
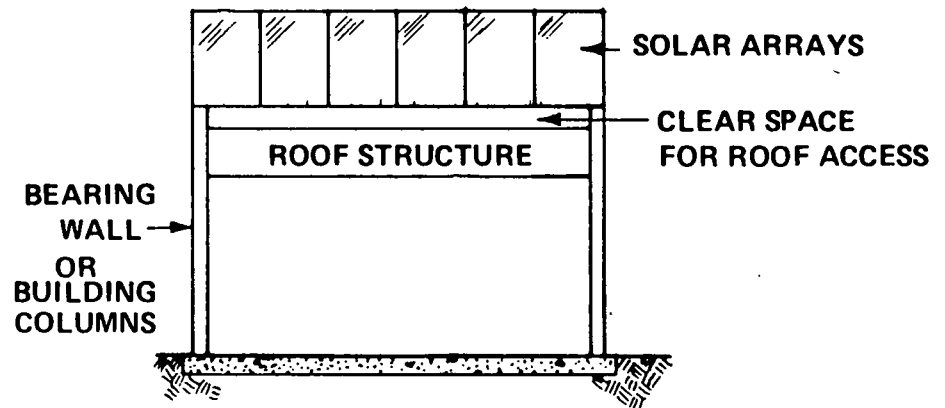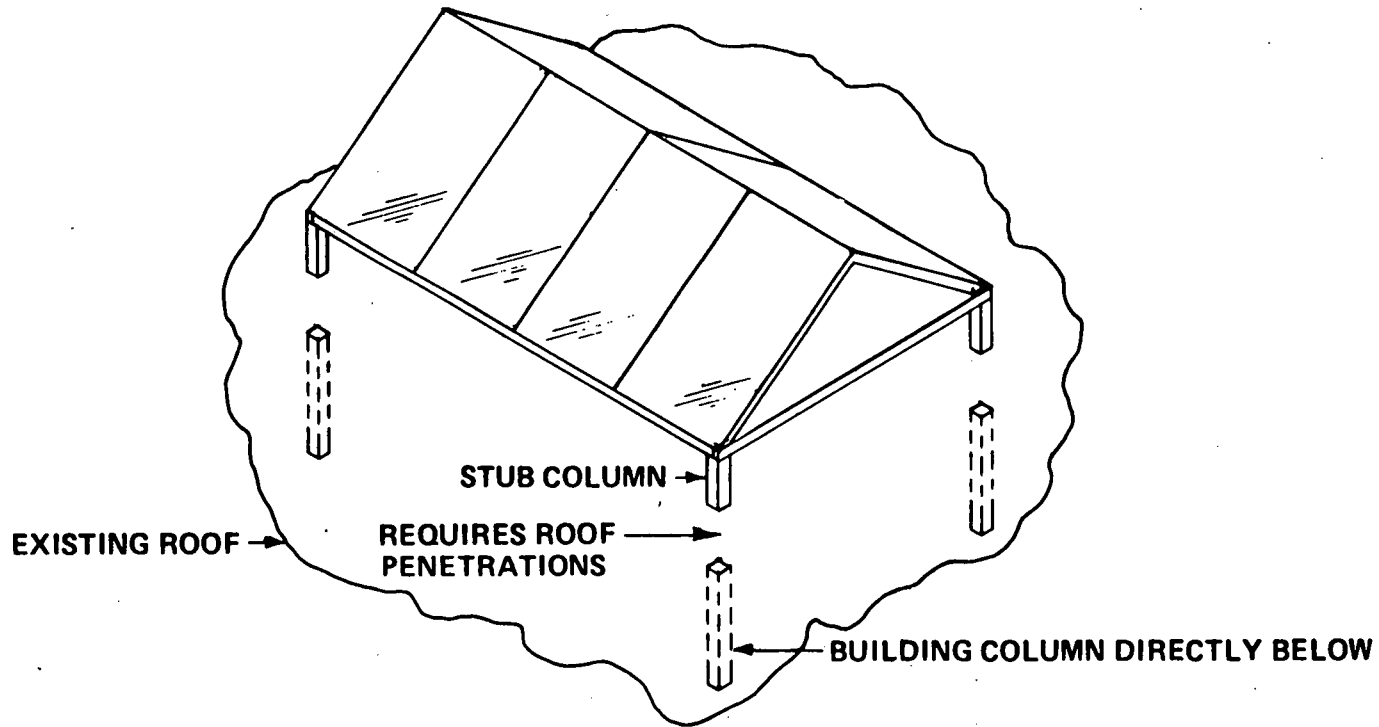
Figure 6—5 Wall-Support Method

approach over the roof support approach for a large photovoltaic installation are discussed in a later section.

Roof Penetrations. Penetrations are generally required at the points where the array support structure loads are transferred to the building. Any penetration of the roofing membrane, especially in retrofit installations, creates potential problems that can result in leaks or failures. Three types of roof penetrations commonly used by the roofing industry, shown in Figure 6-6, are:

- Pitch pockets
- Sleepers
- Curbs.

The pitch pan or pocket is one of the oldest and most common types of roof penetration. However, previous studies have recommended that pitch pockets not be used for any type of solar installation (Refs. 6-13 and 6-14). Pitch pockets cannot be expected to be permanently watertight due to their design, and thus they require periodic maintenance. Hence, any deterioration resulting from poor maintenance allows moisture to enter the roof membrane and the building. This can cause expensive problems for owners and contractors, such as blistering, splitting, and delamination with subsequent damage to building interiors and equipment.

Despite the above, the need to reduce first costs often influences many designers to specify the use of pitch pockets, even though the National Roofing Contractors Association (NRCA) strongly discourages their use.

Sleepers bolted to the roof are also commonly used. These can be effective as an array support except that the bolt penetrations have to be protected against moisture leakage. Also, if the insulation under the waterproof membrane of the roof is not sufficiently dense, large vertical loads may shear the roofing and cause leaks. To date, sleepers used in solar thermal installations have caused a high proportion of leaky roofs.

The third penetration type illustrated in Figure 6-6 is the curb mount. A curb mount requires building up the roof surface with framing members to act as an equipment support. Curbs are an old standby and, if detailed and specified correctly, can be constructed to withstand the horizontal as well as the vertical loads applied to it. The National Roofing Contractors Association recommends the use of curb mounts.

Design Integration. The integration of building and array support structures could result in significant cost savings, especially for new construction.

One approach would involve incorporation of array support elements into the basic building structure. For example, columns might be extended above the roof line to provide a bases for supporting the arrays. The roofing membrane would be installed as usual, treating the projecting columns like any pipe or stack penetration. This would slightly increase the overall roof costs but would eliminate the costs of retrofit roof penetrations. This approach also holds promise to function better than retrofit roof penetrations throughout the life of the building.

A more elaborate integration method involves roof systems embodying trusses.
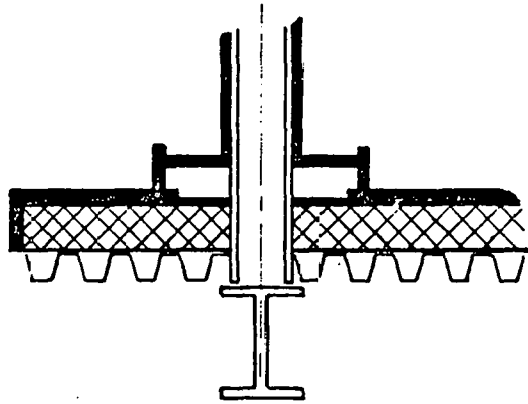
PITCH POCKET
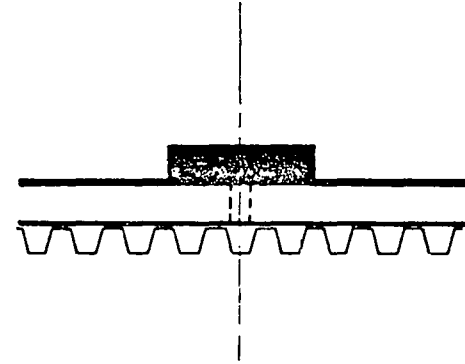
SLEEPER
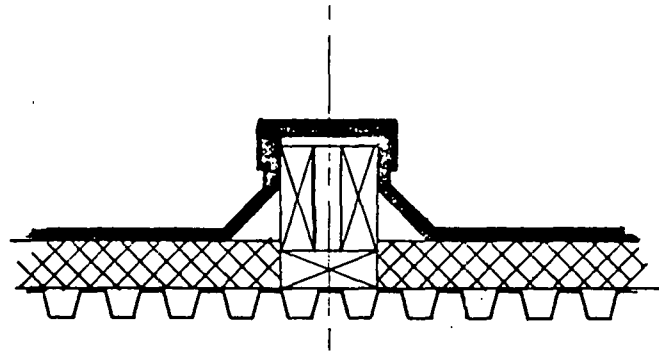
CURB   TAKEN FROM REFERENCE 6-13

Figure 6—6 Types of Roof Penetrations

Here the sloping or vertical truss members might be extended above the roof line and used to support solar arrays. This may succeed for a particular building and roof arrangement but does not lend itself to widespread application because it depends on fortuitous arrangements of roof system trusses.

In conclusion, there is some possibility of integrating array supports with some flat roof structures but practicability will depend greatly on specific building arrangements.

Installation. Scenarios for installing solar arrays on roofs are relatively few. One method is to bring the individual pieces of an array support structure to roof level and then assemble the array piece by piece, using no more than regular hand tools. Another method would be to have the array support structure preassembled on the ground. The entire structure would then be raised onto prefabricated roof supports.

There are numerous hoisting devices available (e.g., bucket truck, cherry picker, crane, or forklift). A simple device is a roof hoist that can be temporarily mounted on the roof. However, its load reactions on the roof require special consideration. Lifting the collectors manually is possible, but might not be economical for large solar installations.

Care must also be taken to ensure that temporary loads created during photovoltaic array installation are not so large as to cause roof damage or failure. Such loads may include the weight of workers or construction equipment. However, with proper construction planning and scheduling,

loads can generally be kept at a minimum to prevent any unanticipated roof distress or failure.

6.1.5   Structural Evaluation

To investigate the structural significance of mounting photovoltaic arrays on the roofs of industrial and commercial buildings, the following scenario was formulated. First, roofs were designed for a typical size industrial building (50 ft wide x 148 ft long x 30 ft high), as shown in Figure 6-7, using both wood and steel construction for two geographic locations:

● Boston, Massachusetts, representative of a region
  of heavy snow and large wind loads

● Albuquerque, New Mexico, representative of a region
  of large wind loads and attractive for solar
  installations.

Structural member sizes for these baseline roof designs were selected from a wide range of standard shapes. Availability of standard member sizes which exactly provide the required characteristics is unusual. Normal practice is to select the smallest (or least costly) member size that exceeds the requirements. In this manner, the baseline designs for the roof members may have some structural margins already built into them.

Second, using these baseline designs, additional loadings were determined for retrofit solar arrays attached to the roof. The roofs were then reanalyzed to determine if member stresses were still within the allowable code limits. To assess the probable worst case situation, roof supports were used in this part of the analysis.

30'

50'

150'
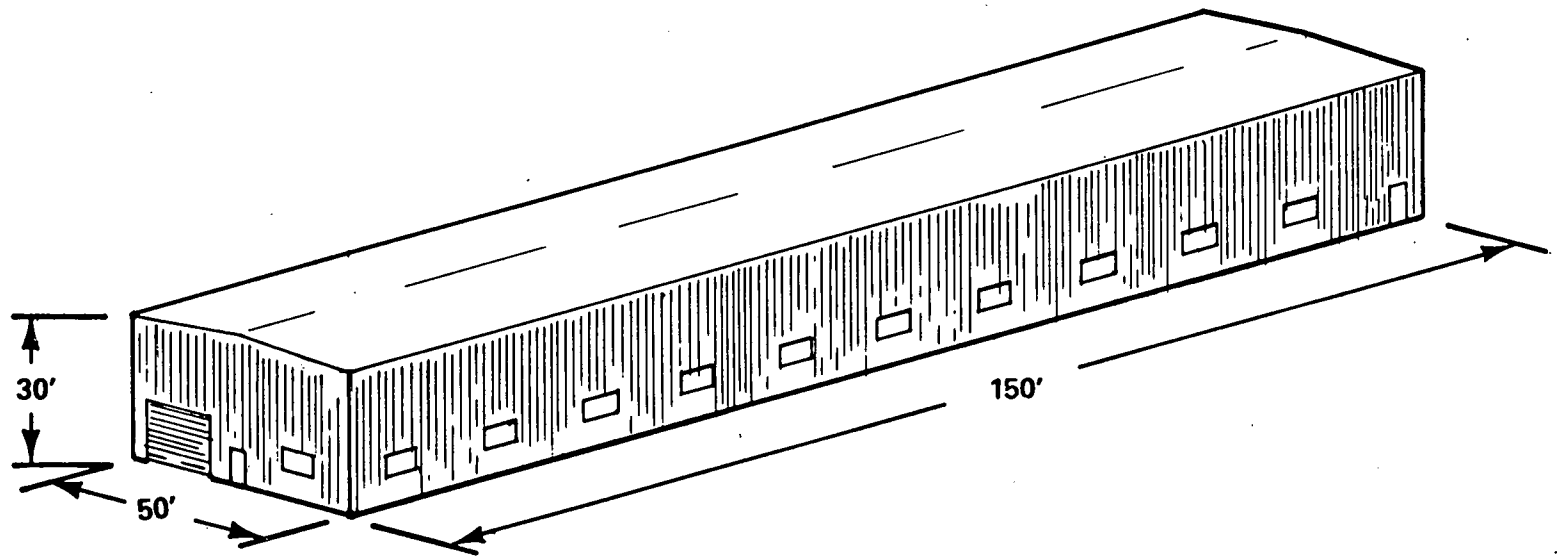
Figure 6—7 Typical Size Industrial Building

<u>Design Criteria</u>. Loadings used in the design of the baseline roof members are shown in Figure 6-8. These loadings were determined using the Uniform Building Code (Ref. 6-15) and ANSI A58.1-1972 Standard (Ref. 6-3). The wind load corresponds to a 90 mph wind. The snow load applies only to the Boston site while the remaining loads apply to both Boston and Albuquerque.

The dead load assumed for panels and array support structure is also shown in the figure.

To keep the analysis within the scope of this study and to facilitate comparison with alternate roof designs, the live, snow, and wind loads were assumed to be uniformly distributed over the entire roof area.

For the baseline designs, the following simplified loading combinations were assumed:

- Dead load plus live load
- Dead load plus snow load (Boston only)
- Dead load plus wind load.

Additional loadings, as well as more complex loading combinations, are possible and would require consideration in a more detailed design analysis. The photovoltaic arrays were assumed to have an 8-ft slant height and to have an angle of 35° with respect to the roof surface. To reduce shadowing effects, the arrays were assumed to be spaced 13-1/2 feet apart as shown in Figure 6-9. This spacing reflects the conventional approach where the clearance between the arrays is taken to be 1-1/2 times the heights of the array. The arrays are assumed to be oriented in an east-west direction.
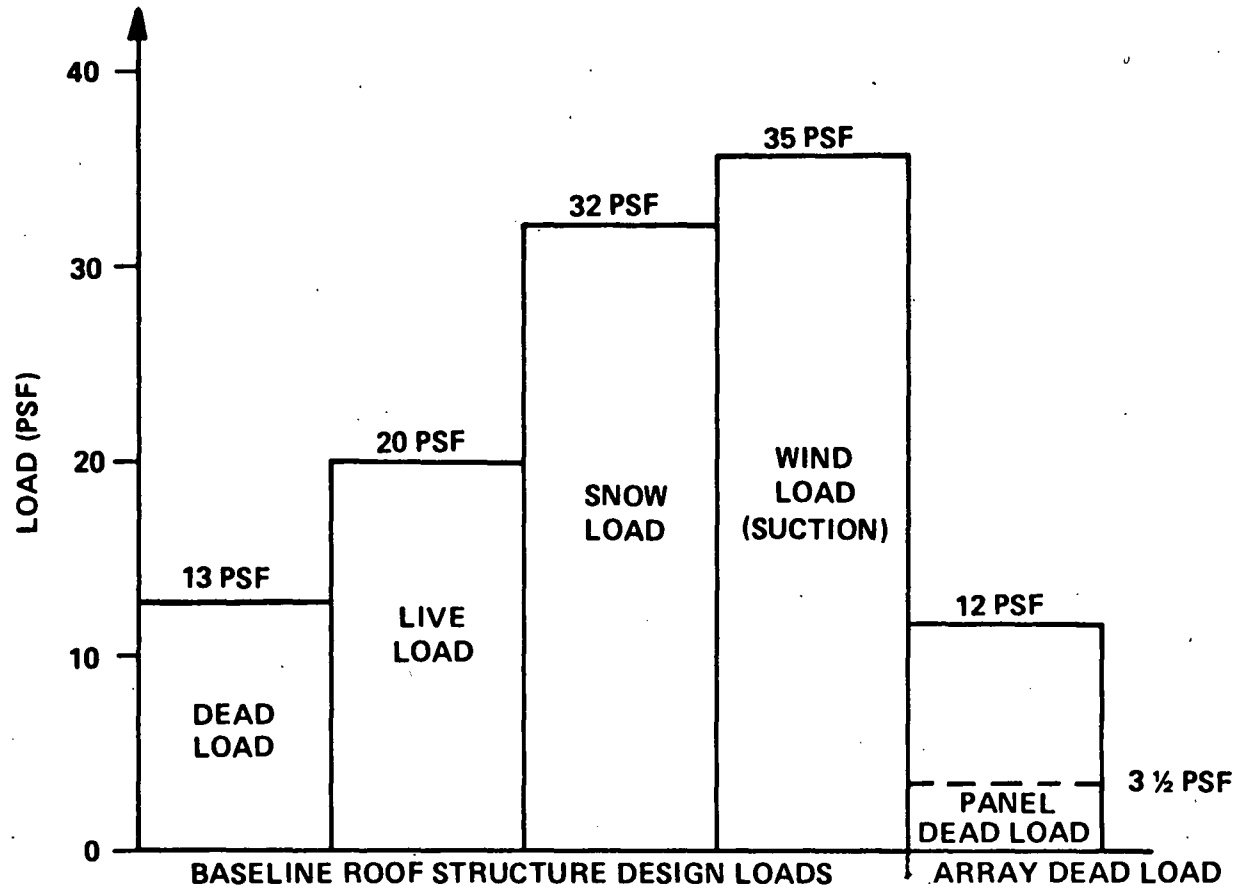
Figure 6—8 Design Loads for Roof Members
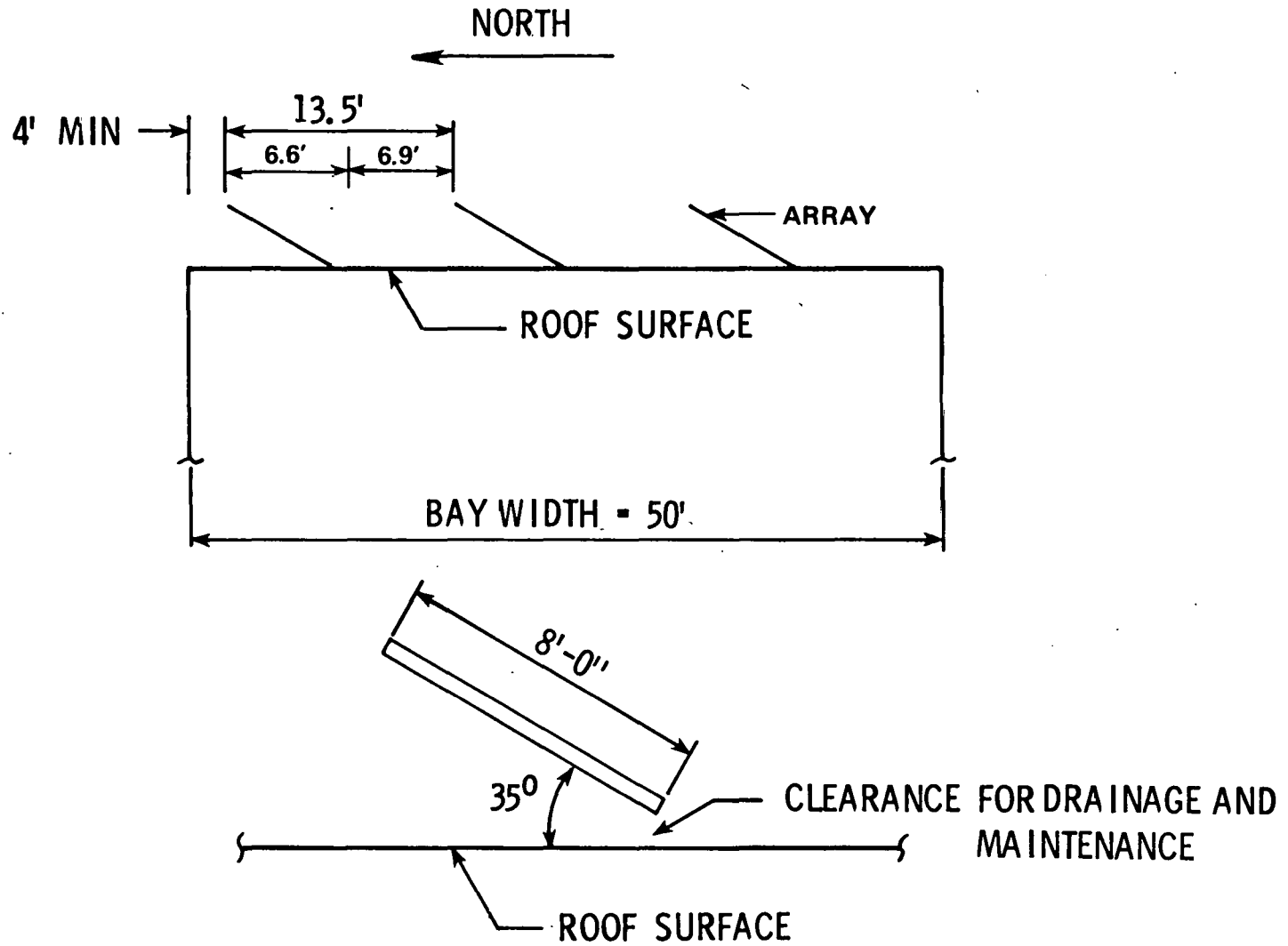
Figure 6–9 Roof Array Geometry

The building, however, can be oriented in any direction. Thus, to evaluate maximum roof loading, the building length was also assumed to be oriented in an east-west direction. For this orientation and array spacing, three rows of photovoltaic arrays can be located across the 50-foot width of the building

As mentioned, the additional loads imposed by the arrays cannot be presently defined using existing codes and therefore must be determined by using approximate procedures and engineering judgement.

Snow was found to be the dominant load for Boston. In reality, drifting of snow between the arrays can occur. However, the development of a rational design approach to define particular snow drift loads would require extensive research. In the absence of this design approach, code values of snow load were used and loading conditions were simplified by assuming snow drifting would not occur between the arrays. Thus, for the Boston retrofit installation, the only additional assumed load imposed on the roof was the self weight of the photovoltaic arrays.

Wind was found to have the most influence in the roof design for Albuquerque. As mentioned, a rooftop solar array installation will obstruct the wind and modify its characteristics (pattern, velocity, and pressure) about a structure. Specific wind design criteria for these rooftop arrangements are not presently available. In the absence of these criteria, an analysis was performed which made the simplifying assumption that the arrays would behave as flat plates under the design wind load (90 mph wind velocity). Forces on the array panels were derived from the wind velocity by applying the appropriate pressure coefficients from the ANSI A58.1-1972 Standard

(Ref. 6-3) which converts wind velocities to wind pressures. Based
on this standard and the 90 mph wind velocity, a wind loading of 21 psf
was used in this portion of the study. Thus for the Albuquerque retrofit
installation, only the wind load on the arrays and the array self weight
were added to the loads in the original baseline design.

Wood Roof Design. Initial designs were performed for a timber roof for
the industrial building shown in Figure 6-7 without considering the
addition of photovoltaic arrays. For this these particular designs,
columns supporting a large, glued-laminated girder are evenly spaced
down the center of the building. Framing into this main girder are roof
beams spaced 4 feet on center that provide support for a plywood deck.
The wood joist design for the building located in Albuquerque is shown
in Figure 6-10.

Arrays were then assumed to be attached and oriented on the roofs in the
manner shown in Figure 6-11. Here, the roof support method is utilized,
the array loads being transmitted to the foundations through the roof
beams rather than directly into the vertical supports (wall support method).
Additional loads imposed by the arrays were then determined, and the roofs
were reanalyzed to identify changes in the design margins.

The design margins for the secondary roof support system (the roof beams)
are plotted in Figure 6-12 for both the baseline designs and with arrays
added, as the ratio of the allowable stress specified by the code to the
actual design stress. A ratio larger than unity indicates that a structural
member is understressed. Figure 6-12 indicates that the roof beams of the

37 @ 4' = 148'

24'

25'

25'

COLUMNS

6-3/4" x 13-1/2" GLUE
LAMINATED GIRDER

A–A

— 3/4" PLYWOOD

4" x 12" ROOF BEAM

48" C-C

SECTION A-A
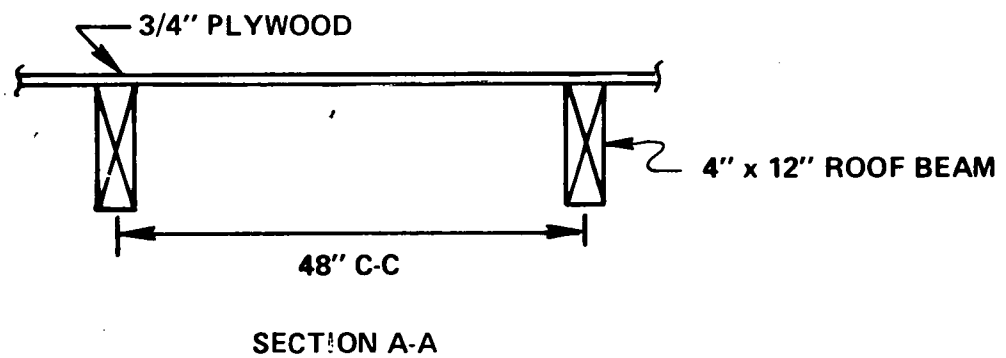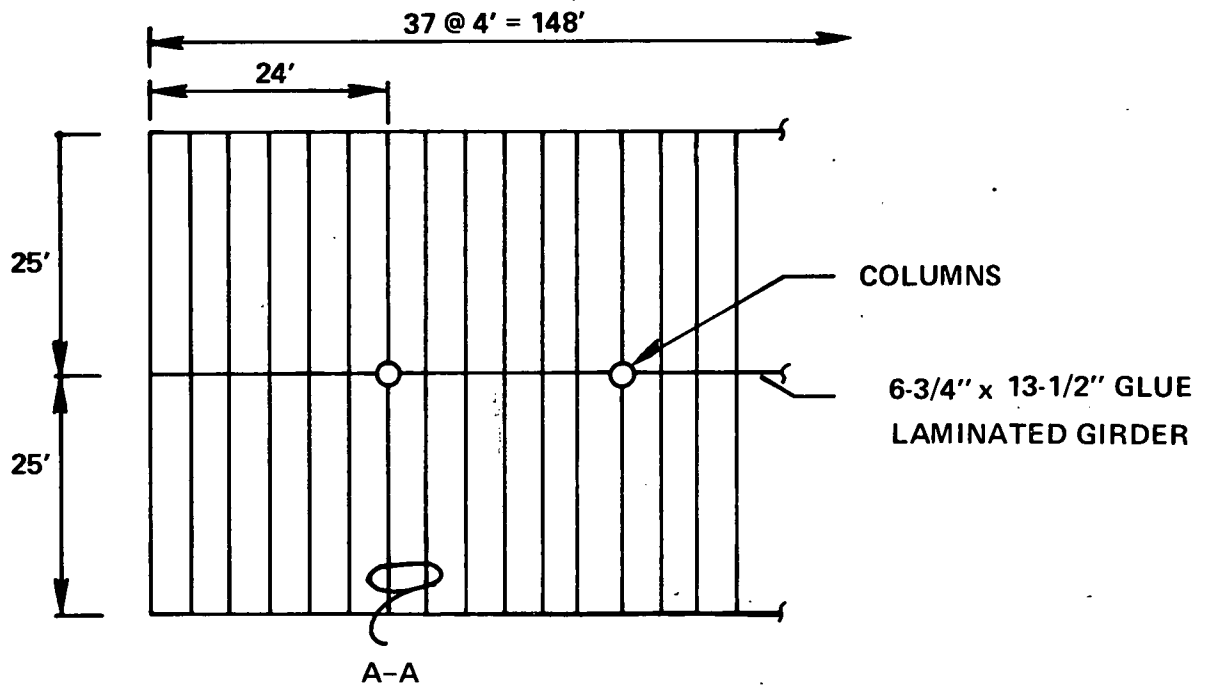
Figure 6-10 Wood Joist Roof Design for Albuquerque

POINTS OF ATTACHMENT

ROOF DECK
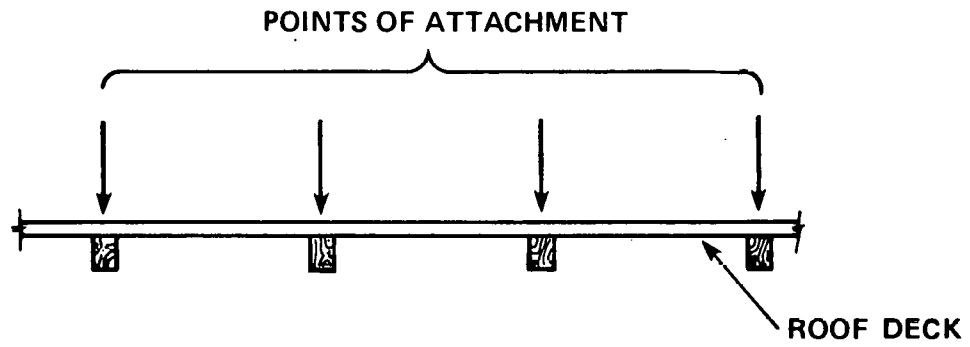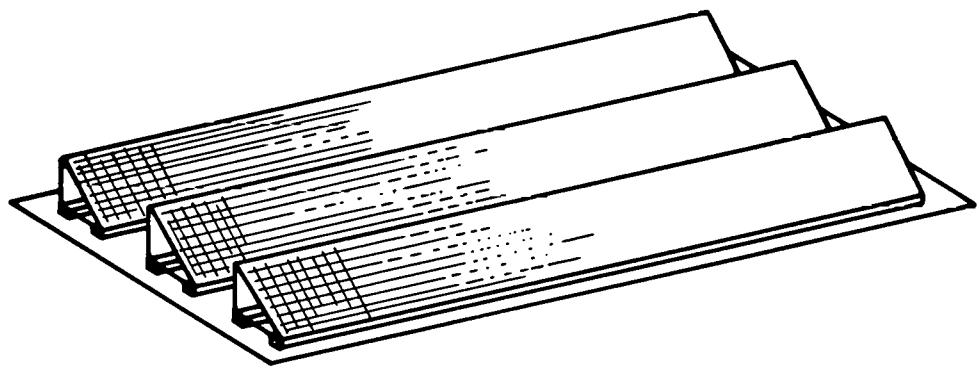
Figure 6-11 Array Supports for Wood Roof
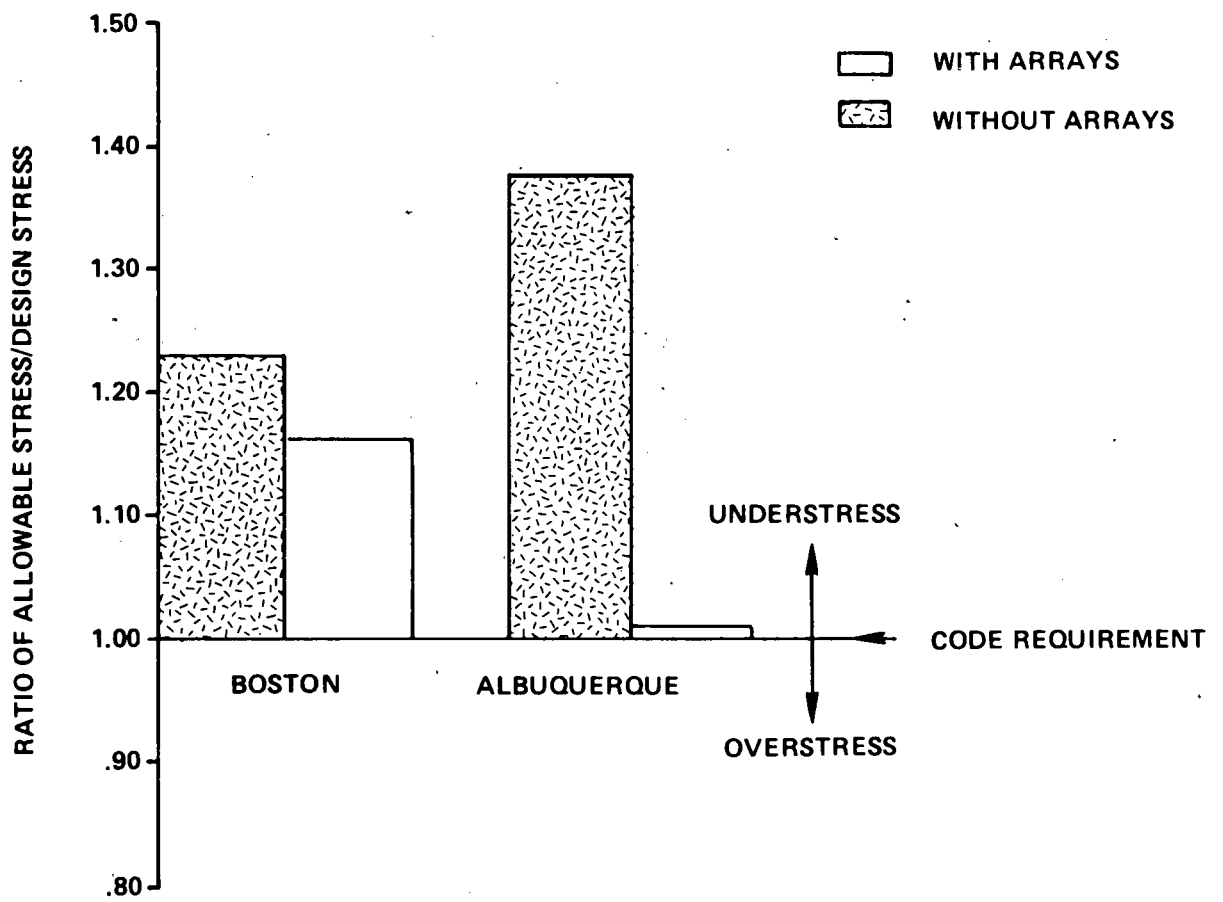
Figure 6-12 Design Margins for Wood Beams

secondary support system are still stressed within the allowable code limits. For the Albuquerque site, the roof beams of this example are seen to have less reserve capacity than those designed for the Boston site. This is primarily due to the fact that the beams designed for the Boston location had larger standard members with more strength capacities than those designed for the Albuquerque site.

The design margins for the primary support system (the roof girders) are shown in Figure 6-13. For both the Boston and Albuquerque designs, these plots clearly indicate overstress in the girders due to the addition of photovoltaic arrays. A later section will present different options for strengthening existing overstressed beams in retrofit applications.

Steel Roof Design. Steel joist/poured gypsum roof designs for the previously specified industrial building were also evaluated. For these particular designs, steel joists span the entire width of the building, thus eliminating the need for central columns.

Using the roof support method, array loadings were assumed to be evenly distributed to the roof system through the steel joists, as shown in Figure 6-14.

The resulting design margins for the steel joist system are shown in Figure 6-15. With the addition of photovoltaic arrays for the Boston site, the roof joists are still within the allowable code stress. However, for the Albuquerque site, the roof joists are slightly over-stressed. This is primarily due to the joists designed for a Boston location having larger standard members with greater strength capacities than those designed for Albuquerque in this design example.
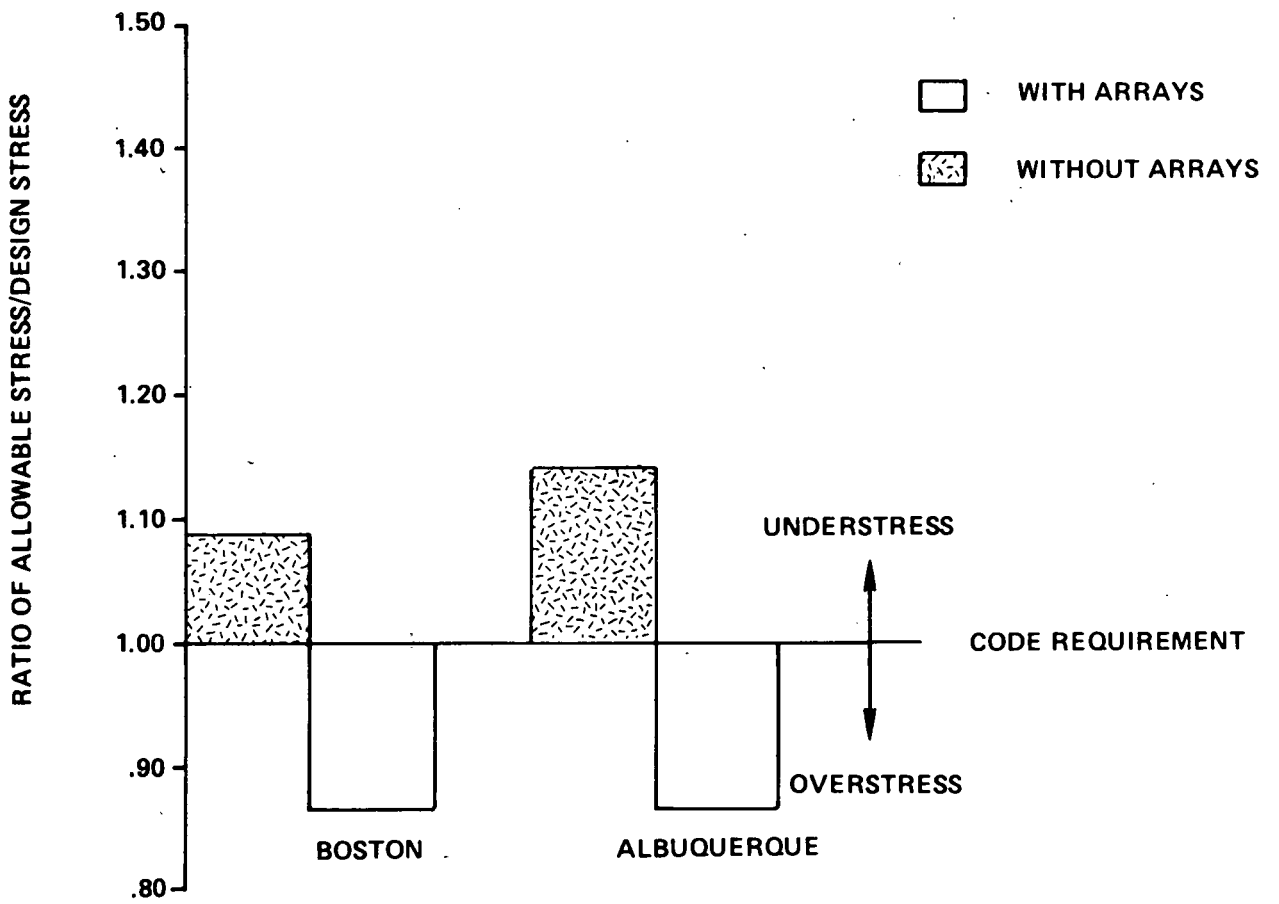
Figure 6-13 Design Margins for Wood Girders

POINTS OF ATTACHMENT
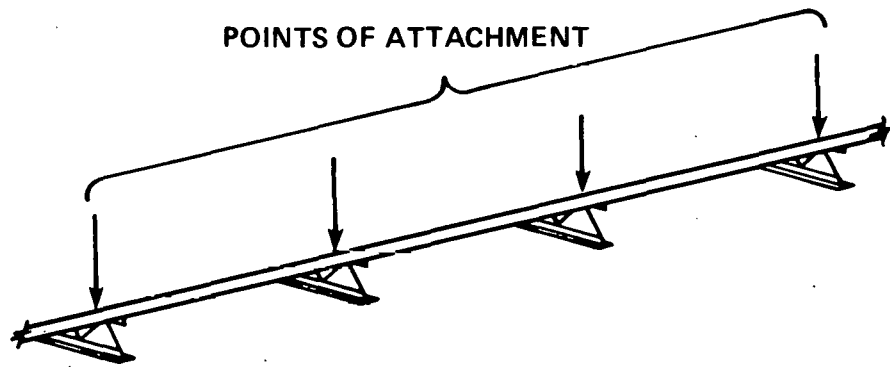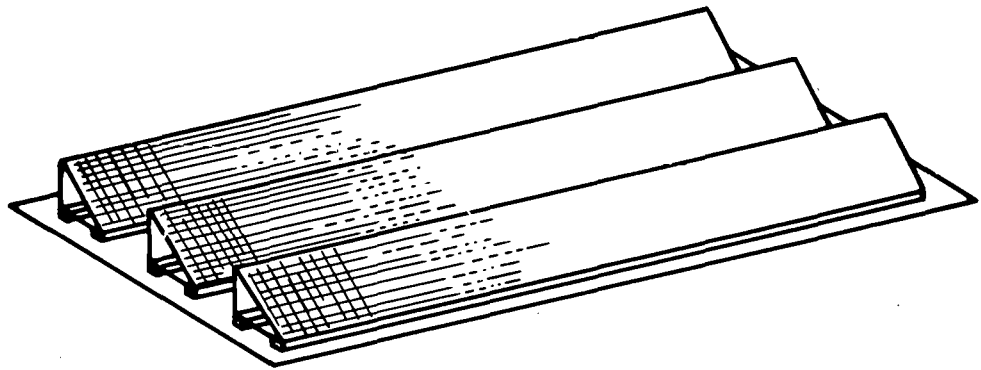
Figure 6-14 Array Supports for Steel Joist Roof
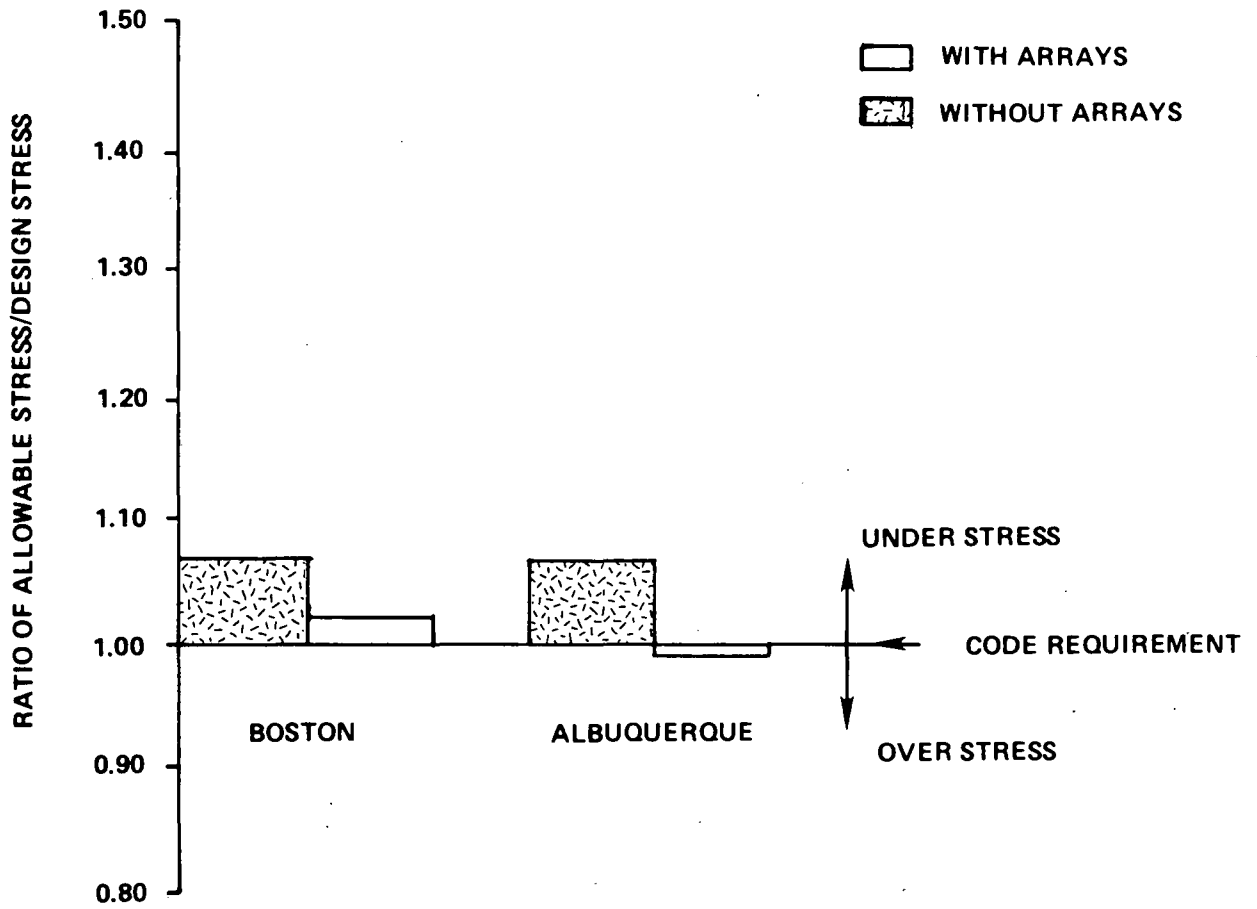
Figure 6-15 Design Margins for Steel Joists

Strengthening Procedures. The previous design examples indicate the possibility of overstressing the structural members of a roof by the addition of photovoltaic arrays, especially in retrofit applications.

One method of relieving the additional array loads on roof members is to avoid such load altogether by using the previously defined wall support method. Panels can be supported by a framing system with the loads being distributed to major roof supporting members, such as walls or columns. In general, the design of walls tends to give them a greater reserve capacity than roofs. However, this cannot be relied upon with inpunity and a prudent designer would check all relevant aspects of the structural design when incorporating photovoltaic arrays. Alternatively, some strengthening method might be selected.

Essentially, two methods are usually suggested to strengthen roof members, such as wood or steel joists. One method uses the kingpost concept in which a post or strut is placed under the beam at midspan and compressed by tensioned cables or bars. Tension in the bars or cables is controlled by turnbuckles. The beam is strengthened much in the same manner as with post-tensioning cables used to reinforced concrete beams. A retrofit kingpost concept for wood girders is shown in Figure 6-16.

A second common method of strengthening existing beams is to temporarily prop and provide a camber to the member. Then, while the beam is relieved of load and deflections, a metal bar (or strip) is attached to its bottom edge by welding or other acceptable method of permanent attachment. The system of propping is then removed. This procedure provides a pre-compression to the lower fibers of the beam, thereby permitting it to
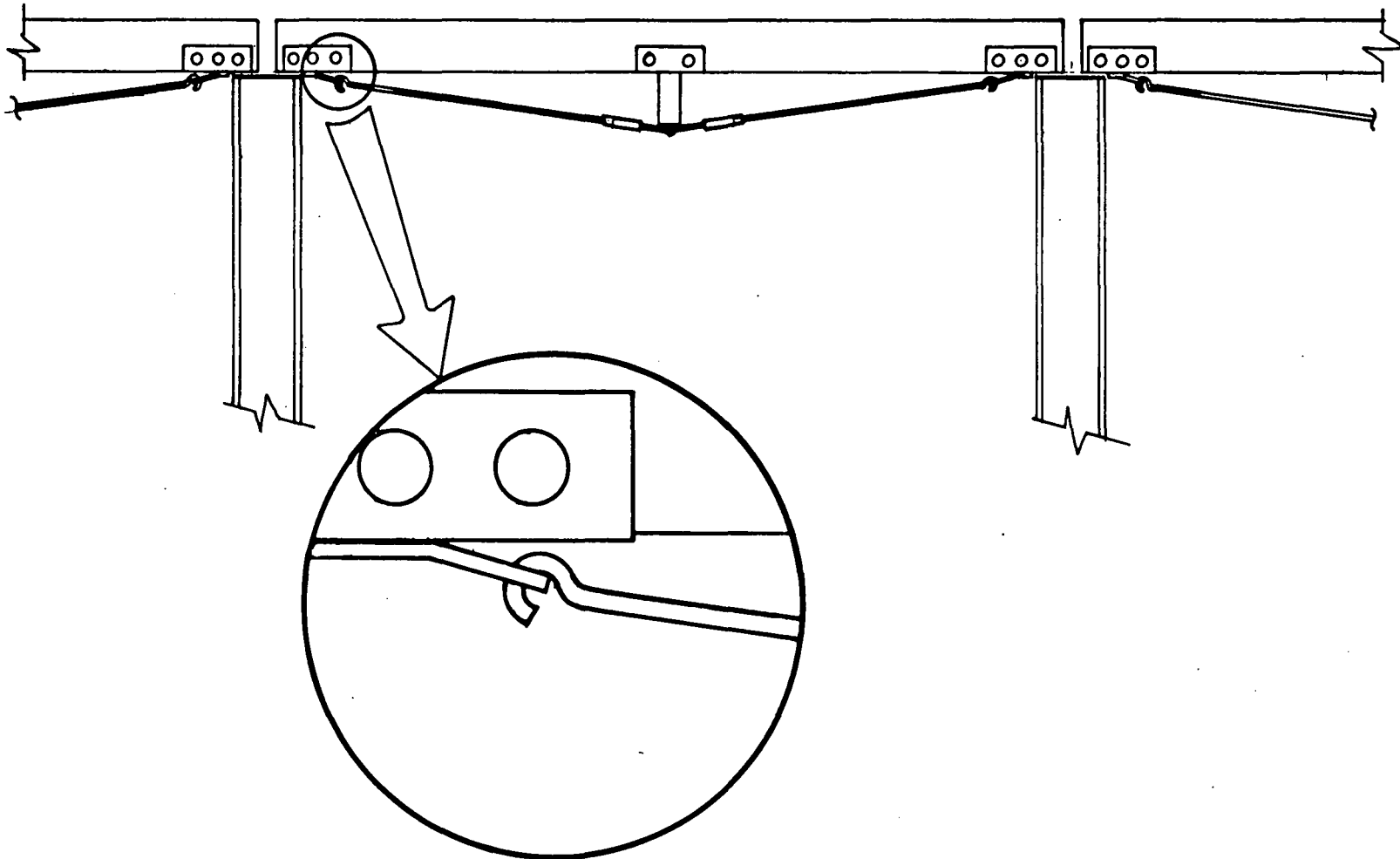
Figure 6—16   Retrofit Kingpost Concept for Wood Joists

carry higher bending loads before bottom-fiber tension stresses are critical. It also provides additional strength by enhancing the structural properties of the cross section through the creation of a composite member. Figure 6-17 illustrates the concept of adding metal reinforcement to a timber beam.

However, these roof beam strengthening methods are likely to be expensive and difficult to perform. As mentioned, the survey of solar installation procedures showed that most firms favored the wall support method over the roof support method of supporting solar arrays. Using the wall support method, the need to strengthen existing beams and joists would be minimal.

Summary. The previous examples of wood and steel roof designs clearly indicate the possibility of overstressing structural members of a roof during a retrofit installation of photovoltaic arrays.

However, it is strongly emphasized that these design examples are not meant to suggest that all roofs would behave structurally in the same manner. Rather, the design examples were utilized to identify potential structural problems and to indicate inadequacies of present codes in defining array loads and loading combinations which may lead to the possibility of overstressing a structural member.

6.1.6   Support Structure Designs

Primary factors influencing the costs of mounting photovoltaic arrays on the roofs of buildings include:

● Type and span length of array framing system
● Location of roof supports

6-49

GLUE LAMINATED BEAM

BOTTOM OF BEAM

METAL BAR OR STRIP

SELF — TAPPING SCREWS
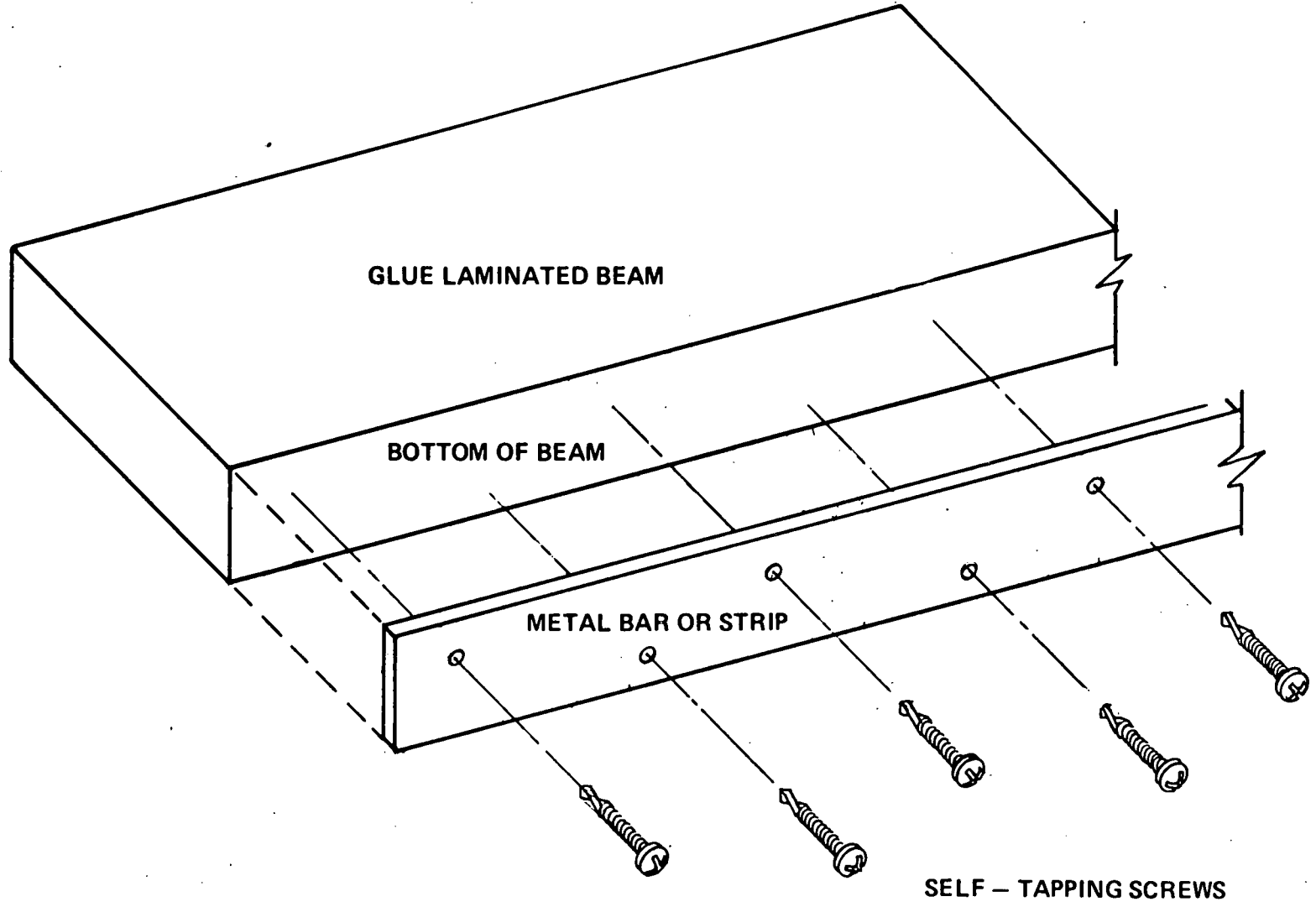
Figure 6—17   Metal Reinforcement for Timber Beams

- ·Anchorage details

- Type and number of roof penetrations

- Installation method

- Integration of arrays with roof supports.

A key question is whether an array framing system should span long distances, thus implying larger structural weights for the frames and fewer roof penetrations, or span shorter distances with a lighter system but requiring more roof penetrations. This part of the study discusses some different types of array framing systems, with regard to the economic significance of spanning various distances and utilizing different types of roof penetrations to achieve a low cost support structure.

Framing Systems. This section examines two leading framing systems, the truss and the torque tube, and compares their potential for low cost application in the design of roof mounted array support structures. From the state-of-development survey of solar space heating and cooling firms performed in this study, it was found that most large solar installations on roofs employ a a truss system for the support of solar arrays.

A previous Bechtel study (Ref. 6-4) for ground-mounted photovoltaic arrays identified the torque-tube concept as an efficient and economically feasible support system. Thus, to provide comparisons for potential low cost support systems for rooftop photovoltaic arrays, both a truss and a torque-tube support system were designed using the following assumptions:

- The framing system spans 20 ft

- Panel attachment points are at their corners.

- The structures are designed to withstand 70 psf loading on the panels.

- Panel twist is not a problem.

- ASTM Grade A 36 structural steel is used.

- Standard structural shapes are used.

A 20-ft-long truss framework designed to support 4 ft x 8 ft photovoltaic panels at a 35° inclination to a flat roof surface is shown in Figure 6-18. The truss is designed to transmit loads to the roof at its four corners. The vertical legs and the top and bottom chords of the truss use rectangular tubes, while the sloped members inclined at 35° are sections designed to support the photovoltaic panels. The remaining structural members consist of angle sections. Total steel weight for this structure was estimated at 1560 lbs (9.75 lb/ft^2 of panel area).

An order-of-magnitude evaluation of the constructed cost of the truss system (exclusive of roof penetrations) was conducted, based upon the following qualifications and assumptions:

- An Albuquerque, New Mexico, site was assumed.

- Material prices and wages were based on the third quarter of 1980.

- 1.20 productivity factor at Albuquerque, based on previous Bechtel in-house data, was assumed.

- The cost estimate was based on 20 frame units (3200 ft^2 of panel area) per typical roof installation.

- Bolted connections for the framing members were assumed.

4' x 8' PANELS

PANEL SUPPORTS

35°

4.6'

20.0'

6.6'

ROOF OR WALL
ATTACHMENT POINTS
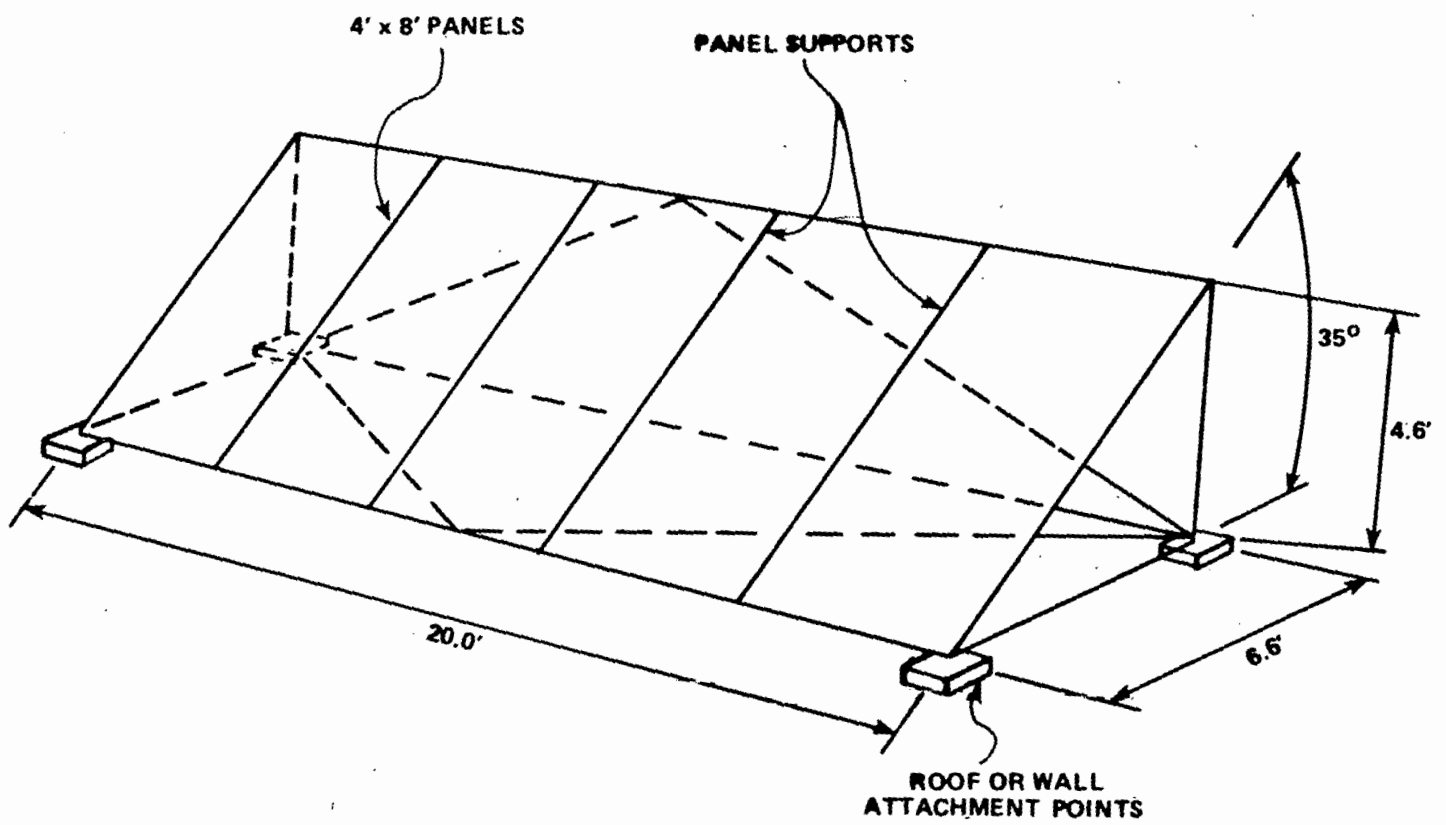
Figure 6—18   Truss Concept

A charge of 60% of the direct labor field cost was chosen as a suitable burden. The installed cost for mounting the truss system on a typical size industrial roof (exclusive of roof penetrations) was estimated to be $2,675 per ton of steel ($13/ft^2 of panel area).

Similarly, a torque-tube system was designed for the same span and to carry the same loads as the truss system, as shown in Figure 6-19. A rectangular cross section was used for the torque tube while M section members were selected for the end legs. Tee section members (fillet welded to the box sections), were used for supporting the 4 ft x 4 ft photovoltaic modules. In this manner, the need for panel support of the modules is eliminated by attaching them directly to the tee section members. This represents an attempt to reduce costs by integrating the photovoltaic modules with the array support system.

Total steel weight for the torque-tube design was estimate at 5 lbs/ft^2 of panel area, almost half of that required for the truss design. Since cost is directly related to steel weight, the torque-tube support system offers better low cost potential for roof mounting than the truss type system typically used in current installations.

Roof Penetrations. Roof penetrations were previously identified as a key factor influencing the costs of installing roof-mounted photovoltaic arrays. To evaluate their significance, costs were estimated for the installation of two different types of penetrations: the pitch pocket and the curb support.
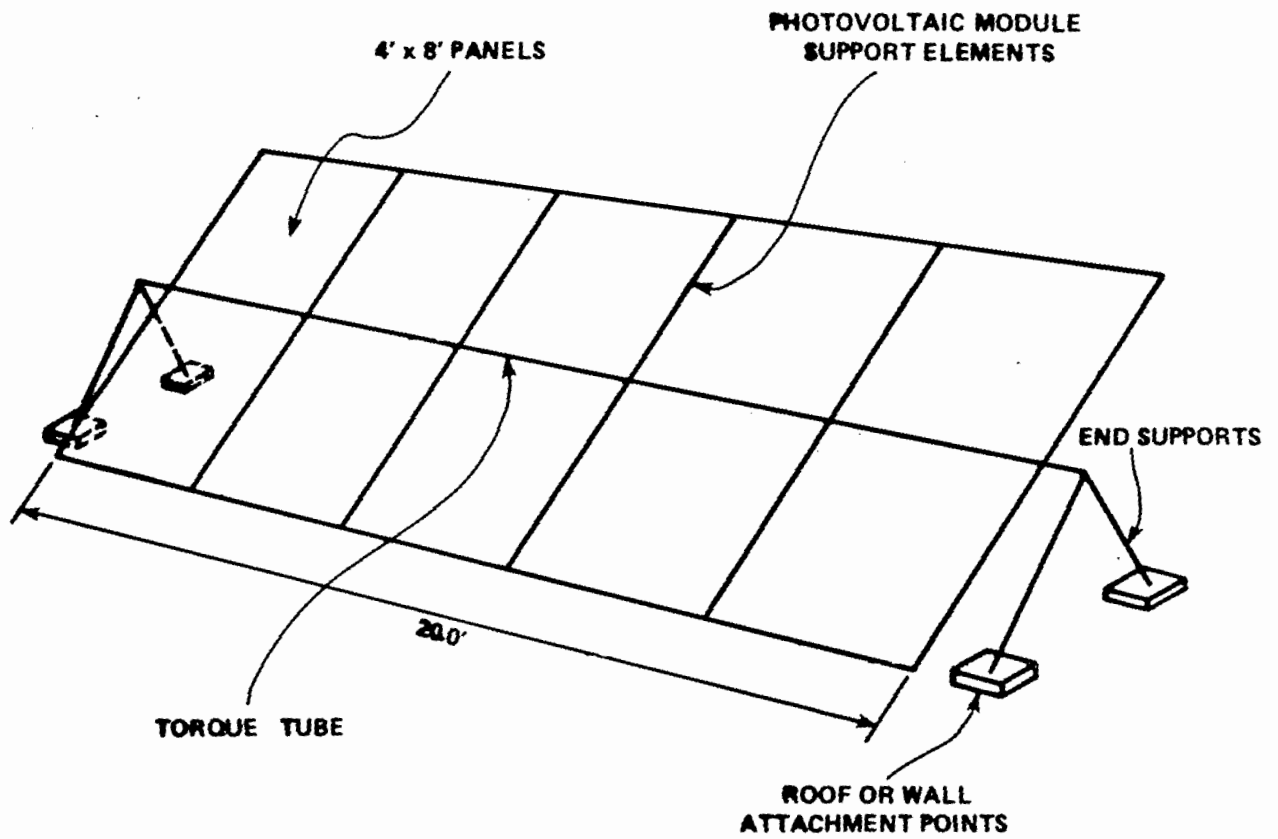
Figure 6—19 Torque Tube Concept

Several steps are necessary in the installation of a pitch pocket on a steel beam/gypsum roof, as shown in Figure 6-20(a). These operations include:

- Removal of the required area of roofing and gypsum

- Installation of an array support column

- Welding of the column to the flange of a main structural roof member

- Pouring replacement gypsum

- Installation of flashing

- Patching of the roof membrane.

An allowance of $150 for material cost and a burden rate of 60% of the direct costs were assumed. The total cost for a roof penetration of this type was estimated at $500.

Likewise, an estimate was made of the costs to install a curb support on a steel bar joist roof system similar to the one shown in Figure 6-20(b). The steps necessary to install this type of roof penetration are:

- Removal of the required curb and support pad plate

- Bolting of the pad plate to the bar joist

- Installation of flashing and patching of the roofing

- Installation of the array support column.

The burden rate was again taken as 60% of the direct labor costs with an allowance of $200 for material costs. The total cost for each roof penetration of this type was estimated at $620.

COL.

PIPE 4 STD

HOT PITCH

ROOFING

FLANGE

POURED GYPSUM FILL

STRUCTURAL MEMBER

(a)

PITCH POCKET

SUPPORT COL.

NEOPRENE PAD
SHEET METAL CAP

FELTS & SHEET METAL CANT

ROOFING

ROOF DECK

BAR JOIST
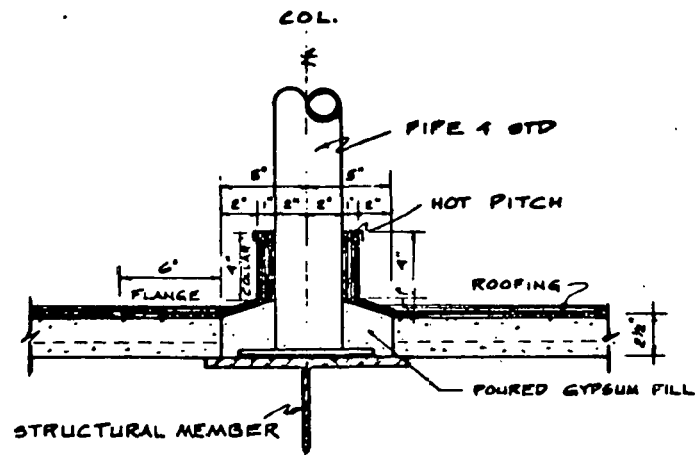
½"DIA'U' BOLT
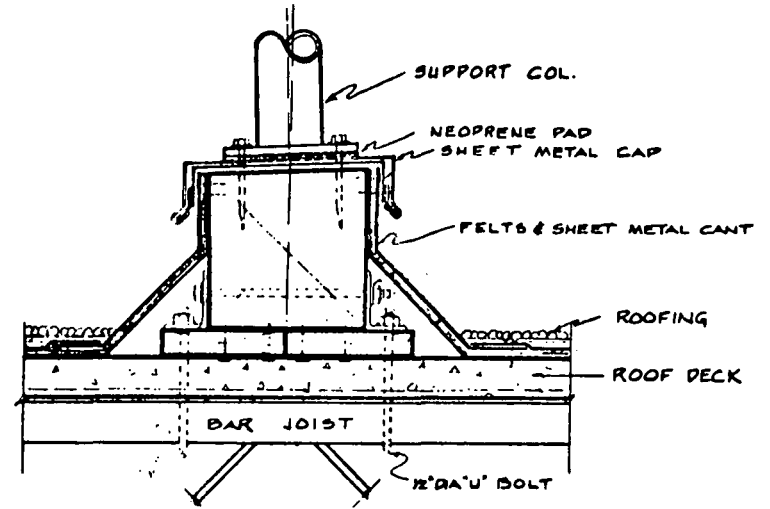
(b)

CURB SECTION

Figure 6—20   Roof Penetration Details

The curb type of roof penetration appears to be slightly more expensive than the pitch pocket type. However, selection of one type of roof penetration over another would not necessarily be made strictly on first costs considerations. Rather, the maintenance requirements, as well as other factors such as the nature and magnitude of the anticipated loads on the supports, should also be considered when selecting a particular type of roof penetration. For example, a curb support would be amenable to sustaining larger forces than a pitch pocket. Thus, the curb support would be more suitable for arrays that employ the wall support approach. Pitch pockets would more likely be used for supporting the lighter loads derived from arrays that use the roof support approach.

Automation and Mechanization. Automation and mechanization are other factors that might influence installation costs of roof-mounted arrays. For ground-mounted arrays, where hundreds or perhaps thousands of arrays are installed, automation may play a key role in lowering field costs. However, automation does not lend itself readily to the installation of roof-mounted arrays where, comparatively speaking, the number of arrays is small.

Mechanization does offer a means of reducing some labor costs. For example, framing systems such as the torque tube can be partially preassembled (by welding) in a factory with assembly being completed on the job site using bolted connections.

Connections can easily lend themselves to mechanization. Conventional welding and bolting are methods which maybe applied to make attachments of array panels to supporting structural framework. However, there exists an

extensive line of industrial fasteners that may be used for quick

attachment of photovoltaic panel supports as well as for modules into

panel frames. Some of these fasteners include:

- Rivets

- Studs

- Insert fasteners

- Quarter-turn fasteners

- Quick-operating fasteners.

Rivets are low-cost, permanent fasteners which are well suited for automation

(Ref. 6-16). The primary reason for riveting is its low in-place cost

that is substantially lower than that of threaded fasteners.

Advantages of using rivets include:

- Materials in various thickness can be joined.

- Almost any part shape having flat parallel surfaces
  can be fastened by a rivet.

- Parts already painted or having other finishing can
  be fastened by rivets.

Disadvantages of using rivets include:

- Tensile and fatigue strengths of rivets are lower than for
  comparable fasteners. Rivets are susceptible to pull out
  under high tension loads and may loosen under severe vibrations.

- Riveted joints are not watertight but may be made watertight at
  added cost by using some type of sealant.

- Riveted parts cannot be disassembled for maintenance or
  replacement without destroying the rivet. This would be
  the most undesirable feature of using rivets where replacement
  and maintenance of photovoltaic panels would become necessary.

Studs have the advantage of eliminating the need for strict tolerances. In this manner, studs reduce the need for large hole clearances and close hole alignments normally required by a cap screw or bolt (Ref. 6-16).

Insert fasteners allow the insertion of a grommet into a hole, followed by the partial pressing of a plunger into the grommet, thus positioning the assembly to be installed in a fixed panel (Ref. 6-17). Using plastic insert fasteners similar to the one shown in Figure 6-21, photovoltaic modules could be quickly attached to the flange of the array support beam of the torque-tube system. This fastener is easy to install, needs no tools and compensates for any minor hole misalignment.

The quarter-turn fastener is a designed for access panels, plates, removable signs, large structural panels, and other applications whenever the movable (or removable) panel overlaps the supporting member, and where very rapid removal or frequent access is necessary (Ref. 6-16).

These fasteners characteristically have excellent ultimate tensile strength and are spring-loaded to engage and lock in a quarter turn. For this reason they have low plate-separation load characteristics up to the distance required to fully compress the spring.

A typical quarter-turn fastener which might be used for the rapid attachment of photovoltaic panels to a supporting structural framework is shown in Figure 6-22. However, this particular fastener has a threaded receptacle which would require an extra operation of threading it into a blind or through hole. This fastener also has the disadvantage of requiring rather restrictive tolerances in the hole alignment for insertion of the

PLASTIC PLUNGER

PLASTIC GROMMET

PV MODULE OR FRAME ELEMENT

PANEL SUPPORT ELEMENT BEFORE ATTACHMENT

PV MODULE

PV MODULE CLAMPED TO SUPPORT ELEMENT
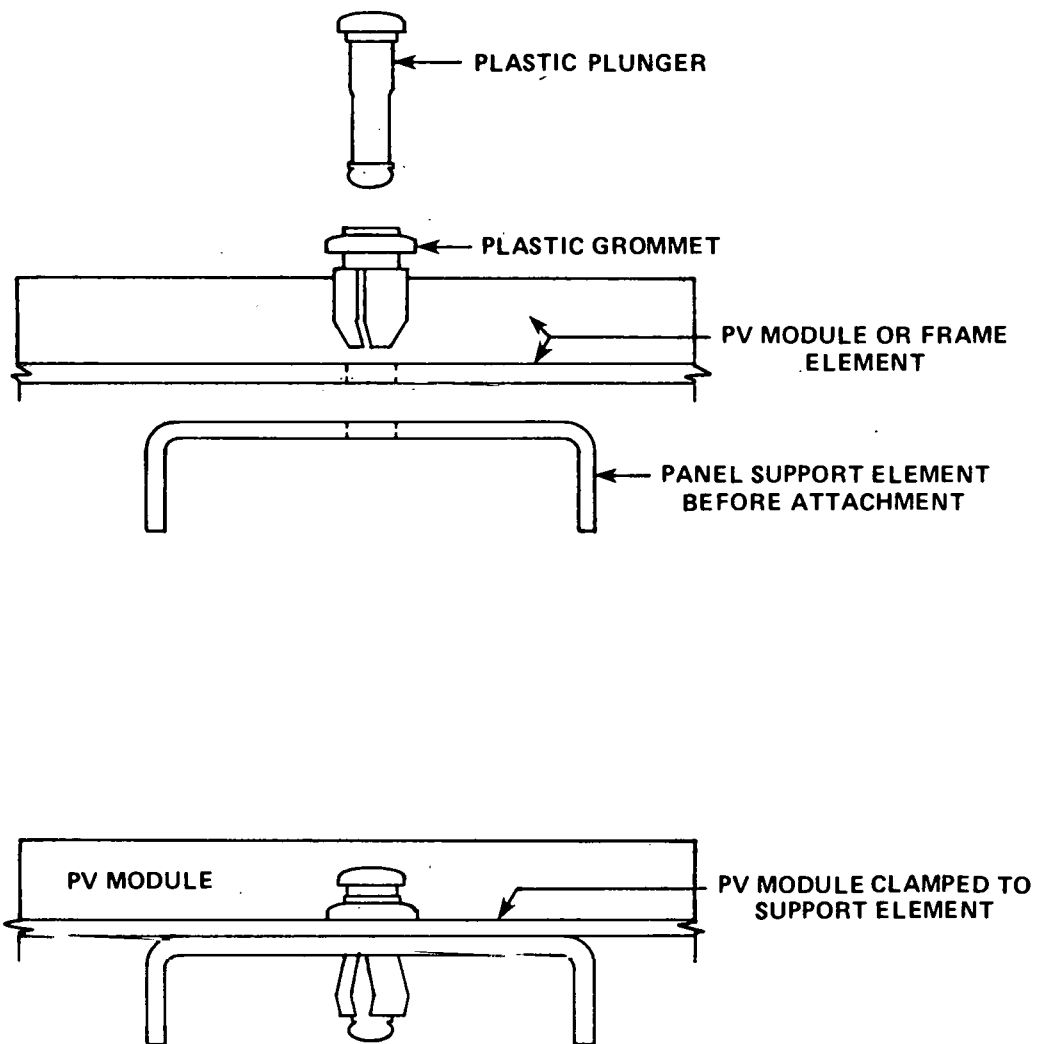
Figure 6—21 Typical Plastic Insert Fastener
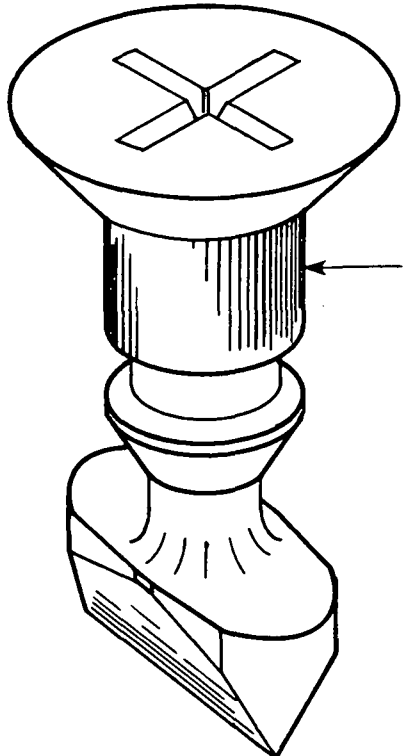
STUD UNIT INSERTS THROUGH FLANGE OF UNIT TO BE ATTACHED
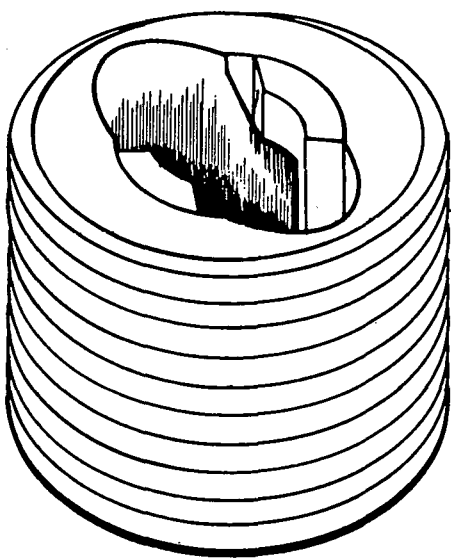
RECEPTACLE THREADED INTO SUPPORT STRUCTURE

Figure 6—22 Typical Quarter - Turn Fastener

stud into the receptacle.

This study does not attempt to recommend specific fastener configurations. The design of fasteners is usually done to suit specific assemblies and can be significant in influencing installation costs. Tradeoff analysis will usually be required to determine which fasteners will provide installation savings compared with the costs required by the fasteners themselves.

6.1.7   Analysis of Promising Support Concepts

Two promising array support concepts have been previously identified:

- Truss system
- Torque-tube system.

The truss support system is an existing concept frequently used in the industry to support solar thermal arrays. The torque tube is a concept that has been identified in previous Bechtel studies as an economically feasible support system for ground-mounted arrays. Both concepts have been previously evaluated for applicability to support roof-mounted arrays (Section 6.1.6), with the torque tube being the least costly. Therefore, the torque-tube support system will be further analyzed in this section.

Several factors were previously identified as contributing to the installation costs for roof mounted arrays. One of these was the type and span length of the array framing system, while another was the type and number of roof penetrations. To evaluate their total significance on costs, a parameter study was made of these factors for the torque-tube system.

For purposes of this analysis, each array support structure was assumed to have a fixed length of 40 ft. Support intervals (span lengths) of 4, 8, 20, and 40 ft along the length were evaluated. Two slanted supports, similar to the ones shown in Figure 6-19, were assumed at each support location. Due to the relatively small support loads for the 4 and 8 ft support intervals, pitch pockets were used. However, the larger support loads occurring for the 20 and 40 ft support intervals resulted in the use of curb supports for these cases.

The costs for roof penetrations, structures, and the total cost to install roof mounted arrays employing the torque-tube system are presented in Table 6-5 and Figure 6-23. The structure costs were based on system weight and the price per ton previously estimated for the truss framework.

For small support intervals, Figure 6-23 shows that frequent roof penetrations contribute significantly to total installed costs while the structure costs remain fairly constant. This would indicate that the wall approach method of supporting arrays, which uses long spans with fewer roof penetrations, offers the best potential for cost savings.

However, within the 20 to 40 ft support interval, the total installation costs appear to be minimum and remain reasonably constant. This would indicate that within this range, the support intervals may be selected to conform with building dimensions with insignificant effects on the total installation costs for roof-mounted arrays. For the lower loading of 20 psf structure costs for the array supports remain rather constant. For the higher load of 70 psf, structure costs appear to increase with longer

Table 6-5

INSTALLATION COSTS FOR ROOF MOUNTED ARRAYS

Torque-Tube System - 40 Foot Span Length

Support Interval (ft)	Roof Penetration			Structure		Total Cost*
	Type	Quantity	Cost*	Wt(lbs)	Cost*	
4	Pitch Pocket	22	370	1203 (944)	54 (36)	424 (406)
8	Pitch Pocket	12	202	1232 (1030)	55 (39)	257 (241)
20	Curb	6	125	1725 (1272)	78 (48)	203 (173)
40	Curb	4	83	2759 (1504)	124 (57)	207 (140)

*Costs are 1980 $/sq. m. for 70 psf; terms in brackets ( ) for 20 psf.
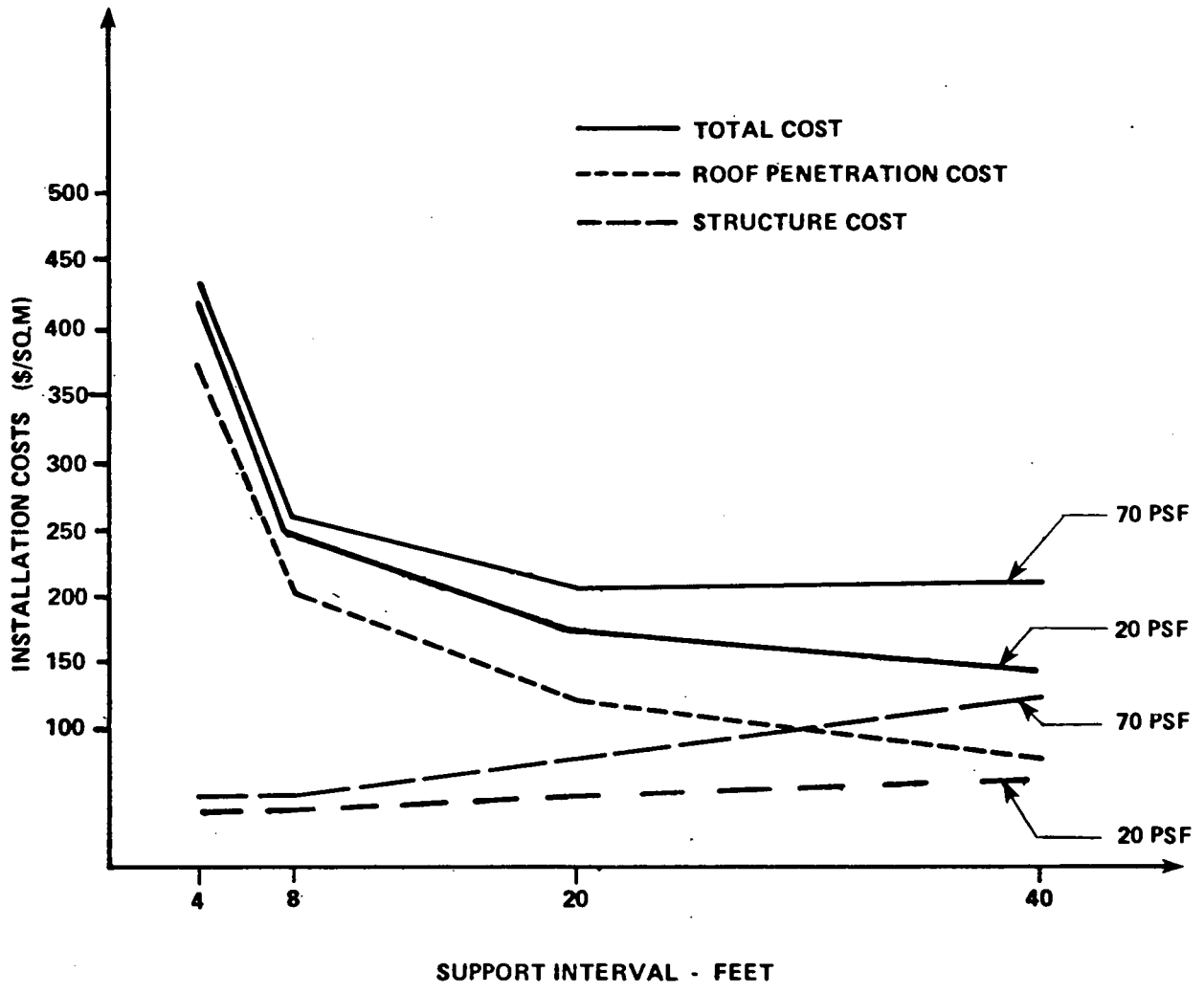
Figure 6—23 Roof-Mounted Array Support Structure Cost Versus Support Interval

support intervals. Within the 20 to 40 ft support interval, total installed costs for the design load of 70 psf appear to have reached a minimum and remain reasonably constant. This would indicate that within this range the support intervals may be selected to conform with building dimensions with an insignificant effect on the total installed costs for roof mounted arrays. However, within that same span range, total installed costs for the design load of 20 psf are still decreasing. This would indicate the total costs for this loading have not reached the minimum and still might be further reduced by increasing the support interval.

It appears that the wall support method of supporting the arrays, which uses long spans with fewer roof penetrations, offers the best potential for cost savings. It also appears that there is an optimum span range from which support intervals might be selected for design purposes that does not significantly affect the total installation costs for roof-mounted arrays.

It can be seen from the data presented in Table 6-5 and Figure 6-23 that the array design loading can be a significant cost driver, especially at the longer span lengths. However, it can also be seen that, even for a loading of 20 psf, total array support structure costs are relatively high ($140/m^2 for a 40 ft span length). This is due in large part to the high cost of roof penetrations used in this study. Therefore, the identification of low cost structure configurations for the support of photovoltaic arrays mounted on flat roofed buildings will require the identification and/or development of innovative, low cost roof attachment methods. Additional cost reductions may also result from further definition of design loadings, as well as a further, detailed support structure design optimization.

6.2 ARRAY SUPPORT STRUCTURE COST REDUCTION

This section discusses several approaches with regard to reducing the installed cost of photovoltaic arrays. This is accomplished by identification and evaluation of:

- Baseline array support structure design concepts and material quantities

- Baseline construction scenarios for the selected array designs

- Design optimization and installation cost reduction techniques.

For purposes of evaluation, the following assumptions were made regarding the photovoltaic power plant characteristics:

- Plant peak power ratings range from 1 to 100MW.

- The site latitude is 35°.

- Fixed flat-plate arrays are tilted at the site latitude.

- The array slant height is 8 ft and the lower edge of the panel is 2 ft above grade.

- The nominal array efficiency is 15% for comparison purposes.

Additionally, two north-south spacings between arrays were evaluated:

- 6.9 ft (1.5 times the vertical array height)

- 10 ft (to facilitate vehicle access).

6.2.1 Baseline Support Designs and Material Quantities

To establish baseline construction scenarios and identify major cost drivers, several representative ground mounted array support structure designs were selected for analysis. A review of previously completed and

ongoing low cost structures design efforts (Refs. 6-4 and 6-19) resulted in selection of three basic designs:

- Caisson-supported frame
- Pile-supported torque tube
- Earth-auger foundation.

These designs were selected to provide a representative range of material types, design configurations, and installation requirements to make the results of this study as widely applicable as possible. It should be pointed out that these three designs had been developed without giving complete consideration to the integration of panel and array structural support members (Ref. 6-4). This was necessitated by the wide divergence and lack of detail regarding panel design existing at the time that the study was conducted, and to facilitate the initial screening of a wide variety of support concepts. Optimum array structure designs will of course result from integrated designs, such as the vertical truss system being developed at JPL (Ref. 6-19).

Therefore, these designs were selected only as baseline concepts to use in identifying construction activities, major cost drivers, and potential areas for cost reductions. They do not represent optimum designs (or support structure costs). This is discussed further in Section 6.2.3. Integrated low-cost designs are currently being developed by Bechtel through another Sandia study for completion in early 1982.

Caisson-Supported Frame. This design, shown in Figure 6-24, is fabricated from standard rolled steel structural shapes. The foundation is a rein-forced concrete caisson that is constructed in a drilled or augered
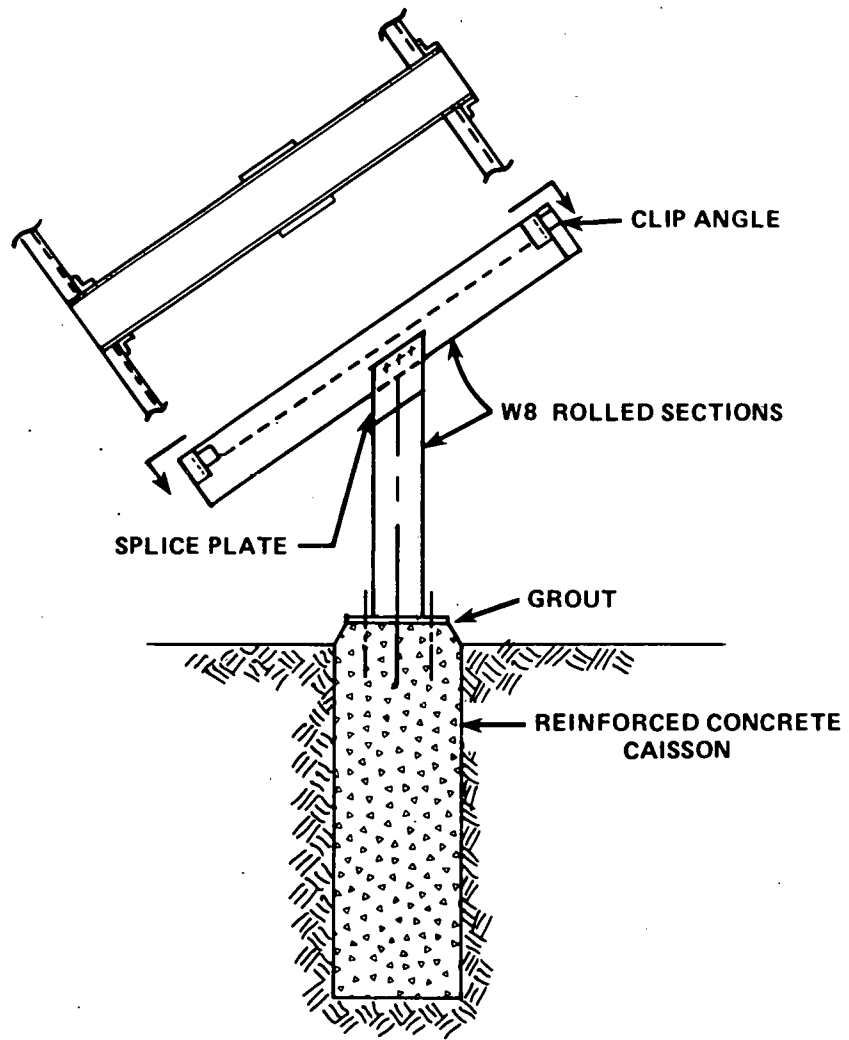
Figure 6-24 Caisson- and Pedestal-Supported Frame

hole. This foundation is applicable to many different types of soil conditions. In addition, the use of rolled steel shapes in the frame results in construction material being readily available in quantity in most parts of the country. The inclusion of the longitudinal beams as part of the support structure makes the design adaptable to a wide range of solar panels. The components required per peak megawatt for this design are: 480 caissons, pedestals, and transverse beams; 900 longitudinal beams; and 2250 photovoltaic panels (4 ft x 8 ft) The design consists of thirty 300-ft long arrays peak per megawatt of plant output.

Pile-Supported Torque-Tube For this design, shown in Figure 6-25, the foundation and above ground pedestal are combined into a single steel wide-flange pile. The principal purpose of this approach is to reduce the number of installation operations. The horizontal structural unit supporting the panels is a rectangular steel tube (torque tube) that replaces the transverse beams of the previous design and eliminates the longitudinal beams and associated connections. The photovoltaic panels are mounted directly onto the torque-tube. The components required per peak megawatt for this design are: 480 piles, 450 torque tubes, and 2250 photovoltaic panels (4 ft x 8 ft). This design would also consist of thirty (300-ft long) arrays per peak megawatt of plant output.

Earth-Auger Foundation System This design, shown in Figure 6-26, is based on the type of earth screw commonly used by utilities to anchor guylines bracing transmission poles. The above ground cables normally used with this anchoring system have been replaced in this design with struts that will resist both compression and tension. The frame is formed from two channels, with the lower ends anchored into a concrete footing to resist

4' x 8' PANELS

ROLLED STEEL PILE SECTION, WOOD
OR PRECAST CONCRETE
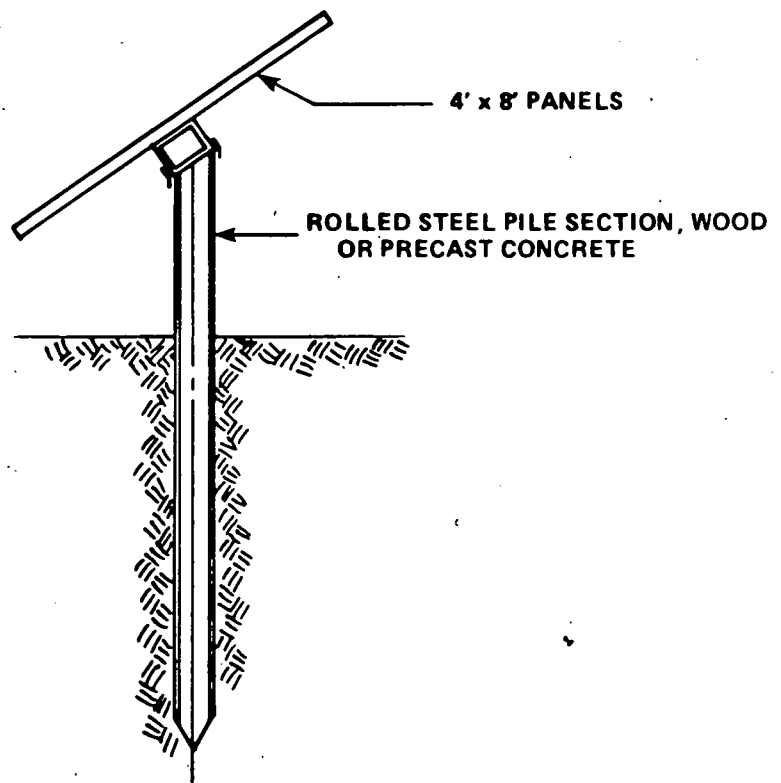
Figure 6—25 Pile-Supported Torque Tube

PLAN VIEW

4' x 8' PANELS

CLEVIS

LUG ANGLE

8" DIA.
EARTH SCREW
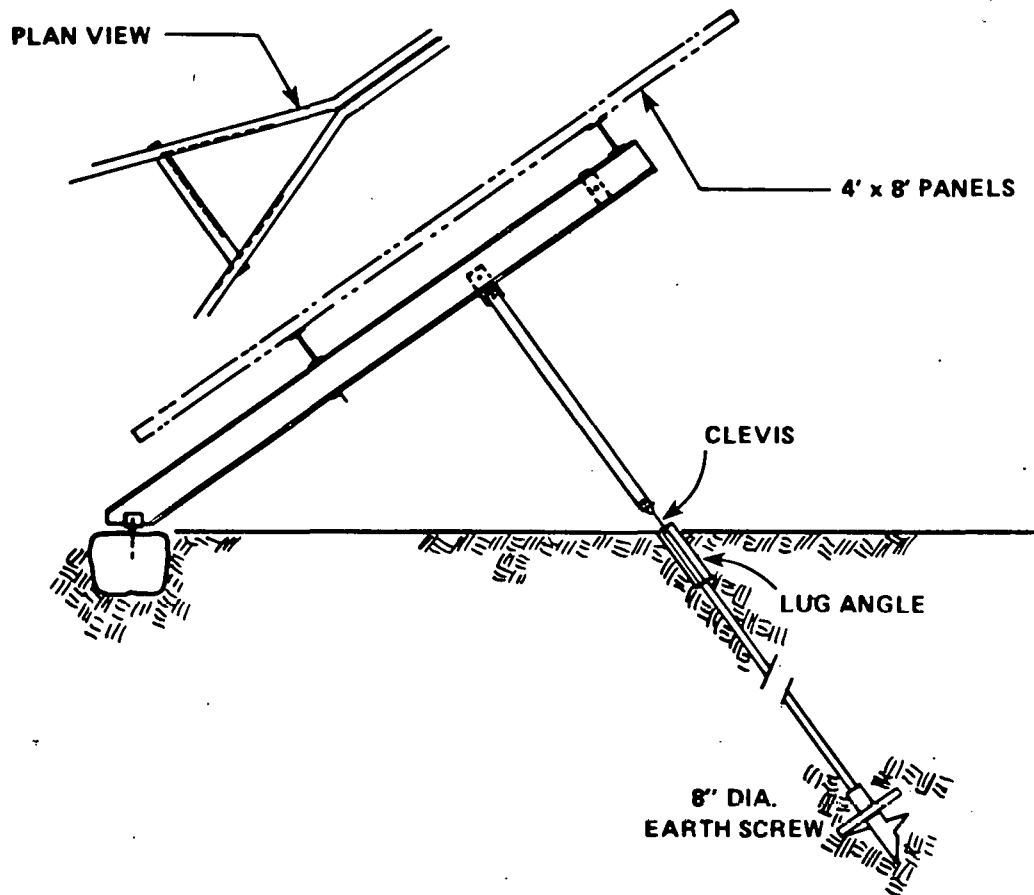
Figure 6—26 Earth-Auger Foundation System

horizontal loads. Components required per peak megawatt for this design are: 480 earth screws, clevises, struts, frames, and foundations; 900 longtudinal beams; and 2250 photovoltaic panels (4 ft x 8 ft). Again there would be thirty 300-foot long arrays per peak megawatt of plant output.

6.2.2 Baseline Construction Scenarios

Baseline construction scenarios and cost estimates were developed for each of the selected designs. These addressed:

- Material costs
- Labor costs (bare costs only)
- Equipment costs
- Operating expenses.

The bare costs of labor include only the direct hourly charges and fringe benefits as listed in Means Building Construction Cost Data 1980. The material costs represent direct costs and the equipment costs are based on monthly rental rates. Operating expenses for the equipment are also taken from Means and include fuel, oil, lubrication, and normal expendables. Cost items not included in the estimates are mobilization, demobilization, profit, contractors' overhead, remote site costs, engineering and management fees, and insurance and taxes.

The sequence of baseline construction operations for each array design is based on the simplest and most direct method for erecting each structure. To establish a consistent baseline, the assumption was made that all components are commercially available at the contruction site. Unless otherwise indicated, the photovoltaic modules are assumed to arrive at

the field assembled into 4 ft by 8 ft panels ready for installation. All construction scenarios were developed assuming 20 ft spacing between vertical array supports.

6.2.2.1 Site Preparation - All Designs

For the purpose of this study, the plant site is assumed to be semi-arid, located in the southwest, reasonably level, and have a sandy soil with light vegetation cover composed of tumbleweed, juniper, grass, cactus, and sagebrush. One quarter of the site is considered to be covered with trees having a maximum diameter of 6 inches. The entire site is considered to require light clearing operations. Site preparation basically consists of clearing, grubbing, and limited site grading. The clearing and grubbing operations involve the removal of trees, stumps, and brush. The sequence of operations postulated for this study was cutting and chipping trees, grubbing stumps and clearing brush.

Table 6-6 lists the requirements for site preparation, including staffing, equipment, time requirements, and resulting costs per unit area of installed arrays.

6.2.2.2 Pedestal Supported Frame

The baseline sequence of installation operations for the pedestal supported frame is as follows:

- Install caissons
- Install pedestals and transverse beams
- Install longitudinal beams and panels.

Caissons. Caissons may be drilled or augered in soil ranging from loose

Table 6-6

GENERAL SITE PREPARATION REQUIREMENTS AND COSTS

| | | | Time (days/MWe) ** | | Costs - $/M²($/ft²)* | | | |
| | | | | | Without Overhead and Profit | | With Overhead and Profit | |
Item	Crew Size	Equipment	Case(1)	Case(2)	Case(1)	Case(2)	Case(1)	Case(2)
Cutting and chipping Trees	1 Foreman 4 Laborers 1 Eqpt Oper (medium)	1 Chipping machine 1 Front end loader 2-18" chain saws	1	1	0.227 (.0211)	0.186 (.0172)	0.278 (.0258)	0.228 (.0212)
Grubbing stumps	1 Equip.Operator 2 Truck drivers (heavy)	1 Hyd. Excavator 1-1/2 yd³ capacity) 2 Dump trucks (16 T capacity)	1.7	1.4	0.275 (.0256)	0.226 (.0210)	0.327 (.0304)	0.269 (.0250)
Cleaning brush	1 Equip.Operator (medium) 1 Laborer	1 Bulldozer (200 hp)	4.5	3.7	0.398 (.0370)	0.326 (.0303)	0.482 (.0448)	0.395 (.0367)
				TOTALS =	0.900 (.0836)	0.737 (.0685)	1.0872 (.1010)	0.892 (.0829)

* Costs are given in $ per unit area of installed modules

** Case (1) = 10' spacing of arrays
   Case (2) = 7' spacing of arrays

sand to rock, with cost highly dependent on ground material and the degree of ground water present. For this study a medium dense sandy soil is assumed with no ground water. Several types of equipment are available to auger the necessary holes. This scenario assumes a truck-mounted gas-engine-powered auger.

The caisson installation sequence begins with the drill rig aligned with a row of caisson locations. The stabilizing pads are then lowered and a hole is drilled. Provided that no unusual conditions (e.g. rocks) are encountered, the drilling rate is 0.4 ft per minute. After the hole is drilled, a temporary plywood cap is placed over it to avoid dirt reentry during spoil removal. The stabilizing pads are then raised and the auger is moved 20 ft to the next location.

Spoil removal is a combination of manual and mechanical operations. A front-end loader would scoop up most of the dirt. Laborers would then shovel the remainder into the bucket for dumping into a truck. Alternatively, laborers could shovel the soil into the front-end loader for dumping into the truck. The latter sequence was assumed for this scenario.

Following spoil removal, the plywood cap is removed from the hole and a preassembled rebar cage is lowered into place. This operation was assumed to require one rodman on the truck bed to hook the crane sling onto the rebar. The equipment operator then lifts, swings, and lowers the cage into position. Two other rodmen position the cage and detach the sling after the cage is set in place. The typical crew used to develop the costs and productivity rates for this study was specified in Means and allows for another rodman, foreman, and an oiler. The oiler, besides servicing the crane, sets the stabilizing pads, adjusts the equipment,

and allows the operating engineer to remain at the controls of the crane. When the maximum extent of the crane boom radius is reached, the crane and truck carrying the rebar cages are moved to a new position.

Concrete placement is based on the use of pumped concrete. It was assumed that the pump truck is set up with a flexible pipe to reach all foundations within a certain radius. Alternatively the pump truck and concrete truck could be moving continuously at a slow rate. The work crew consists of an equipment operator running the pump, one laborer guiding the nozzle, and two laborers vibrating the concrete.

Anchor bolt placement is accomplished immediately after the placement and vibration of the concrete. It was assumed that the anchor bolts come preassembled with templates in units of four are positioned and pushed into the concrete. The assembly is then vibrated to ensure firm positioning in the wet concrete. The template is removed as the final part of the caisson sequence.

Pedestal and Transverse Beams. The pedestal consists of a base plate and a W8 x 24 vertical steel beam matching the W8 x 24 transverse beam. The two components are assumed to be bolted together in the field rather than welded together in a prefabrication shop. This variation is discussed in Section 6.2.3.

Pedestal installation is accomplished in a manner similar to the installation of the rebar cages. The baseline sequence was assumed to be installation of separate pieces for the pedestal and the beam. This was done to establish an upper bound on costs and to clearly identify possible cost savings accruing from moving operations from the field to the shop. In

actuality the two pieces would be shop assembled and installed as a unit. The difference in cost between methods is reported in Section 6.2.3.

Longitudinal Beams and Panels. Longitudinal beam installation proceeds in the same way as the other steel. These beams are C6 x 11.5 structural shapes attached to the supports by 5/8 in. bolts. Panel installation assumes photovoltaic modules arrive in stacks of 4 ft by 8 ft panels. The operation considers the panels stacked on a truck moving slowly down the row while a crane equipped with suction cups lifts a panel one at a time and sets it on the longitudinal beams for two carpenters to fasten in place. An alternative would be to use a larger capacity crane with a greater reach and fewer setups.

Table 6-7 lists the staffing and equipment requirements along with the time required to complete each construction operation.

Material and construction costs are listed in Table 6-8. The data indicate that the foundations account for 24% of the overall cost. The pedestal and transverse beams account for 35%, longitudinal beams 38%, and panel installation 3%. Table 6-9 presents the percentage breakdown of costs for each activity.

6.2.2.3 Pile-Supported Torque-Tube

The construction sequence for this design is:

- Place or drive pile
- Install torque tube between piles
- Install photovoltaic panels.

Table 6-7

CAISSON DESIGN INSTALLATION REQUIREMENTS

ITEM	CREW SIZE	EQUIPMENT	Days/MWe (min/unit)*
Auger Caissons	1 Foreman 3 Bldg Laborers 1 Equip Operator (medium) 1 Oiler	1 4 WD truck 1 Auger (gas power)	20 (20 min/caisson)
Remove Spoils	1 Equip Operator (medium) 1 Truck Driver (heavy) 2 Common Laborers	1-12 T Dump Truck 1 Front end loader (65 HP, 1-1/4 cy)	20 (20 min/caisson)
Set Rebar	1 Foreman 4 Rodmen 1 Equip Operator (medium) 1 Truck Driver (heavy)	1 Hydraulic crane (25 Ton) 1 Flat Bed Truck	13 (13.3 min/caisson)
Place Concrete	1 Foreman 3 Bldg Laborers 1 Equip Operator (medium) 1 Truck Driver (heavy)	1 Concrete Pump 1 Pump Truck 1 Ready-mix Truck (6x4, 45', 240 hp) 2 Gas Vibrators (3 hp)	10 (10 min/caisson)
Install Anchor Bolts	2 Carpenters	1 Pickup truck	12 (12 min/caisson)
Install Pedestal Frames	1 Steel Foreman 2 Ironworkers 1 Equip Operator (medium) 1 Oiler 1 Truck Driver (heavy)	1 Hyd. Crane (25 T)	12 (12 min/caisson)
Install Longitudinal Beams	- as above -	- as above -	23 (24.5 min/span)
Install Panels	2 Carpenters 1 Equip operator (medium)	1 Hyd Crane (25 T) 1 Trailer (2-axle, 25 T) 1 4WD truck (3/4 T)	59 (12.6 min/panel)

* Minutes for each operation are based on 8 hr day, 40 hr week and using the quantity estimates for each concept given in Section 6.2.1

Table 6-8

SUMMARY OF CAISSON DESIGN INSTALLED

Task	Material	Labor	Equip	Oper. Exp.	Total $	%
Caisson	72.05	89.57	17.12	11.90	191	24
Pedestal	109.73	14.92	4.36	1.14	130	17
Transv. Beam	119.48	14.92	4.36	1.14	140	18
Longit. Beams	256.20	29.84	8.72	2.28	297	38
Install Panels	2.40	14.45	3.32	2.01	22	3
TOTALS =	560	164	38	18	780	100
% =	72	21	5	2	100	

Note: 1980 Dollars from Building Construction Cost Data, 1980, R.S. Means Co., Inc., 38th Annual Edition.

Table 6-9

COST BREAKDOWN FOR COMPONENTS OF CAISSON DESIGN

Item	Percentage of Component Cost			
	Caisson	Support and Transverse Beams	Longitudinal Beams	Photovoltaic Panels
Material	38	85	86	11
Labor	47	11	10	65
Equipment	9	3	3	15
Operating Expenses	6	1	1	9
Total Items	100	100	100	100

Placement of Pile. The supports for the torque tube may be placed in one of three ways: driven with an impact hammer, vibrated with a vibratory hammer, or augered and set. Since a medium dense sandy soil was assumed for the construction site the vibratory hammer was chosen as the installation method. This results in higher driving cost, but because of higher driving speeds the unit cost is expected to be lower. The auger and set method would be used as a backup method if the ground refused the pile.

Normal operations would entail the use of a crane supporting the hammer for lifting the pile into position. After the pile is in position and the hydraulically operated jaws on the driver are closed, the hammer is started and the pile driven. Large installations would probably require a racking device for speeding the positioning of the piles prior to driving. This equipment might be similar to that used to handle oil well drilling pipe.

Install Torque-Tube. This operation is similar to that described for piles in the previous design, where a crane would lift the tube from a truck and swing it into position. Iron workers would guide the tube onto seats attached to the pile and fasten it to the pile using bolts. The tube would have elongated holes to allow for adjustment and misalignment.

Install Panels. This task is identical to that described for the previous design except that the connections are at the center of the panel instead of the ends. Four bolted connections are also used in this case. Table 6-10 lists the staffing and equipment requirements along with the time required for each activity. For the larger plants, more than one crew would be used to build the plant in a reasonable period of time.

Table 6-10

PILE SUPPORTED TORQUE-TUBE DESIGN INSTALLATION REQUIREMENTS

ITEM	CREW SIZE	EQUIPMENT	Days/MWe (mins per unit)
Pile Installation	1 Foreman 4 Pile drivers 2 Equip operators (medium) 1 Oiler 1 Truck driver	1 Crane (40 ton) 1 Vibratory hammer (1500 ft-lb) 60 lineal feet of leads 1 Air compressor and 3" hose 1 Tractor (30 ton, 195 hp) 1 Trailer (2 axle, 25 ton)	20 (20 min/pile)
Torque Tube Installation	1 Steel foreman 4 Steel workers 1 Equipment operator (medium) 1 Oiler 1 Truck driver (heavy)	1 Hydraulic crane (12 ton, truck mounted) 1 Tractor (30 ton, 195 hp) 1 Trailer (2 axle, 25 ton)	11 (12 min/tube)
Panel Installation	2 Carpenters 1 Equip Operator (medium) 1 Truck driver (heavy)	1 Hydraulic crane (12 ton, truck mounted) 1 Tractor (30 ton, 195 hp) 1 Trailer (2 axle, 25 ton)	47 (10 mins/panel)

Construction activity costs are listed in Table 6-11. These data indicate that the pile accounts for 49% of the cost, the torque tube 47%, and the panel installation 4%. Although the two-ended support of the photovoltaic panel from the previous design has been changed to a single central support, the installation costs have not changed. This is because four fasteners are still envisioned to attach the panel to the support system. Consequently the cost and percentages are the same as before. Table 6-12 presents the percentage breakdown of costs for each activity.

6.2.2.4 Earth-Auger Foundation System

The construction sequence for this design is:

- Install earth auger
- Install front footing
- Attach rear strut to stem of the earth anchor
- Install frame
- Install longitudinal beams and panels.

Install Earth-Auger. The earth auger resembles the bottom of a regular drill bit. It is installed in a fashion similar to that used to auger holes for the caisson foundations with a drilling rig capable of placing the screw at an angle from the vertical and advancing it into the ground while it rotates. The bit and stem should have an overall length at least equal to the depth of embedment required. After the auger is in place, the stem is unscrewed from the drill rig and the rig moves to the next position.

Install Front Footing. This regular concrete footing can be built very simply. If the soil is sufficiently stiff, the hole for the footing can

Table 6-11

SUMMARY OF TORQUE-TUBE DESIGN INSTALLATION COSTS

Task	Material	Labor	Equip	Oper. Exp.	Total $	%
Pile	242.00	38.22	13.19	7.58	300.99	42.4
Torque Tube	366.00	14.92	4.36	1.14	386.42	54.5
Install Panel	2.40	14.45	3.32	2.01	22.18	3.1
Total	610.40	67.59	20.87	10.73	709.59	100.0
Percentage	86.0	9.5	2.9	1.5	100.0	

Table 6-12

COST BREAKDOWN FOR COMPONENTS OF TORQUE-TUBE DESIGN

Item	Percentage of Component Cost		
	Pile	Torque Tube	Photovoltaic Panels
Material	80	95	11
Labor	13	4	65
Equipment	4	1	15
Operating Expenses	3	0	9
Total Items	100	100	100

be made with one pass of a front-end loader. Forms will be needed if the soil is less cohesive. After the front-end loader has dug the rough hole, laborers would trim the hole prior to carpenters placing the forms. Anchor bolts would then be placed and concrete poured.

Attach Rear Strut To Earth-Auger. The rear strut (possibly a pipe threaded at one end) is coupled to the earth auger. A flange would be attached to the other end to facilitate bolting the frame to the strut. The strut would be threaded onto the stem of the earth anchor and propped in position for later attachment of the frame.

Install Frame. The frames, composed of two channel sections bent to the proper configuration, would be lifted off a truck and positioned on the anchor bolts. The strut would then be aligned with the bolt holes in the frame and the two pieces fastened together.

Install Longitudinal Beams. The longitudinal beams, which weigh 230 lbs each would be lifted off a truck by crane and positioned between two frames. After the iron workers fasten the beams to the frames, the crew would move to the next installation site. If a long-boom crane were used, the crane and truck would move less frequently. This latter arrangement might save enough setup time to justify the cost of a higher capacity long-boom crane. The panels would then be installed on the beams, as previously described.

Table 6-13 lists the staffing and equipment requirements along with the time required for each activity. As with other designs, multiple crews would be used for larger plants to maintain a reasonable construction schedule.

Table 6-13

EARTH-AUGER DESIGN INSTALLATION REQUIREMENTS

ITEM	CREW SIZE	EQUIPMENT	Days/MWe (Units/day)
Install Earth Auger	1 Foreman 1 Equipment operator (medium) 1 Oiler 1 Truck driver (heavy) 2 Building laborers	1 4WD truck 1 Auger (gas driven) 1 Tractor (30 ton, 195 hp) 1 Trailer (2 axle, 25 ton)	20 (24 per day)
Excavate Front Footing	1 Equipment operator (medium) 1 Truck driver (heavy) 1 Building laborer	1 Wheel-type backhoe loader (80 hp, 1-1/4 cy) 1 Dumptruck (12 ton)	12 (40 per day)
Place Concrete	1 Foreman 3 Building laborers 1 Equipment operator (medium) 1 Truck driver (heavy)	1 Concrete pump 1 Truck for pump 1 Ready-mix truck (6x4, 45 ton, 240 hp)	12 (40 per day)
Install Anchor Bolts	2 Carpenters	1 Pick-up truck 1 Vibrator (gas, 3 hp)	12 (40 per day)
Install Rear Strut	2 Steel workers	1 Pick-up truck	12 (40 per day)
Install Frame	1 Steel foreman 2 Steel workers 1 Equipment operator (medium) 1 Oiler 1 Truck driver (heavy)	1 Truck-mounted hydraulic crane (12 ton) 1 Tractor (30 ton, 195)hp 1 Trailer (2 axle, 25 ton)	12 (40 per day)
Install Longitudinal Beams	1 Steel foreman 2 Steel workers 1 Equipment operator (medium) 1 Oiler 1 Truck driver (heavy)	1 Truck-mounted hydraulic crane (12 ton) 1 Tractor (30 ton, 195 hp) 1 Trailer (2 axle, 25 ton)	25 (40 per day)
Install Panels	2 Carpenters 1 Equipment Operator (medium) 1 Truck driver (heavy)	1 Truck-mounted hydraulic crane (12 ton) 1 Tractor (30 ton, 195 hp) 1 Trailer (2 axle, 25 ton)	55 (40 per day)

Construction activity costs are listed in Table 6-14. The data indicate that the footing cost is 15% of the overall cost. The earth screw accounts for 13%, the transverse frame 26%, longitudinal beams 43%, and panel installation 3%. Table 6-15 presents the percentage breakdown of costs for each activity.

6.2.2.5   Comparison of Costs

The three baseline designs were compared on the basis of the construction costs detailed in the preceding sections. The amount of steel required for each design (for a range of plant sizes) is listed in Table 6-16. This table also indicates the sensitivity of steel price to purchase quantity. The resulting costs as functions of plant size are presented in Table 6-17. The data presented in Table 6-17 are based on averages of the two costs presented in Table 6-16 for each purchase quantity.

The data in Table 6-17 indicate that for low-volume production, all three designs are close in cost with the earth-auger foundation system being lowest.

This also holds true for plants sized above about 10 megawatts. The reader is reminded that the three designs evaluated in this study are not based on integrated panel/support structure designs. Therefore, the removal of whatever structural redundancies may exist in these designs would likely result in cost reductions.

6.2.3   Optimization Cost Reduction Study

Optimization of photovoltaic array support structure design involves

Table 6-14

SUMMARY OF EARTH-AUGER DESIGN INSTALLED COSTS

Task	Material	Labor	Eqpt.	Oper. Expense	Total $	%
Footing	54.48	42.40	3.94	4.09	104.91	15.2
Earth Auger	62.40	24.47	3.04	1.53	91.44	13.2
Transverse Frame	125.66	37.28	10.90	2.85	176.69	25.5
Longitudinal Beams	256.20	29.84	8.72	2.28	297.04	42.9
Install Panels	2.40	14.45	3.32	2.01	22.18	3.2
Totals	501.14	148.44	29.92	12.76	692.26	100.0
Percentages	72.4	21.4	4.3	1.8	100.0	

Table 6-15

COST BREAKDOWN FOR COMPONENTS OF EARTH-AUGER DESIGN

Item	Percentage of Component Cost				
	Earth Auger	Footing	Transverse Beams	Longitudinal Beams	Photovoltaic Panel
Material	68	52	71	86	11
Labor	27	40	21	10	65
Equipment	3	4	6	3	15
Operating Expenses	2	4	2	1	9
Total Items	100	100	100	100	100

Table 6-16

STEEL QUANTITIES AND COSTS

(a) Steel Required

Plant Power (MWp)	Pedestal (lb. steel)	Pile (lb. steel)	Earth Auger (lb. steel)
.1	348,360	448,200	357,480
5	1,741,800	2,241,000	1,787,400
10	3,471,990	4,482,000	3,562,880
50	17,359,940	22,410,000	17,814,420
100	34,708,270	44,820,000	35,616,925

(b) Sensitivity of Cost to Quantity Purchase (Base Mill Price)

Quantity (lb.)	LSI - 1980 ($/lb.)		Nat'l Construct. Estimator ($/lb.)	
	$\leq 8"$	$\geq 10"$	$\leq 8"$	$\geq 10"$
$\leq$ 5,000	0.61	0.59	0.52	0.49
$\leq$ 10,000	0.53	0.51	0.46	0.46
$\leq$ 20,000	0.51	0.48	0.43	0.38
$\leq$ 50,000	0.49	0.47	0.41	0.37
$\leq$ 300,000	0.48	0.41	0.38	0.34
$\leq$ 1,000,000	0.41	0.40	-	-
> 1,000,000	-	0.36	-	-

Table 6-17

INSTALLED COST AS A FUNCTION OF STEEL PRICE
($/m^2)

Concept	Steel Price Per Pound		
	61¢	48¢	41¢
Caisson-Pedestal	52.49	45.76	42.26
Pile-Torque Tube	47.78	39.03	34.32
Earth-Auger	46.57	40.71	37.62

Notes: General - Costs given are without overhead
and profit. If included, they
would add 25% to the cost.

consideration of: the structural subsystems and their possible integration

through design modifications, review of connection details and examina-

tion of the labor and materials involved in the production and installation

of photovoltaic array fields.

Detailed optimization requires consideration of specific designs, intended for

specific sites and situations. This study deals with optimization at the

conceptual level to indicate probable avenues for future cost reductions.

Distributed photovoltaic power systems having peak power in the range 1 to

2 MWe will probably be built by local contractors working with regional

consulting firms and local building-supply companies. Consequently, the

available materials and design concepts may be limited by the

local market. For larger sized array fields, into tens of megawatts,

the volume of materials becomes substantial, the economy of bulk purchases is improved, and special designs by custom fabricators can become attractively priced.

Cost reduction possibilities are discussed in terms of:

- Design modifications and integration
- Construction cost reductions.

6.2.3.1 Design Modifications and Integration

Structural optimization can be achieved by applying three basic principles:

- Reduce structural weight
- Reduce numbers of components (especially as shipped to the field)
- Remove structural redundancy.

Changes in subsystem arrangements and designs that achieve the above objectives will generally result in cost reductions. A major cost driver in construction work is the weight of structural elements that must be assembled and/or installed in the field. Reducing the weight of the structure also leads to reductions in material costs, reductions in handling and shipping costs and, consequently reductions in installed costs. Such optimization even reduces demands on the structure from its own dead weight. However, for photovoltaic arrays, reduction in weight can create a design problem in that resistance to wind uplift is diminished. This means that where resistance might have been provided by structural weight, uplift forces must now be resisted by other anchorage methods.

Reducing the number of pieces to be handled in the field generally leads to a reduction in field labor requirements. This suggests that a reduction

in installed costs may be achieved by careful integration of the design elements in addition to the application of prefabrication, where appropriate. Reducing the number of separate pieces by prefabrication is always limited by the need to avoid creating units that are too big, awkward, or heavy to handle and ship cost effectively. Designs should be examined for prefabrication possibilities relative to the actual fabrication-shipping-installation scenario that governs the job. Examples of design integration possibilities are discussed later.

Removing structural redundancy is a form of optimization that typically leads to reduced weight and fewer structural elements. Thus cost reduction is a natural consequence of such design revisions. An area of interest for removing structural redundancy in photovoltaic arrays is in the integration of the panel and supports. The panel framework secures a group of solar modules as a preassembly which is field-attached to the support system. The panel has inherent structural strength which, for an optimum structure, should be utilized after attachment to the supports. This is discussed, for the baseline support designs, in the following examples.

Caisson-supported Frame. This system uses a vertical pedestal attached to a supporting caisson and carries horizontal beams that provide seating for a series of panels. In the baseline configuration considered here, the longitudinal beams span 20 ft between caissons and therefore each support five 4 ft x 8 ft panels. One design variation examined was to substitute a steel pile for the caisson, extending above the ground to replace a separate pedestal. A further variation considered for this element of the design was to attach the sloping transverse beam to the pile and drive the

unit complete. This eliminates an attachment operation during the instal-
lation. For example, based on the data presented in Section 6.2.2, the
combined cost for the caisson and pedestal is $21.60/m^2, while the cost
of the pile is $18.00/m^2. This indicates a potential savings of $3.60/m^2.

Removing the transverse beam installation suggests a further possible
saving of about $1.37/m^2 - that is, if the transverse beam can be
prefabricated to the pile before driving.

A small structural redundancy can be identified in this system at the
panel-beam interface, in that upper and lower framing members of each panel
assembly lie along the support beams. This small redundancy can be re-
moved by assembling a larger panel that is 20 ft x 8 ft to span between
transverse beams at each pile. Such an integration will cause the panel
assembly operations to be changed. However, since the upper and lower edge
beams of the integrated panel will be practically the same as the existing
longitudinal beams, the net result is that only a small weight saving can
be expected.

Torque-Tube. This system has good potential for low cost results in
extensive array fields. Some possibilities for further cost reduction
are considered in the following.

The baseline configuration developed in Section 6.2.2 consists of
a torque tube supported at its ends on the foundation piles. Design
allowances are needed at each support to compensate for pile misalignments,
since pile driving is not a procedure that lends itself easily to precise
spacing and alignments. However, if each torque tube is supported at
its center, to cantilever 10 ft in each direction, the end alignment

concern is eliminated. Each torque tube will be slightly separated from and stand structurally independent of its immediate neighbors.

The previous end-supported tube arrangement provided a situation where maximum moments and shears, from the applied loads, occurred at different locations. This discourages looking for material savings by changing tube sizes. The T-structure arrangement, however, provides maximum moments and shears at the same locations, namely at the support pile. This means that weight reduction by step-tapering the tube may be practically achieved. This step-tapering may occur in the tube wall thickness or in the tube cross-section dimensions or through a combination of both. When a step-tapered tube is compared to the constant cross-section tube, calculations show possible weight reduction of up to 40%. This amounts to a savings of about $6/m^2 in material costs, which will lead to further reductions in shipping and handling costs.

Producing a step-taper (e.g., three different tube sizes) requires shop welds for tube connections. Such welding is relatively simple, lending itself to automation. However, the cost of extra cutting and welding may offset the cost reduction due to weight savings. Only with specific designs and fabrication facilities in mind can this aspect be fully evaluated.

Furthermore, this evaluation will be influenced by the structural require-ments for attaching beams or flanges to the tube to support the panels. A further design consideration is to completely integrate the tube and panel-frame assembly, so that 20 ft x 8 ft units, with central support, are positioned on the piles in the field. In this event, the act of

installing the torque-tube assembly requires no further panel installation. This translates to a possible savings of about $1.50/m^2$ in base costs.

6.2.3.2 Construction Cost Reductions

This section discusses some additional aspects of cost reduction related to prefabrication of assemblies, material selection, changes in member connections, and reduction of the labor content in installation operations.

Prefabrication. Using cost tables from the previous sections, the costs of panel installation are examined. Two construction crew scenarios are considered. One scenario uses iron workers; these costs were used in the earlier tables. The other uses carpenters and assumes the process of installing panels is similar to laying, say, plywood subflooring units. Related costs are listed in Table 6-18, which assumes field-installed panels. In this instance the costs due to prefabrication will also have similar contributors, but advantages will be gained only by reducing the labor content (higher productivity in a preassembly area), by reducing equipment and operating expenses, and perhaps by reducing installation materials requirements. These changes will be effective when the sum of prefabrication costs and the reduced field costs add to less than the original field costs. However, the promise of prefabrication savings, assuming a given scenario, may be offset simply by labor jurisdictional decisions which might direct the employment of more expensive crafts. Prefabrication often provides significant benefits in construction work though it is difficult to quantify them for a general situation.

Table 6-18

PANEL INSTALLATION COSTS

	Costs of Installing Panels	
	Crew 1 (Iron workers)	Crew 2 (Carpenters)
Material (4-5/8in. bolts)	2.40	2.40
Equipment (per panel)	4.44	4.44
Op. expense (per panel)	2.56	2.56
Labor	17.24	10.89
Total per panel	$26.64	$20.29
Add 25% burden	$33.30	$25.36
Cost per sq meter	$11.20	$ 8.53

Materials. Three related considerations for cost reductions are reduc-
tion of material costs with volume purchases, reduction in material
quantities through design changes, and selection of materials offering
lower unit costs. The reduction of unit costs through volume purchases
and the reduction in material quantities by design changes have already
been addressed in the earlier sections. An example of the effect of
changing materials is considered next. The W8 x 24 steel pile of the
torque-tube concept is considered replaced by a precast, prestressed con-
crete pile of 8-in. square section. The steel pile, varying from 41¢
to 61¢ per pound, costs from $9.84 to $14.64 per linear foot. Using the
Means Catalog for average cost data, the 8 in. concrete pile is estimated
to cost $7.20 per lineal foot. This competitive cost indicates that the

designer may gain useful cost savings by switching to precast, prestressed piles. This would require that a suitable production facility be located near enough to ensure cost-effective volumes and deliveries.

Connections. Selection of connections and fasteners must take into account the support structure and panel frame details. Current steel support concepts are suited to the use of bolts and self-tapping screws. Lightweight designs based on sheet metal sections may employ sheet-metal screws or light, rapidly installed fasteners.

A comparison was made to examine the difference between using bolts or sheet metal screws for installations. The baseline structural steel connection used a 2 in. x 5/8 in. diameter A325 bolt, nut and washer (listed in Means at 60¢ ea.). A modified E-2 steel crew was assumed at a bare cost (no burden) of $689.20 per day. For a rate of 160 fasteners per day, crew costs are $4.31 per bolt. The inclusion of material, equipment, operating costs, overhead, and profit brings the total to $9.40 per installed bolt, for the assumed rate of 40 panels per day.

The use of sheet metal screws for the installation work allows a production increase from 40 to 60 panels per day at a lower unit cost. Using a 1-in. No. 14 sheet-metal screw and washer gives a total cost of $1.44 per installed screw with approximately 6.5¢ for the screw cost. This scenario assumes 16 of these screws per panel compared to 4 of the A325 bolts, and results in panel attachment costs of $37.60 with bolts and $23.04 with sheet metal screws.

Probably the ideal panel connection is one where a small crew is used to guide the panel to seat onto supports, and where the panel automatically locks into place, or becomes locked by a simple action by the crew. For example, such a mode is envisioned with the panel assembly lifted off the truck, swung over the supports, with a small amount of guidance to slide the lower panel edge into a channel seat that restrains uplift motions. Lowering the panel pivots it about the lower edge until the upper edge engages with spring-loaded pins on the support structure. Cam-faced pins are pushed aside by the descending panel and then spring into slots like a door latch. Slings are released and the crew moves to the next location, and repeats the sequence. This method would be custom-designed for specific panel and support configurations, and would have to be designed to avoid tight tolerances for installations.

Another approach to quick-locking the panels is to arrange a pivoted locking element that is swung up and over the top edge of the panel by one person throwing a handle after the panel is seated. Again, specific details require the geometry of panels and supports so that cost estimates and design variations can be investigated. Figure 6-27 illustrates these locking concepts for panel installations.

The spring-loaded latches or locking devices all add design detail to panels and structures. This increases the price through material and fabrication costs, but the acceptance criterion for such designs will be the cost-effective reduction in installation costs and time. Such devices would also be scrutinized to arrange mass production along with the panel frames.

PHOTOVOLTAIC PANEL BEING INSTALLED

PHOTOVOLTAIC PANEL INSTALLED

LOCKING BARS

LOCKING ANGLE ROTATES TO HOLD UPPER EDGE OF PANEL

SLOTTED GUIDE

SPRING LATCHES

LOCKING PIN

6-100
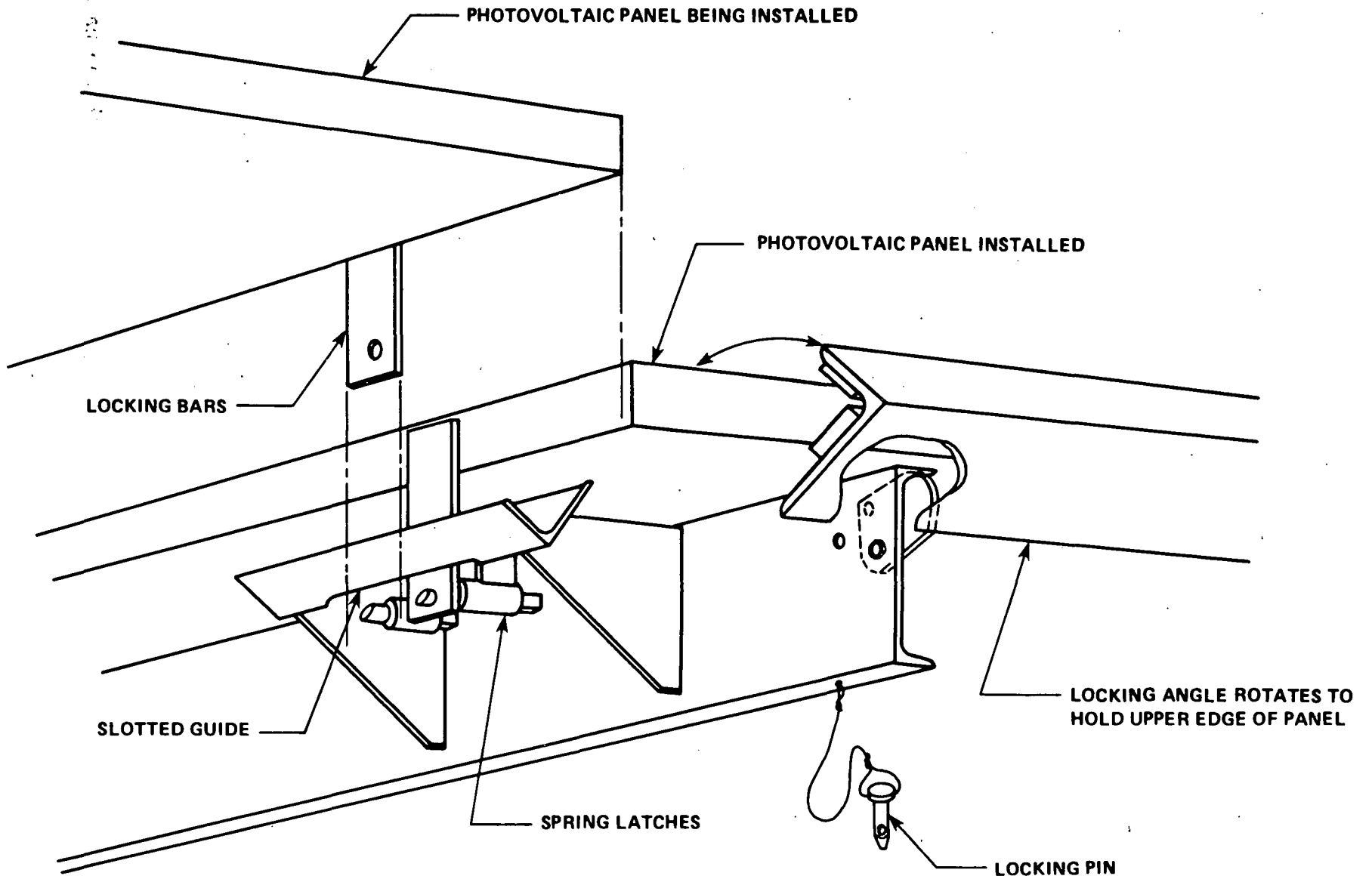
Figure 6-27 Locking Concepts for Photovoltaic Panel Installations

6.2.4 Automated Construction Scenarios

The previous two subsections have documented the development of baseline construction scenarios using conventional methods and various cost reduction techniques. This subsection contains an assessment of potential cost reduction from using construction automation. For the baseline scenarios presented in Section 6.2.2, conventional labor costs account for between 12 and 21% of the total support structure installed costs. After minimizing the material costs, the labor component becomes the next area for reduction.

For cost estimating purposes, the scenarios for this subsection assume the complete elimination of field labor. Throughout the scenarios, it is noted that personnel would be required for certain functions, but it is assumed that these tasks would be accomplished by jobsite supervisory personnel, whose cost was not included in the baseline cases. Although increased sophistication will result in higher equipment and operating costs, the basic functions of construction equipment used for these scenarios is assumed to remain the same as in Subsection 6.2.2. This results in a lower bound on costs and an upper bound on cost savings. More accurate etimates of cost will require more detailed study and prototype engineering, which is beyond the scope of this study.

The following brief discussion of the state of the art in automation is provided prior to developing automated construction scenarios.

Industrial robots have been developed which currently have capabilities for material handling, sensing, and/or decision making. Such capabilities are used in systems consisting of robot helpers, robots with remotely piloted vehicle (RPV) back-up capability, or pure robotics (work cells) (Refs. 6-20 and 6-21).

6-101

The degree of automation envisioned for this study will involve pure robotics and those controlled from a central command point. The field units would consist of a controller, manipulator, tooling/end effectors, and a sensing capability. The degree of complexity of the controller system can range from simple rotary cams to a computer.

For present day construction equipment, cranes, drill rigs, etc., could all be considered to be manipulators. The tooling or end effectors are attach to the manipulator for handling material. These could be a shovel or drill bit. The sensing capability can range from passive sensing to programmed vision and tactile sensing. For the concept envisioned in this study, the more complex capability would be required.

To provide the greatest contrast between conventional and automated construction, the most sophisticated robots currently available have been used in the scenarios postulated herein. The Cincinnati Milacron T^3 unit is in this category and is considered capable of modification for the construction environment. Additional argument for the technical feasibility of the proposed construction equipment has been provided by discussions with personnel in the fields of both automation and construction equipment. As might be expected, firm answers were not available, at this time due to the rapidly expanding nature of the field of robotics, those consulted expressed guarded optimism that the technology would be available to produce the equipment described in this section. Further supporting argument is provided by the current use of remote-controlled equipment being used for underwater pipe burying, such as the Kvaerner Trenching System in use in Norway (Ref. 6-23). The ability of robotics

to be used in a harsh environment has also been graphically demonstrated by the rover and samplers used on Mars by the National Aeronautics and Space Administration (Ref. 6-22).

As mentioned, the postulated scenarios use fully automated equipment. A cost optimization study would undoubtedly show that a blend of pure and partial automation would be most cost effective. Equipment costs will be much lower on machines for which decision making remains with the operator.

Prior to presenting the automated construction scenarios, basic cost data on the proposed mobile construction robot (MCR) are developed. The MCR data is then used with information on other selected automated machines to develop construction scenarios. The basic MCR unit will consist of:

- Mobile platform
- 20 kW diesel generator
- Controller
- Cincinnati Milacron T^3 manipulator
- Tooling end effectors (different for each application)
- Computer vision system
- Interface circuitry.

Table 6-19 contains cost data for the various components. The platform is a 3-ton-rated flatbed truck with cost data from Means. Auxiliary power requirements for the manipulator are assumed to be satisfied by a 20 kW unit. The cost data for the T^3 and the computer vision system are taken from Ref. 6-24. Each controller is assumed to consist of the listed components with prices taken from the spring 1980 Cromemco sales

Table 6-19

ESTIMATED COST OF MOBILE CONSTRUCTION ROBOT (MCR)

Component	Cost $	Monthly Cost ($/mo)	Daily Cost ($/day)	Operating Expense ($/hr)*
Mobile Platform	9,150	425	20.00	3.15
Generator	9,680	450	20.93	1.78
Manipulator	95,000	4,414	203.88	2.55
Controller				
Cromemco Z-2H	9,995			
Cromemco Z-2	995			
3-64K RAM Cards	5,355			
1 - 8 Post I/O Interface Card	295			
CRT Terminal	1,995			
	18,635	866	40.00	0.50
Computer Vision System	20,000	930	42.96	0.54
Interface Circuitry	10,000	465	21.48	0.27
Totals	162,465	7,550	349.25	8.79

*Assumed to be 10 percent of the daily equipment cost divided by the number of hours worked (8 in this case)

catalogue. These data were used due to the reputed reliability of the equipment. The CPU is an 8-bit Z-80 used in many systems. Due to heat, dust, and vibration in the construction environment, any equipment used would require environmental qualification. The monthly equipment cost was calculated using 15% interest and a 3 year payback period, plus 10% for rental fees and/or handling.

6.2.4.1 Site Preparation - All Concepts

As an example, an automated site clearing scenario was developed. The automated equipment for cutting trees would consist of mobile construction robots with end effectors consisting of either an electric or fluid (pneumatic or hydraulic) power saw. A gas-powered saw would also be feasible, but its control would probably be less reliable. The unit's vision system would be used to locate the trees. Software would consist of Cincinnati Milacron's standard software package plus packages for mobility and vision that are currently under development.

The equipment, having located a tree, would position itself and cut down the tree. Additional units would strip the tree and feed pieces to a chipper which would discharge into an automated dump truck. Further units would accomplish the stump grubbing and brush clearing. Table 6-20 tabulates the equipment requirements, costs, and the resulting productivity and costs for operating 8, 16, and 20 hours per day. Staffing will depend on the size of the operation. For a small power plant there may be only two or three people while for large plants there would probably be a main command center with one person supervising several groups.

Table 6-20

SITE CLEARING - EQUIPMENT REQUIREMENTS AND COSTS

Operation and Equipment	Rental $/mo	Rental $/day	Operating Cost $/hr	8 hr day Prod'n acre/day	8 hr day Cost $/acre	16 hr day Prod'n acre/day	16 hr day Cost $/acre	20 hr day Prod'n acre/day	20 hr day Cost $/acre
Tree Cutting									
1 Chipping machine	560	25.87	5. 60						
- automatic control system	143	6.61	0. 66						
1 Dump truck (16 ton)	1,750	80.83	10. 50						
- controller	866	40.00	0. 50						
- computer vision system	930	42.96	0. 54						
- interface circuitry	465	21.48	0. 27						
3 Mobile Construction Robots	22,650	1,047.75	26. 37						
2 Chain saws	320	14.78	0. 60						
Total		1,280.28	45. 04	0.8	2,050.75	1.6	1,256.58	2.0	1,090.54
Stump Grubbing									
1 Hydraulic Excavator (1-1/2 cy)	4,350	201.00	11.25						
- controller	866	40.00	0.50						
- computer vision system	930	42.96	0.54						
- interface circuitry	465	21.48	0.27						
1 Dump truck (16 ton)	1,750	80.83	10.50						
- controller	866	40.00	0.50						
- computer vision system	930	42.96	0.54						
- interface circuitry	465	21.48	0.27						
Total		490.71	24.37	2.0	342.85	4.0	220.15	5.0	195.65
Brush Clearing									
1 Dozer (200 hp)	4,350	201.00	12.60						
- controller	866	40.00	0.50						
- computer vision system	930	42.96	0.54						
- interface circuitry	465	21.48	0.27						
1 Mobile Construction Robot	7,550	349.25	2.55						
Total		654.69	16.46	0.76	1,034,70	1.52	603.98	1.90	517.84

6.2.4.2 Pedestal-Supported Frame Concept

As an example, an automated scenario to install pedestal-supported array frames was developed. The sequence of operations for this concept is:

- Auger hole for caisson

- Remove spoil

- Place rebar

- Pour concrete

- Place anchor bolts

- Install pedestal

- Install transverse beam

- Install longitudinal beams

- Install panels.

Auger Hole. This operation will be the most difficult to program because of uncertainty in subgrade conditions. If the soil is uniform to a depth of about 10 ft, the operation can be expected to run smoothly. Conversely, large rocks (volume greater than 10 cubic in.) may require different bits or drilling approaches. It is at this point that having remotely piloted vehicle capability may prove cost effective due to reduced programming costs, less complexity or uncertainty, and more productivity from the equipment with less manpower.

In addition to subgrade conditions, location of the holes is critical to this operation. The postulated method of positioning the drilling rig within the plant grid system is to use a laser or radio-distance measuring equipment. Coarse location would be accomplished by maneuvering

the drill rig while fine adjustment would be achieved by moving the drill stem with respect to the vehicle carriage.

After the hole is augered to the specified depth, the rig's controller would retract the stabilizers, start the engine, and move the unit to the next location.

Remove Spoil. A mobile construction robot (MCR) would follow the drillrig to remove spoil. It is envisioned that the end effector would consist of a central post to plug the hole and a scoop that would operate around the perimeter. The loaded scoop would then be emptied into an automated dump truck.

Place Rebar. The equipment used for this task is similar to that used for the baseline operation, but with controllers and MCRs replacing the operating engineer and rodmen. The crane would be equipped with a vision system enabling the controller to locate a cage on the bed of a truck and the hole in the ground. The programming would enable the crane end effector to pick up a cage and set it in the hole. A communications link between the crane's controller and the MCRs would expedite the operation by providing triangulation measurements.

Pour Concrete. This would be a simple operation compared to augering. The concrete pump truck is approached by the automated ready-mix concrete truck and connected for the transfer of concrete. The transfer operation would be controlled by the pump's controller using data from a vision system mounted close to the nozzle of the hose. After sensing that the hole was filled, the coupled units would move to the next location.

After the ready-mix truck had been emptied, the two units would be disconnected to allow the ready-mix truck to return to the batch plant for refilling. Concreting could be completed by an MCR with a combination vibrator and trowelling end effector.

Place Anchor Bolts. To facilitate automation, the anchor bolts are pre-assembled. An MCR would pick up an anchor bolt assembly, position it over the fresh concrete, and then insert it into the concrete. After the assembly reaches the correct depth, the concrete would be vibrated to ensure good consolidation around the bolts.

Install Pedestal. This operation is similar to the placement of rebar cages. The additional operation involved is the placement of nuts and washers on the bolts by the MCR after the baseplate is leveled.

Install Transverse Beams. While cost reduction efforts generally include assembly of this unit in the shop prior to shipment, it is assumed to be field assembled in this scenario to allow more compact packaging and higher production rates. The equipment used would be similar to that described previously with assembly techniques using a combination of the Draper Lab's RCC end effector and SRI's vision system.

Install Longitudinal Beams. The longitudinal beams might be installed separately or have panels attached to them in a field shop using the MCRs, with the whole assembly then installed on the transverse beams. In either case, the procedure would consist of an automated crane removing the beams from a trailer and positioning them over the pedestal. MCRs would assist in final positioning and fasten the beams to the pedestal.

Install Panels. The following description is based on the individual installation of panels onto field-installed beams although operations would be similar to those in a field shop used for prefabrication. A crane, equipped with a vacuum lifting attachment and a vision system, would lift a panel from the bed of a waiting truck and move it into position over the beams. MCRs would provide sensory feedback to the crane's controller. The panel would then be set on and fastened to the beams while another MCR or a fixed unit on the crane would be unpacking another panel.

Table 6-21 tabulates the automated equipment required for this concept, associated costs, and the resulting productivity and costs developed by operating 8, 16, or 20 hours per day.

6.2.4.3 Torque-Tube Concept

The sequence of operations for the concept is:

- Install pile
- Install torque tube
- Install panels.

Although the panels may be preassembled to the torque tube in a manufacturing facility or field shop, they are assumed to be installed in place for consistency with the other scenarios.

The pile installation consists of delivery of the pile, placing it in the mandrel, and driving it. Closer tolerances will be required if the design requires the torque tube to be supported at each end. After delivery,

Table 6-21

CAISSON CONCEPT - EQUIPMENT REQUIREMENTS AND COSTS

Operation and Equipment	Rental $/mo	Rental $/day	Oper Cost $/hr	Production and Unit Cost 8 hr day Prod'n units/day	8 hr day Cost $/unit	16 hr day Prod'n units/day	16 hr day Cost $/unit	20 hr day Prod'n units/day	20 hr day Cost $/unit
Auger Caisson									
4 WD Truck	305	14.10	3.60						
Gas auger	1,140	52.65	4.40						
- controller	866	40.00	0.50						
Mobile Construction Robot	7,550	349.25	2.55						
Total		456.00	11.05	20	27.22	40	15.82	50	13.54
Remove Spoil									
Front End Loader (1-1/4 cy, 65 hp)	1,300	60.05	5.30						
Dump truck (12 ton)	1,325	61.20	7.20						
- controller	866	40.00	0.50						
- computer vision system	930	42.96	0.54						
- interface circuitry	465	21.48	0.27						
Mobile Construction Robot	7,550	349.25	2.55						
Total		574.94	16.36	20	35.29	40	20.92	50	16.36
Place Rebar Cage									
Hydraulic Crane (25 ton)	3,850	177.85	8.50						
- controller	866	40.00	0.50						
- computer vision system	930	42.96	0.54						
- interface circuitry	465	21.48	0.27						
Flat Bed Truck	425	19.65	2.75						
- controller	866	40.00	0.50						
- computer vision system	930	42.96	0.54						
- interface circuitry	465	21.48	0.27						
2 Mobile Construction Robots	15,100	698.50	5.10						
Total		1,104.88	18.97	40	31.40	80	17.60	100	14.85

Table 6-21 (Continued)

CAISSON CONCEPT - EQUIPMENT REQUIREMENTS AND COSTS

Operation and Equipment	Rental $/mo	Rental $/day	Oper Cost $/hr	8 hr day Prod'n units/day	8 hr day Cost $/unit	16 hr day Prod'n units/day	16 hr day Cost $/unit	20 hr day Prod'n units/day	20 hr day Cost $/unit
Place Concrete									
Truck Mounted Concrete Pump (4" lines, 80' boom)	4,755	219.60	12.44						
- controller	866	40.00	0.50						
- computer vision system	930	42.96	0.54						
- interface circuitry	465	21.48	0.27						
Ready Mix Truck (6x4, 45 ton, 240 hp)	1,775	82.00	9.85						
- controller	866	40.00	0.50						
- computer vision system	930	42.96	0.54						
- interface circuitry	465	21.48	0.27						
2 Mobile Construction Robots	15,100	698.50	5.10						
Gas vibrator (3 hp)	145	6.70	0.45						
Total		1,212.18	45.94	40	39.49	80	24.34	100	21.31
Place Anchor Bolts									
Pick-up truck	245	11.32	3.50						
- controller	866	40.00	0.50						
- computer vision system	930	42.96	0.54						
- interface circuitry	465	21.48	0.27						
2 Mobile Construction Robots	15,100	698.50	5.10						
Total		814.26	9.91	40	22.34	80	12.16	100	10.12
Install Pedestal									
Hydraulic Crane (25 ton)	3,850	177.85	8.50						
- controller	866	40.00	0.50						
- computer vision system	930	42.96	0.54						
- interface circuitry	465	21.48	0.27						
Tractor (30 ton, 195 hp)	1,275	58.89	6.45						
- controller	866	40.00	0.50						
- computer vision system	930	42.96	0.54						
- interface circuitry	465	21.48	0.27						
Trailer (2 axle, 25 ton)	570	26.33	0.74						
2 Mobile Construction Robots	15,100	698.50	5.10						
Total		1,170.45	23.41	40	33.94	80	19.31	100	16.39

Table 6-21 (Continued)

CAISSON CONCEPT - EQUIPMENT REQUIREMENTS AND COSTS

Operation and Equipment	Rental $/mo	Rental $/day	Oper Cost $/hr	Production and Unit Cost					
				8 hr day Prod'n units/day	Cost $/unit	16 hr day Prod'n units/day	Cost $/unit	20 hr day Prod'n units/day	Cost $/unit
Install Transverse Beams									
Hydraulic Crane (25 ton with control package:	6,111	282.26	9.81						
Tractor (30 ton, 195 hp) with control package:	3,536	163.32	7.76						
Trailer (2 axle, 25 ton)	570	26.33	0.74						
2 Mobile Construction Robots	15,100	697.46	17.58						
Total		1,169.37	35.89	40	36.35	80	21.77	100	18.85
Install Panels									
Hydraulic Crane (25 ton)	3,350	177.85	8.50						
- controller	366	40.00	0.50						
- computer vision system	930	42.96	0.54						
- interface circuitry	465	21.48	0.27						
Tractor (30 ton, 195 hp)	1,275	58.89	6.45						
- controller	366	40.00	0.50						
- computer vision system	930	42.96	0.54						
- interface circuitry	465	21.48	0.27						
Trailer (2 axle, 25 ton)	570	26.33	0.74						
2 Mobile Construction Robots	15,100	698.50	5.10						
Total		1,170.45	23.41	40	33.94	80	19.31	100	16.39

	8 hr day	16 hr day	20 hr day
Concept Totals =	395.73	228.47	193.37
$ per sq meter =	26.60	15.36	13.00

the pile would be placed in the mandrel using either mobile construction robots or tooling similar to oil drilling equipment. For this scenario, an MCR with an end effector similar to that used to set drill pipe is assumed. The robot would locate a pile, rotate it to the vertical, and place it in a positioning jig. The necessary equipment is a vision system and modified search routine. This would provide the greatest flexibility, as it would allow flexibility in stacking piles on the trailer.

Once the pile is engaged in the positioning jig, the hammer would be positioned to commence driving. Subsequently, the pile driver would move to the next location and repeat the operation.

The installation of the torque tube requires an automated crane and at least one MCR. The crane would pick up a 20-foot long torque-tube using a special attachment which allows it to level the tube, and move it over the pile top. The pile location would be determined by sensors, with the information used to modify the placement routine of the crane. As the tube is lowered onto the pile top, the position information would be updated by the MCRs sensors. After placement, the MCR would attach bolts or make alternative structural connections. The above procedure assumes that the tube is cantilevered from one pile and is not structurally connected to adjoining tubes. Panel installation would proceed as described previously.

The one area of possible difficulty would be the development of software for the control of the pile driving operations. The uncertainty associated with this operation may make the choice of a heavier steel section

desirable to allow the driving operation to punch through soil that might stop wood or concrete piles.

Table 6-22 tabulates the automated equipment required for installation, associated costs, and the resulting productivity and unit costs developed by operating 8, 16, or 20 hours per day.

6.2.4.4 Earth Auger Concept

The sequence of operations for this concept is:

- Install earth screw or anchor
- Install front footing
- Attach rear strut to stem of the earth anchor
- Install frame
- Install longitudinal beams
- Install panels.

Install Earth Auger. The work group would consist of the drill rig, an automated tractor and flatbed trailer, and at least one mobile construction robot (MCR). Operating in a similar fashion to the pile driving equipment, the MCR would pick up an earth auger from a trailer and position it in the chuck of the drill rig. The controller on the drill would make final position adjustments using the laser generated plant grid system as a reference, begin drilling and, when the prescribed depth is reached, disengage the stem from the drill chuck.

Install Front Footing. There are several operations required for this task, necessitating a work group consisting of the following units:

Table 6-22

TORQUE-TUBE CONCEPT - EQUIPMENT REQUIREMENTS AND COSTS

Operation and Equipment	Rental $/mo	Rental $/day	Oper Cost $/hr	8 hr day Prod'n units/day	8 hr day Cost $/unit	16 hr day Prod'n units/day	16 hr day Cost $/unit	20 hr day Prod'n units/day	20 hr day Cost $/unit
Install Pipe									
Crane (40 ton)	4,350	200.92	9.65						
- controller	866	40.00	0.50						
- computer vision	930	43.00	0.54						
- interface circuitry	465	21.48	0.27						
Pile Driving Hammer (15000 ft lb, 60' leads)	1,625	75.06	4.20						
- controller	866	40.00	0.50						
Air compressor, 3" hose	600	27.71	-						
Tractor (30 ton, 195 hp)	1,275	58.89	6.45						
- controller	866	40.00	0.50						
- computer vision	930	42.96	0.54						
- interface circuitry	465	21.48	0.27						
Trailer (2 axle, 25 ton)	570	26.33	0.74						
3 Mobile Construction Robots	22,650	1,042.00	26.37						
Total		1,679.83	50.53	24	86.83	48	51.84	60	49.84
Install Torque Tube									
Hydraulic Crane (25 ton) with controller, computer vision, interface circuitry:	6,111	282.29	9.81						
Tractor (30 ton, 195 hp) with controller, computer vision, interface circuitry:	3,536	163.33	7.76						
Trailer (2 axle, 25 ton)	570	26.33	.74						
3 Mobile Construction Robots	22,650	1,042.00	26.37						
Total		1,513,95	44.68	40	46.78	80	27.86	100	24.08
Install Panels									
Hydraulic Crane (25 ton) with controller, computer vision, interface circuits:	6,111	282.29	9.81						
Tractor (30 ton, 195 hp) with controller, computer vision, interface circuits:	3,536	163.33	7.76						
Trailer (2 axle, 25 ton)	570	26.33	.74						
2 Mobile Construction Robots	15,100	695.00	17.58						
Total		1,166.95	35.89	40	36.35	80	21.77	100	18.85

Concept Totals = 315.36   188.55   168.17
$ per sq meter = 21.21   12.68   11.31

- Trencher or excavator

- Spoil removal unit

- Concrete placement unit

- Anchor bolt installation unit.

To simplify the work, it is assumed that the footing is built without the use of formwork. This may use more concrete but will save the many steps involved in erecting and stripping forms. The equipment consists of a backhoe-loader converted to automatic and RPV control capability and an automated dump truck. The backhoe would position itself using the plant grid system described above and dig the trench. The spoil will be placed in a dump truck, which will return to the command position when the load sensors of the truck indicate that it is full At the command position, it will pick up a driver and proceed to dump its load. Meanwhile, an empty truck will move to the vacated position and allow the excavation to continue.

Prefabricated rebar cages will be brought to the site on flatbed trailers and towed by automated tractors to the installation site. There, either an automated crane or an MCR with suitable end effectors will pick up the cage and place it in the hole.

Placement of concrete and anchor bolts will proceed in a manner similar to that described for the caissons (Subsection 6.2.4.2). Location for the anchor bolts will be determined from the plant grid.

The installation of the rear strut (the extension of the earth auger) would involve only a truck and an MCR. The MCR would pick up a rear strut

and thread it on the end of the earth auger. Fine adjustment of length would be accomplished during frame installation.

Install Frame. The frame would be installed using equipment similar to that used to install the pedestals or the torque tube. The equipment involved would be an automated crane, an automated tractor with a flatbed trailer, and at least two MCRs. The crane would lift a frame off of the trailer and position it over the anchor bolts and rear strut. One MCR would adjust the rear strut while the other would provide final positioning of the front bolt holes. Once the frame is correctly positioned, the MCRs would complete the connections. Panel installation would be similar to that described for previous concepts.

Table 6-23 tabulates the automated equipment required for installation, associated costs, and the resulting productivity and unit costs developed by operating 8, 16, or 20 hours per day.

6.2.4.5 Summary

Current applications of automation technology in the laboratory and in manufacturing facilities have demonstrated the feasibility of the various components described previously. Trends in robotics indicate that it would be reasonable to assume that similar equipment could be developed for construction applications.

Costs developed were based on available data for similar automation equipment and do not reflect the large costs expected to be necessary for the development of specific equipment or construction environment qualification.

Table 6-23

EARTH-AUGER CONCEPT - EQUIPMENT REQUIREMENTS AND COSTS

Operation and Equipment	Rental $/mo	Rental $/day	Oper Cost $/hr	8 hr day Prod'n units/day	8 hr day Cost $/unit	16 hr day Prod'n units/day	16 hr day Cost $/unit	20 hr day Prod'n units/day	20 hr day Cost $/unit
Install Earth Auger									
4WD Truck with controller package	2,566	118.54	4.91						
Auger with Interface Circuits:	465	21.48	0.27						
Tractor (30 ton, 195 hp) with controller package,etc.	3,536	163.33	7.76						
Trailer (2 axle, 25 ton)	570	26.33	0.74						
2 Mobile Construction Robots	15,100	695.0	17.58						
Total		1,077.33	35.66	24	56.78	48	34.33	60	29.84
Excavate Front Footing									
Wheel-type Backhoe (65 hp) w/control package	3,561	164.48	6.61						
Dump truck (12 ton) and control package:	3,586	165.64	8.51						
Mobile Construction Robot	7,550	347.50	8.79						
Total Excavation		678.11	23.91	40	21.73	80	13.26	100	11.56
Place Concrete									
Truck-Mounted Concrete Pump (4" line, 80' boom) with control package	7,016	324.06	13.75						
Ready-Mix Truck (6x4, 45 ton, 240 hp) with control package	4,036	186.42	11.18						
2 Mobile Construction Robots	15,100	697.46	17.58						
Vibrator, 3 hp	145	6.70	0.45						
Total Concrete Placement		1,214.64	42.96	40	39.49	80	24.34	100	21.31
Install Anchor Bolts									
Pickup Truck with Control Package with control package	2,506	115.75	4.81						
2 Mobile Construction Robots	15,100	697.46	17.58						
Total for Anchor Bolts		813.21	22.39	40	24.75	80	14.61	100	12.59

Table 6-23 (Continued)

EARTH-AUGER CONCEPT - EQUIPMENT REQUIREMENTS AND COSTS

	Rental		Oper Cost	Production and Unit Cost					
				8 hr day		16 hr day		20 hr day	
Operation and Equipment	$/mo	$/day	$/hr	Prod'n units/day	Cost $/unit	Prod'n units/day	Cost $/unit	Prod'n units/day	Cost $/unit
Install Rear Struts									
- As above -		813.21	22.39	40	24.75	80	14.61	100	12.59
Install Frames									
Hydraulic Crane (25 ton) with control package	6,111	282.26	9.81						
Tractor (30 ton, 195 hp) with control package	3,536	163.32	7.76						
Trailer (2 axle, 25 ton)	570	26.33	0.74						
2 Mobile Construction Robots	15,100	697.46	17.58						
Total for Frames		1,169.37	35.89	40	36.35	80	21.77	100	18.85
Install Longitudinal Beams:									
- As above-		1,169.37	35.89	40	36.35	80	21.77	100	18.85
Install Panels									
- As above-		1,169.37	35.89	40	36.35	80	21.77	100	18.85

Concept Totals = 422   253   220
$ per sq meter = 28.38   17.05   14.78

The potential for incresed productivity and reduced costs fields is shown by the cost summaries of Tables 6-24 and 6-25. Data in Table 6-24 relates to three different lengths of workday. The automated equipment shows the expected reduction in unit cost for utilization over larger periods of time. However, these results are still based on a 5-day week and further gains will be achieved by using a 7-day operation. The 20-hour workday costs are compared in Table 6-25 with the baseline 8-hour workday scenario costs. Recalling that the automated construction scenarios are hypothetical and use the most sophisticated equipment, then Table 6-25 suggests there is a possibility for cost savings, but automation must be examined in greater depth. Actual productivity of crews or automated equipment is uncertain but the chances of increased productivity for the automation scenario are possible. Table 6-25 includes a column of costs that reflect what happens when assumed productivity rates are doubled. Further encouragement comes from the realization that moving the baseline scenarios to 20-hour workdays by shift scheduling raises the baseline unit costs rather than decreases them, due to premium wage requirements. This was not included in the present effort but is important in considering schedule compression by use of longer days and work weeks.

Although the subject could not be fully explored in this study, automated construction scenarios may have some promise. Further studies are required to identify optimum blends of manual and automated techniques for construction of photovoltaic power plants, identify equipment development requirements and costs, and identify potential cost benefits.

Table 6-24

SUMMARY OF AUTOMATED INSTALLATION COSTS

Concepts	1980 $ Per Sq. Meter		
	8 hr. day	16 hr. day	20 hr. day
1. Caisson-pedestal	26.60	15.36	13.00
2. Torque Tube	21.21	12.68	11.31
3. Earth Auger	28.38	17.05	14.78

Table 6-25

BASELINE AND AUTOMATED INSTALLATION COSTS COMPARISON

Concepts	1980 $ Per Sq. Meter		
	Baseline 8-hr. days	Automated 20-hr. day	Productivity Doubled
1. Caisson-pedestal	14.79	13.00	6.50
2. Torque Tube	6.67	11.31	5.65
3. Earth Auger	12.85	14.78	7.39

Notes: (a) Baseline bare costs for 8 - hour days.
      (b) Automated bare costs for 20 - hour days.
      (c) Costs are labor, equipment, and operating costs for installing concepts.

Section 7

CONCLUSIONS AND RECOMMENDATIONS

This section presents the major conclusions resulting from this study, along with recommendations for future work.

7.1   CONCLUSIONS

Significant conclusions relating to subfield layout and wiring considerations include:

- A major distinction exists between vertical axis arrays (primarily two axis tracking concentractors) and horizontal axis arrays (such as fixed flat-plate and single axis tracking line focus systems) due to the respective locations of the array electrical terminals. Vertical axis arrays require the dc wiring subsystem to extend to the center of the arrays (point of rotation) while the dc wiring subsystem for horizontal axis arrays only extends to the ends of the arrays.

- First costs and I^2R energy losses for the dc wiring subsystem generally decrease for both array types with increasing dc voltage levels in the range of 500 to 5000 V. However, decreases are less significant above about 2000 V. Also, dc wiring subsystem first costs and I^2R losses are generally lower for horizontal axis arrays than for equivalently rated vertical axis arrays.

- Comparison of aluminum versus copper conductors for the dc wiring subsystem indicates that there may be little economic difference

between the two alternatives when both first costs and the value of the I^2R energy losses are considered. This could change depending on application specific factors, including the relative prices of copper and aluminum as well as the value of the energy losses.

● Similar tradeoff analyses with regard to the size of the conductors versus the maximum current loading indicate that there may be some economic advantage in slightly oversizing the dc power wiring conductors to reduce the I^2R energy losses.

● Costs for overhead ac power collection wiring may be somewhat lower than for underground construction. However, the actual costs are relatively small compared to total plant costs, especially for the higher field power densities.

● The requirements for the array field grounding subsystem are presently not well defined. Therefore, better definition of grounding requirements is necessary to determine the level of protection that can be provided in a cost effective manner. A major cost driver in grounding subsystem design is site soil resistivity (over which the system designer has little control).

● Similarly, the requirements for transient overvoltage protection in the dc power collection subsystem are also not well defined. Analysis conducted in this study indicate that if varistor type surge protectors are adequate, they can likely be

provided at an acceptable cost (e.g., in the range of 10 mills/Wp for one array design evaluated in this study).

- Requirements and costs for array control, instrumentation, and auxiliary power wiring subsystems are extremely array and application specific. These subsystems must therefore be designed and optimized during detailed design of specific photovoltaic power systems.

Major conclusions with regard to power conditioning equipment include:

- Selling price ($/kW) generally decreases with increasing power level (in the range of 1 to 25MW).

- Selling price for fixed power level LCI and SCI systems is relatively insensitive to dc voltage, especially in the higher power levels (5 to 25MW).

- SCI systems tend to have comparable, or slightly lower, selling prices than equivalently rated (in terms of dc power and voltage levels, as well as power factor and harmonic injection levels) LCI systems.

- Efficiency increases as power level increases for both SCI and LCI systems.

- The efficiencies of identically rated SCI and LCI systems are approximately equal.

- SCI system efficiency decreases as dc voltage increases.

- LCI system efficiency at higher power levels increases as dc voltage increases. At lower power levels, LCI system efficiency decreases as dc voltage increases.

- Selling price ($/kW) for both LCI and SCI converters decreases for narrower voltage window designs (between 1.5 and 1.1).

- Efficiency of both LCI and SCI converters increases for narrower voltage window designs (between 1.5 and 1.1)

- For the schemes evaluated in this study, the use of in-field dc up-converters results in higher first costs and lower operating efficiencies than the use of in-field dc to ac converters.

- SCI systems offer lower installation costs, less site-specific engineering, greater application flexibility, and greater tolerance to utility line disturbances than LCI systems.

- LCI systems may, in some installations, offer slightly higher efficiency than SCI systems.

- LCI and SCI equipment are generally comparable on an overall basis and further study will be required to determine which type of converter would be best suited for a particular application.

Major conclusions with regard to array field design optimization include:
- Yearly power conditioner energy efficiency is a function of inverter efficiency, site location (i.e., insolation), and array type (i.e., response to direct and diffuse sunlight).

7-4

- Total equivalent costs (first costs plus the value of the yearly energy losses) for identically rated SCI and LCI systems are approximately equal.

- Evaluation of the combined costs for dc wiring and power conditioning equipment indicates that there is little economic incentive to postulate array subfields with ratings much above about 5MW and 2000 Vdc.

- Consideration of other factors, including the requirements and costs for branch circuit shorting and disconnect switches as well as the costs of providing solar cell module electrical insulation may result in somewhat reduced optimum dc voltage levels.

- Power conditioning equipment with voltage windows as narrow as 1.2 or 1.1 may be economically attractive in many applications.

- High first costs and/or low operating efficiencies result in the in-field dc up-converter schemes evaluated in this study being economically unattractive.

- Depending on land costs, site latitude, and other application-specific factors, flat-plate array spacings of up to 3 times the vertical array height may be economically attractive.

Major conclusions with regard to array support structures include:

- The wide variety of construction types used in flat-roofed commercial and industrial buildings makes generalization of roof-mounted array design requirements extremely difficult.

- At present, existing building codes do not specifically address design requirements for roof-mounted photovoltaic arrays.

- Design requirements, including loadings, are presently not well defined and are subject to interpretation by individual building code officials.

- If roof structural members are used to transfer array loads to vertical building supports (i.e., walls or columns), overstress conditions may result, especially in retrofit installations.

- Design loading is a significant cost driver.

- The development of innovative, low cost roof penetrations having minimum maintenance requirements will be necessary to realize roof-mounted photovoltaic array support structures with acceptably low costs.

- The realization of low installed cost array support structures for large array fields can only be achieved through integration of panel/support structure designs, as well as through innovative use of low cost materials.

- For the three array designs and baseline construction scenarios evaluated in this study, labor costs represent from 12 to 21% of the total installed costs and they are sensitive to purchase quantity (ie., plant size).

- For fully optimized designs, there may be little economic incentive in postulating sophisticated, highly automated construction scenarios and this would require further study.

7.2 RECOMMENDATIONS

Based on the results of this study, several recommendations can be made regarding the need for additional evaluation.

These include:

- The need for branch circuit disconnect and/or isolating switches, as well as the costs for providing increased module electrical isolation, should be further identified to facilitate selection of optimum power conditioner dc voltage and power ratings.

- The requirements for array grounding and transient surge protection should be better defined to facilitate determination of detailed design requirements and associated subsystem costs.

- Utility interface requirements with regard to power factor and harmonic injection should be evaluated both to facilitate detailed power conditioning equipment specification, as well as the comparison between SCI and LCI technologies.

- Operating efficiency estimates, especially at low load, as well as installation costs and other inverter design specific parameters, should be further evaluated to facilitate identification of optimum inverter configurations.

- The effects of aging on array IV characteristics should be identified to facilitate identification of acceptable dc voltage windows.

- Loading conditions for roof-mounted photovoltaic arrays should be better defined, along with other specific design requirements.

- Low cost roof penetrations, or other methods of attaching roof-mounted array support structures to the building structural members, should be developed.

- Array support structure designs should be fully optimized, including the integration of panel and support structure, prior to the investigation of automated installation techniques.

REFERENCES

1-1   Interim Performance Criteria for Photovoltaic Energy Systems, Draft Document, prepared for the U.S. Department of Energy by the Solar Energy Research Institute under Contract No. EB-77-C-01-4042, Golden, Colorado, May 1980.

1-2   Building Construction Cost Data 1980, Robert Snow Means Company, Inc. 38th Edition, Kingston, Mass., 1979.

1-3   1980 Dodge Manual for Building Construction Pricing and Scheduling, McGraw-Hill Cost Information Systems, Annual Edition No. 15, New York, New York 1979.

1-4   National Photovoltaics Program - Multi-Year Program Plan, U.S. Department of Energy, Photovoltaic Systems Division Office of Solar Applications for Buildings, Washington, D.C., September 1980.

3-1   Summary of Photovoltaic Application Experiments Designs, ed E.L. Burgess and E.A. Walker, United States Department of Energy, Albuquerque Operations Office, October 1979.

3-2   F.J. Mosna Jr. and J. Donlinger, Photovoltaic Module Electrical Termination Design Requirement Study, prepared by Motorola, Inc./ITT Cannon for the Jet Propulsion Laboratory under Contract No. 955367, Final Report, July 1980.

3-3   Bechtel National, Inc., Study of Curved Glass Photovoltaic Module and Module Electrical Isolation Design Requirements, Final Report prepared for the Jet Propulsion Laboratory under Contract No. 954698, June 1980.

3-4   National Electrical Code 1981 Edition, National Fire Protection Association, NFPA No. 70-1981, Boston, Mass., 1980.

3-5   Burt Hill Kosar Rittelmann Associates, Residential Photovoltaic Module and Array Requirement Study, DOE/JPL955149-1 (APP) performed for the Jet Propulsion Laboratory under Contract No. NAS-7-100-955149, Butler, PA, June 1979.

3-6   Reported in the "Solar Energy Intelligence Report," August 14, 1980.

3-7   National Electric Safety Code 1981 Edition, Institute of Electrical and Electronic Engineers, ANSI C2 1981, New York, September 1980.

3-8   Bechtel Corporation, Engineering Study of the Module Array Interface for Large Terrestrial Photovoltaic Arrays, Final Report prepared for the Jet Propulsion Laboratory under Contract No. 954698, June 1977.

3-9   Bechtel National, Inc., <u>Requirements Definition and Preliminary</u>
        <u>Design of a Photovoltaic Central Station Test Facility</u>, Final
        Report prepared for Sandia Laboratories under Contract No. 07-6926,
        April 1979.

3-10   IEEE Red Book - STD 141-1976

3-11   Westinghouse Electric Corporations, <u>Distribution Systems</u>,
        East Pittsburg, PA, 1965

3-12   Guide for Safety in Alternating-Current Substation Grounding,
        IEEE Std., 80-1961, IEEE, New York (R 1971).

3-13   Georgia Institute of Technology, <u>Grounding Bonding and Shielding</u>
        <u>Practices and Procedures for Electronic Equipments and Facilities</u>
        <u>Volume I</u>, prepared for the Federal Aviation Administration,
        December 1975.

3-14   H. Fowles, et al., <u>Transient Effects From Lightning</u>, report
        prepared by Mission Research Corporation for Sandia Laboratories
        under Contract No. 13-0215, Volume I, January 1980.

3-15   Westinghouse Electric Systems, <u>Electrical Transmission and</u>
        <u>Distribution Reference Book</u>, Westinghouse Electric Corp., East
        Pittsburg PA, 1950, P. 557.

3-16   Joslyn Electric Systems, <u>Electrical Protection Guide For Land-Based</u>
        <u>Facilities</u>, Joslyn Manufacturing and Supply Company, Inc.,
        Goleta, CA, 1971, p. 15.

3-17   Climatological Services Division, <u>Mean Number of Thunderstorm</u>
        <u>Days in the United States</u>, U.S. Department of Commerce Weather
        Bureau, Technical Paper No. 19, September 1952.

3-18   Bechtel National, Inc., <u>Terrestrial Central Station Array Life-Cycle</u>
        <u>Analysis Support Study</u>, Final Report prepared for the Jet Propulsion
        Laboratory under Contract No. 954848, August 1978.

3-19   Bechtel National, Inc., <u>Improvement of Civil Engineering Techniques</u>
        <u>for Buried Transmission Cables</u>, Final Report prepared for the
        Electric Power Research Institute under Contract No. 7870-1,
        January 1979.

3-20   Stuart M. Lewis, "URD Cable Instllation Practices", <u>Transmission</u>
        <u>and Distribution</u>, May, 1979, pgs. 42 and 44.

3-21   Nelson J. Anello, "Grounding Grid Connections Simplified",
        <u>Transmission and Distribution</u>, January, 1981, p. 40.

4-1   <u>AC/DC Power Converter for Batteries and Fuel Cells</u> (EPRI RP841-1),
        Ramon W. Rosati, et al.., Annual Report EM-1286, Power Systems
        Divisions of United Technologies Corporation, December, 1979.

4-2   IEEE Guide for Harmonic Control and Reactive Compensation of
        Static Power Converters, IEEE Project No. 519, July, 1979.

4-3   Evaluation of Battery Converters Based on 4.8-MW Fuel Cell
        Demonstrator Inverter (DOE EX-76-C-01-2122), John W. Walton,
        et al., Power Systems Division of United Technologies Corporation,
        Final Report FCR-0926, October, 1980.

4-4   Advanced Converter Technology for Battery Applications (DOE DE-AC-01-
        79-ET-29079), Power Systems Division of United Technologies
        Corporation, November 1, 1979.

4-5   Conceptual Design of Electrical Balance Of Plant For Advanced
        Battery Energy Storage Facility, annual report prepared for
        Argonne National Laboratory by United Technologies' Power Systems
        Division under contract number 31-109-38-4308, March 1979.

4-6   Conceptual Design and Systems Analysis of Photovoltaic Power
        Systems (DOE EY-76-C-04-2744), P. Pittman, Westinghouse Electric
        Corporation, March, 1977.

4-7   Conceptual Design and Systems Analysis of Photovoltaic Systems
        (DOE EY-76-C-04-3686), General Electric Company, June, 1975 -
        March, 1977

4-8   W. Kimbark, Direct Current Transmission, Vol. 1, 1971, Wiley-
        Interscience Division of John Wiley & Sons, Inc., New York.

4-9   B.R. Pelly, Thyristor Phase-Controlled Converters and Cycloconverters
        1971, Wiley-Interscience Division of John Wiley & Sons, Inc.,
        New York

4-10   Development of Advanced Batteries for Utility Applications (EPRI
        RP128-4,-5) General Electric Company, Interim Report EM-1341,
        February, 1980.

4-11   "Power Conditioning for DC Energy Souces", EPRI Journal, September,
        1980, pp. 45-47.

4-12   AC/DC Power Conditioning and Control Equipment for Advanced
        Conversion and Storage Technology (EPRI RP390-1), Peter Wood,
        Westinghouse Electric Corporation, Final Report EM-271, November,
        1976.

4-13   Thristor Voltage Safety Factor (EPRI RP840), John Mungenast and Del
        Kirk, Power Semiconductors, Inc., Final Report EM-825, July, 1978.

4-14   Open-Cycle MHD Power Conditioning and Control Requirements
        Definition (EPRI RP642-1), S. Petty and K. Williams, AVCO
        Everett Research Laboratory, Inc., Final REport AP-1345, March,1980

4-15   Airesearch Manufacturing Company of California, "Battery Energy
        Storage Test (BEST) 2.5 MW Reversible Converter", presented at the
        DOE Battery and Electrochemical Contractors Conference, Arlington,
        Virginia, December, 1979.

5-1   Bechtel National, Inc., Study of Curved Glass Photovoltaic Module
        and Module Electrical Isolation Design Requirements, Final Report
        prepared for the Jet Propulsion Laboratory under Contract No.
        954698, June, 1980.

5-2   Jet Propulsion Laboratory, Thermal Performance Testing and Analysis
        of Photovoltaic Modules in National Sunlight, JPL Publication No.
        5101-31, July 29, 1977.

6-1   Architectural Graphic Standards by Ramsey and Sleeper,
        6th Edition, 1970, pp. 498-499.

6-2   Residential Photovoltaic Module and Array Requirement Study, June
        1979, DOE/JPL/955149-1.

6-3   Building Code Requirements for Minimum Design Loads in Building and
        Other Structures, A58.1-1972, American National Standards Institute,
        Inc.

6-4   Design of Low-Cost Structures for Photovoltaic Arrays, Volume 2 of 3,
        Technical Studies, Bechtel National Inc., July 1979, SAND 79-7002.

6-5   Timber Construction Manual, American Institute of Timber Construction,
        2nd Edition, 1974, John Wiley & Sons.

6-6   Installation Guidelines for Solar DHW Systems In One- And Two-Family
        Dwellings, May 1980, HUD-PDR-407(2)

6-7   O'Rouke, M. J., Snow and Ice Accumulation Around Solar Collector
        Installations, August 1979, NBS GCR 79-180

6-8   HUD Intermediate Minimum Property Standards Supplement, 1979,
        prepared by the Department of Housing and Urban Development.

6-9   "Winter Roof Collapses: Bad Luck, Bad Construction, or Bad Design",
        Civil Engineering, ASCE, December 1979, pp. 42-45.

6-10   "Snow-Prone Roof's Strength Tripled", Civil Engineering, ASCE,
        Jaunary 18, 1979, pp. 41.

6-11   "Collapsed Space Truss Roof Had a Combination of Flaws", ENR,
        June 22, 1978, pp. 36-37.

6-12   "Active Solar Energy System", Design Practice Manual, DOE National
        Solar Data Program, October 1979, Solar 10802-79-01.

6-13   Weinstein, Stephen, Architectural Concerns in Solar System Design
        and Installation, PRC Energy Analysis Company, March 1979, SOLAR/
        0801-79/01

6-14   Mertz, E. C., "Solar Collectors, Another Roof Design Problem",
        The Construction Specifier, May 1979, pp. 69-72.

6-15   Uniform Building Code, The International Conference of Building Officials, 1979.

6-16   "Fastening and Joining", Machine Design, Vol. 48, No. 26, November 18, 1976.

6-17   Parmley, R. O., Standard Handbook of Fastening and Joining, McGraw-Hill, 1977, pp.

6-18   Module/Array Interface Study, Bechtel National Inc., August 1978, DOE/JPL-No. 954698-78/1.

6-19   Abe Wilson, "Array Structure Cost Reduction Study", Progress Report 15 and Proceedings of the 15th Project Integration Meeting (for the low cost solar array project), JPL Publication 80-27, Jet Propulsion Laboratory.

6-20   Aderhold, J.R., Gordon, G., and Scott, G.W., "Civil Uses of Remotely Piloted Vehicles", Summary Report, NASA CR-137895, July 1976.

6-21   Garber, V., "Remotely Piloted Vehicles for the Army", pp. 46-51, Astronautics and Aeronautics, Oct. 1974.

6-22   Dobrotin, B., et al, "A Design for a 1984 Mars Rover", A1AA 16th Aerospace Sciences Conference, Huntsville, Alabama, Paper No. 78-81, Jan. 1978.

6-23   "Kvaerner Trenching System, Remote-Controlled Pipe Burying System", Kvaerner Brig A/S, P.O. Box 3610, Gb Oslo 1, Norway

6-24   Saveriano, J.W. "Industrial Robots Today and Tomorrow", pp. 4-17, Robotics Age, Vol. 2, No. 2, Summer 1980.

Appendix

LCI AND SCI OPERATIONAL CHARACTERISTICS

THIS PAGE

WAS INTENTIONALLY

LEFT BLANK

CONTENTS

ILLUSTRATIONS

TABLES

Appendix

LCI AND SCI OPERATIONAL CHARACTERISTICS

After completing the work described in the main body of this report, a
further study was conducted to evaluate LCI and SCI power conditioning
units (PCUs). Characteristics of the two types of PCUs were compared
in the following areas:

- Bidirectional operation
- Reactive power operation
- Immunity to ac system disturbances
- Contributions to ac system faults
- Stand alone operation
- Operation of parallel modules
- Effects of dc side faults on the ac system
- Installation costs

Except for installation costs, the work presented in this Appendix was per-
formed by United Technologies Corporation under a subcontract to Bechtel.

The results of this work indicate that both LCI and SCI units can be
designed to have acceptable performance with regard to the operational
characteristics listed above. Achieving this performance does not produce
major impacts on the results of the work presented in the preceeding main
text. The estimated specific costs to install the LCI and SCI units are
$0.016/W and $0.0097/W, respectively (exclusive of PCU purchase price).

The following sections of this Appendix present details on the specifications to which the converters were designed. The two types of converter designs are described in Section A-2. Sections A-3 through A-10 discuss each of the eight areas of the study listed above. Conclusions are presented in Section A-11.

A.1 PCU SPECIFICATIONS

A set of baseline specifications for photovoltaic PCU equipment was developed and used in both the initial study and the assessment presented in this Appendix. These specifications are patterned after the PCU specifications for battery and fuel cell applications developed in the Electric Power Research Institute Project 841-1 (Ref. A-1). Both the LCI and SCI systems evaluated herein are designed to meet the specifications described in this subsection:

A.1.1 Electrical Specifications

Power Rating. The nominal PCU system rated power is 10 MW ac at unity power factor.

Efficiency. A conversion efficiency of 95% is required at the lowest dc voltage at which 10 MW ac output (rated power) is obtained. The efficiency shall not be below 90% at 25 percent of rated power.

Dc Voltages. The minimum dc bus voltage for the baseline designs is 1,600 volts. For other designs, this voltage may be changed to accommodate array operating conditions. The maximum voltage must be established by the dc voltage range described below.

Dc Voltage Range. The ratio of maximum to minimum dc voltage is 1.5:1 (i.e., 1,600 to 2,400 volts).

Dc Source Characteristics. The PCU dc input must be designed to accomodate the characteristics of connected arrays of photovoltaic cells. Typical cell characteristics are shown in Figure 5-14 (Page 5-26).

Ac Voltage. The PCU must be designed to operate into a 3∅, 60 Hz utility system at a standard utility distribution or subtransmission line voltage (e.g., 4.16, 13.8, 34.5 or 69 kV).

Ac Voltage Range. Operation is expected to be at distribution voltage levels, where voltage regulation is not as continuous as on transmission networks. To allow utilities to meet voltage regulation needs on distribution systems as specified by ANSI C84.1-1977, the following more stringent voltage/performance criteria will be used for the PCU (i.e., generator):

Line Voltage Range: ±5% normal continuous, no effect on performance.

+5% to +10% (maximum continuous), up to 85% of rated power output, power factor may be less than unity).

-5 to -10% (minimum continuous), up to 95% of rated power at unity power factor.

-10 to -20% (short time operation up to 85% of rated power output at unity power factor).

> +10%, < -20% (not acceptable, power conditioner may turn itself off).

Ac Voltage Unbalance. One per unit ac power will be maintained with a 2 percent phase-to-phase voltage unbalance.

Percent Voltage Unbalance = 100 x (highest or lowest rms phase voltage - average rms phase voltage) ÷ (average RMS phase voltage)

Power Factor. The power factor at the ac side of the transformer must be no worse than .95 lagging at full-rated power. Operation can be at power factors other than unity (leading or lagging). This may be useful for controlling line voltage, depending on the specific characteristics of the utility system at the point where the PCU is connected.

Harmonics. Harmonic voltages introduced into the utility ac network should not exceed a total harmonic distortion (THD) of 5 percent RMS of the fundamental voltage on power systems at 13.8 kV levels (Ref. A-2) when operating into a utility line with 250 MVA short-circuit capacity. If needed, filters should be provided for this purpose.

Electromagnetic Interference (EMI). The PCU must not cause malfunctions of local utility or communications equipment.

A.1.2   Protection and Protection Coordination Specifications

The converter system shall have three primary zones of protection:

- Dc source and buswork
- Power conditioner
- AC interface including switchgear and step-up transformer

The converter system must be designed so that its protection system is coordinated in an overall systems plan in order to automatically correct for internally or externally generated malfunctions that could cause operation of any zone beyond its design capability.

Dc Input. The PCU should provide a protective device(s) to interrupt dc source fault currents into inverter internal faults. If the dc source is made up of several dc submodules, then the dc source must include a means of preventing one dc submodule or the ac source from contributing to a fault in another dc submodule (e.g., by isolating interruptors or fault isolation).

Silicon Controlled Rectifier (SCR) Protection. Power SCRs must be protected against faults or overload conditions. Fuses used for this purpose must be coordinated so as not to clear unnecessarily under conditions such as distribution line faults and recovery, switching transients, and most lightning strokes. The fuses shall be easily accessible for inspection, maintenance, and replacement. Protection trip indication shall be provided. Such fuse protection of SCR's may not always be possible for LCI systems.

Ac Protection. The PCU output shall contain a circuit breaker and differential protection against short circuits and faults in the ac side of the inverter system. The circuit breaker shall be capable of interrupting the fault current of the connected ac system short circuit capability.

Isolated Operation. The use of a photovoltaic power system in an isolated operating mode (i.e., stand-alone operation with no other utility generators connected to the loads served by the system) provides increased availability of electric service for the area served and may therefore be desirable.

Development of an isolated operation specification will be deferred until solar arrays systems are commercialized. An earlier study for EPRI (Ref. A-4) showed that isolated operation would produce minimal impact on PCU characteristics.

A.1.3 Environmental Specifications

The PCU must be able to survive and operate under the following environmental conditions:

Ambient Air Temperature	-35 to 43°C (-30 to 110°F)
Altitude	Up to 2440 m (8000 ft), derate above 1000 m
Humidity	99% Relative Humidity
Wind Load (Side Wall)	45 m/sec., 2.2kPA (100 MPH, 45 lbs/ft^2)
Snow or Ice Roof Load	3.9kPA (80 lbs/ft^2)
Wind, Simultaneously Applied with Snow and Ice	Calculated per Reference ANSI A58.1 for Configuration
Solar Radiation	1.1 kW/m^2
*Seismic Loads (Ground Motion) Horizontal Vertical	0.33G (2.1G maximum without damping) 0.22G (1.4G maximum without damping)
Dust	0.180 micrograms/meter^3
Salt Entrained in Air	.003 - .01 ppm
Rain/Wind	25 mm/hr, 16m/sec (1 in/hr, 35 MPH)

*Seismic loads not simultaneous with wind loads.

A.1.4 Other Criteria

Cooling. The PCU cooling system must ensure suitable performance of the equipment with final heat transfer to ambient air.

<u>Acoustic Noise</u>. The noise level generated must be less than 55 db, "A-weighting" when measured at a distance of 100 ft from the installation perimeter.

<u>Safety</u>. Safety guidelines must be estabished to minimize the occurrence of a hazardous event. Failure analysis conventionally defines a hazardous event as either a serious personal injury or major equipment damage. No single failure should result in a hazardous event.

Design guidelines must be consistent with NEMA, ANSI, OSHA, National Electrical Safety Code, and ASME when applicable. The National Electric Code is not binding for utilities (but may be for privately-owned plants up to 80 MW under PURPA regulations.)

<u>Maintenance</u>. The PCU must be easy to maintain (i.e., its components and subsystems must be accessible), and required preventive maintenance must be held to a minimum. Maintenance requirments should be appropriately balanced with equipment costs and reliability.

<u>Modularity</u>. Modularity is encouraged to enhance maintainability and reliability as well as to permit use of a standard-sized unit for a variety of plant sizes and to enable phased expansion.

A.1.5   <u>Cost and Life Considerations</u>

<u>Cost Base</u>. For photovoltaic applications, the power base used to determine specific cost of the equipment should be the rated power of the PUC (10 MWac for the designs presented in this appendix).

Life. To be consistent with the design life of other utility equipment, the expected life of the PCU in this application should not be less than 20 years with nominal maintenance and repair.

Cost. This selling price (to the user) is for mass-produced equipment in a mature technology (i.e., not a "first-of-a-kind" product). Production levels of one hundred 10 MW converter units per year are assumed herein.

A.2 SYSTEM DESCRIPTIONS

This section presents descriptions of LCI and SCI systems.

A.2.1 Line-Commutated Inverters

The block diagram for a 10 MW line-commutated inverter is shown in Figure A-1. The design shown is a commonly used arrangement in which two bridges are used to feed wye-delta windings on the low side of a main transformer. Theoretically, this cancels the 5th and 7th family of harmonics (5, 7, 17, 19, 29, 31, etc.). In practice, however, cancellation is imperfect. With analog gating controls, the 5th and 7th are about 70% cancelled and the higher order harmonics may or may not undergo some degree of cancellation. With modern digital gating controls, from 85% to 90% cancellation of the 5th and 7th harmonics can be obtained.

With the wye-delta arrangement, the 11th, 13th and higher harmonics are commonly controlled by filtering. In large HVDC transmission systems, tuned filters are normally used to attenuate the 11th and 13th, with a high pass filter used to attenuate the higher harmonics. In smaller
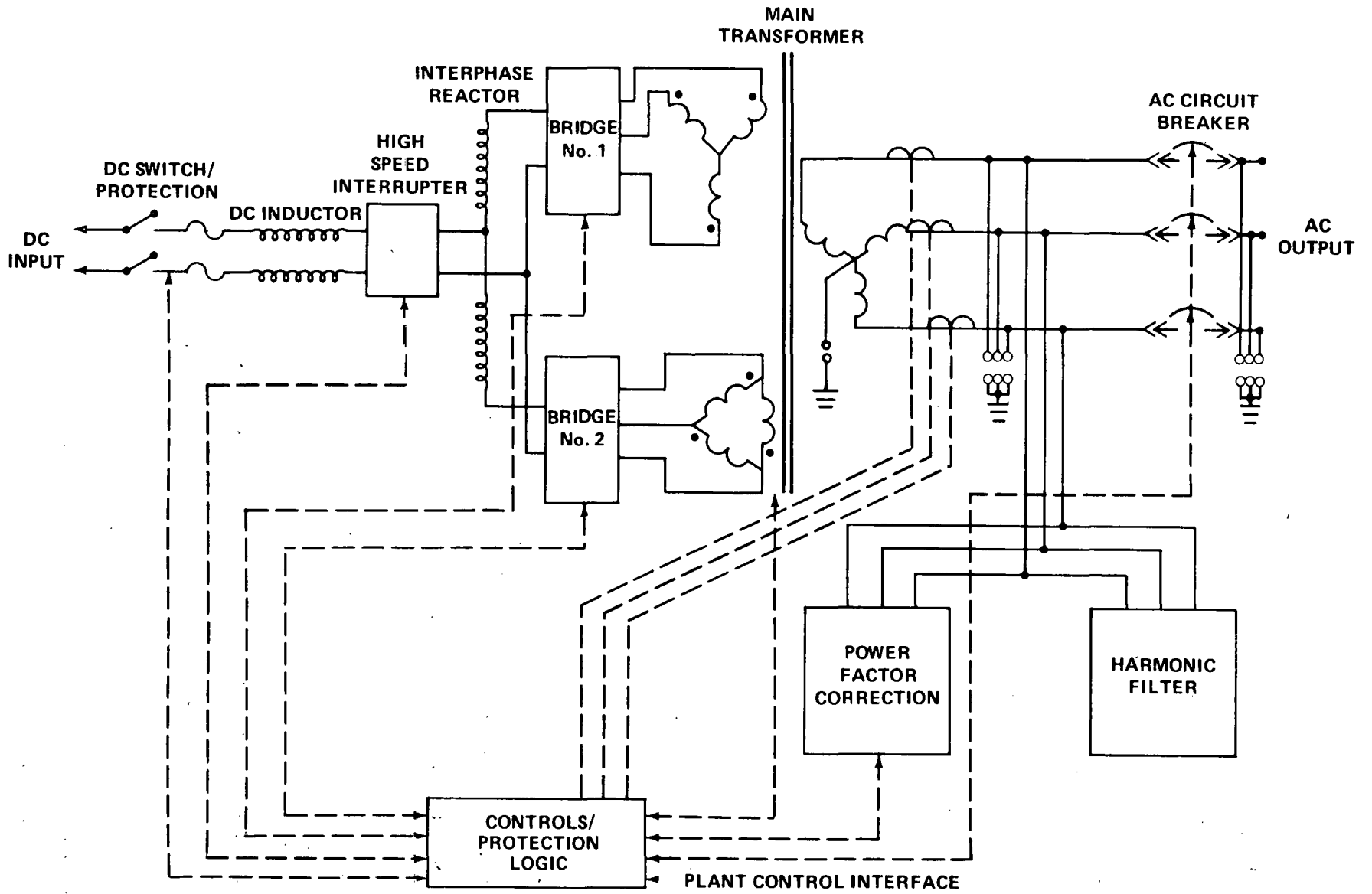
Figure A-1 LCI Electrical Diagram

systems, a high pass filter is sometimes used to attenuate harmonics above the 11th and thereby eliminate the need for tuned filters.

Line-commutated inverters must have a positive means for commutating-off (shutting-off) the dc input when the line voltage required for normal commutation deviates beyond allowable limits due to ac system faults and switching transients. Dc circuit breakers could be used for this purpose. However, due to contact arcing, breakers in the voltage and current range of this application have a limited number of operations available before they must be maintained. Since ac line disturbances are fairly frequent, a static commutation circuit can be incorporated into the dc input to handle these routine events and eliminate the contact maintenance problem. A dc breaker is included as backup for the static commutation circuit and for faults on the dc input side. With a solar array as the dc source, dc fault currents are only slightly higher than the normal operating currents and the breaker requirements are much less rigorous than with a stiff dc source such as a battery. Thus, it may be possible to develop a dc breaker for solar applications that is capable of a large number of operations before requiring maintenance. If both solar arrays and battery energy storage are used, the dc breaker requirement is severe due to the high fault current capability of the battery. Accordingly, consideration should be given to adding a dc input emergency commutation circuit in applications that include batteries.

It should be noted that this is a large commutation circuit. The recovery time for the large, phase-controlled SCRs in line-commutated

systems is about 4 times the recovery time for the fast inverter-grade SCRs used in self-commutated systems. This means that the energy storage in the LCI emergency commutation circuit components would have to be on the order of 4 times that for the SCI's inverter-grade SCRs.

Before the advent of high power semiconductors, mercury arc valves were used for HVDC transmission line installations. These valves were subject to frequent arc-backs which jarred the main transformer windings due to the large currents involved. This required use of specially braced transformers called "rectifier transformers" which are considerably more expensive than standard units with the same rating. Since semiconductors do not arc-back, such bracing is not required. However, the main transformer is not quite a standard unit. There will be some dc offset current fed into the transformer. The amount depends on the degree of symmetry in the bridge and bus geometries, and how well the SCRs are matched for forward voltage drop. Designers often reduce the design flux density in the main transformer or incorporate a small air gap to accommodate dc offset current without saturating the core. Also, economics favor locating the harmonic filters on the high-voltage side rather than on the low-voltage side for the voltages considered herein. This means that all the harmonic currents must flow through the main transformer. This increases losses in the windings as well as in the core. These effects are not large but do impose a penalty on the order of a few percent in transformer size and cost.

A.2.2 Self-Commutated Inverters

The block diagram for a 10-MW self-commutated, pulse-width-modulated inverter is shown in Figure A-2. Protection against dc faults is provided by a current-limiting protector. It opens automatically when a dc fault is sensed and will also open when activated by other control signals. This highly current-limiting protector is small and its cost is a small fraction of the cost of a dc breaker. However, it cannot be used for routine isolation of the converter from the dc source. A disconnect can be used for this purpose.

With pulse-width modulation, the ac voltage waveform generated by the inverter does not require tuned filters for harmonic cancellation. Thus, the probability of establishing unwanted resonances with the other system impedances is reduced markedly. Accordingly, the two bridges feed two 3 phase low-side transformer windings through small series reactors.

The main transformer is a standard-design substation unit. The pulse-width modulated bridges control lower order harmonic currents to small values. The small series reactors present large impedances to high frequencies and thereby limit higher order harmonic currents. Hence the main transformer sees only low levels of harmonic currents which have negligible effects on transformer losses.

The high-precision, digital gating controls make it possible to reduce dc current content to negligible values despite normal component voltage drop tolerances and circuitry unbalances.
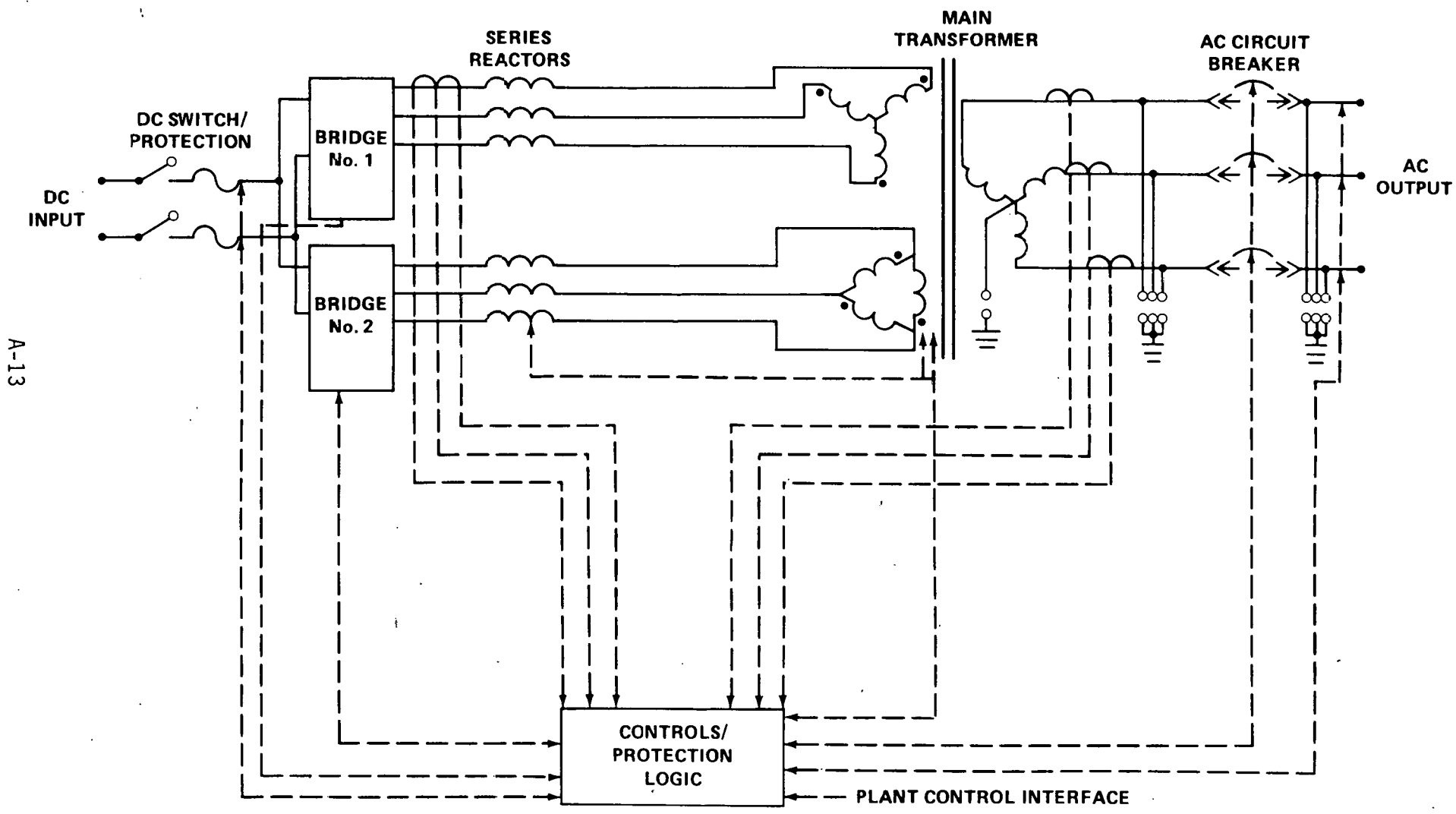
Figure A-2 SCI Electrical Diagram

A.3 BIDIRECTIONAL OPERATION

Both the LCI and the SCI are capable of handling full rated power in either direction. They can operate as an inverter or a rectifier, i.e., a converter. This feature would be required if on-site battery energy storage were to be charged from the utility line.

A.3.1 Line-Commutated Inverters

The LCI can smoothly change the level of (slew) real power from full power in the forward (inverter) direction to zero. However, as this is taking place, the reactive power (VARs) consumed by the converter is changing. It is necessary to reduce the VARs supplied by the power factor correction capacitors to counterbalance the converter's reduced VAR consumption in order to prevent the system voltage from rising due to excessive VAR generation by the power factor correction capacitor banks. Thus, the power factor correction supplied must track (to some degree) as the real power is changed.

For example, consider a 25 MVA substation such as shown in Figure A-3.
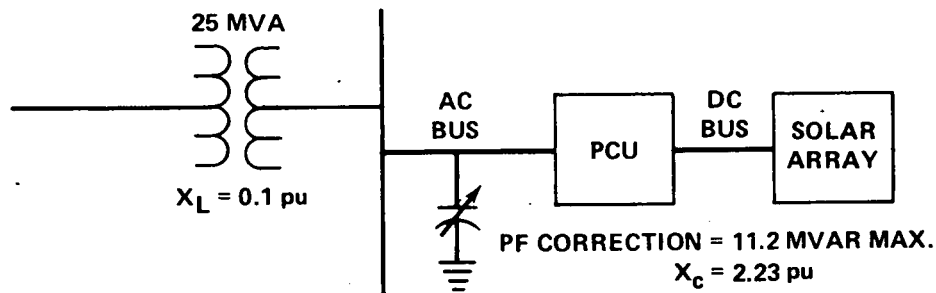
Figure A-3 System Electrical Configuration

The converter requires a maximum of 11.2 MVAR of power factor correction capacitors in order to be able to deliver its full rated power of 10 MW at

at unity power factor with the dc input at the minimum voltage of 1600 volts. At this point, the net VAR flow into the PCU system (converter and power factor capacitor banks) is zero. If the converter's real power is reduced to zero without changing the power factor capacitor, the capacitor banks will deliver 11.2 MVARs into the substation 13.8 kV bus. The voltage will rise about 7%. The presence of loading on the 13.8 kV bus will decrease the voltage rise somewhat. While this is not necessarily a dangerous level, it would be desirable to limit the imbalance betweeen power factor correction and the converter VAR consumption to about half of the total VAR loading of the converter at worst-case power factor. This is 5.5 MVAR for the present design.

Continuous VAR control and close tracking are possible with a static VAR generator. With switched-capacitor power factor correction, the 5.5 MVAR limit can also be held without difficulty.

After the converter real power goes to zero, it is necessary to reverse either the bridge dc polarity or the dc source polarity. In either case, DPDT switching action is required. This requires four single-pole dc breakers, which are expensive. A better alternative is to use solid-state dc switches. Back-to-front SCR connections could also be used in each valve position in the converter. With this configuration, only one set of SCRs is gated for inversion operation; the other set is only gated for rectification operation.

After the dc polarity has been switched, the LCI can slew smoothly to full real power in the rectifier direction. Again, with switched

capacitors, the discrepancy between VAR consumption by the converter and VAR generation by the power factor correction capacitor bank should not exceed about 5.5 MVAR, as described above.

A.3.2 Self-Commutated Inverters

The SCI can slew smoothly from supplying power to the ac system from a dc source to supplying power to a dc source from the ac system. This is accomplished by simply changing the power demand setting from a positive demand to a negative demand. The slew rate is controlled to provide the power-versus-time curve shown in Figure A-4.
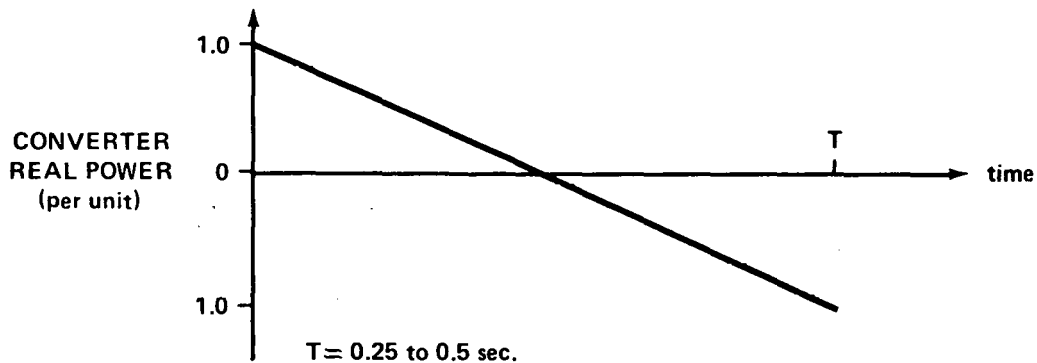
Figure A-4 SCI Slew Characteristics

During the transition, reactive power (Q) can be controlled independent of real power (P) over the range where

$$|Q| \leq (1 - P^2)^{1/2} \text{ per unit}$$

A.3.3 Summary

Both LCI and SCI units can be designed for bidirectional operation. However, the requirement for LCI dc polarity reversal plus the need to balance the VARs generated by the power factor correction capacitors

and consumed by the converter adds some penalty to the LCI. The polarity reversal will add to the PCU cost in applications requiring bidirectional power flow. VAR balance during the transition can be accomplished either with continuous VAR control using static VAR generators or with switched capacitors. There is no such penalty with the SCI system.

A.4 REACTIVE POWER OPERATION

Utilities prefer high power factor loads and co-generators for two purposes:

- To minimize circuit voltage drops. Since the reactive voltage drop (V_R) produced by reactive current (I_R) is

$$V_R = X \cdot I_R$$

where the line impedence is primarily reactive (X_L). This voltage drop becomes much more appreciable than does the resistance drop if the reactive current becomes a significant part of the total line current. It should be noted that this is the case with lagging power factor loading. With leading power factor loading, the above reactive voltage is a voltage rise.

- To minimize I^2R loss in the lines and transformers by minimizing line current.

Both converter types can generate or absorb VARs. In both cases there are some limitations. The ability to generate VARs is widely regarded as an advantage. Somewhat less widely recognized is the advantage of a converter's ability to absorb VARs. Many utility

systems have stability problems at light loads due to the presence of un-switched capacitor banks and, in some cases, large effective capacitances created by extensive underground cable networks. Under these conditions, a utility's generators can see leading power factor loading due to the genera-tion of excess VARs in their system. This in turn drives generation excita-tion levels downwards (to hold voltage down). As a result, the coupling between the generators in the system is decreased and it is easier to lose synchronization or become unstable during and following major system dis-turbances. Hence, depending upon the location of the converter within the utility system, the ability to absorb VARs may be useful to utilities with this problem.

A.4.1 VAR Generation and Consumption with SCI Systems

Just as with a conventional rotating generator, the SCI controls VAR generation and consumption by varying its driving ac voltage. If the voltage (behind the series reactors) exceeds the ac line voltage, it delivers VARs to the ac system. If this internal voltage is less than the ac line voltage, the SCI will consume VARs from the ac system. The SCI can consume VARs up to its full rating if no real power is being delivered. A rotating machine can consume only about 50% of its rating with no real loading. VARs (Q) can be controlled independently of real power (P) but there are some limits.

- The VARs generated or consumed must be

$$|Q| \leq (1 - P^2)^{1/2} \text{ per unit}$$

  to keep a line current at-or less than 1.00 per unit. This gives an upper limit of ± 10 MVAR for the 10 MW system being considered. This limitation is shown by the curve in Figure A-5 for rated ac voltage.

- With 105% ac line voltage and with dc source at minimum voltage, the SCI cannot generate VARs. However, it can consume VARs. Above dc voltages of about 1,800V, the preceeding equation (illustrated in Figure A-5) is the determining factor.

- At 110% ac line voltage and minimum dc voltage for emergency operation, VARs will be consumed from the ac line. The VARs consumed wil be in the area of 0.23 per unit.
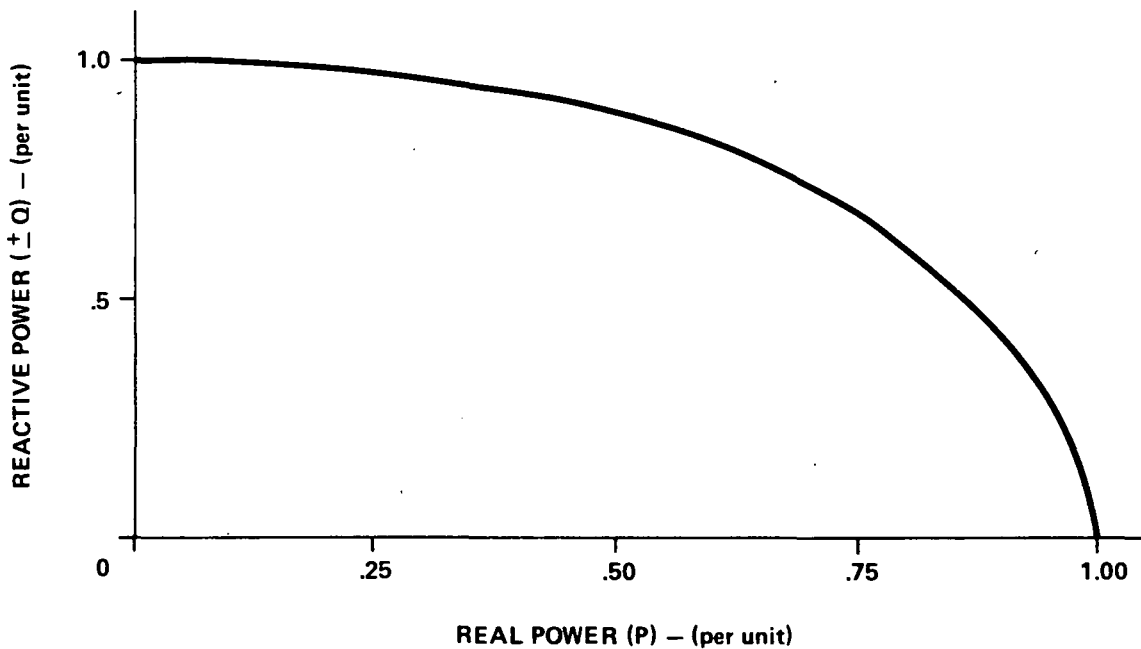
Figure A-5 SCI VAR Limits

The SCI is inherently capable of stand-alone operation as a VAR generator or consumer. With the proper control, it can operate in this mode without being connected to a dc source or sink. This has the following advantages to a utility using an SCI converter as a static VAR generator when the dc source is unavailable (e.g., at night for photovoltaic systems):

A-19

- · There is no impact on output transformer size or losses
- Response time is very rapid (e.g., 200 milliseconds for full leading to 90 percent of full lagging, Ref. A-1)
- Control resolution is continuous from full leading to full lagging
- Voltage transients (such as occur with switched power factor capacitors) are not generated

Operation of an SCI system for standalone operation has been studied and verified experimentally (Ref. A-5).

A.4.2   VAR Generation and Consumption with LCI Systems

VAR control in the LCI is quite different from the SCI and conventional rotating machines. In the LCI system, VAR consumption of the converter is a function of the real power flow and the dc voltage level. However, the capacitor banks used to accomplish power factor correction are variable, either continuously (with SCR-controlled corrective spoilers as in a static VAR generator) or in steps (with switched capacitors). The power factor correction must be sized for the converter's worst steady-state operating conditions of maximum (105%) ac voltage and minimum (1,600 Vdc) dc voltage. As a result, there is excess VAR generation available at all other normal operating points. The power factor correction bank can be adjusted to control the net VAR flow into the ac line. Similarly, the LCI can draw VARs from the ac line by reducing the power factor correction below the level required by the converter. Thus, the LCI system can provide VAR generation control.

As with the SCI, the VAR generation capability of the LCI has limits on the combination of real power, dc voltage level, and ac line voltage level. These limits are described by the following:

- There must be real power flow into or out of the converter for it to consume VARs.

- If the converter has no real power loading, all or a portion of the power factor correction banks are available to feed VARs into the ac line.

- At low dc voltages, VAR consumption by the converter tends to be large (depending on the real power level) and the excess VAR generation available in the power factor correction banks becomes small. At high dc voltge, much more VAR generation is available from the power factor correction banks to feed into the ac line.

The VAR generating and consumption capabilities of the baseline 10 MW LCI are listed in Table A-1.

<u>Voltage Regulation Penalties For No Power Factor Correction.</u> Consider the previous example (see Figure A-3) of a transformer connected to the sub-transmission or transmission line. If no power factor correction is used, the LCI converter will draw 9.8 MVARs at 95% ac bus voltage of and 1,600 V_{dc}. This will produce a drop of:

$$\Delta V = -0.1 \times 9.8/25 = -.04 \text{ per unit}$$

Since the station bus was already at 95% of rated voltage, the added drop produced by not correcting the power factor will result in a station bus voltage of about 90%. This is unacceptable for steady state operation.

Table A-1

LCI REACTIVE POWER CAPABILITY

-10 MW SYSTEM-

Dc Voltage (volts)	Real Power (MW)	Reactive Power	
		Generation (MVAR)	Consumption (MVAR)
1600 (minimum)	0	11.2	0
	2.5	8.4	2.8
	5.0	5.6	5.6
	7.5	2.8	8.4
	10.0	0	11.2
2000	0	11.2	0
	2.5	9.5	1.7
	5.0	7.9	3.3
	7.5	6.2	5.0
	10.0	4.6	6.6
2400 (maximum)	0	11.2	0
	5	11.2	0
	10.0	11.2	0

Reactive Power Consumed $= P_{real} \times \tan [\cos^{-1} (V_{dc}/V_{dc\ max})]$

Reactive Power Generated $= 11.2 - P_{real} \times \tan [\cos^{-1} (V_{dc}/V_{dc\ max})]$

This can be corrected by using a ±10% load tap changer on the 25-MVA transformer, but this is costly. If the transformer already has a load tap changer, it most likely would be used to keep the station bus within the allowable range during load changes. If this is the case, the VAR loading added by the converter may cause the bus voltage to be below the allowable range.

The above considers only the effect of the 25-MVA transformer leakage drop. If the converter is the only one in the network, the drop in the sub-transmission and transmission networks will be negligible. However, if converter installations become 10% of the total generation, there will be additional voltage drops in these networks to add to the 25 MVA transformer drop. These drops require compensation by some means and this adds cost.

<u>Transformer Size Penalties For No Power Factor Correction</u>. If no power factor correction is used, the substation transformer size would have to be increased. Consider the converter's VAR loading on the 25 MVA transformer at 105% ac bus voltage and 1,600 Vdc. This is 11.2 MVAR. If the loading on the station bus is assumed to be at 0.85 PF, the capacity of this transformer available for the loads is

$$\text{Load VA} \cong 10 \text{ MVA @ load PF} = .85$$

That is, the transformer can supply only 40% (10 MVA/25 MVA = .40) of its rating to the substation loading. To supply the full 25 MVA from the station transformer to the loading, the transformer size would have to be increased to 35 MVA.

Total Penalties for No Power Factor Correction. The total cost penalty can
be calculated as follows for an installation of a 10 MW LCI converter in a
25 MVA substation, without using power factor correction in the converter.
Since a load tap changer increases transformer cost by a factor of about
1.5, the cost penalty for the transformer will be:

Cost Penalty = (35 MVA x 1.5)-25 MVA = 27.5 MVA = 27,500 kVA

That is, given the cost per kVA for a standard transformer, the incremental cost
will be roughly

Cost Increase = 27,500 kVA X cost/kVA

This does not include the costs of removing the 25 MVA unit and installing a
35 MVA unit with a load tap changer and assumes that the 25 MVA transformer
is fully usable elsewhere for the lifetime of a new transformer. If it is
already about 10 years old, the reduced lifetime available will add signifi-
cantly to the above incremental cost.

Other areas of cost increases are those caused by the increased losses in the
larger transformer and in the subtransmission system. Transformers in this
size range will have full load losses of about 0.8% of their rating. Thus,
there will be a transformer loss of about 280 kW with a 35 MVA unit versus a
loss of about 200 kW for a 25 MVA unit, an increase of 80 kW due to the in-
creased VAR loading caused by the converter. This is the worst case for the
LCI and is the same as reducing converter efficiency nearly 1%. At higher dc
voltages this penalty will decrease. On the average, the converter efficiency
due to this factor may be decreased by about 0.3% to 0.5%.

Again, the impact of a single installation on subtransmission and transmission losses may be insignificant, but the impact will become noticeable with 10% of the total generation in such installations.

To sum up, the penalties are:

- Substation transformer   Cost = 27,500 x cost/kVA
- Reduction in effective converter efficiency - 0.3% to 0.4% (Avg.)

Based on these penalties, there is little question that power factor correction will more than pay for its cost.

Voltage Resolution. Standard load tap-changing transformers often cover a ± 10% voltage range in 1.25% steps. These are very widely used in utility systems. Therefore, it can be assumed that this resolution is satisfactory for utility needs. If the LCI is in a substation supplied by a 25 MVA trans- former, the equivalent circuit is as shown in Figure A-6, in per unit on the 25 MVA base.
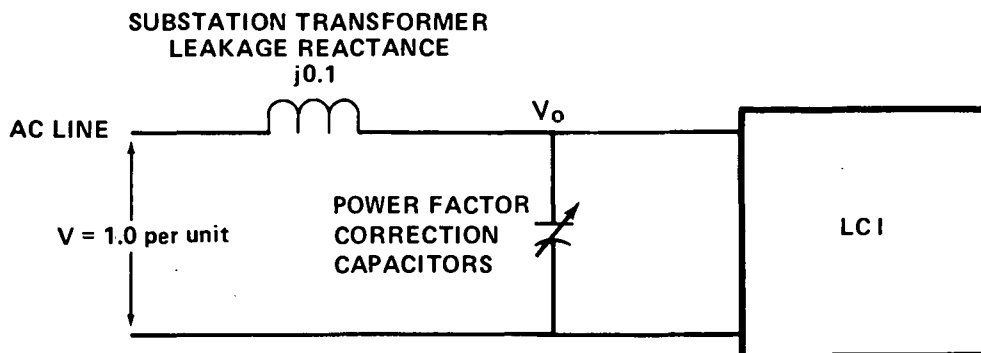
Figure A-6   Equivalent Circuit

The following analysis is used to calculate the value of power factor correction capacitor step size required to counteract a 1.25% change in the substation bus voltage. The effect of LCI power level and substation loading are neglected. This simplifying assumption results in a worst case analysis, since loading reduces the change in bus voltage for the calculated step size.

Using voltage division,

$$V_0 = - j \Delta X_c/j(.1 - \Delta X_c) = \Delta X_c/(\Delta X_c - .1)$$

Also,

$$\Delta V_0 = V_0 - 1 = .1/(\Delta X_c - .1)$$

Where ΔV_0 is a voltage rise. Then, for a 1.25% step,

$$.0125 = .1(\Delta X_c - .1)$$

whence

$$\Delta X_c = 8.1 \text{ per unit}$$

and the step of 1.25% is obtained when

$$\text{Capacitor bank step size} = 25/8.1 \sim 3 \text{ MVAR}$$

Steps of about 3 MVAR will be acceptable. Thus, 4 steps are used to cover the range from 0 to 11.2 MVAR in this case.

With static VAR generation equipment, operation is smooth and no steps are needed.

Response Time. With switched capacitors, the switches have a finite life in terms of the number of operations. Economy considerations dictate the use of a dead-band and/or time-delay to hold operation rates to suitably low levels. Controls for transformer tap-changers usually incorporate a dead-band of about 1% to reduce switching rates.

The response time during normal operation is of little concern; it can be seconds with no appreciable adverse effects on system operation. There have been cases where a part of the utility system voltage drops as a result of this capacitor limitation when an overload causes the line voltage to drop sharply. This has occurred in areas with heavy motor loading and relatively weak ties to the transmission system. As line voltage sags, motor VAR demand increases but the VARs supplied by the capacitors decreases. The VAR shortage causes the line voltage to drop even farther. To alleviate this effect, it is desirable to increase capacitor VAR generation fairly rapidly in such situations. If the LCI is in operating near full rated power, it can be quickly slewed down to zero real power (and zero VAR consumption), thus reducing the total VAR demand. This can be backed up by switching in more power factor correction capacitors, if they are not already in use. This should be accomplished within a few tenths of a second to be most effective.

With static VAR generators, the LCI power level can be changed as rapidly as above, and excess capacitance can be brought on line very rapidly by reducing the reactive spoiler current. Thus, all the available VAR generation capacity can be brought on line very quickly.

Switching Transients. Every time a capacitor is switched onto the line, an inrush transient takes place. If there are no other capacitors on line, the voltage transient peak will be nearly double the peak of the ac voltage wave and high frequency ringing will be present. It is evident that such disturbances can cause commutation failure in the LCI. However, this effect is mitigated by the following factors:

- Many substations already contain switched capacitors, some of which are usually on line.

- In the great majority of the cases, other power factor correction capacitors will already be on line.

- The LCI gating control can be designed such that the unit will ride through most commutation failures without distress.

- If other capacitors are on line, the switching voltage transient is greatly reduced. If one 3 MVAR bank is switched on line with only 3 MVAR already on line, the transient is reduced by about 50%. If considerably more than 3 MVAR of capacitors are already on line, the voltage transient is negligible.

- If the LCI is located in a substation that already has switched capacitors, the LCI will be subjected to switching transients no matter how the LCI power factor correction is effected.

The use of static VAR generators with inductive spoilers for continously variable power factor correction will eliminate the effects of switching transients originating in the LCI power factor correction capacitor. However, as seen above, the presence of such transients is not very troublesome, and the use of static VAR generators will not eliminate switching transients in substations that already contain switched capacitors.

On balance, the use of static VAR generators can be expected to reduce LCI commutation failure rates somewhat but certainly will not eliminate them in

all substation locations. With all else equal, the static VAR generator does offer some advantages over switched capacitors in this area.

Resonance Problems. Consider the case used in the preceding discussion where a 25 MVA transformer feeds the station bus in parallel with the LCI. The equivalent circuit for harmonics is shown in Figure A-7.

$X_L = j\,0.1n$ I_n $X_c = -j\,2.23/n$
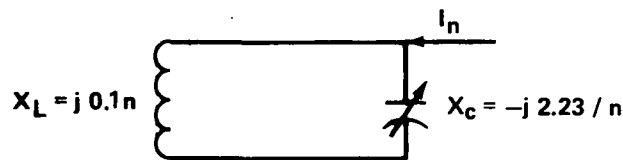
Figure A-7 Harmonic Equivalent Circuit

In this figure, I_n is a current harmonic produced by the LCI bridge. This tank circuit will resonate at

$$f = 1/(.223K)^{1/2} \text{ per unit}$$

where K is the percentage of 11.2 MVAR connected, so that

$$f = 2.12/K^{1/2}$$

is the resonant frequency.

If f coincides with the frequency of I_n, the circuit will build up the harmonic voltage seen at the station bus. It is evident that this resonant frequency can coincide with the frequency of any of the harmonic currents present in the bridge.

Thus, the filter must be designed so that its impedance to these harmomics is low enough to prevent harmonic voltages from building up beyond specifications in spite of these resonances. This is simply a factor that has to be considered in filter design.

The use of a static VAR generator would offer an advantage in that K = 1 for all normal operating conditions. This will reduce filter design problems and result in a smaller filter. However, in substations that already have switched capacitors, K will usually not be 1.0 since other capacitors are on line and must be accounted for in filter design.

Equipment. Power factor corection can be implemented by two types of equipment, banks of switched capacitors and static VAR generators (SVG).

Switched capacitor banks can be built with standard utility components. Where no other capacitors are in the substation, the switching control would sense total VARs out of the LCI and switch appropriately to reduce the VAR imbalance to less than ± 1.5 MVAR (for 3 MVAR steps, see page A-26). Where other substation capacitors are present, the control should be integrated with the station controls to obtain the most efficient use of all the capacitors. Capacitors will be individually fused and the whole bank will be protected by the LCI main breaker. With this arrangement, a shorted capacitor will clear its own fuse and be isolated without much disturbance to the system.

The SVG is very nearly another inverter with sufficient capacity to handle 11.2 MVA at 105% ac voltage. The SVG tends to be less expensive if long strings of SCRs in its inverter bridge valve positions to permit operation at a 13.8 kV line voltage rather than to use a lower-voltage bridge and a

transformer. This is because the current level is much lower than in the
LCI bridge and the SCRs can be smaller, thereby reducing the cost penalty
for the longer strings. In all, the SVG should be considerably less expensive
than the inverter and main transformer. SVG equipment is presently available
from several major manufacturers.

A.4.3 VAR Generation and Consumption Comparison

Figures A-8 and A-9 show the VAR generation and consumption capabilities of
the two conversion systems as functions of the real power level and the dc
voltage. The LCI system includes power factor correction capacitor as shown
in Figure A-1.

A.5 IMMUNITY TO AC SYSTEM DISTURBANCES

Typical ac systems can have many disturbances, some of which are quite severe.
The converter must either be able to ride through these disturbances or
automatically take whatever action is required to maintain its integrity.
In some areas (such as lightning surges) it is not economic to design for
the worst possible condition. Designs should be based on acceptable utility
practice with regard to outage rates and maintenance costs.

There is one fundamental difference between the LCI and SCI. The SCRs in the
SCI are directly exposed to ac line voltage disturbances (reflected through
the transformer) and they must have sufficient voltage withstand capability to
handle all but the most extreme voltage surges on the ac line. The rule-of-
thumb often used for LCI design is that the SCR strings must be able to with-
stand 2.5 times the peak line-to-line bridge output voltage at rated conditions.
Experience has shown this to be a means of obtaining low outage rates and
low maintenance costs in systems with properly applied lightning arresters
and transient voltage suppressors.
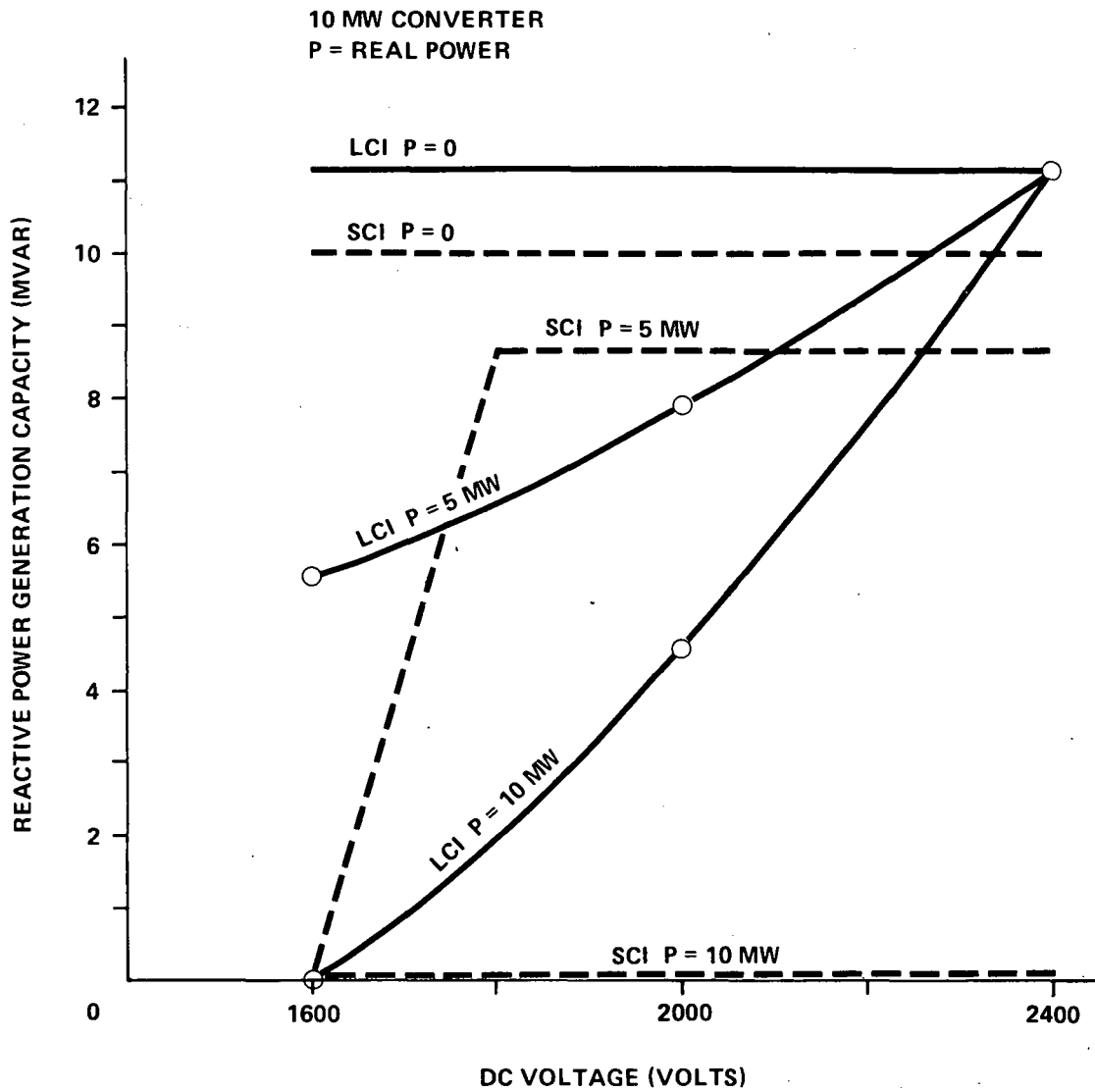
Figure A-8 VAR Generation Capability
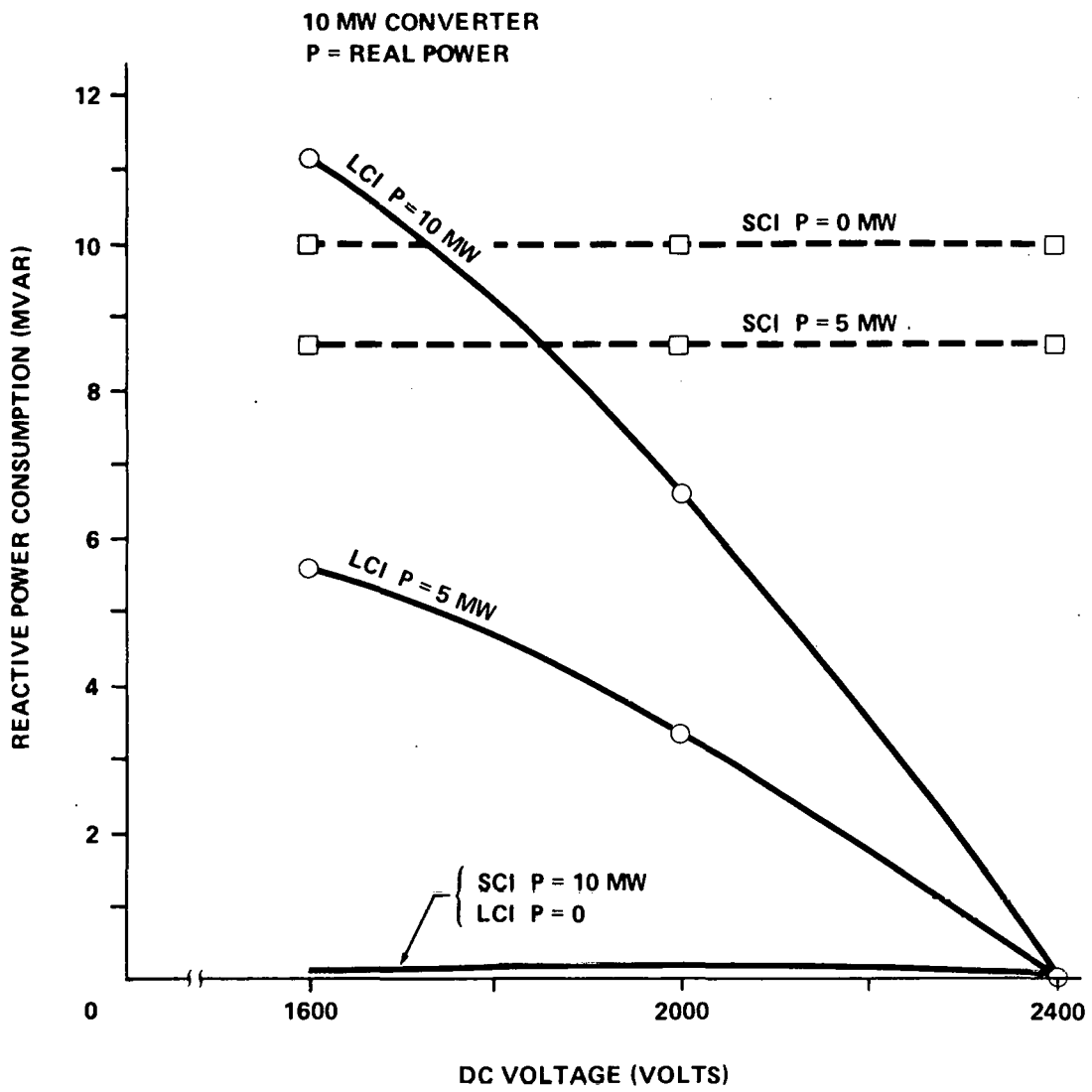
Figure A-9 VAR Consumption Capability

In the SCI, the SCR voltage level is fixed by that of the dc source. Voltage sources on the ac line cause current surges in the bridges. Since most dc sources are exposed to far fewer major disturances than the ac line, the SCRs in the SCI very rarely see voltages greater than normal. However, the SCI still must be designed to survive and accommodate the current surges driven by ac line voltage surges (Ref A-6).

With proper design, both types of converter are capable of operating with acceptable outage rates due to ac line voltage surges. The SCI has an advantage in that failure to commutate a large current surge (resulting from an extremely large line voltage surge) causes shoot-through in one or more poles. In nearly all cases, this is cleared by a fuse with no further damage. In the LCI, such an unusual surge will fail SCRs due to overvoltage. Thus, with the same outage rates from this cause, the SCI maintenance cost will be less because fuses are easier and less expensive to replace than SCR/heatsink assemblies.

The actions taken by each system during and after major ac system disturbances are tabulated in Table A-2. It is seen that with good design, either system can accommodate and survive ac system disturbances. The SCI has some advantage in voltage surges as discussed in the foregoing. This advantage is not decisive and can be removed by using more SCRs in the LCI strings, but with penalties in cost and efficiency (Ref. A-7).

A.6   CONTRIBUTIONS TO AC SYSTEM FAULTS

One of the major advantages of generating systems that include converters is the fact that it is possible to add generation without increasing distribution system fault currents appreciably.

Table A-2

PCU ACTIONS DUE TO AC SYSTEM DISTURBANCE

AC Line Disturbance	LCI Actions	SCI Actions
Short Circuits	Commutation failure; high speed interrupter operates and the bridges are shut down.	Line undervoltage causes bridges to commutate off within 280 microseconds and the bridges are shut down.
	Can restart when line voltages return to normal range.	Can restart when line voltages return to normal range.
Lightning Surges	None unless commutation failure takes place. Control can be designed to enable LCI to ride through most such commutation failures if the bridges can handle the very large dV/dt without false gating.	If the surge is large, line overvoltage will cause the system to take the action shown above.
	The commutation failure ensures the high speed interrupter will act to shut the bridges down and restart can take place when line voltages return to normal range.	
Large Line Voltage Unbalance	Commutation failure; high speed interrupter operates and shuts bridges down.	Within limits unbalance override will reduce P and Q to keep bridg currents within normal ranges. If unbalance is large enough, same actions as with line short circuits above.
	Can restart when voltage is within normal levels.	At first, will ride through at reduced output until unbalance returns to normal levels.
Line Overvoltage (60 Hz)	Will stay on line up to 110% (typical design set point) and shut bridges down for larger overvoltages.	Will stay on line up to 110% (typical design set point) and shut bridges down on larger overvoltages.
Line Undervoltage (60 Hz)	If large, commutation failure and some actions as with line short circuits above.	Will stay on line down to 80% (typical design set point) at reduced P and Q. Below 80%, same action as for line short circuits as above.
Line Frequency Deviations	Can follow reasonable deviations. Protection can be set to shut down below 57 Hz or above 61 Hz.	As with the LCI.
	Can be restarted when frequency returns to normal range.	
Switching Surges	As with lightning surges above.	As with lightning surges above. More tolerant than the LCI for there are fewer bridge shutdowns.

A-35

A.6.1 LCI Systems

Fault contributions by LCI systems will depend on the type of high-speed interrupter used. With the static type, the fault current contribution will be reduced from its maximum value to zero in less than 1 cycle. Conventional breakers do not begin opening in less than 1 cycle. Therefore, it can be argued that the converter makes no contribution to system fault currents. Since the contribution disappears before the breaker begins arcing, it has added nothing to the breaker "duty".

A.6.2 SCI Systems

The SCI is also commutated-off by its internal circuitry, and the preceding remarks on the LCI apply to this system as well, except that the SCI contribution to system faults is reduced to zero in considerably less time. However, this is of little consequence since the contribution of both systems is zero in a practical sense.

A.7 STAND ALONE OPERATION

A.7.1 LCI Capabilities

Theoretically, the LCI can operate without being paralleled to an ac voltage source. However, this is difficult to accomplish in practice due to the very large quantity of VARs that must be supplied to support the system ac voltage.

A.7.2   SCI Capabilities

With very little modification the SCI system can be used as an isolated gener-
rator. In fact, the SCI can be designed to operate both in parallel with a
line and in isolated operation at virtually no cost penalty. Since it
provides its own commutation energy, there is no startup problem and limited
fault current is available. However, this fault current limit (set by the
commutation capabilities of the converter) imposes a limit on the size of
circuit breakers that can be operated by the converter. Because of this, the
largest individual circuit connected to an isolated 10 MW SCI should not be
more than 3 to 4 MVA. The total of all connected circuits may, of course, be
10 MW. Fault current capability can be increased by increasing commutation
capability, but this may increase cost and decrease efficiency.

A.7.3   Summary

The SCI is superior to LCI for stand-alone operation. LCI type bridges can
be designed to have stand-alone capability but this may cause operational
difficulty and it incurs a higher capital cost.

A.8   OPERATION OF PARALLELED UNITS

It is anticipated that in large systems such as photovoltaic central stations
the power level is some multiple of 10 MW and consideration should be given
to any special problems attendant to such installations. It is assumed herein

that each 10 MW unit will have its own dc source (i.e., array subfield), main transformer, controls, protection, and switchgear.

A.8.1   Control Stability

In any system, that has more than one control system on paralleled units, there is a possibility of instability in the controls. This is more likely with installations where the coupling to the utility system is weak. Since there has been little operating experience with such installations, it is recommended that computer simulations be used to evaluate control stability in parallel operation before the system design is finalized. It is easier and less expensive to study and modify the controls before the installation is completed than to accomplish this on site.

A.8.2   Harmonic Interaction

LCI. LCI converter bridges generate harmonic currents. For each harmonic, the currents generated by LCI converters paralleled on the ac side are in phase with one another. Thus, there are no appreciable harmonic currents circulating between the paralleled converter units. The harmonic currents, attenuated by filters, are injected into the ac lines. However, obtaining load division between separate, tuned filters can be difficult. Studies are needed to determine whether such filters can be paralleled successfully with reasonable levels of component tolerances or whether it is necessary to incorporate a single filter for entire plant. If a single filter is used for several PCUs in parallel, it may be necessary to install more power factor correction capacity than needed with filters on each PCU.

<u>SCI</u>. With the SCI, harmonic voltages are generated by the inverter bridges. Since these harmonics differ in phase and magnitude in each module, the possibility of circulating harmonic currents is certainly present. With the 0.22 per unit series reactor typically used on the ac side of such SCI units, a minimum of (2 x 0.22 x n) per unit reactance is available to limit these circulating currents, where n is the harmonic number. At high harmonic numbers, this impedance becomes large. For example, at the 17th harmonic, it becomes

$$X_{17} = 17 \times 2 \times 0.22 = 6.4 \text{ per unit.}$$

At lower harmonic numbers, the impedance is, of course, smaller. Lower harmonic generation is reduced to small values by voltage waveform modulation control, but it may be necessary to restrict lower harmonic generation even further to hold this spectrum of circulating currents to acceptably small values.

In the few installations where high-pass filters are required, such filters can be paralleled easily since they are typically low-Q filters with large band-pass characteristics.

<u>Summary</u>. Paralleling either SCI or LCI systems is possible but may require limited modifications of the control and filter designs. In both cases, computer studies of the possible problems should be carried out before control and filter designs are finalized. There is less site-specific engineering required for SCI systems since filters do not have to be considered. Large UPS systems are usually installed with several modular units connected in parallel.

A.9   EFFECTS OF DC SIDE FAULTS ON THE AC SYSTEM

A.9.1   LCI Systems

Shorted SCR String.   If one SCR in a string becomes shorted, the string's overvoltage margin is reduced by the rating of one device.   Since appreciable design margins are usually used, operation may continue for a long period. When a large enough ac voltage surge occurs, the entire string cascades into shorted SCRs due to overvoltage.

When an entire string does short out, it is the same as an arc-back in a mercury valve except that an arc-back can be cleared and the valve can resume normal operation.   With a shorted SCR string, the ac system will see a bolted line-to-line fault on the low side which will continue until the ac breaker for the module clears the fault.   The dc-side current will be commutated off by the high-speed interrupter.   A shorted SCR string must be replaced before normal operation can resume.

Dc Short Circuit at the Bridge Input.   During operation as an inverter, the bridges will commutate-off and open the ac-side.   Hence, the ac system will see a small disturbance which disappears very quickly.   The dc current will be commutated-off by the high speed interrupter and is backed up by the dc source fault protection.

In rectifier operation, the control system will sense the fault and phase back the gates to produce zero dc voltage and the dc source protection will clear the dc-side.   The ac system will see a momentary low-side fault which will disappear well before the ac breaker operates.

Dc Short Circuit at the Dc Source End of the Dc Inductor. During operation
as an inverter, the ac system will see a decaying set of ac curents (starting
at the prefault currrent level) until the energy stored in the dc inductor
is pumped into the ac system. At this time, ac side conduction ceases and
the dc-side fault is removed by dc source fault protection.

In rectifier operation, the ac current rises slowly due to the large dc
inductor. As the gate control senses this condition, the SCRs are phased
back to produce zero dc voltage. At this time, conduction on the ac side
ceases. The source protection then clears the dc side.

A.9.2 SCI Systems

Shorted SCR String. If one SCR in a string fails, operation can continue
until the dc voltage rises above the level that the remaining SCR's can
withstand. At this time, the remaining SCRs cascade into a shorted string.
When the string fails, a shoot-through (short across the dc bus through the
SCRs) ensues very quickly and is cleared by the fuse in each powerpole.
This occurs within a few hundred microseconds and, in turn, causes the gating
controls to commutate off all the other powerpoles. The ac breaker is opened.
A final level of protection is provided by the current-limiting interrupter
which clears on the dc side as a backup for commutating the bridges off. The
ac system will see a transient of a few hundred microseconds duration followed
by rapidly decaying currents until the series reactors have pumped their
stored energy into the ac line and dc source.

Dc Filter Capacitor Short Circuit. Each capacitor can is protected by its
own fuse. Since there are multiple cans in parallel, the defective can will
clear its fuse with only slight disturbance to the dc bus voltage or the ac

system; operation will continue in most cases, since there are redundant filter capacitor cans provided in the system. This is expected to be the most frequent source of dc bus faults.

Other Dc Bus Faults. The diodes in the bridges may feed a fault from the ac side until the ac breaker opens. With the series reactors of 0.22 per unit each, the fault current will not exceed about 4.5 times the rated current of the high side of the main transformer. This will be about 420 amperes total fault current on the 13.8 kV side.

Summary. For both the LCI and SCI converters, sufficient ac and dc protection are provided to ensure that the connected ac system is not adversely affected by dc-side faults. For most of the severe dc fault conditions, the ac breaker will ultimately open and disconnect the converter from the line.

A.10   INSTALLATION COSTS

A.10.1   Estimate Basis

The PCU subsystem is part of a photovoltaic power system, such as described by Figure 1-1 (page 1-4). Certain items possibly associated with the PCU are normally included in other cost code-of-accounts. The following items are excluded from the PCU cost-to-install estimate:

- General site preparation
- Fences
- Area lighting
- Security systems
- Fire protection

- Dc, ac and plant instrumentation/control wiring subsystems and grounding subsystem. These subsystems are considered to exist with their wiring termininating at the PCU. The cost of terminating is considered to be associated with each of the individual subsystems.

- The portion of overall plant design related to the PCU

- Contingency (normally 20 percent)

- The FOB selling price of the PCU itself

- Rework or engineering, should the equipment not perform satisfactorily

The estimate does include the costs of the following:

- Shipping (by truck for a distance of 1000 miles)

- Equipment foundations and mounting pads

- Installation and mounting of PCU equipment (identified in Section A.10.2)

- Electrical connections

- Checkout and testing

- Site-specific engineering

The PCU site is assumed to have been graded as part of the grading operation for the total plant. Civil work included in the PCU installation includes the following, as appropriate for the size and weight of each component:

- Foundation excavation and backfill

- Formwork

- Reinforcing steel

- Embedments

- Concrete

- Gravel

- Asphalt paving

A minimum 4-foot separation is provided between all major PCU components. This area is paved with 6-inch-thick subbase and 2-inch-thick asphalt. Installation includes off-loading of components by means of a rented crane and standard lifting cables, chains and hooks. Components are lifted into place and bolted to their foundations.

In addition to the components listed in the Bill of Materials for each type of PCU, an auxiliary power transformer and uninterruptable power supply (UPS) are required. These items are identified separately because in some instances they may be incorporated into other plant subsystems. In particular, they may be incorporated into a tracking drive power supply system in plants using concentrator arrays. For plants using flat plate arrays, the items would be furnished with the PCU installation. Their costs are not included in the PCU selling price but are included with the installation costs.

Electrical connections are made per the specifications for each type of PCU and its components.

Checkout and testing include visual inspections, point-to-point continuity tests of electrical connections, operational tests of circuit breakers and switches, and operational testing at full voltage and power.

Engineering services include specifying harmonic filter and power factor correction requirements, and determining ac system impedance at the fundamental as well as at harmonic frequencies. Engineering also includes development of site layout, specification of equipment foundations and similar functions.

A-44

Determining the optimum PCU size, ac and dc voltage levels and similar items are considered to be part of overall plant engineering and are not included with the cost to install the PCU.

The costs presented in this Appendix were estimated at third quarter 1981 levels and converted to 1980 dollars by dividing by a factor of 1.12. Costs were also rounded off to the nearest $100.

Field labor is estimated at a rate of $28.8/hr (1980$) which includes indirects at 60% of direct labor. Engineering was estimated at $45/hr including burden.

The cost estimate for the total plant would also include a contingency of 15 to 25 percent, depending on the level of design completeness and overall engineering to cover design of the plant. This is not included in the present estimates.

The estimated costs to install LCI and SCI units were developed for single unit installations. These costs are presented in Sections A.10.2 and A.10.3. The estimate for a 150 MW installation, a comparison of the two PCU types and additional factors are presented in Section A.10.4.

A.10.2   LCI System

The 10 MW LCI system is as described in Section A.2.1 and meets the specifications presented in Section A.1. This system and its installation are further described by the Bill of Materials and layout drawing, as follows:

Bill of Materials. The LCI system is made up of the following major items:

ITEM	SIZE (LxWxH in feet)	WEIGHT(lbs.)
DC Switch/Protecton	6 x 6 x 10	7,500
DC Inductor	8 x 10 x 6	5,000
High Speed Interrupter	6 x 6 x 10	6,000
Bridge Pallet	25 x 10 x 10	32,000
Main Transformer	14 x 14 x 14	120,000
Power Factor Correction	23 x 4 x 10	15,000
Harmonic Filter	20 x 6 x 12	23,000
AC Breaker	6 x 6 x 8	8,000
		216,500 ∿ 108 tons

For the LCI system, the auxiliary transformer loads total 90 kVA and include:

● DC switch motor

● DC inductor cooling fans

● High-speed interrupter logic controls and fans

● Bridge module logic, controls, heat, lighting, fans and outlets

● Main transformer fans

● AC breaker motor

● Power factor correction switch motors and controls

Included in the above are UPS loads totaling 7 kVA. A 15-minute battery storage capability is included in the UPS.

Layout. The physical layout of the LCI system and its components is shown in Figure A-10.

Cost Estimate. The estimated cost to install the LCI system is presented in Table A-3.
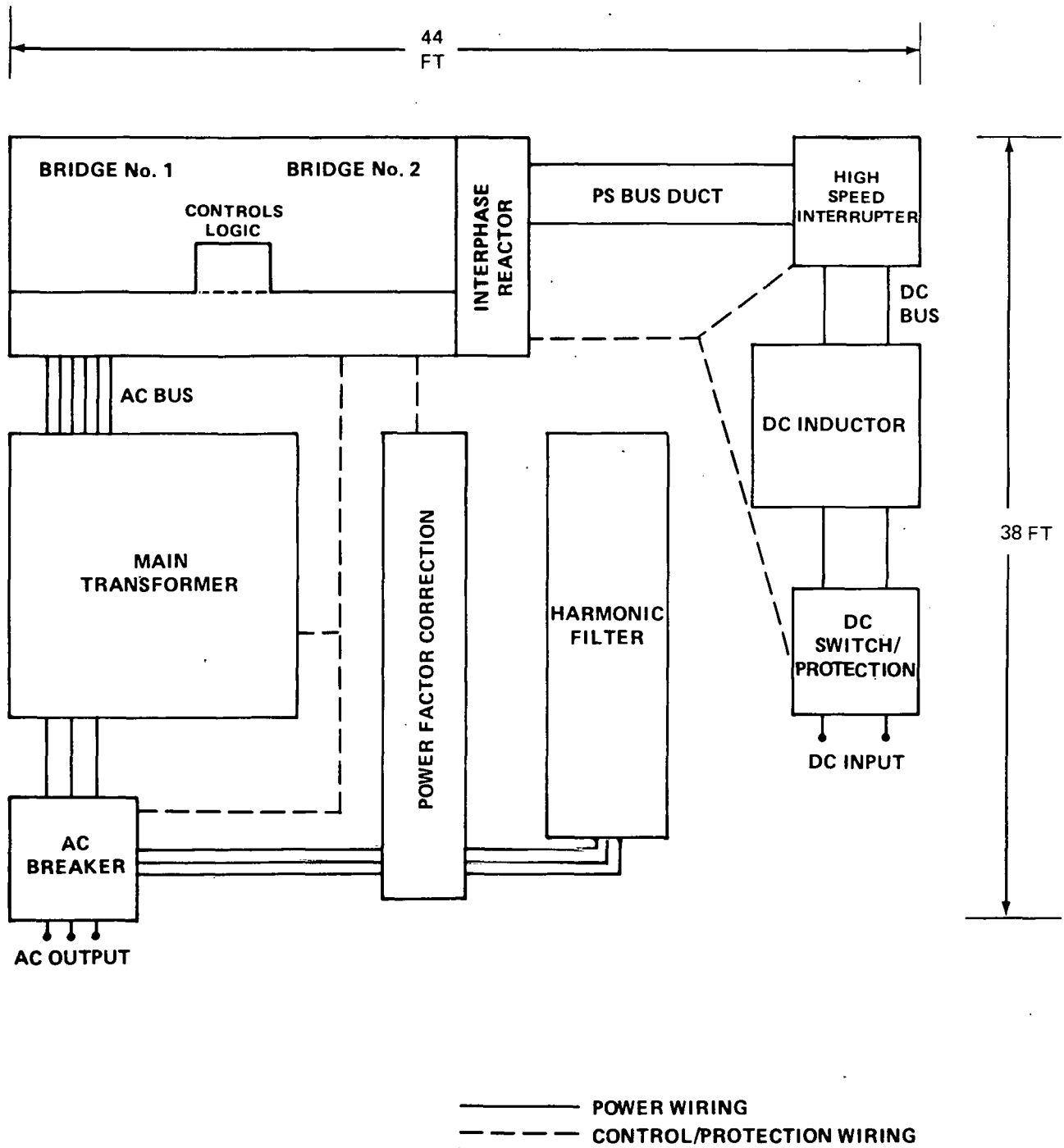
Figure A-10 LCI Equipment Layout

INSTALLATION COSTS - LCI

| ITEM | MANHOURS | COSTS (1980$) | | | | % Of |
		LABOR	MATERIALS	SUBTOTAL	$/W	TOTAL
Civil Work	520	15,000	12,100	27,100	.0027	14
Shipping	-	-	9,600	9,600	.0010	5
Equipment Install.	2120	61,100	2,700	63,800	.0064	33
Busways	100	2,900	500	3,400	.0003	2
Conduit & power wiring	600	17,300	5,400	22,700	.0023	11
Instrumentation wiring	80	2,300	400	2,700	.0003	1
Auxiliary power transformer	250	7,200	7,600	14,800	.0015	8
UPS	50	1,400	17,900	19,300	.0019	9
Checkout & testing	640	18,400	-	18,400	.0018	9
Engineering	360	16,200	-	16,200	.0016	8
Total		141,800	52,600	198,000	.0198	100

A.10.3 SCI System

The 10 MW SCI system is as described in Section A.2.2 and meets the specifications presented in Section A.1. This system and its installation are further described by the Bill of Materials and layout drawing as follows:

Bill of Materials.   The SCI system is made up of the following major items:

ITEM	SIZE (LxWxH in feet)	WEIGHT (lbs.)
DC Switch/Protection	6 x 6 x 10	7,500
Bridge Pallet	25 x 10 x 10	57,300
Main Transformer	12 x 10 x 14	88,000
AC Breaker	6 x 6 x 8	8,000
		160,800 ～ 80 tons

For the SCI system, the auxiliary transformer loads total 75 kVA and include:

- DC switch motor

- Bridge module logic, controls, heat, lighting, fans and outlets

- Main transformer fans

- AC breaker motor

Included in the above are UPS loads totaling 5 kVA. A 15-minute battery storage capability is included in the UPS.

Layout.   The physical layout of the SCI system and its components is shown in Figure A-11.

Cost Estimate.   The estimated cost to install the SCI system in presented in Table A-4.
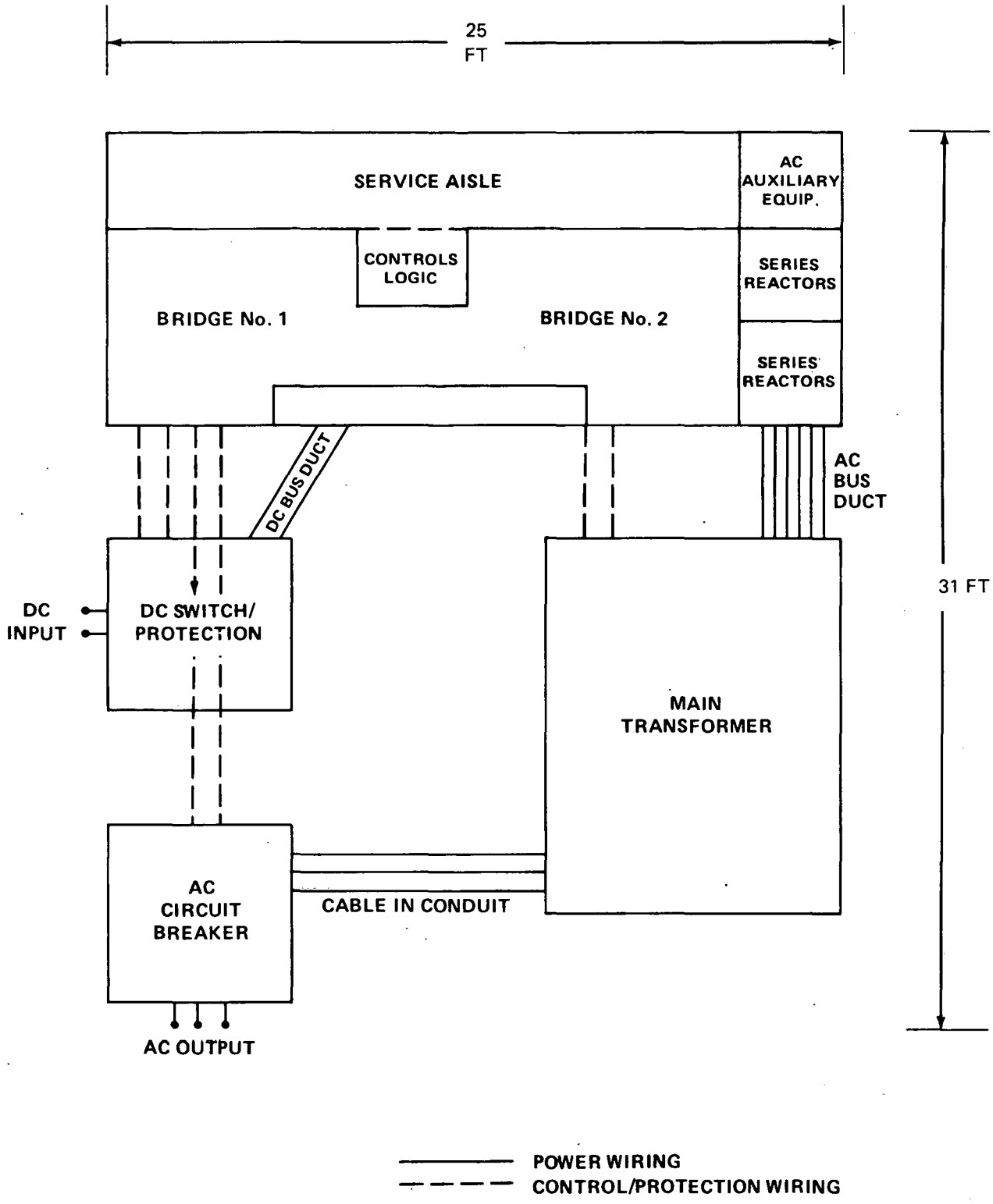
Figure A-11 SCI Equipment Layout

TABLE A-4

INSTALLATION COSTS - SCI

| ITEM | MANHOURS | COSTS (1980$) | | | | % Of TOTAL |
		LABOR	MATERIALS	SUBTOTAL	$/W	
Civil Work	280	8,100	3,800	11,900	.0012	10
Shipping	-	-	7,100	7,100	.0007	6
Equipment Install.	1300	37,400	1,800	39,200	.0039	32
Busways	90	2,600	400	3,000	.0003	2
Conduit & power wiring	150	4,300	800	5,100	.0005	4
Instrumentation wiring	70	2,000	400	2,400	.0002	2
Auxiliary power transformer	170	4,900	6,400	11,300	.0011	9
UPS	50	1,400	15,800	17,200	.0017	14
Checkout & testing	360	10,400	-	10,400	.0011	9
Engineering	320	14,400	-	14,400	.0014	12
Total		85,500	36,500	122,000	.0122	100

A.10.4 150 MW Installation

As mentioned, the costs presented in Table A-3 and A-4 were derived for installation of a single 10 MW unit._ For a 15 unit installation at a 150 MW photovoltaic control station, the previously presented specific costs ($/w) would be reduced. It is estimated that a learning curve would reduce labor costs costs by 10 percent. An exception is engineering which need only be performed once for all of the units. It is also estimated that volume purchase of

bulk materials would reduce their costs by 10 percent. Exceptions are shipping and the UPS. Although contracts at reduced cost might be negotiated, it is estimated that the shipping cost will remain essentially unchanged. For the UPS, an order of 15 units is expected to result in a reduction in specific cost of about 20 percent. The effects of these factors is shown in Table A-5 which also compares the cost categories for installation of LCI and SCI units.

TABLE A-5

INSTALLATION COSTS AT 150 MW

| ITEM | COST (1980 $/WP) | |
	LCI	SCI
Civil Work	.0024	.0011
Shipping	.0010	.0007
Equipment Install.	.0057	.0035
Busways	.0003	.0003
Conduit & power wiring	.0020	.0005
Instrumentation wiring	.0002	.0002
Auxiliary power transformer	.0013	.0010
UPS	.0016	.0014
Checkout & testing	.0017	.0009
Engineering	.0001	.0001
Total	.0163	.0097

As can be seen, the estimated cost to install the LCI unit is higher than the cost to install the SCI unit. This is because more separate and modular components, such as harmonic filter and power factor correction equipment, are used in LCI. It is possible that further design efforts might enable packaging of filter and power factor correction equipment onto a single pallet. This would reduce the LCI installation cost by reducing the number of field electrical connections, the number of separate components to be installed and the area occupied. This would in turn shorten the lengths of wire runs and reduce the amount of civil work. Unless the basic design was changed, the auxiliary power requirements and shipping weight would remain the same. The effect of shipping distance on shipping cost is shown in Figure A-12.
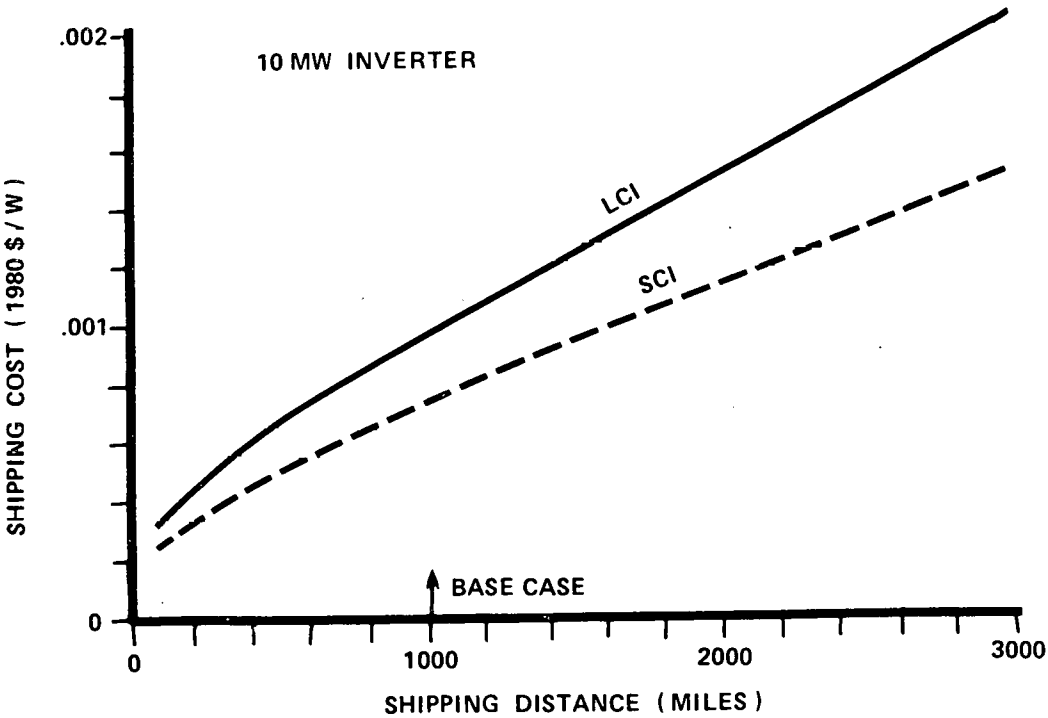
Figure A-12 Shipping Costs

A.11   CONCLUSIONS

The following major conclusions are derived from the work presented in this appendix:

- If utility line charging of onsite energy storage is required, both the LCI and SCI units can be designed for bidirectional operation. However, the LCI system requires a dc polarity reversing switch.

- Similarly, both types of PCU can be designed to have acceptable performance in the areas of reactive power, immunity to ac system disturbances, contribution to ac system faults, operation of parallel modules, and dc side faults. Several if not all of these areas require specific site characteristics to be defined before final design of the PCU.

- The SCI is superior for stand alone operation.

- The installation cost for the LCI is 50 percent higher than for SCI. Further design effort may reduce this cost difference.

Additional conclusions drawn by considering this appendix in conjunction with the main text are as follows:

- The estimated costs to insall the PCU are significant when compared to its purchase price.

- Although not addressed specifically, it is expected that the cost to install (in terms of $/W) will tend to increase with decreasing PCU power level. This is because the major cost driver, labor for installation and checkout, will generally involve handling,

connecting, and testing the same number of (smaller-sized) components for lower power PCUs. Combining this conclusion with estimated PCU price characteristics increases the bias toward high power systems for the lowest specific costs.

● In general, the results of evaluating the operational characteristics of the PCUs does not alter the results of the study presented in the main text.

REFERENCES

A-1 United Technologies, <u>AC/DC Power Converter for Batteries And Fuel Cells</u>, annual report EM-1286 prepared for the Electric Power Research Institute under contract RP 841-1, December, 1979.

A-2 "IEEE Guide for Harmonic Control and Reactive Compensation of Static Power Converters," IEEE Standard 519-1979

A-3 United Technologies, <u>Evaluation of Battery Converters Based on 4.8 MW Fuel Cell Demonstrator Inverter</u>, final report prepared for DOE under contract No. EX-76-C-01-2122

A-4 United Technologies, <u>Advanced Technology Fuel Cell Program</u>, final report EM-335 prepared for the Electric Power Research Institute under contract RP 114, October 1976

A-5 United Technologies, <u>Program to Develop Advanced Converter Technology for Battery Applications</u>, annual report prepared for DOE under contract No. De-AC-01-79 ET 29079, May 22, 1980

A-6 Power Semiconductors, Inc., <u>Thyristor Voltage Safety Factor</u>, final report EM-825 prepared for the Electric Power Research Institute under contract RP 840, July 1978

A-7 G.A. Phillips, J.W. Walton and F.J. Kornburst, Progress in Self-Commutated Invertors for Fuel Cells and Batteries", <u>IEEE Transactions on Power Apparatus and Systems</u>, Vol. PAS-98, No. 4, July/August 1979, pp. 1466-1475

DISTRIBUTION:

TID-4500-R66, UC-63a (224)

L. A. Barrett (25)
Department of Energy
Division of Photovoltaic Energy Systems
Forrestal Bldg.
1000 Independence Ave. SW
Washington, DC 20585
Attn: M. B. Prince
      V. Rice
      A. Krantz

Department of Energy
Division of Active Heating and Cooling
Office of Solar Applications for Bldgs.
Washington, DC 20585
Attn: Robert D. Jordon, Director

Department of Energy
Division of Passive and Hybrid
Office of Solar Applications
Washington, DC 20585
Attn: Michael D. Maybaum, Director

Jet Propulsion Laboratory (15)
4800 Oak Grove Drive
Pasadena, CA 91103
Attn: R. V. Powell (4)
      R. Ferber
      K. Volkmer
      W. Callaghan
      R. Ross
      R. S. Sugimura
      R. Weaver
      S. Krauthamer
      A. Lawson

Jet Propulsion Laboratory
Solar Data Center
MS 502-414
4800 Oak Grove Drive
Pasadena, CA 91103

R. Tabors (2)
MIT-Energy Laboratory
E40.172
Cambridge, MA 02139

Solar Energy Research Institute (6)
1536 Cole Boulevard
Golden, CO 80401
Attn: D. Feucht
      S. Sillman
      T. Basso
      M. DeAngelis
      G. Nuss
      R. DeBlasio

SERI, Library (2)
1536 Cole Boulevard, Bldg. #4
Golden, CO 80401

SERI
Mail Stop 15-3
1617 Cole Blvd.
Golden, CO 80401

NASA Lewis Research Center
21000 Brookpark Laboratory
Cleveland, OH 44135

Florida Solar Energy Center
300 State Road 401
Cape Canaveral, FL 32920.
Attn: S. Chandra

EPRI (3)
P.O. Box 10412
Palo Alto, CA 94303
Attn: Frank Goodman
      Edgar Demeo
      Roger Taylor

House Science and Technology Committee
Room 374-B
Rayburn Building
Washington, DC 20515
Attn: Don Teague

MIT-Lincoln Laboratory (6)
P.O. Box 73
Lexington, MA 02173
Attn: M. Pope
      M. Russell (2)
      E. Kern (3)

Office of Technology Assessment
U.S. Congress
Washington, DC 20510

New Mexico Solar Energy Inst. (25)
New Mexico State University
Box 3SOL
Las Cruces, NM 88003
Attn: John Schaeffer

Sandia National Laboratories:
2525   D. L. Caskey
2525   R. P. Clark
3141   L. J. Erickson (5)
4700   E. C. Beckner
4720   D. G. Schueler
4721   W. P. Schimmel
4723   D. Chu
4723   J. L. Jackson
4723   G. J. Jones (100)
4723   T. S. Key
4723   H. N. Post
4724   L. C. Beavis
4724   E. C. Boes
4724   A. B. Maish
4723   M. Rios
4724   C. B. Stillwell
4724   M. W. Edenburn
4726   H. H. Baxter, Jr.
4726   K. L. Biringer
4726   E. L. Burgess
4726   C. B. Rogers

3151   W. L. Garner (3)
3154-3 C. H. Dalin (25)
        For DOE/TIC (Unlimited Release)
8214   M. A. Pound

A. D. Little, Inc.
Attn: C. E. Maytum
Acorn Park
Cambridge, MA 02140

A.A. Serregamo Architects
Attn: Anthony Serregamo Architects
P.O. Box 332
East Sandwich, MA 02537

Aerospace Corporation (2)
Attn: S. Leonard
Attn: B. Siegel
P.O. Box 902957
Los Angeles, CA 90009

AIA Research Corporation
Attn: Joel H. Vicars, III
1735 New York Avenue, NW
Washington, DC 20006

Alan McGree
P.O. Box 2004
Austin, TX 78768

Alexander Associates Architects
Attn: Fred Alexander
8200 E. Pacific Place #204
Denver, CO 80231

Anderson Architects
Attn: Alan Gass, AIA
1522 Blake St.
Denver, CO 80202

Anderzhon/Diehl + Associates
Attn: James D. Castner, AIA
120 W. Golf Road
Schaumburg, IL 60195

Angelo Vitiello Nilya Ryan Inc.
Attn: Ralph E. Vitiello, AIA
1915 I Street
Sacramento, CA 95814

Applied Research & Technology of
Utah, Inc
Attn: Don Sorenson
2555 South 900 West
Salt Lake City, UT 84119

Architect, Inc.
Attn: Larry W. Taylor
2570 South Harvard
Tulsa, OK 74114

Architects
Attn: Douglas Juller, AIA
1951 Brookview Drive
Kent, OH 44240

Architects Forum
Attn: Douglas S. Nichols, AIA
211 E. 11th Street
Suite 105
Vancouver, WA 98660

Architects Hawaii Ltd.
Attn: Dennis Daniel, AIA
60 Church Street
Wailuku Maui, HI 96793

Architects Weeks & Ambrose
Attn: William L. Ambrose III, AIA
30 Market Square Mall
Knoxville, TN 37902

Architecture, Architectural Planning,
   Interior Design, Graphics & Photography
Attn: John G. Lewis, AIA
P.O. Box 711 - Capitol Station
Richmond, VA 23206

ARCO Solar, Inc.
Attn: W. Hawley
20542 Plummer St.
Chatsworth, CA 91311

Arizona State University
Attn: Jeffrey Cook, AIA
College of Architecture
Tempe, AZ 85281

Arizona Sunworks
Attn: Bill Otwell
502 Hill Avenue
Prescott, Az 86301

Arnold J. Aho AIA Architect
Attn: Arnold J. Aho, AIA
P.O. Box 5291
Mississippi State, MS 39762

Arthur Lewis Davis Architect
Attn: Arthur Lewis Davis, AIA
30 Journal Square
Jersey City, NJ 07306

Bahm, Raymond J.
2513 Kimberley Ct. NW
Albuquerque, NM 87120

Barkmann Engineers
Attn: Herman Barkmann, PE
107 Cienega Street
Santa Fe, NM 87501

Barth & Ramsbottom
Attn: Bill Barth
5006 Whitaker Drive
Knoxville, TN 37919

Bartos & Rhodes Architects
Attn: Robert Rhodes, AIA
10 East 40th Street
New York, NY 10016

Beale's Wharf
Attn: Rock Salvando
Box 254
SW Harbor, ME 04609

Benham-Blair & Affiliates, Inc.
Attn: Mr. William J. Judge
1200 Northwest 63rd Street
P.O. Box 20400
Oklahoma City, CK 73156

Beverly Brandon
4600 Roland Avenue
Baltimore, MD 21210

Black & Veatch Consulting Engineers
Attn: Donald C. Gray
P.O. Box 8405
Kansas City, MO 64114

Bob Schmitt
P.O. Box 8196
Strongsville, OH 44136

Bohlin Powell Brown
Attn: Frank Grauman
182 N. Franklin Street
Wilkes-Barre, PA 18701

Brenda Ellis
109 12th Street, NE
Washington, DC 20002

Brooks Waldman Associates
Attn: Brooks H. Waldman
162 Adams Street
Denver, CO 80206

Bruce, Campbell, Grahm Associates
Attn: Ray Sullivan
16 Bridge Street
Westport, CT 06880

Burns & Roe, Inc. (2)
Attn: C. A. Fontana
800 Kinderkamack Road
Oradell, NJ 07649

Burran and Smith AIA Partners
Attn: James A. Burran, Jr., AIA
P.O. Box 6724
Lubbock, TX 79413

Burt Hill Kosar Rittlemann
Attn: John Oster
400 Morgan Center
Butler, PA 16001

Calcara Duffendack Foss Manlove, Inc.
Attn: Michael H. Foss, AIA
4610 J. C. Nichols Parkway
Kansas City, MO 64112

California Energy Commission
Attn: Arthur J. Soinski
1111 Howe Avenue
Sacramento, CA 95825

Carnegie Mellon University
Attn: Volker Hartkopf
519 College of Fine Arts
Pittsburgh, PA 15213

Cataldo and Waters Architects, P.C.
Attn: J. Charles Cataldo, AIA
142 Droms Road
Scotia, NY 12302

Central States Energy Research Corp.
Attn: James L. Schoenfelder, AIA
Box 2623
Iowa City, IA 52244

CHI Housing Inc.
Attn: Doug Coonley
68 South Main Street
Box 566
Hanover, NH 03755

Circus Studios
Attn: W. Ted Montgomery
Box 500
Waitsfield, VT 05673

Clayton Yong Associates
Attn: Clayton Yong
2366 Eastlake Avenue
Seattle, WA 98102

Clifford S. Nakata & Associates
Attn: Clifford S. Nakata, AIA
525 North Cascade Avenue
Colorado Springs, CO 80903

Clovis Helmsath Associates
Attn: Clovis Helmsath, FAIA
On the Square
Fayetteville, TX 78940

Communico
Attn: Wayne Nicholas
Seton Village R.R. 3
Box 810
Santa Fe, NM 87501

Competition Advisory Service
Attn: Will Lehr
AIA 3rd Floor
1735 New York Ave., NW
Washington, DC 20006

Comprehensive Design Associates, Inc.
Attn: Steven Bottiger, AIP
P.O. Box 332
State College, PA 16801

Cooperson Breck Associates
Attn: Todd Breck
4000 Thomps Bridge Road
Montchanin, DE 19710

Cromwell, Neyland, Truemper, Levy & Gatchell, Inc.
Attn: Ray K. Parker, AIA
One Spring Street
Little Rock, AR 72201

Crowther/Architects Group
Attn: Lawrence Atkinson, AIA
310 Steele Street
Denver, CO 80206

CRS Design Associates, Inc.
Attn: Larry W. Bickle
2700 S. Post Oak Road, Suite 2300
Houston, TX 77056

Cynthia Howard AIA & Associates
Attn: Cynthia Howard
34 Ash Street
Cambridge, MA 02138

Dale Roth, Architect
RD 2 Box 165-D
New Tripoli, PA 18066

Daniel Aiello
516 West Parkway Blvd.
Tempe, AZ 85281

Daniel, Mann, Johnson & Mendenhall
Attn: Walter Meisen
3250 Wilshire Blvd.
Los Angeles, CA 90010

David Francis Costa Jr. & Associates
Attn: David Francis Costa, Jr., AIA
210 Ellsworth Street
Albany, OR 97321

David Jay Feinberg Architect
Attn: David Feinberg, AIA
Suite 302
10700 Caribbean Blvd.
Miami, FL 33189

David L. Smith Architect
Attn: David L. Smith
505 Hamilton Street
Schenectady, NY 12305

David Wong & Associates
Attn: David Wong, P.E.
American Security Bank Bldg.
1314 S. King St., Suite 1461
Honolulu, HI 96814

Dayton Power & Light Co.
Attn: Bruce Curtis
P.O. Box 1247
Dayton, OH 45401

Denny Long
Route 1 Box 158
Woodland, CA 95695

Design Direction
Attn: Dennis John Becker, AIA
1588 Tanglebriar
Fayetteville, AR 72701

Dick Jenkins, Vice President
Product Development
10221 Wincopin Circle
Columbia, MD 21044

Dick Lamar Architect
Attn: Dick Lamar, AIA
201 Woodrow Street
Columbia, SC 29205

Donald F. Monell Architect
Attn: Donald F. Monell, AIA
11 Pleasant Street
Gloucester, MA 01930

Donald M. Watts Architect
Attn: Donald M. Watts
1649 Huntington Drive
South Pasadena, CA 91030

Downing Leach & Associates
Attn: Jim Leach
3985 Wonderland Hill Avenue
Boulder, CO 80302

Dr. Stephen K. Young   (10)
SAI
1710 Goodridge Drive
McLean, VA 22102

Dublin Bloome Associates
Attn: H. Robert Sparkes, P.E.
312 Park Road
West Hartford, CT 06107

Dyer and Watson Architects
Attn: James Watson
24100 Chagrin Blvd.
Cleveland, OH 44122

EAI Inc.
Attn: Dr. Jerry Alcone
13300 Hugh Graham Rd. NE
Albuquerque, NM 87111

Earth Dynamics
Attn: Peter Slack
P.O. Box 1175
Boulder, CO 80002

Earthworks
Attn: Steven E. Golubski
20 West 9th Street
Kansas City, MO 64105

Edwards & Daniels Associates
Attn: A. Brett Bullock
525 E. 300 S
Salt Lake City, UT 84102

Ekosea
Attn: Lee Porter Butler
573 Mission Street
San Francisco, CA 94105

Ellerbe Associates, Inc.
Attn: Jim Gelfer
Manager of Professional Services
Electrical Design Department
One Appletree Square
Bloomington, MN 55420

Ellmore/Titus/Architects/Inc.
Attn: S. A. Titus, AIA
736 Chestnut Street
Santa Cruz, CA 95060

Energy Architects Inc.
Attn: Ski Milburn
885 Arapahoe
Boulder, CO 80302

Energy Conversion Devices
Attn: Mr. Lionel Robbins
1675 West Maple Road
Troy, MI 48084

Energy Design & Analysis Co.
Attn: David Schwartz, AIA
1001 Connecticut Ave., NW
Suite 632
Washington, DC 20036

Energy Design Associates
Attn: Steve Nearhoof
114 E. Diamond Street
Butler, PA 16001

Energy Planning & Investment Corp.
Attn: Richard Larry Medlin AIA
833 North Fourth Avenue
Tucson, AZ 85705

Energy Services Organization of
The Georgia Power Co.
Attn: Edward Ney
7 Solar Circle
Shenandoh, GA 30265

Engineers-Architects P.C.
Attn: Arnold Hanson, AIA
1407 24th Avenue South
Grand Forks, ND 58201

Engineers-Architects P.C.
Attn: Gord Rosey
408 First Avenue Building
Minot, ND 58701

Environmental Concern
Attn: Bruce Mauser, AIA
Box 2128
Spokane, WA 92210

Environmental Design Alternatives
Attn: Douglas G. Fuller
1951 Brookview Drive
Kent, OH 44240

Environmental Institute of Michigan
Attn: Reed Maes
P.O. Box 618
Ann Arbor, MI 48107

Environmental Research Laboratory
Attn: Helen Kessler
Tucson International Airport
Tucson, AZ 85706

Environomic Design
Attn: Dennis N. Young, AIA
W. 905 Riverside
Spokane, WA 99201

ERG, Inc.
Attn: Chuck Sherman
1650 W. Alameda Drive
Suite 140
Tempe, AZ 85282

Erwin and Akers Associates
Attn: Charles DeLisio
Benedum-Trees Bldg.
Pittsburgh, PA 15222

Everett Zeigel Tumpes and Hand
Attn: R. J. Martin, AIA
1215 Spruce Street
Boulder, CO 80302

Ezra D. Ehrenkrantz & Associates
Attn: William Meyer
19 West 44th Street
New York, NY 10036

Fando Martin and Milstead
Attn: Hank Walker
608 Tennessee Avenue
Charleston, WV 25302

Fischer Stein Associates
Attn: Hans J. Fischer, AIA
Route 51 South
Carbondale, IL 62901

Fisk Rinehart Keltch Meyer Inc.
Attn: Harley B. Fisk, AIA
100 Kentucky Exec. Building
2055 Dixie Highway
Ft. Mitchell, KY 41011

Frank H. Witchey Corbett Associates
Box 1009
86 East Broadway
Jackson, WY 83001

Fred Meyer, AIA
3611 5th Avenue
San Diego, CA 92103

Fred W. Forbes & Associates, Inc.
Architects AIA and Engineers NSPE
P.O. Box 443
Xenia, OH 45385

Galliher Schoenhardt & Baier
Attn: Robert P. Morcarsky
The Courtyard No. 10
Simsbury, CT 06070

Gary Copeland
31-81 Poplal Avenue
Memphis, TN 38111

Gary Marciniak
6582 N. 90th
Milwaukee, WI 53224

Geiger Berger & Associates
Attn: Karl Beitlin, PE
500 Fifth Avenue
New York, NY 10036

General Electric Co.
Attn: E. M. Mehalick
Advanced Energy Programs
P.O. Box 8661
Philadelphia, PA 19101

Gensler Architects, Inc.
Attn: James L. Gensler, AIA
819 N. Marshall Street
Milwaukee, WI 53202

George A. Roman & Associates, Inc.
Attn: George A. Roman, AIA
One Gateway Center
Newton, MA 02158

Georgia Institute of Technology
Attn: Richard Williams
College of Engineering
Atlanta, GA 30332

Georgia Institute of Technology
Engineering Exp. Station
Attn: Joan Wood
225 North Avenue, NW
Atlanta, GA 30332

Georgia Power Company
Attn: Gary Birdwell
P.O. Box 4545
Atlanta, GA 30303

Gerken & Upham Architects, Inc.
Attn: Mr. Carl Gerken
P.O. Box 155
Ormond Beach, FL 32074

GK Associates
Attn: Drew Gillette
319 Holbrook Road
Bedford, NH 03102

Class Energy Electronics
Attn: Ron Wilson
4463 Woodland
Park Avenue North
Seattle, WA 98103

Grahm Hubenthal
Box 777
Soap Lake, WA 98851

Greenles/Reese Associates, Ltd.
Attn: Frank L. Reese, AIA
6400 Flying Cloud Drive
Suite 210
Eden Praire, MN 55344

Grimball/Gorrondona/Savoye
Attn: Michael D. Cortner
2352 Metarle Road
Metarle, LA 70001

Gunnar, Birkerts & Associates
Attn: Charles Eleckenstein
292 Harmon Street
Birmingham, MI 48009

Hahn Jackson Lloyd Thresher Arch. & Eng.
Attn: Timothy A. Henning, AIA
Top Hat Road
Princeton, IN 47670

Hankins & Anderson, Inc.
Attn: H. C. Yu
1680 Santa Rosa
Richmond, VA 23288

Harthorne Hagen Gross AIA & Assoc.
Attn: Cliff Gross, AIA
220 Marina Mart 1500 Westlake N.
Seattle, WA 98109

Harvard University
Attn: John Martin
204 Pierce Hall
Cambridge, MA 02138

Heery Energy Consultants Inc.
Attn: Marvin Wiley, P.E.
880 W. Peachtree Street, NW
Atlanta, GA 30309

Heery & Heery, Architects & Engineers, Inc.
Attn: Mr. Richard Yelvington
880 West Peachtree Street, NW
Atlanta, GA 30309

Helen McEntire
4160 S. 1785 W.
Heritage Bank Building
Suite 200
Salt Lake City, UT 84119

Herbert Sands
2013 S. Melborne Ct.
Melbourne, FL 23901

Hood Miller Associates
Attn: Bobbie Sue Hood, AIA
2051 Leavenworth St.
San Francisco, CA 94133

Interactive Resources, Inc.
Attn: Carl Bouville
117 Park Place
Point Richmond, CA 94801

Iowa State University (2)
Attn: David Block, AIA
Attn: Laurent Hodges
Physics Department
290 College of Design
Ames, IA 50011

J. L. Harter Associates
Attn: James L. Harter, Sr., AIA
41 S. Tenth Street
Allentown, PA 18102

Jackson Labs
Attn: Tom Hyde
Otter Creek Road
Bar Harbor, ME 04609

James Sudler Associates
Attn: Joal Cronewett, AIA
200 Cable Building
Denver, CO 80202

James Sudler, FAIA
1201 18th Street
Suite 200
Denver, CO 80202

James T. Barretta Architect
Attn: James T. Barretta, AIA
1832 NW 2nd Avenue
Boca Raton, FL 33432

Jammel Finn & Associates
Attn: Arnold Finn
1516 E. Hillcrest Street
P.O. Box 8963
Orlando, FL 32856

Jim Dennison
Water Street
Ellsworth, ME 04605

Joe Melendez
444 Executive Center Blvd.
Suite 130
El Paso, TX 79902

John D. Swetish
No. 7 Wildwood Trail
Bettendorf, IA 52722

John Martin Associates Architects
Attn: John T. Martin, AIA
506 Heights Blvd.
Houston, TX 77007

John R. Taylor Architect
Attn: John R. Taylor, AIA
815 Shady Bluff Drive
Charlotte, NC 28211

John Yellott Engineering Association
Attn: John Yellott
901 West El Caminito
Phoenix, AZ 85021

Johnstown Architects, Inc.
Attn: Benjamin J. Policicchio, AIA
GKI Building
777 Goucher Street
Johnstown, PA 15905

Jones & Mayer
Attn: Charles Mayer
13100 Manchester Road
St. Louis, MO 63131

Jones & Strange-Boston Ross Building
Attn: Donald L. Strange-Boston, AIA, PE
Main Street at 8th
Richmond, VA 23219

Joseph J. Del Ciotto, Jr., Architect
Attn: Joseph Del Ciotto, AIA
201 Church Road
Lansdale, PA 19446

JSR Associates
Attn: Dr. John S. Reuyl
2280 Hanover Street
Palo Alto, CA 94306

Kammeraad Stroop van der Leek
Attn: Paul van der Leek
355 Settlers Road
Holland, MI 49423

Keith Vaughan Associates
Attn: Keith Vaughan
3136 E. Madison Street
Seattle, WA 98112

Kelbaugh and Lee Architects
Attn: Douglas Kelbaugh, AIA
240 Nassau
Princeton, NJ 08540

Kitchen & Associates
Attn: Deborah K. Gawthrop
Office Manager
Box 935
Philadelphia, PA 19105

Knoell/Quidort Architects
Attn: Hugh Knoell, Jr. AIA
1131 East Highland
Phoenix, AZ 85014

Korsunsky Krank Erickson Architects
Attn: Daryl P. Fortier, AIA
Director of Design
570 Galaxy Building
330 Second Avenue South
Minnesota, MN 55401

Kruger Kruger Albenberg
Attn: Kenneth Kruger
2 Central Square
Cambridge, MA 02139

Lancaster and Lancaster Architects
Attn: Earl M. Lancaster AIA
P.O. Box 10
Auburn, AL 36830

Lane & Associates Architects
Attn: John E. Lane, AIA
1318 North B Street
P.O. Box 3929
Fort Smith, AR 72913

Lapicki/Smith Associates
Attn: Carol A. Moore
617 Park Avenue
Baltimore, MD 21201

Lee R. Connell Architect, Inc.
Attn: Lee R. Connell, Jr., AIA
2500 Joseph Street
New Orleans, LA 70115

Leo A. Daly
Attn: Arturo Bantog
1025 Connecticut Ave., NW
Suite 712
Washington, DC 20036

Leon Deller
911 22nd Street
Santa Monica, CA 90403

Leonard Wrinberg, AIA
160 Hilair Circle
White Plains, NY 10605

Living Systems
Attn: Johathan Hammond
Route 1 Box 170
Winters, CA 95616

Londe Parker Michels Consultants
Attn: Timothy I. Michels
7438 Forsyth
Suite 202
St. Louis, MO 63105

Long Hoeft Architects
Attn: Mr. Gary Long, AIA
1228 Fifteenth Street, Suite 401
Denver, CO 80202

Louisiana Institute of Building Sciences
Attn: Richard C. Thevenot
830 North Street
Baton Rouge, LA 70802

Lydia Straus-Edwards Arch. Designer
Attn: Lydia Straus-Edwards
331 Main Street South
Woodbury, CT 06798

M. David Egan, PE
P.O. Box 365
Anderson, SC 29621

Manuel Perez
1056 Hunting Lodge Drive
Miami Springs, FL 33166

Marcel E. Sammut Arch. & Struct. Eng.
Attn: Marcel E. Sammut, AIA
30 Anthony Circle
Newtonville, MA 02160

Mark Beck Associates
Attn: Peter Powell, AIA
762 Fairmount Avenue
Towson, MD 21204

Marlin H. Andersen Homes
Attn: Marlin Grant, President
8901 Lyndale Avenue South
Bloomington, MN 55420

Martin Marietta Corp.
Attn: M. S. Imamura
P.O. Box 179
Denver, CO 80201

Mass Design
Attn: Gordon Tully
138 MT. Auburn St.
Cambridge, MA 02138

Massachusetts Institute of Technology
Attn: Tim Johnson
Department of Architecture
Cambridge, MA 02139

Matrix Inc.
Attn: Edward Mazria
400 San Felipe NW
Suite 6
P.O. Box 4883
Albuquerque, NM 87106

Mayhill Homes Corp.
Attn: John Odeguard
P.O. Box 1778
Gainesville, GA 30501

McCleer Architect
Attn: Mike McCleer
2249 First National Bldg.
Detroit, MI 48226

MCM
Attn: Michael C. Merchant
P.O. Box 7707
Stanford, CA 94305

Merriam, Deasy & Whisenant, Inc.
Attn: Bruce D. Fraser, AIA
979 Osos Street
Suite C
San Luis Obispo, CA 93401

Metcalf and Associates
Attn: Susan Shaw
3222 N Street NW
Washington, DC 20007

Miami University of Ohio
Attn: Fuller Moore
Department of Arch.
Oxford, OH 45056

Michael Albanes
2368 Cherry Street
Denver, CO 80207

Miller Hanser Westerbeck Bell Architects, Inc.
Attn: Jay Johnson
Suite 300 Butler Square
100 N 6th Street
Minneapolis, MN 55403

Miller Wagner Coenen, Inc.
Attn: Robert M. Miller, AIA
250 N. Green Bay Road
P.O. Box 396
Neenah, WI 54956

Mogavero & Unruh
Attn: David J. Mogavero
811 J Street
Sacramento, CA 95814

Moore, Grover & Harper
Attn: Robert L. Harper, AIA
Maine Street
Centerbrook, CT 06049

More, Combs, Burch Arch. & Eng.
Attn: Donald H. More, AIA
3911 E. Exposition Avenue
Denver, CO 80209

Morton, Wolfberg, Alvarez, Taracidi & Associates
9400 S. Dadeland Blvd.
Miami, FL 33156

Motorola, Inc. A110
Attn: Bob Hammond
P.O. Box 2953
Phoenix, AZ 85062

Mr. J. Marshall Mauney, AIA
Division of Plant Operation
306 Education Building
Raleigh, NC 27611

Mr. William Dorsett
930 Thurston
Manhattan, KS 66502

Mueller Associates
Attn: Bob Hedden
1900 Sulphur Spring Road
Baltimore, MD 21227

N.C. Solar Energy Assoc.
Attn: Bruce Johnson, AIA
P.O. Box 12235
Research Triangle Park, NC 27709

National Homes Corp.
Attn: Steven J. Wilson
Director of Research & Technology
P.O. Box 7680
Lafayette, IN 47903

Nelis O. Brown Development Company
Attn: Nelis O. Brown, President
368 Sunway Lane
RR #1
Creve Coeur, MO 63141

Nixon Brown Brokaw Bowen
Attn: Paul G. Flehmer AIA
1800 Commerce Street
Boulder, CO 80301

Northeast Design Distribution
Attn: David Campbell
727 - 11th Ave.
New York, NY 10019

Northeast Solar Energy Center
Attn: Drew A. Gillett
470 Altantic Avenue
Boston, MA 02110

Oceanside Solar Consultants
Attn: Ralph L. Sherwood
10 East Main Street
Hyannis, MA 02601

Office of Franz Peter Scheuermann
Attn: Franz P. Scheuermann, AIA
Park Street P.O. Box 1008
Stowe, VT 05672

Office of Glen H. Mortensen, Inc.
Attn: Glen H. Mortensen, AIA
Suite 201
1036 W. Robinhood Dr.
Stockton, CA 95207

Omer Mithun, FAIA
2000 112th Avenue, NW
Belevur, WA 98004

Optical Sciences Group, Inc.
Attn: Dieter W. Grabis
24 Tiburon Street
San Rafael, CA 94901

Pacific Power & Light Company
Attn: Bill McTavish
Box 720
Casper, WY 82602

Parker Croston Associates
Attn: M. E. Croston, Jr., AIA
P.O. Box 1927
3108 W. 6th Street
Fort Worth, TX 76101

Perez & Hurtado Architects, Inc.
Attn: Jess F. Perez
850 E. Chapman Avenue
Suite A
Orange, CA 92666

Perkins & Will
Attn: Bill Bobenhausen
445 Hamilton Avenue
White Plains, NY 10601

Peter D. Paul, AIA
P.O. Box 271
50 Galesi Drive
Wayne, NJ 07470

Peter Dobrovolny, AIA
Box 133
Old Snowmass, CO 81654

Peter Van Deesser
634 Garcia Street
Santa Fe, NM 87501

Peterson Construction Company
Attn: Robert Peterson, President
6100 S. 14th Street
Lincoln, NE 68512

Pettit & Bullinger Architects
Attn: Hell C. Pettit, AIA
P.O. Box 2726
1202 East First
Wichita, KS 67201

Philip West, Donald Bergstrom & Assoc.
Attn: Edward J. Marcyn, AIA
33 East First Street
Hinsdale, IL 60521

Phineas Alpers Architects, Inc.
Attn: Phineas Alpers, AIA
344 Newbury Street
Boston, MA 02115

Potomac Energy Group
Attn: David Johnston
401 Wythe Street
Alexandria, VA 22314

Price and Partners
7301 Birch Avenue
Takoma Park, MD 20012

Price Roth & Muse Architects
Attn: William Price
P.O. Box 1014
Tri-City Airport
Blountville, TN 37617

Princeton Energy Group
Attn: Harrison Fraker, AIA
729 Alexander Road
Princeton, NJ 08540

RA Solar Consultants, Inc.
Attn: Harry E. Burns, Jr., AIA
Park 20 West
Blountstown Highway
Tallahassee, FL 32304

Ralph E. Kiene & Associates
Attn: Ralph E. Kiene, AIA
1006 Grand Avenue
Kansas City, MO 64106

Ralph Jefferson, AIA Architect
497 Springfield Avenue
Summit, NJ 07901

Ramon Zambrano & Associates
Attn: Dan Holland
1015 Battery Street
San Francisco, CA 94111

Rasmussen Hobbs Architects/Planners
Attn: D. L. Hobbs, AIA
#9 Saint Helens
The Henry Drum House
Tacoma, WA 98402

Raymond E. Phillips, Architect
Attn: Raymond E. Phillips, AIA
703 SW McKinley
Des Moines, IA 50315

Raymond J. Bahm
2513 Kimberley Ct. NW
Albuquerque, NM 87120

Reyn Hendrickson
4480 Grand River Street
Novi, MI 48050

Richard Schwarz/Neil Weber
Attn: Neil Weber, AIA
3601 Park Center Boulevard
Minneapolis, MN 55416

Riddick Engineering Corporation,
Consultants
Attn: James R. Balley, P.E.
2310 First National Building
Little Rock, AR 72201

Robb Axton, AIA
4741 Laurel Canyon Blvd.
North Hollywood, CA 91607

Robert Dincecco Architect
Attn: Robert Dincecco
326 W. Lawrence Lane
Phoenix, AZ 85021

Robert G. Werden & Associates, Inc.
Attn: William F. Milburn
P.O. Box 414
Jenkintown, PA 20736

Robert J. Johnson, Architects
1220 Santa Barbara St.
P.O. Box 2673
Santa Barbara, CA 93101

Roche Dinkeloo Associates
Attn: Ms. Curtain
20 Davis Street
Hamden, CT 06517

Rogers-Nagel & Langhart, Inc.
Attn: Mr. Roger Crosby
1576 Sherman Street
Denver, CO 80203

Ron Piotras
Northeast Carry Building
110 Water Street
Hallowell, ME 04347

Ron Yeo, FAIA Architect, Inc.
Attn: Ron Yeo, FAIA
500 Jasmine Avenue
Corona Del Mar, CA 92625

Ronald R. Campbell & Associates
Attn: Jan Kafranic
2150 North 107th Street
Seattle, WA 98133

Rotz Engineers, Inc.
Attn: Thomas Chiplis
2828 North High School Road
P.O. Box 24357
Indianapolis, IN 46224

Rowe Holmes Assoc. Arch. Inc.
Attn: Dave Fronccok
215 S. Adams Street
Tallahassee, FL 32301

RRI
Attn: Kurt Johnson
157 Church Street
New Haven, CT 06670

Sadiron Deck
Attn: Bruce Brownell
Alternative Energy
c/o Brownell Lumber
Route 4
Edenburgh, NJ 12134

Sam Cravotta
One Design
Mountain Fall RTE
Winchester, VA 22601

Sargent, Webster, Crenshaw, Folley
Attn: Donald Skowron
2112 Erie Blvd. East
Syracuse, NY 13224

Schaffer Bonavolonta Arch., Inc.
Attn: Martin Schaffer
24 West Erie Street
Chicago, IL 60610

Schipporeit Inc.
Attn: David Urschel
One American Plaza
Evanston, IL 60201

SEAGroup
Attn: David Wright AIA
418 Broad
Nevada City, CA 95959

Sierra Engineering
Attn: Tom Carver
1129 Tudor Street
Lodi, CA 95240

Skoler & Lee Architects, P.C.
Attn: Kermit J. Lee, Jr., AIA
1004 University Building
Syracuse, NY 13202

SMALC/XRE
Attn: Jim Pestillo
McClellan AFB
Sacramento, CA 95652

Smith, Hinchman, and Grylls
Attn: Randal E. Swelch
455 West Fort Street
Detroit, MI 48226

Sol Tec
Attn: Jim Crouch
2160 Clay Street
Denver, CO 80211

Solar Building Corp.
Attn: John Newman
1004 Allen
St. Louis, MO 63104

Solar Design Associates
Attn: Steven J. Strong
Conant Road
Lincoln, MA 01773

Solar Environmental Engineering
Attn: Dave Gunther
2524 East Vine Drive
Fort Collins, CO 80524

Solar Processes Inc.
Attn: Gordon Preiss
11 Velvet Lane
Mystic, CT 06355

Solar Technology Systems
Attn: Charles Orr
81A Upper St. Giles St.
Norwich, ENGLAND NR21AB

SolArc
Attn: Anthonly Outri
2040 Addison Street
Berkeley, CA 92704

Solarex Corporation
Attn: Marth Bozman
1335 Piccard Drive
Rockville, MD 20850

South Street Design
Attn: Don Prowler
2233 Grays Ferry Avenue
Philadelphia, PA 19146

Southern Solar Energy Center
Attn: S.C. Nelson
61 Perimeter Park
Atlanta, GA 30341

Steelcraft Corporation
Attn: Gary Ford
Box 12408
Memphis, TN 38112

Sunrise Builders
Attn: Rich Schwolsky
P.O. Box 125
Grafton, VT 05146

Sverdrup and Parcel Eng & Arch
Attn: Frank Kessler
1650 W. Alameda Drive
Tempe, AZ 85282

Tackett Way Lodholz
Attn: George Way
3121 Buffalo Speedway
Suite 400
Houston, TX 77098

Talbot & Associates
Attn: Thomas L. Ainscough, AIA
P.O. Box 2224
Virginia Beach, VA 23452

Texas Tech University
Attn: Professor Carl Childers
Division of Architecture
Box 4140
Lubbock, TX 79409

The Architects Collaborative
Attn: Ms. Gail Flynn
46 Brattle Street
Cambridge, MA 02138

The Architects Taos
Attn: William Mingenbach
Box 1884
Taos, NM 87571

The Architectural Alliance
Attn: Peter Pfister, AIA
400 Clifton Avenue
Minneapolis, MN 55403

The Burns/Peters Group
Attn: William L. Burns, AIA
8000 Pennsylvania Circle NE
Albuquerque, NM 87110

The Burr Associates, Architecture & Planning
Attn: Donald F. Burr, FAIA
P.O. Box 99885, Lakewood Center
Tacoma, WA 98499

The Clark Enerson Partnership
Attn: Charles L. Thomsen
600 NBC Center
Lincoln, NE 68508

The Hawkeed Group Ltd.
Attn: Rodney Wright, AIA
4643 N. Clark Street
Chicago, IL 60640

The Orcutt/Winslow Partnership
Attn: Paul Winslow AIA
1109 North Second Street
Phoenix, AZ 85004

The Royal Arch. Institute of Canada (RIAC)
Attn: Robbins Elliott
151 Slater
Ottawa Canada KIP 5H3

The Wolf Partnership Architects
Attn: William G. Schimeneck, AIA
Attn: Paul J. Schmitz, AIA
7 South 7th Street
Allentown, PA 18101

Thomas Russell
80 Shield Street
West Hartford, CT 06110

Thomas Vonier Associates
Attn: Peter H. Smeallie
Suite 413
2000 P Street, NW
Washington, DC 20036

Thomas W. Merrill Architects
Attn: Thomas W. Merrill
321 SW Sixth
Albany, OR 97321

Total Design Four
Attn: Carter Howard
P.O. Drawer 3947
Corpus Christi, TX 78404

Total Environmental Action
Attn: Peter Temple
Church Hill
Harrisville, NH 03450

Trellis & Watkins
6565 Pennacook Court
Columbia, MD 21045

Trynor Hermanson & Hahn Architects
Attn: Gilbert F. Hahn, AIA
311 Medical Arts Building
Box 156
St. Cloud, MN 56301

University of Arizona
Attn: Merle Jensen
Environmental Research Laboratory
Tucson, AZ 85706

University of Arkansas
Attn: James Lambeth, AIA
1591 Clark
Fayetteville, AR 72701

University of North Carolina
Attn: Dean Charles Hight
College of Architecture
UNCC Station
Charlotte, NC 28223

University of Puerto Rico
Attn: Angel Lopez
Ctr for Energy and Environmental Research
College Station
Mayaquez, P.R. 00708

University of Southern California
Attn: Ralph Knowles
School of Architecture and Fine Arts
Los Angeles, CA 90007

USDA Forest Service Engineering
Attn: Robert LeCain
P.O. Box 7669
Missoula, MT 59807

VanDerRyn Calthorpe & Partners
Attn: Peter Calthorpe
Drawer 7
Inverness, CA 94937

Walter S. Withers Architect
Attn: Walter S. Withers, AIA
1250 Chambers Road
Columbus, OH 43212

Warehouse Specialist, Inc.
Attn: Mark van Deyaclat
655 Brighton Beach Road
Manasha, WI 54952

Warner Burns Toan Lunde
Attn: Fritz Lunde
330 W. 42nd Street
New York, NY 10036

WED Enterprises
Attn: Mike McCullough
1401 Flowers Street
Glendale, CA 91201

Wendell H. Lovett Architect
Attn: Wendell H. Lovett, FAIA
2134 Third Avenue
Seattle, WA 98121

William Drevo Architect
Attn: William Drevo, AIA
6125 29th Street, NW
Washington, DC 20015

William J. Bates Architect
Attn: William J. Bates, AIA
57 Marlin Drive West
Pittsburgh, PA 15216

William Morgan Architect
Attn: Thomas A. McCrary, AIA
220 East Forsyth Street
Jacksonville, FL 32202

William Tao & Associates
Attn: Richard Janus
2357 59th Street
St. Louis, MO 63110

William Thomas Meyer, AIA
Attn: William T. Meyer
353 East 72nd Street
New York, NY 10021

Wright, Pierce, Eng. & Arch.
Attn: Douglas Wilkie
38 Roosevelt Avenue
Glen Head, NY 11545

Wright-Pierce Associates & Eng.
Attn: Barbara Freeman
99 Main Street
Topsham, ME 04086

ZOEworks
Attn: Garth Collier, AIA
70 Zoe Street
San Francisco, CA 94107

Zomeworks Inc.
Attn: Steve Baer
P.O. Box 712
Albuquerque, NM 87103

Dist-16